Oceanic and climatic variability in the eastern tropical North Atlantic and over western Sahel during the last deglaciation and the Holocene

Dissertation zur Erlangung des Doktorgrades der Naturwissenschaften
(Dr. rer. Nat) am Fachbereich Geowissenschaften
der Universität Bremen

Vorgelegt von

Ilham Bouimetarhan

Bremen, January 2009

Tag des Kolloquiums

17.04.2009

Gutachter:

Frau PD Dr. Karin Zonneveld

Frau Prof. Dr. Gesine Mollenhauer

Prüfer:

Frau Dr. Lydie Dupont

Herr Prof. Dr. Tilo von Dobeneck

Bouimetarhan, Ilham 24th of January, 2009

Department of Geosciences/Marum, Universität Bremen, Klagenfurter Strasse, D-28359 Bremen, Germany

Erklärung

Hiermit versichere ich, dass ich

1. die Arbeit ohne unerlaubte fremde Hilfe angefertigt habe,

2. keine anderen als die von mir angegebenen Quellen und Hilfsmittel benutzt habe und

3. die den benutzten Werken wörtlich oder inhaltlich entnommenen Stellen als solche kenntlich gemacht habe.

Bremen, den 24. Januar 2009

Ilham Bouimetarhan

Il faut se servir de toutes les ressources de l'intelligence,

de l'imagination, des sens, de la mémoire

pour avoir une intuition distincte

des propositions simples.

Régle 12

(Les régles pour la direction de l'esprit, 1629)

René Descartes

Acknowledgements

I owe my gratitude to PD Dr. Karin Zonneveld who gave me the opportunity to undertake this PhD project and, with accurate suggestions, advised me throughout.

My most sincere thanks go to Dr. Lydie Dupont who introduced me to the beautiful world of pollen and who shared with me her knowledge about African vegetation and climate. Her permanent support, interest, generosity, and encouragment has made possible for me to complete this thesis. I would like to warmly thank Dr. Enno Schefuß who always helped me to face with optimism and enthusiasm "all" scientific problems. I feel very lucky to have worked with him. Special thanks go to Dr. Stefan Mulitza and Prof. Dr. Gesine Mollenhauer for the fruitful discussions and suggestions.

I would like to sincerely thank all the people at the Department of Geosciences and Marum in Bremen University who somehow contributed to this work. Many thanks to Dr. Fabienne Marret, who received me during two months at Liverpool University, for her endless help and support. Sven Forke and Mirja Hoins are thanked for their help with the laboratory work, *you made my life so easy and my slides so nice to look at…you always did a great job…Thank you*. I would like also to thank everybody in the "Historical Geology/Paleontology" group, especially Prof. Dr. Helmut Willems, Dr. Gerhard Versteegh, Maria, Nicole, Kara, Maike, Anne, Monika, Angelika, Marion, Katarzyna, Stijn, Rehab, Ines, Sonja. Monika Kodrans-Nsiah is thanked for all the fun we had at our office…*I miss our Tee Pause*. Thanks to all my friends and colleagues, especially Jeroen, Heather, Cletus, Martin, Jörg, Chrsitian März (for the *Französich/Deutch/Spanish* Tandem), Jean, Rosella, and Nourredine. Many thanks to my dear friend Catalina González who always made me feel at home with her love, support and patience. She was always my example of discipline, enthusiasm, and passion for marine palynology. At the end, I would like to thank Igaratza Fraile for the beautiful friendship and also for her support with all my problems that did not regard Science.

I am immensely grateful to my parents for their permanent support and encouragement during all my life and esepecially during these three years in

distance. *Vous étiez toujours présents et vous continuez de l'être pour faire mon bonheur*, *je vous en suis très reconaissante. Merci d'être mes parents, j'en ai toujours été fière et j'espère que vous l'êtes aussi de moi. Merci aussi à ma soeur chérie, à l'unique soeur que j'ai au monde Mariam et à mon petit frère Bakr. Merci d'être toujours à mes côtés*. This thesis is dedicated to the memory of my beloved grandfather who left us in December 2008. *J'espère que, du monde qui est sien maintenant, il accepte cet humble geste comme preuve de reconnaissance de la part de sa petite fille qui a toujours apprécié son optimisme, sa générositè et sa joie de vivre et qui a toujours prié pour le salut de son âme*.

Most of all, I thank my "*chèr fiancé"* for his treasured love, without him my life and work here in Bremen would not have been possible.

This work was funded by the German Research Foundation *Deutsche Forschungsgemeinschaft* as part of the DFG-Research Center/Excellence cluster "The Ocean in the Earth System".

Table of Contents

Abstract

For the last decades, climatologists and paleoecologists have focused their attention on the semi-arid Sahel region, one of the most sensitive areas on the planet to even small climatic shifts. Previous studies of West African paleohydrology largely focused on the Holocene and the last deglaciation have revealed alternating arid and humid conditions as reconstructed from records of lake-level fluctuations across the continent as well as from marine cores recovered off west tropical Africa. These hydrological changes are thought to be associated with weakening and strengthening of the African monsoon circulation that occurs on both short - and long - time scales. They are forced by shifts in the average latitudinal position of the Intertropical Convergence Zone (ITCZ) and its associated tropical rainbelt in close association with changes in sea surface temperature (SST) patterns and northern high-latitude climate.

The present study is based on the high-resolution palynological analysis of marine sediment cores recovered off the Senegal River mouth and provides a detailed reconstruction of the hydrological variability of western Sahel during the last deglaciation and the late Holocene. It also concerns the past oceanic circulation variability in the eastern tropical Atlantic with respect to abrupt climate changes. We used pollen and spores, and organic-walled dinoflagellate cyst to 1) describe and assess changes in vegetation and operating transport agents (winds and rivers) in relation to rainfall variability over the Sahel, 2) describe marine productivity changes recorded in the eastern tropical Atlantic, 3) investigate the underlying local and regional mechanisms controlling the observed patterns, and 4) establish direct land-sea correlations of terrestrial and marine environmental changes.

This investigation first determined the relation between dinoflagellate cyst distribution in the marine surface sediments and the present-day upper water conditions such as sea-surface temperature, salinity, fresh water input, and marine productivity based on a palynological analysis carried out on 53 surface sediment samples taken along the coast of West Africa. The composition of organic-walled dinoflagellate cyst assemblages and changes in their concentrations allows the identification of four hydrographic regimes; 1) the northern regime between 14° and

17°N characterized by high productivity associated with seasonal coastal upwelling, 2) the southern regime between 6° and 12°N associated with high-nutrient waters influenced by river discharge 3) the intermediate regime between 12° and 14°N influenced mainly by seasonal coastal upwelling additionally associated with fluvial input of terrestrial nutrients and 4) the low productivity regime characterized by low chlorophyll-*a* concentrations in upper waters and high bottom water oxygen concentrations.

As a second step, late Holocene oceanic and environmental variations were addressed in detail using a marine palynological record from the mud-belt deposited off the Senegal River mouth. The record is based on changes in the assemblages, concentrations and fluxes of pollen and dinoflagellate cysts as well as changes in sedimentation rates, and cover the period from ca. 4200 and 1200 cal yr BP. This period saw alternating arid and humid phases where initial dry conditions from ca. 4200 to 2900 cal yr BP were followed by a period of stronger fluvial transport; and, by inference, greater monsoonal humidity between ca. 2900 and 2500 cal yr BP, which we refer to as “Little Humid Phase”. A return to dry conditions was recorded between ca. 2500 and 2200 cal yr BP when Senegal River runoff decreased and Sahelian winds increased. Around ca. 2200 cal yr BP, this relatively dry period ended with periodic pulses of high terrigenous contributions and strong fluctuations in fern spore and river plume dinoflagellate cyst percentages and in the total accumulation rates of pollen, dinoflagellate cysts, fresh-water algae, and plant cuticles indicating episodic flash flood events of the Senegal River between ca. 2200 and 2100 cal yr BP. The observed oscillations reflect most probably the strengthening and weakening of the African monsoon in close association with the latitudinal migration of the ITCZ and its associated tropical rainbelt.

Finally, vegetation development in the western Sahel and ocean surface conditions in the eastern tropical Atlantic were reconstructed during the last deglaciation with focus on Heinrich event 1 (H1) and implications for abrupt climate change were addressed. The high-resolution palynological and geochemical record covering the period from ca. 20,000 to 12,000 cal yr BP reveals the complexity of the H1 stadial. We identified two aridity maxima between ca. 18,800 and 17,400 cal yr BP and between ca. 16,400 and 15,400 cal yr BP. Both phases were characterized by a

maximum occurrence of the Saharan plant community simultaneously with a maximum of Ti/Ca ratio indicating extremely dry conditions and strong NE trade winds. Interestingly, dinoflagellate cyst assemblages were dominated, during both intervals, by the upwelling association suggesting nutrient-rich surface waters characteristic for high marine upwelling-related productivity. After ca.15,400 cal yr BP, an increase of mangroves and hygrophile plants along with fern spores and fresh water algae and a simultaneous increment of the runoff dinoflagellate cyst association, point to a shift towards more humid and relatively warm climate as a response to the Indian monsoon ractivation. The results show that both, the composition and the regional distribution of the vegetation sensitively responded within decades to abrupt climate changes indicating the importance of paleovegetation studies for comparing and validating Earth System Models including dynamic vegetation modelling. These results primarily reflect the important role played by the latitudinal migration of the inter tropical convergence zone and its associated tropical rainbelt during periods of the AMOC weakening (strengthening), and corroborate the hypothesis that during the last deglaciation tropical and high latitudinal climate systems were tightly coupled.

Zusammenfassung

In den letzten Jahrzehnten haben Klimatologen und Paläoökologen der semi-ariden Sahel-Region grosse Aufmerksamkeit gewidmet, eine der empfindlichsten Gebiete der Erde, die auf kleinste Klimaänderungen reagiert Bisherige Arbeiten über die Paläo-Hydrologie von West Afrika, die sich vor allem auf das Holozän und die letzte Enteisung konzentrierten, zeigten Wechsel zwischen ariden und humiden Bedingungen, die aus verschiedenen terrestrischen Anzeigern für den Wasserstand von afrikanischen Seen und aus marinen Sedimenten vor dem westliche tropische Afrika rekonstruiert wurden. Es wird angenommen, dass diese Änderungen in der Hydrologie mit der Abschwächung und Intensivierung des afrikanischen Monsuns zusammenhängen, und sowohl auf kurzen wie auf langen Zeitskalen auftreten. Die klimatischen Änderungen werden durch Verschiebungen der mittleren Position der innertropischen Konvergenzzone (ITCZ) und dem daran gekoppelten tropischen Regengürtels (TRB) induziert, und stehen in Wechslwirkungen mit der Oberflächentemperatur des Meerwassers (SST) und dem Klima der nördlichen hohen Breiten.

Diese Arbeit basiert auf der hochauflösenden palynologischen Analyse von marinen Sedimentkernen aus dem Bereich der Mündung des Senegal und liefert eine detaillierte Rekonstruktion der hydrologischen Variabilität der westlichen Sahel während der letzten Enteisung und im späten Holozän und der Paläo-Zirkulationsänderungen im östlichen tropischen Atlantik in Bezug auf abrupte Klimaänderungen. Wir verwenden Pollen, Sporen und Dinoflagellatenzysten mit organischen Schalen, um Änderungen in der Vegetation und den Transportmechanismen (äolisch / fluviatil) in Bezug zum Niederschlag in der Sahel zu beschreiben und zu bewerten, Änderungen in der marinen Produktivität im östlichen tropischen Atlantik zu beschreiben, die lokalen und regionalen Mechanismen, die diese Muster kontrollieren zu untersuchen und direkte Land-Meer-Korrelationen mariner und terrestrischer Umweltänderungen zu erstellen

Dazu wurde zunächst der Ausdruck von heutigen Oberflächenwasserbedingungen wie Oberflächentemperatur, Salinität, Süsswassereintrag und mariner Produktivität in der Palynologie von 53 Oberflächenproben von Sedimenten vor West-Afrika

analysiert. Die Zusammenetzung von Vergesellschaftungen organischwandiger Dinoflagellatenzysten-und von Pollen erlaubt die Identifizierung von vier hydrographischen Regionen: Eine nördliche Region zwischen 14° und 17°N, die durch hohe Produktivität mit saisonalem Auftrieb gekennzeichnet ist, eine südliche Region zwischen 6° und 12°N mit durch Flusseintrag nährstoffreichen Wässern, eine mittlere Region zwischen 12° und 14°N die vor allem durch saisonalen Auftrieb und fluvialen Eintrag terrestrischer Nährstoffe gekennzeichnet ist, und eine Region mit niedriger Produktivität gekennzeichnet durch niedrige Konzentrationen von Chlorophyll-a im Oberflächenwasser und durch hohe Konzentrationen von Sauerstoff im Oberflächenwasser.

In einem zweiten Schritt wurden die Änderungen der spätholozänen terrestrischen und marinen Umweltbedingungen detailliert anhand der Palynologie eines Sedimentkerns aus dem Mud-belt im Bereich der Senegal-Mündung untersucht. Der Kern zeigt sowohl Änderungen in der Vergesellschaftung, der Konzentration und dem Flux von Pollen und Dinoflagellatenzysten, als auch Änderungen in der Sedimentationsrate, und umfasst den Zeitraum 4200 bis 1200 cal yr BP. In dieser Periode gab es alternierende aride und humide Phasen mit zunächst ariden Bedingungen von ca.4200 bis 2900 cal yr BP, die von einer Phase mit mehr fluviatilen Transport zwischen ca. 2900 und 2500 cal yr BP gefolgt wurde, die wir als monsungesteuerte humide Phase interpretieren und als "Little Humid Phase" bezeichnen. Die Palynologie des Kerns zeigt zwischen ca. 2500 und 2200 cal yr BP eine Rückkehr zu trockenen Bedingungen mit weniger Wasserführung des Senegal und einer Zunahme des Windes in der Sahel. Um 2200 cal yr BP endete diese relativ trockene Phase mit periodischen Schüben von hohem terrigenen Eintrag und starken Fluktuationen im Anteil an Farn-Sporen und Dinoflagellatenzysten, die Süsswassereintrag anzeigen, und in den Gesamt-Akkumulationsraten von Pollen, Dinoflagellatenzysten, Süsswasseralgen und Pflanzenresten, was wir als episodische "flash flood events" des Senegal zwischen 2200 und 2100 cal yr BP deuten. Die beobachteten Wechsel spiegeln sehr wahrscheinlich die Intensivierung und die Abschwächung des afrikanischen Monsun in engem Zusammenhang mit der Migration der ITCZ und des damit gekoppelten TRB.

Schliesslich wurden die Vegetationsentwicklung der westlichen Sahel sowie die ozeanischen Bedingungen im Oberflächenwasser des tropischen Ost-Atlantiks während der letzten Enteisung mit Schwerpunkt auf dem Heinrich-Event 1 (H1) rekonstruiert und Anzeiger für abrupte Klimaänderungen untersucht. Die Palynologie und Geochemie eines hochauflösenden Sedimentkernes im Zeitraum von ca. 20.000 bis 12.000 cal yr BP zeigt eine komplexe Struktur des Heinrich Stadials, wobei wir zwei Ariditätsmaxima zwischen 18.800 und 17.400 cal yr BP und zwischen 16.400 und 15.400 cal yr BP beobachten. Beide Phasen sind gekennzeichnet vom Maxima im Auftreten einer Sahara-Pflanzenvergesellschaftung zusammen mit Maxima im Ti/Ca-Verhältnis, was extrem trockene Bedingungen und starken NE-Passat anzeigt. Interessanterweise wird die Dinoflagellatenzysten-Vergesellschaftung in beiden Phasen von Arten dominiert, die Auftriebsanzeiger sind, und damit einen Hinweis auf nährstoffreiche Oberflächenwässer liefern, die charakterisctisch für auftriebsgesteuerte hohe marine Produktivität sind. Nach ca. 15400 cal yr BP liefert ein Anstieg im Anteil an Pollen von Mangroven und hydrophilen Pflanzen zusammen mit Farn-Sporen, Süsswasseralgen und einem Anstieg an Flusseintrag anzeigenden Dinoflagellatenzystengemeinschaften Hinweise für eine Rückkehr zu feuchterem und relativ warmem Klima. Die Ergebnisse zeigen, dass die Zusammensetzung und die regionale Verbreitung der Vegetation und der marinen Produktion empfindlich und innerhalb von Jahrzehnten auf abrupte Änderungen des Klimas reagieren. Die Ergebnisse weisen besonders auf die Bedeutung der Lage der ITCZ und des daran gekoppelten TRB in Phasen mit abgeschwächter oder intensivierter Ozeanzirulation (Atlantic Meridional Overturning Circulation, AMOC) hin, und unterstützen die Annahme, dass während der letzten Enteisung die Klimasysteme der Tropen und der hohen Breiten eng gekoppelt waren.

Chapter 1

Introduction

1.1 Late Quaternary climatic fluctuations

One of the most conspicuous outcomes of the study of earth's history during the late Quaternary is the discovery of rapid millennial-scale climate fluctuations manifested as a series of high-amplitude abrupt climate changes shifting from glacial to interglacial conditions within a few decades (Figure 1.1) (Adams et al., 1999). Previous reviews (e.g., Alley et al., 1999, 2003; Lockwood, 2001; Rahmstorf, 2002; Rial et al., 2004) have defined these abrupt changes as a result of instabilities, threshold crossing, and other types of nonlinear behaviour of the global climate system, triggering a sudden climate transition to a new state at rates faster than their known or suspected cause (Ganopolski and Rahmstorf, 2001).

Two main types of rapid climate changes are recorded in ice cores from Greenland (Dansgaard, 1993) and in detailed marine records from the North Atlantic during the last glacial period (Heinrich, 1988; Bond et al, 1992; Broecker et al., 1992), and are known respectively, as Dansgaard-Oeschger (D-O) oscillations and the so-called Heinrich events (HEs). D-O cycles show an abrupt temperature increase (up to ~8°C) in Greenland (interstadials) within a few decades followed by gradual cooling (stadials) lasting several centuries (Bond et al., 1999). HEs are documented in the North Atlantic as anomalous and wide spread occurrences of ice-rafted debris layers that coincided with the coldest final phases of some consecutive cold stadials (Hemming, 2004). They occur every 7-10 kyrs and appear to have had a global impact (Heinrich, 1988; Voelker et al., 2002). The driving mechanism behind these events remains unclear, they are thought to be related to ice sheet instability (MacAyeal, 1993), orbital variations of insolation and solar activity (Heinrich, 1988; McIntyre and Molfino, 1996) as well as changes in deep sea circulation (Sarnthein et al., 2000; Rahmstorf, 2002). Sudden discharge of large freshwater quantities from melting of the Northern Hemisphere continental ice-sheets lowers the salinity and density of surface waters at about 45°-55°N and subsequently reduces North Atlantic Deep Water (NADW) formation interrupting the thermohaline circulation and the

Atlantic meridional overturning circulation (AMOC) (e.g., Broecker et al., 1986; Rahmstorf, 2002; McManus et al., 2004).

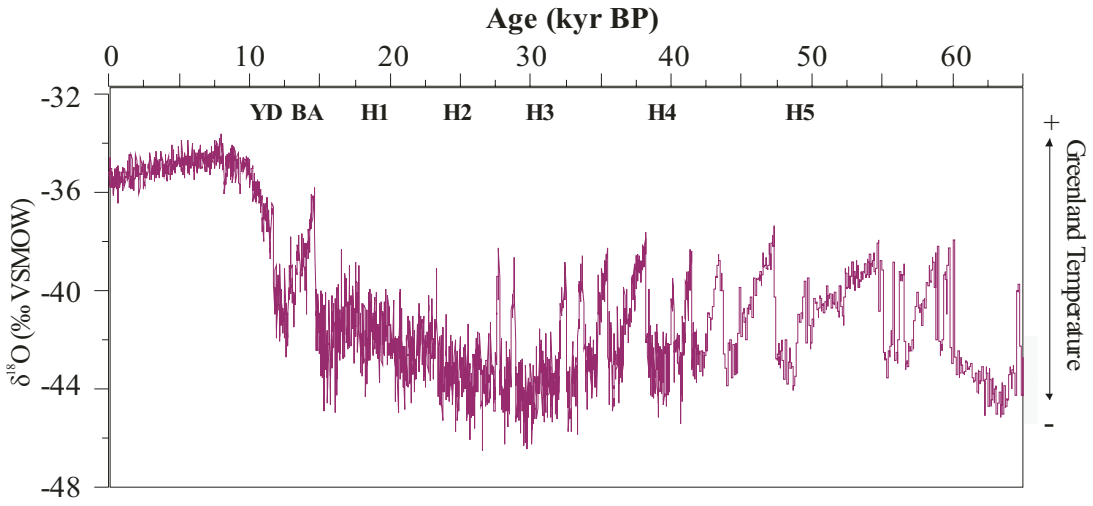

Figure 1.1 Stable isotope stratigraphy ($\delta^{18}O$) of the North Greenland Ice Core Project (NGRIP; 75.10°N and 42.32°W) (NGRIP-members, 2004) showing the Heinrich Events (H), the Bølling-Allerod warm event (BA) and the Younger Dryas (YD).

In parallel, extensive and consistent evidences from several subtropical and tropical records have identified millennial scale variability in hydrological patterns to be synchronous with HEs cycles (Figure 1.2) (e.g. Zhao et al., 1995 (NW Africa); Arz et al., 1998 (NE Brazil); Leuschner and Sirocko, 2000 (Arabian Sea); Wang et al., 2001 (China); Burns et al., 2003 (Arabian sea); Dupont and Behling, 2006 and Dupont et al., 2008 (Namibia and Angola); Jullien et al., 2007 (Eastern tropical North Atlantic); González et al., 2008 (Cariaco basin); Itambi et al., 2008; Mulitza et al., 2008; Tjalingii et al., 2008 (NW Africa)). Atmospheric linkages, such as the Intertropical Convergence Zone (ITCZ) and the monsoon system, have been proposed as driving mechanisms in transporting the effects of HEs to mid- and low-latitude locations (Schulz et al., 1998; Wang et al., 2001; Broecker, 2003; Mulitza et al., 2008). Whereas other studies suggest a reduction of the NADW formation and the slow-down of the AMOC as the primary trigger for propagating the effect of HEs (Ganopolski and Rahmstorf, 2001; Hemming, 2004).

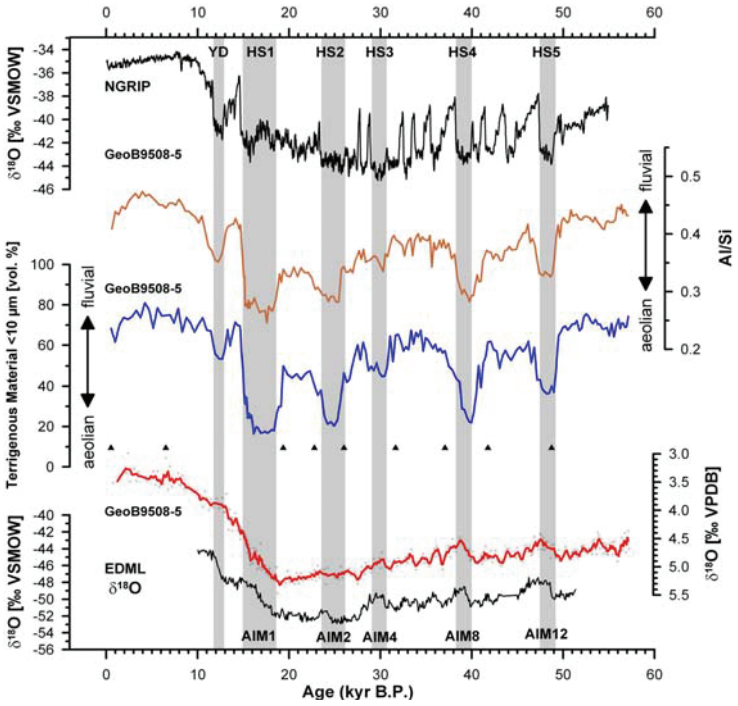

Figure 1.2 Comparison of sedimentary records of Core GeoB9508-5 off NW Africa with **(A)** $\delta^{18}O$ of Greenland (NGRIP) and **(E)** Antarctic (EDML, bottom) ice cores [*EPICA, 2006*]. **(B)** Bulk Al/Si ratios, **(C)** relative abundance of terrigenous sediments with grain size < 10µm and **(D)** oxygen isotope record of benthic foraminifera in core GeoB9508-5. Grey bars indicate the approximate occurrence of Dansgaard-Oeschger Stadials associated with Heinrich Events (i.e., Heinrich Stadials, HS) and the Younger Dryas (YD) in the Northern Hemisphere, and the corresponding Antarctic Isotope Maxima (AIM) in the Southern Hemisphere. Arrows indicate dominant mode of terrigenous sediment transport (Mulitza et al., 2008).

The climate of Africa, a continent that represents up to 20% of the earth's surface, is a very important element in climate modelling studies. Especially the semi-arid Sahel region, where rainfall depends on the intensity, width and latitudinal position of the tropical rainbelt (Nicholson, 2008), that has experienced most recently, severe droughts from the late 60s to early 80s of the last century. This causes distressing social and economic decline (e.g., Nicholson, 2000) resulting in famine, death, and large population migration. This region has also been frequently affected, since the Pliocene, by changes towards more arid climate (Leroy and Dupont, 1994; deMenocal, 1995), which resulted in extreme hydrological and environmental variations from extensive grassland with numerous lakes during the early Holocene African Humid Period (AHP) to the present day arid conditions (Claussen et al., 1999; Gasse, 2000; deMenocal et al., 2000).

Historical records from the tropical eastern Atlantic and over western Sahel, suggest millennial scale Sahel droughts to be synchronous with cold north Atlantic sea surface temperature (SST) anomalies (Street-Perrot and Perrot, 1990; Gasse, 2000; Zhao et al., 1995; Julien et al., 2007; Itambi et al., 2008; Mulitza et al., 2008; Tjalingii et al., 2008) during times of reduced AMOC (Newell and Hsiung, 1987). Climate modelling studies propose the southward shift of the ITCZ and its associated tropical rainbelt in conjunction with an intensification and southward expansion of the mid-tropospheric African Easterly Jet as driving mechanisms for the extreme aridity over western Sahel (Mulitza et al., 2008). These different results show that the ultimate mechanisms behind this abrupt climate variability still remain uncertain. Studying and understanding the causes, extent, and frequency of these changes is essential to predict future climate change. High-temporal-resolution records reconstructing paleoceanographic and paleoclimatic conditions in regions covering the latitudinal extent of the modern tropical rainbelt allow the reconstruction of decadal- to millennial-scale variability in ocean circulation and changes in tropical rainfall in Sahel. This will enable the recognition of simultaneous changes in both oceanic and atmospheric conditions and therefore, allow for a detailed land-sea correlation through the complementary use of marine palynology alayzing terrestrial (pollen and spores) and marine originated (organic-walled dinoflagellate cysts) palynomorphs.

1.2 Marine palynology

Next to a wide range of isotopic, biostratigraphic and geochemical methods, marine palynology has shown to provide valuable information on past environments of the adjacent continent and past surface ocean conditions allowing for a correlation of terrestrial and marine paleoclimatic and paleoceanographic reconstructions. Marine palynology is the study of palynomorphs, defined as organic-walled microfossils of both animal and vegetal structures (from ~5 to 500µm) including pollen, spores, dinoflagellates, acritarchs, chitinozoans and scolecodonts. They are extracted from rocks and marine sediment cores by standard palynomorph-extraction procedures that include strong acids, bases, acetolysis and density separation (Traverse, 2007).

1.2.1 Pollen

Pollen is a fine to coarse powder consisting of microgametophytes (pollen grains). Most pollen grains are spherical and very small, their sizes vary from ~6 to 100µm, they contain three cells, one is responsible for the growth of the pollen tube when the pollen grain arrives at the stigma, one vegetative cell (non-reproductive) and one is generative cell (reproductive). They are protected within a thick and resistant organic wall made of sporopollenin. Once pollen grains are released by the plants, they can be transported over long distances by winds and/or by rivers, and then potentially reach the sea floor. Therefore, they are present in marine sediments from estuarine to abyssal environments and from the tropics to the Polar Regions. Consequently, their broad occurrence makes them valuable paleoclimatic and paleoenvironmental markers especially along the coast of arid environments where terrestrial records are scarce and other common microfossils are badly preserved.

Pollen data derived from marine sediments integrate palynological information on large shifts in vegetation over long and continuous periods, covering often more than one climatic cycle. They have shown to be suitable for tracing large-scale climatically related vegetation changes as well as hydrological variability (Dupont, 1999) and for reconstructing a direct land-sea correlation (Hooghiemstra et al., 2006). However, the interpretation of pollen records from marine sediments should be done carefully and several aspects must be taken into account. These include 1) source and production of pollen grains that varies remarkably from one species to another, 2) transport to the ocean floor and through the water column, 3) displacement by ocean currents, 4) sedimentation process, 5) taphonomic processes and early diagenisis, 5)fossilisation in the sediment (Dupont, 1999). Because pollen grains are transported over long distances reflecting the ease with which they can be transported from their source area to the site of sedimentation, the evaluation of transport agents is always part of the interpretation of marine pollen records. Aeolian transport of pollen grains predominates in deep-sea sediments located far from the coast and along arid areas with no or small river discharge (Heusser and Morley, 1985; Hooghiemstra et al., 1986). Whereas fluvial transport is especially dominant in humid areas and at sites close to river mouths.

1.2.2 Organic-walled dinoflagellate cysts

Dinoflagellates are a large group of unicellular eukaryotic algae living in most types of aquatic environments from lakes to open ocean and from the tropical realm to the high-latitudes polar regions (e.g., Taylor and Pollingher, 1987; Matthiessen et al., 2005). These microscopic protists (~ 30-200μm) belonging to the division of Dinoflagellata possess two flagella, one transverse flagellum encircling the body and one longitudinal enabling the vertical migration through the water column with a "whirling" motion (Fensome et al., 1993). About 2000 dinoflagellate species (~90%) are known to live in marine environments in almost all climatic regimes but show particularly high diversity in the tropics and neritic temperate waters (e.g., Stover et al., 1996) where they represent the majority of marine phytoplankton and together with diatoms and coccolithophorids account for the main constituents of the marine primary producers (e.g., Parsons et al., 1984; Taylor and Pollingher, 1987). Dinoflagellates exhibit diverse feeding strategies. Besides the autotrophic species depending on the availability of light to photosynthesise nutrients taken up directly from the water column (Schnepf and Elbrächter, 1992), many dinoflagellates are heterotrophic or mixotrophic (combination of heterotrophic and autotrophic) feeding on other organisms mainly diatoms or on dissolved organic substances (Jacobson and Anderson, 1986).

The life cycle of dinoflagellates is relatively complex involving several stages, asexual and sexual, motile and non-motile (cyst) (Figure 1.3). During the sexual reproduction, dinoflagellates produce gametes, pairs of which fuse to produce a hypnozygote. Some hypnozygotes can be protected by a thick cyst wall called "resting cyst", which permits survival of the organism during a certain dormancy period (e.g. Wall and Dale, 1967; Fensome et al., 1993). 10 to 20% of the species produce a highly resistant organic walled cyst known as dinosporin which has been compared to the sporopollenin of pollen grains (Fensome et al., 1993; Kokinos et al., 1998). The process of encystment occurs mostly after blooms and might be influenced by temperature, day length, irradiance and endogenous encystment rhythm (e.g., Anderson and Keafer, 1987). After the dormancy period, the protoplast hatches through an excystment opening in the cyst wall called archeopyle.

Excystment can be triggered or inhibited by several factors such as anoxia, low temperature or nutrient/light availability (Dale, 1983).

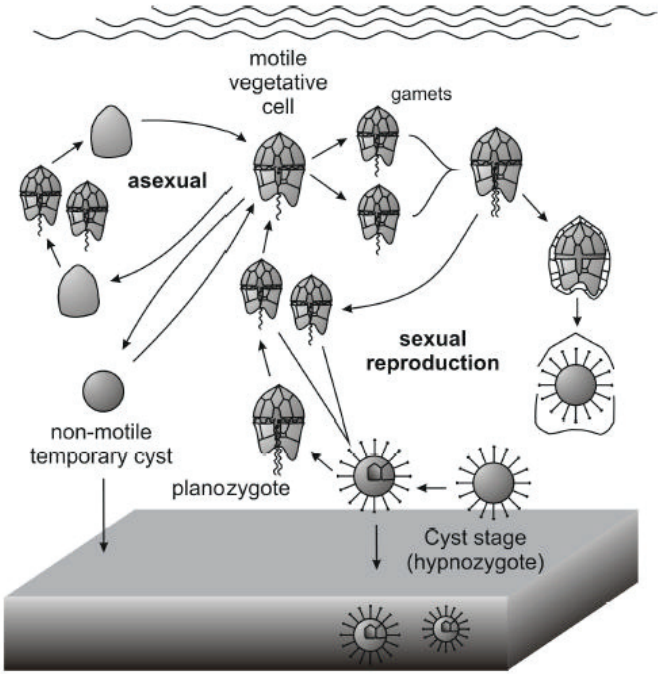

Figure 1.3 Simplified life cycle of cyst producing dinoflagellates (From Bockelmann, 2007, after Dale, 1986))

Since the 90's, studies of modern dinoflagellate cysts in marine surface sediments increased remarkably (Lewis et al., 1990; de Vernal et al., 1994; Harland, 1994; Marret, 1994; Dale, 1996; Marret and de Vernal, 1997; Versteegh, 1997; Zonneveld, 1997; Rochon et al., 1998, 1999; Santarelli et al., 1998; Zonneveld and Brummer, 2000; de Vernal et al., 2001; Zonneveld et al., 2001; Radi et al., 2001; Dale et al., 2002; Marret and Zonneveld, 2003; Radi and de Vernal, 2004; Pospelova et al., 2005, 2006, 2008; Holzwarth et al., 2007). They have shown that the spatial and seasonal distribution of dinoflagellate cysts is strongly correlated with physical/chemical sea surface conditions such as sea-surface temperature, salinity, nutrient availability, turbulence and freshwater discharge (e.g. Wall et al., 1977; Dale, 1996; de Vernal et al., 1994, 2001, 2005; Rochon et al., 1999; Vink et al., 2000; Radi and de Vernal, 2004). Concurrently, they became increasingly used for paleoceanographic and paleoenvironmental studies to document aspects of changes in the ocean conditions during the period of major global climatic and environmental changes, especially in neritic highly-productive environments where the microbial

degradation of the organic matter causes carbonate dissolution restricting the use of calcareous proxies (e.g., planktonic foraminifera, diatoms and coccolithophores).

However, as with all other proxies, the use of dinoflagellate cyst assemblages as a proxy for paleoceanography has certain limitations. First, it is worth emphasizing that several species can be laterally displaced by oceanic currents from their point of origin to the site of sedimentation while sinking to the ocean floor. Some authors, in fact, consider the large abundance of dinoflagellate cysts beyond the shelf break to have been transported from neritic environments (e.g., Dale, 1983; 1996). Secondly, though the majority of dinoflagellate cyst are made of highly resistant organic complex biomolecules (e.g., Kokinos et al., 1998; Versteegh and Blokker, 2004) and are generally very well preserved in marine sediments. Recent studies have shown that oxidation may selectively destroy cysts of some species notably the brown-walled cysts (i.e. Protoperidinoids). The species-selective post-depositional degradation of dinoflagellate cysts could be a limitation, especially in areas characterized by oxygenated bottom waters and low sedimentation rates, preventing rapid burial of the organic-matter (e.g. Zonneveld et al., 1997, 2001, 2007; Hopkins and McCarthy 2002; Versteegh and Zonneveld, 2002; Reichart and Brinkhuis 2003; Kodrans-Nsiah et al., 2008).

1.3 Scientific objectives

Because the semi-arid Sahel region is one of the most ecologically vulnerable areas on the planet, due to the alternation of arid and humid phases associated with weakening and strengthening of the African monsoon circulation (Gasse, 2000; Nicholson, 2000), it has been the focus of numerous climatic and paleoecological studies. Although the general trend of paleoclimate history of western Sahel is reasonably well established for the last glacial-interglacial cycle as a whole, the amplitude and timing of rainfall variations remain imprecise due to the major discontinuities in lacustrine sediments (Lézine, 1998) and the low time resolution as well as large dating uncertainties (Gasse, 2000). The continental record of the hydrological variations associated with the strengthening of the Atlantic monsoon at the glacial-deglacial transition comes only from two permanent crater lakes from the Guineo-Congolian forest domain: Lake Bosumtwi in Ghana (Talbot and Johanessen, 1992; Beuning et al., 2003) and Lake Barombi Mbo in Cameron (Giresse et al.,

1994; Maley and Brenac, 1998). In contrast, climate reconstructions from oceanic cores recovered off West tropical Africa are numerous but only few of them give access to information on river mouth zones sensitive to hydrological changes (e.g. Dupont and Weinelt, 1996; Schneider et al., 1997; Marret et al., 2001, 2008; Zabel et al., 2001; Adegbie et al., 2003; Mulitza et al, 2008)

The main objective of this project is to work out a detailed reconstruction of ocean circulation and climatic variability in the eastern tropical Atlantic and over western Sahel from cores off the mouth of the Senegal River, in order to document the hydrological history of western Sahel during the last deglaciation and the late Holocene as well as the past oceanic conditions in the eastern tropical Atlantic with respect to abrupt climate changes. This paleo-climatic and -environmental study will contribute to better understand the climate system of this region hoping it will aid in developing reliable models that can predict future climate change at regional and global scales. The fundamental questions that arise from this study are:

- What is the degree of variability in Sahel rainfall during the late Holocene?
- Are decadal- and millennial-scale Sahel droughts associated with latitudinal migration of the ITCZ and its associated tropical rainbelt?
- What is the impact of ocean circulation and SST variability on terrestrial environments, especially on the hydrological cycle and vegetation of western Sahel?
- What is the impact of ocean circulation variability on marine primary productivity in the eastern tropical Atlantic?

This work attempts to answer the mentioned questions by using two independent proxies: 1) Terrestrial palynomorphs (pollen and spores) to assess vegetation changes on the adjacent continent and operating transport agents (mainly winds and rivers) in relation to changes in climate (mainly precipitation), and 2) organic-walled dinoflagellate cysts (dinocysts) to independently investigate the variability of the past sea-surface conditions (e.g., primary productivity, salinity, temperature, nutrient availability, freshwater discharge) in relation to climate changes. The combination of the vegetation information and the paleoceanographic information potentially

enables the recognition of simultaneous changes in both oceanic and atmospheric mechanisms allowing for a detailed land-ocean correlation.

1.4 Outline

The outcomes of this project are presented in three manuscripts that correspond to Chapter 4, 5 and 6 of this thesis.

The first manuscript (Chapter 4) - *Dinoflagellate cyst distribution in marine surface sediments off West Africa (17 – 6°N) in relation to sea-surface conditions, freshwater input and seasonal coastal upwelling* - aims to examine to which extent we can use dinocysts as environmental indicators in the tropical eastern Atlantic and to explore which species or combination of species provide the best information about changes in environmental conditions. For this purpose a dinocyst analysis was carried out on 53 surface sediment samples from West Africa (17 – 6°N) to obtain insight in the relationship between their spatial distribution and hydrological conditions in the upper water column as well as marine productivity. The composition of cyst assemblages and dinocyst concentrations allows the identification of four hydrographic regimes that are related to the current position and seasonal variability of the ITCZ and as such the position of its associated tropical rainbelt. The results presented in the first manuscript are of crucial importance to the rest of the thesis. They show that the fossil dinocyst association in this region forms a very accurate tool to reconstruct, in detail, the past ocean circulation changes.

The second manuscript (Chapter 5) - *Palynological evidence for climatic and oceanic variability off NW Africa during the late Holocene* - a high temporal resolution reconstruction of late Holocene fluctuations in climate of NW Africa. The reconstruction is based on pollen and dinocyst analyses from a marine sediment core GeoB9503-5 retrieved from the mud-belt deposited off the Senegal River mouth. The core registred high sedimentation rates (~1.5 $cm.yr^{-1}$) that allowed a decadal-scale reconstruction. The results provided insights into changes in continental moisture conditions over western Sahel and variability in oceanic conditions in the eastern tropical North Atlantic for the time interval ca. 4200-1200 cal yr BP, a period which has been generally considered relatively stable. The palynological record displays two main humid periods that occur between ca. 2900 and 2500 cal yr BP we refer to

as “Little Humid Phase” and between ca. 2200 and 2100 cal yr BP caused by episodic flash flood events of the Senegal River.

The third manuscript (Chapter 6) - *Two aridity maxima in western Sahel during Heinrich event 1* - addresses the last deglaciation climatic and hydrologic changes over the western Sahel. Here, the focus is on Heinrich event 1 (H1) stadial. Pollen, dinocysts and bulk sediment geochemistry from a marine sediment core GeoB9508-5 recovered from the continental slope off Northern Senegal, are presented. Again, high sedimentation rates of the studied core allowed a high-resolution reconstruction of regional vegetation changes, marine paleoproductivity, and tropical African rainfall variability during H1. The results show that H1 stadial is a complex period characterized by four distinct phases among which two aridity maxima were distinguished. These findings highlight the important role played by the latitudinal shifts of the ITCZ in modifying the regional climate patterns and support the hypothesis of the close relationship between the variability in AMOC strength, changes in SST patterns and Sahel precipitation.

Additionally to the results presented in the three manuscripts, the appendix of this thesis includes another manuscript that is not in the focus of the main research theme of the study but is closely related to it. We contributed to this paper, which describes the use of morphological variance in a dinocyst species *Lingulodinium machaerophorum* as a salinity and temperature indicator, with material, data and scientific discussions. The data of this thesis including counts of organic-walled dinoflagellate cysts and pollen are also presented in the appendix

References

Adams, J., Maslin,M., Thomas,E., 1999. Sudden climate transitions during the late Quaternary. Progress in Physical Geography 23, 1-36.

Adegbie, A.T., Schneider, R.R., Röhl, U., Wefer, G., 2003. Glacial millenial-scale fluctuations in central African precipitation recorded in terrigenous supply and freshwater signals offshore Cameroon. Paleogeography, Paleoclimatology, Paleoecology 197, 323-333.

Alley, R.B., Clark, P.U., Keigwin, L.D., Webb, R.S., 1999. Making sense of millennial scale climate change. In: Clark, P.U., Webb, R.S., Keigwin, L.D. (Eds), Mechanisms of global climate change at millennial time scales, Geophysical Monograph Vol. 112, American Geophysical Union, Washington, pp. 385-395.

Alley, R.B., Marotzke, J., Nordhaus, W.D., Overpeck, J.T., Peteet, D.M., Pielke Jr., R.A., Pierrehumbert, R.T., Rhines, R.T., Stocker, T.F., Talley, L.D., Wallace, J.M., 2003. Abrupt climate change. Science 299, 2005-2010.

Anderson, D.M., Keafer, B.A., 1987. An endogenous annual clock in the toxic marine dinoflagellate Gonyaulax tamarensis. Nature 325, 616-617.

Arz, H., Pätzold, J., Wefer, G., 1998. Correlated millenial-scale changes in surface hydrography and terrigenous sediment yield inferred from last-glacial marine deposits off northeastern Brazil. Quaternary Research 50, 157-166.

Beuning, K.R.M., Talbot, M.R., Livingstone, D.A., Scmukler, G., 2003. Sensitivityof carbon isotopic proxies to paleoclimatic forcing: a case study from lakeBosumtwi, Ghana, over the last 32,000 years. Global Geochemical Cycles 17, 1121.

Bockelmann, F.D., 2007. Selective preservation of organic-walled dinoflagellate cysts in Quaternary marine sediments: an oxygen effect and its application topaleoceanography. PhD thesis, university of Bremen, 130pp.

Bond, G., Heinrich, H., Broecker, W., Labeyrie, L., McManus, J., Andrews, J., Huonparallel, S., Jantschik, R., Clasen, S., Simet, C., Tedesco, K., Klas, M., Bonani, G., Ivy, S., 1992. Evidence for massive discharges of icebergs into the North Atlantic sediments and Greenland ice. Nature 365, 143-147.

Bond, G.C., Showers, W., Elliot, M., Evans, M., Lotti, R., Hajdas, I., Bonani, G., Johnson, S., 1999. The North Atlantic's 1–2 kyr climate rhythm: relation to Heinrich events, Dansgaard-Oeschger cycles and the little ice age", In: Clark, P.U., Webb, R.S., Keigwin, L.D.: Mechanisms of Global Change at Millennial Time Scales, Geophysical Monograph. American Geophysical Union, Washington DC, pp. 59–76.

Broecker, W.S., 1986. Oxygen isotope constraints on surface temperatures. Quaternary Research 26, 121-134.

Broecker, W.S., Bond, G., Klas, M., Clark, E., McManus, J., 1992. Origin of the northern Atlantic's Heinrich events. Climate Dynamics 6, 265-273.

Broecker, W.S., 2003. Does the trigger for abrupt climate change reside in the ocean or in the atmosphere? Science 300, 1519-1522.

Burns, S.J., Fleitmann, D., Matter, A., Kramers, J., Al-Subbary, A.A., 2003. Indian Ocean climate and an absolute chronology over Dansgaard-Oeschger Events 9 to 13. Science 301, 1365-1367.

Claussen, M., Kubatzki, C., Brovkin, V., Ganopolski, A., 1999. Simulation of an abrupt change in Saharan vegetation in the mid-Holocene. Geophysical research letters 26, 2037-2040.

Dale, B., 1983. Dinoflagellate resting cysts: “benthic plankton”. In: Fryxell, G.A. Editor, Survival strategies of the algae, Cambridge University Press, pp 69-136.

Dale, B., 1996. Dinoflagellate cyst ecology: modeling and geological applications. In: Jansonius, J., McGregor, D.C. (Eds.), Palynology: Principles and Applications, vol. 3. American Association of Stratigraphic Palynologists Foundation, Salt Lake City, pp. 1249-1275.

Dale, B., Dale, A.L., Jansen, J.H.F., 2002. Dinoflagellate cysts as environmental indicators in surface sediments from the Congo deep-sea fan and adjacent regions. Palaeogeography, Palaeoclimatology, Palaeoecology 2893, 1 – 30.

Dansgaard, W., Johnsen, S.J., Clausen, H.B., Dahl-Jensen, D., Gundestrup, N.S., Hammer, C.U., Hvidberg, C.S., Steffensen, J.P., Sveinbjörnsdottir, A.E., Jouzel, J., Bond, G., 1993. Evidence for general instability of past climate from a 250-kyr ice-core record. Nature 364, 218-220.

deMenocal, P., 1995. Plio-Pleistocene African climate. Science 270, 53-59.

de Menocal, P., Oritz, J., Guilderson, T., Sarnthein, M., 2000. Coherent High- and low-latitude climate variability during the Holocene warm period. Science 288, 2198-2202.

de Vernal, A., Turon, J.-L., Guiot,J., 1994. Dinoflagellate cyst distribution in high latitude environments and quantitative reconstruction of sea-surface temperature, salinity and seasonality. Canadian Journal of Earth Sciences 31, 48-62.

de Vernal, A., Henry, M., Matthiens, J., Mudie, P.J., Rochon, A., Boessenkool, K.P.,Eynaud, F., Grøsfjeld, K., Guiot, J., Hamel, D., Harland, R., Head, M.J., Kunz-Pirrung, M., Levac, E., Loucheur, V., Peyron, O., Pospelova, V., Radi, T., Turon, J.-L., Voronina, E., 2001. Dinoflagellate cyst assemblages as tracers of sea-surface conditions in the Northern Atlantic, Arctic and sub-Arctic seas: the new "n=677" data base and its application for quantative paleoceanographic reconstruction. Journal of Quaternary Science 16(7), 681-698.

de Vernal, a., Eynaud, F., Henry, M., Hillaire-Marcel, c., Londeix, L., Mangin, S., Matthiessen, J., Marret, F., Radi, T., Rochon, A., Solignac, S., Turon, J.-L., 2005. Reconstruction of sea surface conditions at middle to high latitudes of the Northern hemiphere during the Last Glacial Maximum (LGM) base don dinoflagellate cyst assemblages. Quaternary science Review 4 , 897-924.

Dupont, L.M., Weinelt, M., 1996. Vegetation history of the savannah corridor between the Guinean and Congolian rain forest during the last 150,000 years. Vegetation history and Archeobotany 5, 273-292.

Dupont, L.M., 1999. Pollen and spores in marine sediments from the East Atlantic: a view from the ocean into the African continent. In: Fischer, G., Wefer, G. (Eds), Use of proxies in paleoceanography: examples from the South Atlantic. Springer, Berlin, pp. 523-546.

Dupont, L.M., Behling, H., 2006. Land-sea linkages during deglaciation: High resolution records from the eastern Atlantic off the coast of Namibia and Angola (ODP site 1078). Quaternary International 148, 19-28.

Dupont, L.M., Behling, H., Kim, J-.H., 2008. Thirty thousand years of vegetation development and climate change in Angola (Ocean drilling Program Site 1078). Climate of the Past 4, 107-124.

Fensome, R.A., taylor, F.J.R., Norris, G., Sarjeant, W.A.S., Wharton, D.I., Williams, G.L., 1993. A classification of living and fossil dinoflagellates. American Museum of Natural History. Micropaleontology Special publication number 7, pp. 1-351.

Ganopolski, A., and Rahmstorf, S., 2001. Rapid changes of glacial climate simulated in a coupled climate model. Nature 409, 153-158.

Gasse, F., 2000. Hydrological changes in the African tropics since the Last Glacial Maximum. Quaternary Science Reviews 19, 189-211.

González, C., Dupont, L.M., Behling, H., Wefer, G., 2008. Neotropical vegetation response to rapid climate changes during the last glacial: palynological evidence from the Cariaco Basin. Quaternary Research 69, 217-230.

Giresse, P., Maley, J., Brenac, P., 1994. Late Quaternary palaeoenvirenments in the Lake Barombi Mbo (West Cameroon) deduced from pollen and carbon isotopes of organic matter. Palaeogeography, Palaeoclimatology, Palaeoecology, 107: 65-78.

Harland, R., 1994. Dinoflagellate cysts from the glacial/post-glacial transition in the northeast Atlantic Ocean. Palaeontology 37, 263 – 283.

Heinrich, H., 1988. Origin and consequences of cyclic ice-rafting in the northeast Atlantic Ocean, during the past 130,000 years. Quaternary Research 29, 142-152.

Hemming, S., 2004, Heinrich events: massive late Pleistocene detritus layers of the North Atlantic and their Global Climate imprint. Review of Geophysics 42, 1-43.

Heusser, L.E., Morley, J.J., 1985. Pollen and radiolarian records from deep-sea-core RC14-103: climatic reconstructions of Northeast Japan and Northwest Pacific for the last 90,000 years. Journal of Quaternary Research 24, 60-72.

Holzwarth, U., Esper, O. and Zonneveld, K. 2007. Distribution of organic-walled dinoflagellate cysts in shelf surface sediments of the Benguela upwelling system in relationship to environmental conditions. Marine Micropaleontology 64, 91-119.

Hooghiemstra, H., Agwu C.O.C., 1986. Distribution of palynomorphs in marine sediment: a record for seasonal wind patterns over NW Africa and adjacent Atlantic. Geologische Rundschau 75, 81 - 95.

Hooghiemstra, H., Lézine, A.-M., Leroy, S.A.G., Dupont, L., Marret, F., 2006. Late Quaternary palynology in marine sediments: a synthesis of the understanding of pollen distribution patterns in the NW African setting. *Quaternary International 148*, 29-44.

Hopkins, J. A., McCarthy, F. M. G., 2002. Post-depositional palynomorph degradation in Quaternary shelf sediments: a laboratory experiment studying the effects of progressive oxidation. Palynology 26, 167-184.

Itambi A, von Dobeneck T, Mulitza S., Bickert T, Heslop D., 2008. Millennial-scale North West African droughts relates to H Events and D O Cycles: Evidence in marine sediments from off-shore Senegal. Paleoceanography, PA001570.

Jacobson, D.M., Anderson, D.M., 1986. Thecate heterotrophic dinoflagellatetes: feeding behavior and mechanisms. Journal of Phycology 22, 249-258.

Jullien, E., Grousset, F., Malaizé, B., Duprat, J., Sanchez-Goni, M.-F., Eynaud, F., Charlier, K., Schneider , R., Bory, A., Bout, V., Flores, J.-A., 2007. Low-latitude "dusty events" vs. high-latitude "icy Heinrich events". Quaternary Research 68, 379-386.

Kodrans-Nsiah, M., 2008. A natural exposure experiment on short-term species selective aerobic degradation of dinoflagellate. Review of Paleobotany and Palynology 152, 32-39.

Kokinos, J.P., Eglinton, T.I., Goni, M.A., Boon J.J., Martoglio, P.A., Anderson, D.M., 1998. Characterization of a highly resistant biomacromolecular material in the cell wall of a marine dinoflagellate resting cyst. Organic Geochemistry 28, 265-288.

Leroy, S.A.G., Dupont, A., 1994. Developpmement of vegetation and continental aridity in Northwestern Africa during the late Pliocene: the pollen record of ODP 658. Paleogeography, Paleoclimatology, Paleoecology 109, 295-316

Leuschner, D.C., and Sirocko, F., 2000. The low-latitude monsoon climate during Dansgaard-Oeschger cycles and Heinrich events. Quaternary Science Reviews 19, 243-254.

Lewis, J., Dodge, J.D., Powell, A.J., 1990. Quaternary dinoflagellate cysts from the upwelling system offshore Peru, Hole 696B, ODP Leg 112. In: Suess, E., von Huene, R., et al. (Eds.), Proceeding of the Ocean Drilling Program. Scientific results, vol. 112, pp. 323-327.

Lézine, A.M., 1998. Pollen record of past climate changes in West Africa since the Last Glacial Maximum. In: Issar, A.S., Brown, N. (Eds.), Water, environment and society in times of Climate Changes. Kluwer Academic Publishers. The Netherlands, pp. 295-317.

Lockwood, J.G., 2001. Abrupt and sudden climate transitions and fluctuations: A review. International Journal of Climatology 21, 1153-1179.

MacAyeal, D.R., 1993. Binge/Purge oscillations of the Laurentide Ice-Sheet as a cause of the North-Atlantics Heinrich Events. Paleoceanography 8, 775–784.

Maley, J., Brenac, P., 1998. Vegetation dynamics, palaeoenvironments and climatic changes in the forests of western Cameroon during the last 28,000 years B.P. Review of Palaeobotany and Palynology, 99: 157-187.

Marret, F., 1994. Distribution of dinoflagellate cysts in recent marine sediments from the east Equatorial Atlantic (Gulf of Guinea). Review of Paleobotany and Palynology 84, 1-22.

Marret, F., de Vernal, A., 1997. Dinoflagellate cyst distribution in surface sediments of the Southern Indian Ocean. Marine Micropaleontology 29, 367-392.

Marret, F., Zonneveld, K., 2003. Atlas of modern organic-walled dinoflagellate cyst distribution. Review of Palaeobotany and Palynology 125, 1-200.

Marret, F., Scourse, J.D., Versteegh, G., Jansen, J.H.F., Schneider, R., 2001. Integrated marine and terrestrial evidence for abrupt Congo River palaeodischarge fluctuations during the last deglaciation. Journal of Quaternary Science 16, 761-766.

Marret, F., Scourse, J.D., Kennedy, H., Ufkes, E., Jansen, J.H.F., 2008. Marine production in the Congo-influenced SE Atlantic over the past 30,000 years: A novel dinoflagellate cyst –based transfer function approach. Marine Micropaleontology 68, 198-222.

Matthiessen, J., de Vernal, A., Head, M.J., Okolodkov, Y.B., Zonneveld, K.A.F., Harland, R., 2005. Modern organic-walled dinoflagellate cysts in Arctic marine environments and their (paleo) environmental significance. Paläontologische Zeitschrift 79, 3-51.

McIntyre, A., Molfino, B., 1996. Forcing of Atlantic equatorial and subpollar millennial cycles by precession. Science 274, 1867-1870.

McManus, J.F.; Francois, R., Gherardi, J.-M., Keigwin, L.D., Brown-Leger, S. 2004. Collapse and rapid resumption of Atlantic meridional circulation linked to deglacial climate changes. Nature 428, 834-837.

Mulitza, S., Prange, M., Stuut, J.B., Zabel, M., von Dobeneck, T., Itambi, C.A., Nizou, J., Schulz, M., Wefer, G., 2008. Sahel Megadrought triggered by glacial slowdowns of Atlantic meridional overturning. Paleoceanography 23, PA4206.

Newell, R.E., Hsiung, J., 1987. Factors controlling free air and ocean temperature of the last 30 years and extrapolation to the past, in Aprupt climate change; evidence and implications, edited by Berger, W.H. and Labeyrie, L.D., pp. 67-87.

Nicholson, S.E., 2000. The nature of rainfall variability over Africa on time scales of decades to millenia. Global and planetary change 26, 137-158.

Nicholson, S.E., 2008. The intensity, location and structure of the tropical rainbelt over West Africa as factors in interannual variability. International Journal of Climatology, in press.

Parsons, T. R., Takahashi, M., Hargrave, B., 1984. Biological oceanographic processes, 3rd ed., Pergamon Press, Oxford, 330p.

Pospelova, V., Chmura, G.L., Boothman, W.S., Latimer, J.S., 2005. Spatial distribution of modern dinoflagellate cysts in polluted estuarine sediments from Buzzards Bay (Massachusetts, USA) embayments. Marine Ecology Progress Series 292, 23 – 40.

Pospelova, V., Pedersen, T.F., 2006. Dinoflagellate cyst evidence for Late Quaternary climate and marine productivty changes along the californian Margin. In: Poulsen, N.E. (Ed.), The International Workshop on Dinoflagellate and their Cysts: their ecology and Databese for Paleoenvironmental Reconstrutions. Geological Survey of Denmark and Greenland (GEUS), Copenhagen, Denmark, pp. 26 – 27.

Pospelova, V., de Vernal, A., Pedersen, T.F., 2008. distribution of dinoflagellate cysts in surface sediments from the northeastern Pacific Ocean (43 – 25°N) in realtion to sea-surface temperature, salinity, productivity and coastal upwelling.

Radi, T., de Vernal, A., Peyron, O., 2001. Relationships between dinocyst assemblages in surface sediments and hydrographic conditions in the Bering and Chukchi seas. Journal of Quaternary Science 16, 667-680.

Radi, T., de Vernal, A., 2004. dinocyst distribution in surface sediments from the northeastern Pacific margin (40 - 60°N) in relation to hydrographic conditions, productivity and upwelling. Review of Paleobotany and Palynology 128, 169-193.

Rahmstorf, S., 2002. Ocean circulation and climate during the past 120,000 years. Nature 419, 207-214.

Rahmstorf, J.M., Lamb, J.P., 2003. Ocean circulation and climate during the past 120,000 years. Nature 419, 207-214.

Reichart, G. J., Brinkhuis, H., 2003. Late Quaternary *Protoperidinium* cysts as indicators of paleoproductivity in the northern Arabian Sea. Marine Micropaleontology 937, 1-13.

Rial, J.A., Pielke Jr., R.A., Beniston, M., Claussen, M., Canadel, J., Cox, P., Held, H., De Noblet-Ducoudre, N., Prinn, R., Reynolds, J.F., Salas, J.D., 2004. Nonlinearities, feedbacks and critical thresholds within the Earth's climate system. Climate change 65, 11-38.

Rochon, A., de Vernal, A., Sejrup, H.-P., Haflidson, H., 1998. Palynological evidence of climatic and oceanographic changes in the North Sea during the last deglaciation. Quaternary Research 49, 197-207.

Rochon, A., de Vernal, A., Turon, J.L., Matthiessen, J., Head, M.J., 1999. Distribution of recent dinoflagellate cysts in surface sediments from the North Atlantic Ocean and adjacent seas in relation to sea-surface parameters. American Association of Stratigraphic Palynologists Foundation, 23, 1- 150.

Santarelli, A., Brinkhuis, H., Hilgen, F., Lourens, L., Versteegh, G.J.M., Visscher, H., 1998. Orbital signatures in a late Miocene dinoflagellate record from Crete (Greece). Marine Micropaleontology 33, 273-297.

Sarnthein, M., Stattegger, K., Dreger, D., Erlenkeuser, H., Grootes, R., Haupt, B., Jung, S., Kiefer, T., Kuhnt, W., Pflaumann, U., Schäfer-Neth, C., Schulz, H. Schulz, M., Seidov, D., Simstich, J., Van Kreveld, S., Vogelsang, E., Völker, A.,Weinelt, M., 2000. Fundamental Modes and abrupt changes in North Atlantic circulation and climate over the last 60 ky – Concepts, reconstruction and numerical modeling, In: Schäfer, P., Ritzrau, W., Schlüter, M., Thiede, J. (Eds). The Northern North Atlantic: A changing environment. Springer, Berlin, pp.365–410.

Schneider, R.R., Price, B., Müller, P.J., Kroon, D., Alexander, I., 1997. Monsoon related variations in Zaire (Congo) sediment load and influence of fluvial silicate supply on marine productivity in the east equatorial Atlantic during the last 200,000 years. Paleoceanography 12, 463-481.

Schnepf, E., Elbrächter, M., 1999. Dinophyte chloroplasts and phylogeny- A review. Grana 38, 81-97.

Schulz, H., von Rad., U., Erlenkeuser, H., 1998. Correlation between Arabian Sea and Greenland climate oscillations of the past 110,000 years. Nature 393, 54-57.

Stover, L.E., Brinkhuis, H., Damassa, S.P., Verteuil, L., Helby, R.J., Monteil, E., Partridge, A., Powell, A.J., Riding, J.B., Smelror, M., Williams, G.L., 1996. Mesozoic-Tertiary dinoflagellates, acritarchs and prasinophytes. In: Jansonius, J. and McGregor, D.C., (Eds), Palynology: principles and applications. Pp. 641-750, AASP Foundation, Dallas, TX.

Street-Perrott, F.A., Perrott, R.A., 1990. Abrupt climate fluctuations in the tropics: The influence of Atlantic Ocean circulation. Nature 343, 607-611.

Talbot, M.R., Johannessen, T., 1992. A high resolution paleoclimatic record of the last 27,500 years in Tropical West Africa from the carbon and nitrogen composition of lacustrine organic matter. Earth and Planetary Science Letters 110, 23-37.

Taylor, f.J.R., Pollingher, U., 1987. The ecology of dinoflagellates. In: Taylor, F.J.R. (Ed), the biology of dinoflagellates. pp. 398-529. Oxford: Blackwell Scientific Publications.

Tjallingii, R., Claussen, M., Stuut, J.B., Fohlmeister, J., Jahn, A., Bickert, T., Lamy, F., Röhl, U., 2008. Coherent high- and low-latitude control of the northwest African hydrological balance. Nature Geosciences 1, 670-675.

Traverse, A., 2007. Paleopalynology. 2nd ed. Topics in Geobiology, Vol. 28, 813p. Versteegh, G.J.M., 1997. The onset of northern hemisphere glaciations and its impact on dinoflagellate cysts and acritarchs from the Singa section (south Italy and ODP core 607 (North Atlantic). Marine Micropaleontology 30, 319-343.

Versteegh, G.J.M., Zonneveld, K.A.F., 2002. Use of selective degradation to separate preservation from productivity. Geology 30, 615 – 618.

Versteegh, G.J.M., Blokker, p., 2004. Resistant macromolecules of extant and fossil microalgae. Phycological Research 52, 1-15.

Vink, A., Zonneveld, K.A.F., Willems, H., 2000. Organic-walled dinoflagellate cysts in western equatorial Atlantic surface sediments: distributions and their relation to environment. Review of Palaeobotany and Palynology 112. 247 – 286.

Voelker, A.H.L., workshop participants, 2002. Global distribution of centennial-scale records for Marine Isotope Stage (MIS) 3: a database. Quaternary Science Reviews 21, 1185–1212.

Wall, D., Dale, B., 1967. The resting cysts of modern marine dinoflagellate cysts and their paleontological significance. Review of Palaeobotany and Palynology 2, 349-354.

Wall, D., Dale, B., Lohmann, G.P., Smith, W.K., 1977. The environmental and climatic distribution of dinoflagellate cysts in modern marine sediments from regions in the North and South Atlantic Ocean and adjacent seas. Marine Micropaleontology 2, 121-200.

Wang, Y.J., Cheng, H., Edwards, R.L., An, Z.S., Wu, J.Y., Shen, C.-C., Dorale, J.A., 2001. A high-resolution absolute-dated late Pleistocene monsoon record from Hulu Cave, China. Science 294, 2345-2348.

Zabel, M., Schneider, R., Wagner, T., Adegbie, A.T., deVries, U., Kolonic, S., 2001. Late Quaternary climate changes in Central Africa inferred from terrigenous input to the Niger fan. Quaternary Research 56, 207-217.

Zhao, M., Beveridge, N.A.S. , Shackleton, N. J., Sarnthein, M., and Eglinton, G., 1995. Molecular stratigraphy of cores off northwest Africa: Sea surface temperature history over the last 80 ka. Paleoceanography 10, 661–675.

Zonneveld, K.A.F., 1997. Dinoflagellate cysts distribution in surface sediments of the Arabian sea (Northwestern Indian Ocean) in relation to temperature and salinity gradients in the upper water column. Deep-Sea Research II 44, 1411-1443.

Zonneveld, K.A.F., Brummer, G.A., 2000. Ecological significance, transport and preservation of organic-walled dinoflagellate cysts in the Somali Basin, NW Arabian sea. Deep-sea research. Part 2,9, 2229-2256.

Zonneveld, K.A.F., Hoek, R., Brinkhuis, H. and Willems, H., 2001. Geographical distributions of organic-walled dinoflagellate cysts in surface sediments of the Benguela upwelling Region and their relationship to upper ocean conditions. Progress in Oceanography 48, 25-72.

Zonneveld, K.A.F., Mackensen, A., Baumann, K-H., 2007. Stable oxygen isotopes of *Thoracosphaera heimii* (Dinophyceae) in relationship to temperature; a culture experiment. Marine Micropaleontology 64, 80-90.

Chapter 2

Environmental setting

2.1 Regional climate

The study area encompasses the eastern tropical North Atlantic Ocean and is located at the continental margin off Senegal (western Sahel, NW Africa). Atmospheric circulation in this region is mainly controlled by the West African monsoon system which determines the amount and distribution of precipitation. The climate is tropical, characterized by intense precipitation in summer and dry conditions in winter as a result of the seasonal migration of the tropical rainbelt associated to the Intertropical Convergence Zone (ITCZ) (Figure 2.1) (Hsu and Wallace, 1976). The ITCZ is a low pressure belt that forms where the Northeast (NE) Trade Winds converge with the Southeast (SE) Trade Winds and migrates seasonally between ~ 2° and 15°N over the eastern North Atlantic Ocean and between ~ 8° and 24°N over the continent (Nicholson and Grist, 2003).

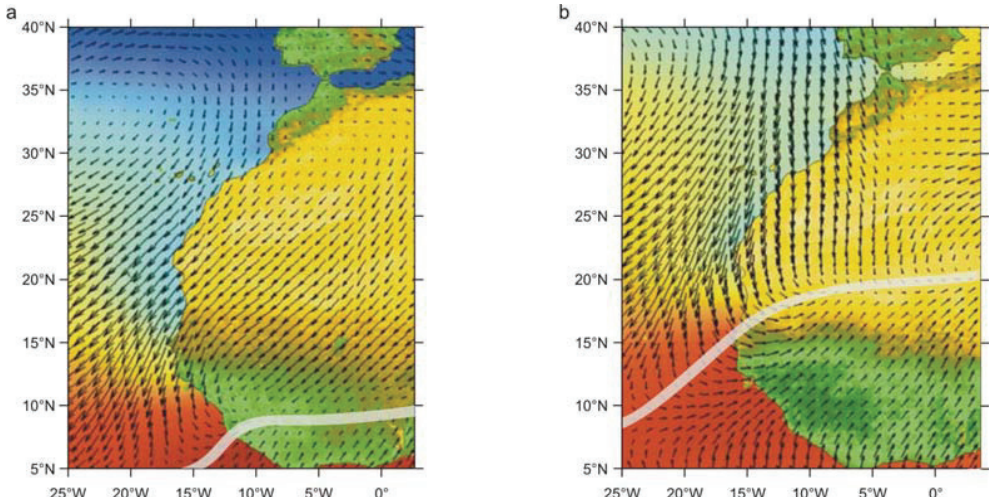

Figure 2.1 Map showing the present-day NW African surface wind systems (black arrows). a) Boreal winter conditions when the ITCZ (white zone) migrates southward. b) Summer conditions (Tjallingii, 2008).

During boreal summer, between July and September, the ITCZ reaches its northern most position bringing moist air upward (Figure 2.1). This causes water vapour to condense resulting in a band of heavy precipitation over the Sahel region as a humid

monsoon flow (Nicholson and Grist, 2003) bringing most of the 700 mm of annual rainfall (Figure 2.2). A contrasting dry season develops during the boreal winter, from December to February, when the ITCZ reaches its southern most position causing dry conditions in the study area associated with strong NE Trade Winds blowing almost parallel to the coast in a southwesterly direction.

Another major component of the atmospheric circulation in NW Africa is the Saharan Air Layer (SAL) a mid-tropospheric zonal wind system occurring at higher altitudes (1500 – 5500 m) related to the African Easterly Jet (AEJ). SAL is responsible for transporting dust and terrestrial remains such as pollen grains from the Sahara and Sahel belt to the Atlantic Ocean (Figure 2.3) (Prospero and Nees, 1986; Prospero et al., 2002; Colarco et al., 2003; Stuut et al., 2005)

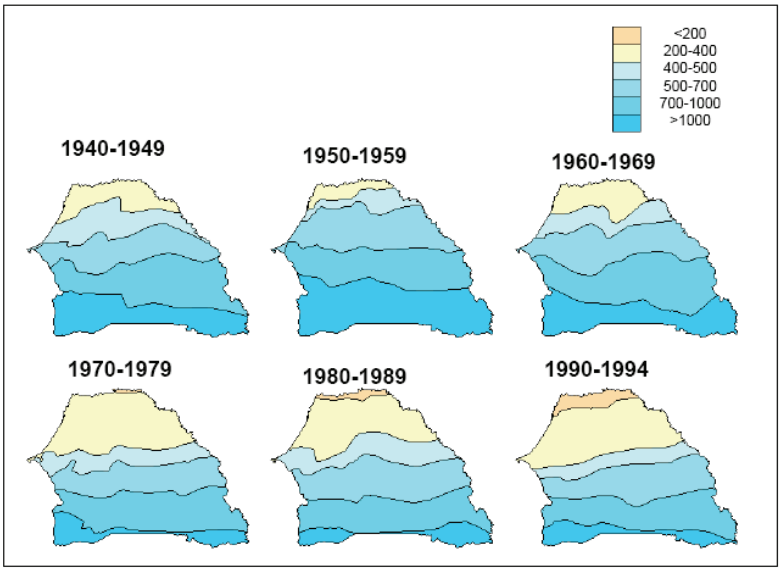

Figure 2.2 Interannual variability of rainfall (mm) in Senegal for the period 1940-1994 (Dia, 2005).

2.2 Oceanic circulation

The eastern tropical North Atlantic Ocean is influenced by several oceanic currents. The dominant surface water current is the Canary Current (CC), the easternmost branch of the Azores Current (Figure 2.3). The CC flows southwestward along the NW African coast as far south as Senegal where it turns westward at ~ 22°N to join the Atlantic North Equatorial Current (NEC) (Mittelstaedt, 1991).

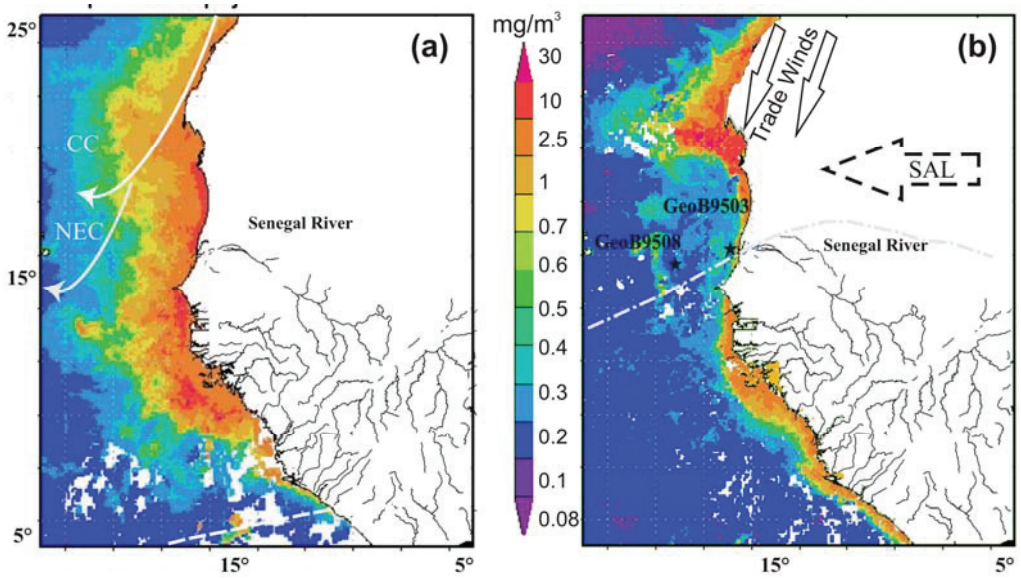

Figure 2.3 Distribution of chlorophyll-*a* concentrations (mg/m^3) averaged from the year 2005 at the sea surface in boreal winter (a) and boreal summer (b) (http://seawifs.gsfc.nasa.gov) with major surface oceanic circulation. CC: Canary Currents, NEC: North Equatorial Current, GC: Guinea Current (after Sarnthein et al., 1982 and Mittelstaedt, 1991) and main wind belts (Saharan Air Layer (SAL) and trade winds). The dash lines indicate the present-day positions of the Intertropical Convergence Zone (ITCZ).

The subtropical surface waters of the CC are underlain by the southward flowing oxygen-rich and relatively low-nutrient North Atlantic Central Water (NACW) (Siedler and Onken, 1996; Hagen, 2001) and by the northward flowing low oxygen and nutrient-rich South Atlantic Central Water (SACW) which is the main source of the upwelling water masses. Below this, the Mediterranean Outflow Water (MOW) occurs at a depth of 1700 m and is underlain by the southward flowing North Atlantic Deep Water (NADW) (Sarnthein et al., 1982; Knoll et al., 2002; Llinás et al., 2002).

Wind-induced upwelling occurs over the continental shelf when the position of the subtropical high pressure system strengthens the NE Trade Winds (Nykjaer and Van Camp, 1994). The upwelling region shifts seasonally between 20° and 32°N during boreal summer and between 10° and 25°N during boreal winter (Nykjaer and Van Camp, 1994; Santos et al., 2005) in connection with the seasonal shift of the ITCZ and the NE Trade Winds (Wefer and Fischer, 1993; Helmke et al., 2005). The water masses from the upwelling areas are transported far offshore by filaments and eddies (Johnson and Stevens, 2000) that entrain cool and nutrient-rich waters from the coast up to several hundred km offshore (Mittelstaedt, 1991). Primary productivity reaches

its maximum in surface waters off NW Africa during the upwelling season which supports a vigorous phytoplankton growth near the surface mainly dominated by diatoms, coccolitophores (Nave et al., 2001), dinoflagellates (Margalef, 1973) and planktonic foraminifera (Meggers et al., 2002) that are responsible for the biomass production.

2.3 Senegal River

The 1790 km-long Senegal River is one of the largest rivers and the most active drainage systems of West Africa. The total area of the Senegal River basin is ~ 419,650 km^2 (World Resources Institute, 2003). The annual sediment load delivered to the Atlantic Ocean is ~$2x10^9$kg (Gac and Kane, 1986) and the average water discharge at the last downstream point immediately landward of the estuary is ~641 m^3/s. The Senegal River source is located in the Fouta Djalon region where the mean annual rainfall reaches 1780 mm and its mouth area lies in the Sahel region between a dry Saharan climate in the North and wet subequatorial climate in the South. The River's flow regime is characterized by a high-water season from July to October with a peak flow generally occurring in late September and early October due to the boreal summer monsoon rain. The water discharge during this season is ~1370 m^3/s and the sediment suspended load is >200 mg/l (Gac and Kane, 1986). In contrast, during the boreal arid winter from November to June, the water discharge of the Senegal River decreases to ~120 m^3/s, as well as the sediment suspended load that does not exceed ~10 mg/l (Gac and Kane, 1986). The low flow regime of the Senegal River during dry season allows seawater to penetrate the reduced river bed over a distance of ~250 km inland (Gac et al., 1985).

2.4 Regional vegetation and pollen sources

The most important overall factor in determining the vegetation structure in tropical NW Africa is climate (the mean annual rainfall and the length of dry season) although local conditions such as soils and water availability are also important (White, 1983). The main vegetation belts reflect the North-South precipitation gradient (Figure 2.4) encompassing the steppes of the semi-desert area of the western Atlas region, desert vegetation of the Sahara, semi-desert grassland and shrubland of

Sahelian (dry savannah) vegetation, and the Sudanian savannah zone as well as the tropical rainforest along the Gulf of Guinea (White, 1983).

In the arid Sahara desert, where the mean annual rainfall does not exceed 150 mm, vegetation is rare and consists mainly of herbaceous steppe formations or shrubs according to the nature of the soil. Sandy regions are mainly dominated by grass (Poaceae) formation (e.g. *Stipagrostis pungens* association), whereas species of *Acacia* are the dominant trees of the rocky slopes with *Acacia tortilis* the most common, along with *A. ehrenbergiana*. *Acacia* is locally associated with other tree species including *Maerua crassifolia*, *Balanites aegyptiaca*, *Capparis decidua*, *Salvadora persica*, *Ziziphus mauritania* and desert shrubs such as *Panicum turgidum*, *Cassia italica*, *Caylusea hexagyna* (White, 1983). Along arid coastline, hypersaline conditions develop in marshes or shallow lakes when the water evaporates causing the formation of salt crusts over wide areas known as "Sebkha" where scattered drought and salt resistant herbaceous plants occur (e.g. Chenopodiaceae, Amaranthaceae, *Salsola baryosma*, *Suaeda vermiculata*, *Zygophyllum cornutum*, *Tamarix sp*.) (Naegelé, 1958; Assémien, 1971).

The semi-desert grassland and shrubland of Sahelian (dry savannah) vegetation develop in the transition zone between the Sahara desert and Sahel, where the annual rainfall ranges from 150 to 500 mm. Common shrub species are *Grewia bicolor*, *Adansonia digitata*, *Combretum micranthum*, *Combretum glutinosum*, *Dichrostachys cinerea*, *Acacia ataxacantha*, *A. macrostachya*, *Sclerocarya birrea*, *Celtis integrifolia*, *Lannea acida*, *Sterculia setigera* (Trochain, 1940).

Woodland and Sudanian savannah occupy the region where annual rainfall ranges between 500 and 1000 mm. Vegetation associations are mainly dominated by Mimosaceae and Combretaceae associated with *Oxytenanthera abyssinica*, *Daniellia oliveri*, *Detarium microcarpum*, *Syzygium guineense*, *Prosopis africana*, *Piliostigma thonningii*, *Nauclea latifolia*, *Borassus aethiopium*, *Hymenocardia acida*, *Bridelia ferruginea*. Xerophytic species are mostly dominated by *Balanites aegyptiaca*, *Grewia bicolor*, *Boscia senegalensis*, *Acacia senegal*, *Commiphora africana*.

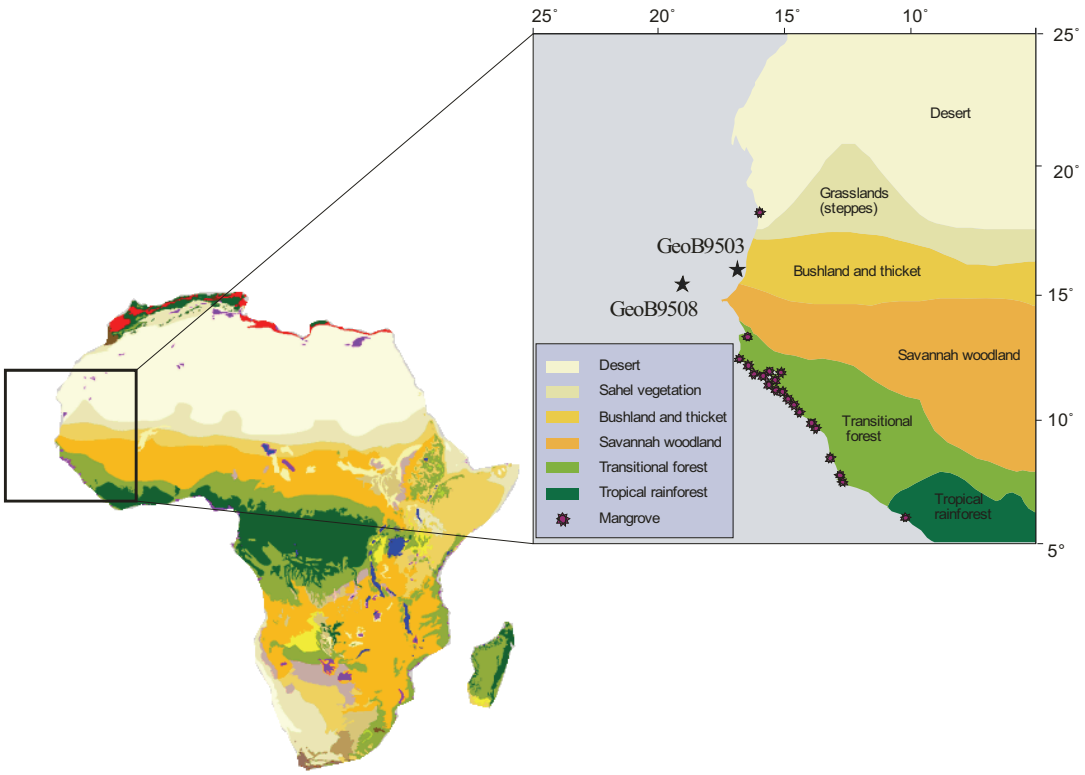

Figure 2.4 Simplified phytogeography and biomes in NW Africa (after White 1983).

Gallery forests that occur along the Gulf of Guinea where the mean annual rainfall exceeds 1000 mm are dominated by *Elaeis guineensis* and *Lophira alata*. The Guinean vegetation located in gallery forests is dominated mostly by *Anthostema senegalense*, *Antiaris africana*, *Anthocleista frezoulsii*, *Dialium guineense*, *Pseudospondias microcarpa*, *Alchornea cordifolia* (Trochain, 1940; White, 1983).

Mangrove stands of *Rhizophora racemosa*, *R. mangle*, *R. harrisonii*, *Avicennia nitida*, *Laguncularia racemosa* and *Conocarpus erectus* mostly dominate the littoral vegetation in estuaries and near the River mouths of Casamance, Gambia, Saloum and Senegal (Spalding et al., 1997) and of which the distribution depends on the increasing salinity gradient. Mangroves are usually associated with Poaceae (e.g. *Sesuvium portulacastrum*, *Philoxerus vermicularis*), Cypercaeae (e.g. *Cyperus*) and *Thypha*.

In the NW African region, aeolian transport of pollen is mainly dependent on the two dominating wind systems, the NE trade winds and the SAL (Hooghiemstra and

Agwu, 1986; Hooghiemstra et al., 2006). The Senegal River, on the other hand, is the most important fluvial source of pollen and other terrestrial remains in the study area.

References

Assémien, P., 1971. Etude comparative de flores actuelles et quaternaires récentes de quelques paysages végétaux de l'Afrique de l'Ouest. PhD thesis, University of Abidjan, 257p.

Colarco, P.R., Toon, O.B., Reid, J.S., Livingston, J.M., Russel, P.B., Redmann, J., nSchmid, B., Maring, H.B., Savoie, D., Welton, E.J., Campbell, J.R., Holben, B.N., Levy, R., 2003. Saharan dust transport to the Caribbean during PRIDE: 2. Transport, vertical profiles and deposition in simulations of in situ and remote sensing observations. Journal of Geophysical Research 103, 8590.

Dia, A.M., 2005. Climate variability in the Senegal River valley: Mapping flood extension with satellite images and GIS tools. PhD thesis, university of Dakar.

Gac, J.Y., Kane, A., Saos, J.L., Carn, M., Villeneuve, J.F., 1985. L'invasion marine dans la basse vallée du fleuve Sénégal. –Dakar-Hann : ORSTOM, 64 p.

Gac, J.Y., Kane, A., 1986. Le fleuve Sénégal : Bilan hydrologique et flux continentaux de matières particulaires à l'embouchure. Sciences géologique bulletin 39, 1, p. 99-130. Strasbourg.

Hagen, E., 2001. Northwest African upwelling scenario. Oceanologica Acta 24, 113-128.

Helmke, P., Romero, O., Fischer, G., 2005. Northwest African upwelling and its effect on offshore organic carbon export to the deep sea. Global Biogeochemical Cycles 19, GB4015, doi:10.1029/2004GB002265.

Hooghiemstra, H., Agwu C.O.C., 1986. Distribution of palynomorphs in marine sediment: a record for seasonal wind patterns over NW Africa and adjacent Atlantic. Geologische Rundschau 75, 81 - 95.

Hooghiemstra, H., Lézine, A.-M., Leroy, S.A.G., Dupont, L., Marret, F., 2006. Late Quaternary palynology in marine sediments: a synthesis of the understanding of pollen distribution patterns in the NW African setting. *Quaternary International 148*, 29-44.

Hsu, C.P.F., Wallace, J.M., 1976. The global distribution in annual and semiannual cycles in precipitation. Monthly Weather Review 104(9), 1093-1101.

Knoll, M., Hernández-Guerra, A., Lenz, B., Laatzen, F.L., Machin, F., Müller, T.J., Siedler, G., 2002. The Eastern Boundary Current system between the Canary Islands and the African coast. Deep Sea Research Part II 49, 3427-3440.

Llinás, O., Rueda, M.J., Marrero, J.P., Pérez-Martell, E., Santana, r., Villagarcia, M.G., Cianca, A., Godoy, J., Maroto, L., 2002., Variability of the Antarctic intermediate waters in the Northern canary box. Deep Sea Research Part II 49, 3441-3453.

Margalef, R., 1973. Assessment of the effects on plankton, p.301-306. In E.A. Pearson and E. De Farja Fragipane (eds.), marine pollution and marine waste disposal proceedings of the 2nd International Congress, san Remo, 17-21 December 1973.

Meggers, H., Freudenthal, T., Nave, S., Targarona, J., Abrantes, F., Helmke, P. 2002. Assessment of geochemical and micropaleontological sedimentary parameters as proxies of surface water properties in the Canary Islands region. Deep Sea Research II 49, 3631-3654.

Mittelstaedt, E., 1991. The ocean boundary along the northwest African coast: Circulation and oceanographic properties at the sea surface. Progress in Oceanography 26, 307-355.

Naegelé, A., 1958. Contribution à l'étude de la flore et des groupements végétaux de la Mauritanie. In : note sur quelques plantes récoltées à Chinguetti (Adrar Tmar). Bulletin institut fondamental d'Afrique noire.

Nave, S., Freitas, P., Abrantes, F., 2001. Coastal upwelling in the Canary Island region: spatial variability reflected by the surface sediment diatom record. Marine Micropaleontology 42, 1-23.

Nicholson, S.E., Grist, J.P., 2003. The seasonal evolution of the atmospheric circulation over West Africa and Equatorial Africa. Journal of Climate 16 (7), 1013-1030.

Nykjaer, L., Van Camp, L., 1994. Seasonal and interannual variability of coastal upwelling along Northwest Africa and Portugal from 1981 to 1991. Journal of Geophysical Research 99, 14197-14207.

Prospero, J.M., Nees, R.T., 1986. Impact of the North African drought and El Nino on mineral dust in the Barbados trade winds. Nature 320, 735-738.

Prospero, J.M., Ginoux, P., Torres, O., Nicholson, S.E., Gill, T.E., 2002. Environmental characterization of global sources of atmospheric soil dust identified with the nimbus 7 total zone mapping spectrometer (TOMS) absorbing aerosol product. Review of Geophysics 40, 2-1/ 2-31.

Santos, M.A., Kazmin, A.S., Peliz, A., 2005. Decadal changes in the canary upwelling system as revealed by satellite observations: Their impact on productivity. Journal of Marine Research 63, 359 – 379.

Sarnthein, M., Thiede, J., Pflaumann, U., Erlenkeuser, H., Fütterer, D., Koopmann, B., Lange, H.E.S., 1982. Atmospheric and oceanic circulation patterns off Northwest Africa during the past 25 million years. *In* Von Rad, U., Hinz, K., Sarnthein, M., Seibold, E. (Eds), Geology of the Northwest African continental margin. Springer, Berlin, pp. 584-604.

Siedler, G., Onken, R., 1996. Eastern recirculation. In "The warmwatersphere of the North Alantic Ocean" (W. Krauss, Ed.), pp. 339-364. Gebrücher Bornträger, Berlin Stuttgart.

Spalding, M., Blasco, F., Field, C., 1997. World mangrove Atlas. The International Society for mangrove Ecosystems (ISME), Smith Settle, Otley, UK: 178p.

Stuut, J-B., Zabel, M., Ratmeyer, V., Helmke, P., Schefuß, E., 2005. Provenance of present-day eolian dust collected off NW Africa. Journal of Geophysical Research 110, 4202 – 5161.

Tjallingii, R., Claussen, M., Stuut, J.B., Fohlmeister, J., Jahn, A., Bickert, T., Lamy, F., Röhl, U., 2008. Coherent high- and low-latitude control of the northwest African hydrological balance. Nature Geosciences 1, 670-675.

Trochain, J., 1940. Contibution à l'étude de la vegetation du Sénégal. Paris: Larose, 433p., 30 planches.

Wefer, G., Fischer, G., 1993. Seasonal patterns of vertical particle flux in equatorial and coastal upwelling areas of the eastern Atlantic. Deep Sea Research Part I: Oceanographic research papers 40, 1613-1645.

White, F., 1983. The vegetation of Africa. UNESCO, Paris, 384 pp.

World Resources Institute, 2003. http://www.wri.org/

Chapter 3

Material and methods

3.1 Marine sediment samples

The marine sediment samples examined in this thesis were taken during R/V *Meteor* cruise M65-1 in June 2005 (Mulitza et al., 2006).

37 surface samples were collected from the first upper centimeter of multicores that were recovered from water depths ranging between 10 and 4000 m off West Africa extending from ~ 17° to 8°N.

Marine sediment core GeoB9503-5 was recovered from the Senegal mud-belt off the Senegal River mouth at approximately 50 meters water depth (16°03.99'N, 16°39.15'W). The total length of the recovered core was 791 cm consisting of homogenous dark olive green mud with few carbonated shell fragments (Mulitza et al., 2006).

Marine sediment core GeoB9508-5 was recovered from the continental slope off Northern Senegal, west of the Senegal River mouth from a water depth of ~ 2384 meters (15°29.90'N, 17°56.88'W). The 965 cm-long core consists of homogenous olive green muddy sediments with very few shell fragments (Mulitza et al., 2006).

3.2 Radiocarbon dating

The most common dating tool for the study of late Quaternary climatic and oceanic fluctuations is radiocarbon dating. This radiometric dating method uses the radioisotope carbon-14 (^{14}C) to determine the age of carbonaceous material in samples of peat, paleosols, bone, shell, marine and lacustrine sediments, corals…etc, up to about 50,000 years. Because oceanic circulation prompts the mixing of the ^{14}C-depleted waters with modern waters, the radiocarbon dated marine sediment samples must be corrected for the reservoir effect. Franke et al. (2008) shows a temporal reservoir-age variation raging between ~300 years in parts of the subtropics and ~1000 years in the Southern Ocean. To estimate the effect of reservoir-age on our

radiocarbon dating we used the constant reservoir correction of ~ 400 years (Bard, 1988; Bard et al., 2000).

Additionally, it's well known that atmospheric ^{14}C concentration levels were not constant and have varied through time resulting in the variations of the radiocarbon production rates, variations in the rate of exchange of radiocarbon between various geochemical reservoirs, and variations in the total amount of CO_2 in the atmosphere, biosphere and hydrosphere (Damon et al., 1978). Therefore, ^{14}C ages have to be calibrated in order to convert them to calendar ages.

3.3 Palynological processing

Samples for palynological investigations were prepared according to standard laboratory procedures (Faegri and Iversen, 1989). Oxidative steps (e.g. acetolysis) were excluded in order to avoid degradation of organic-walled dinoflagellates (Figure 3.1). A known volume of 1 to 2 cm^3 of wet sediments was oven-dried for 24h and subsequently weighed and decalcified using 10% hydrochloric acid (HCl). One tablet of exotic *Lycopodium* spores was added to each sample during the decalcification process in order to calculate palynomorph concentrations and accumulation rates.

The siliceous fraction was dissolved using 40% hydrofluoric acid (HF). Samples were agitated for 2 hours and left in the HF solution for one day without agitation. The resulting fraction was treated with 30% HCl for ca. 24h to remove fluorosilicates. Subsequently the solution was decanted and demineralised water was added to the samples. We neutralize the supernatant solution with 10% KOH prior to disposal. Finally, demineralised water was added to the samples and after 24 h the residual was washed and sieved over a 8 µm mesh size sieve using an ultrasonic bath to disintegrate lumps of organic matter.

The residue was concentrated by centrifuging for 8 minutes at 3500 rotations per minute and resuspended in 1 ml water. An aliquot of 40 to 60 µl was mounted in a gelatine-glycerine medium for investigation under the microscope.

Palynomorphs were counted up to 200 pollen grains including those of herbs, shrubs, trees and aquatics and 300 organic-walled dinoflagellate cysts (hereafter dinocysts) where possible. Besides dinocysts and pollen other microfossils such as fern spores, plant cuticles, fresh water algae (*Botryococcus*, *Cosmarium*, *Pediastrum*, *Scenedesmus* and *Staurastrum*), eggs and remains of copepods, organic-walled linings of foraminifera and fungal spores were counted as well but not included in the sum on which the percentage calculation is based.

Main dinocyst types were identified based on published morphological descriptions (de Vernal et al., 1997; Zonneveld, 1997; Pospelova and Head, 2002; Fensome and Williams 2004). Pollen grains were identified using the African Pollen Database (Vincens et al., 2007) and Pollens des savanes d'Afrique orientale (Bonnefille and Riollet, 1980).

Palynological results are expressed as percentages of the total palynomorph sums, as palynomorph concentrations and as palynomorph accumulation rates (flux). Pollen counts are expressed as percentages of total pollen (including pollen of trees shrubs, herbs, and aquatics), spores are expressed as percentages of total pollen and spores, and dinocyst counts are expressed as percentages of total cysts.

Palynomorph concentrations were calculated according to the equation:

$$C_1 = (N \times L) / (l \times v) \qquad (1)$$

$$C_2 = (N \times L) / (l \times wg) \qquad (2)$$

Where

C_1: Palynomorph concentration (### / cm^3)

C2: Palynomorph concentration (### / g)

N: Palynomorph counts

L: Lycopodium spores added

l: Lycopodium spores counted

v: Original volume of sediment in cm^3

wg: dry weight in gram.

Similarly, The total accumulation rates or palynomorph flux are expressed as numbers of individuals per cm^2 per year (### / cm^2 / yr) using bulk sediment accumulation rates. This relation can be described by the following equation:

$$AR = C_1 \times SR \qquad (3)$$

Where

AR: palynomorph total accumulation rate (flux) (### /cm^2 / yr).

C_1: Palynomorph concentration (### / cm^3)

SR: sedimentation rates (cm / yr)

3.4 Statistical methods

The multivariate ordination techniques Detrended Correspondence Analysis (DCA), Principal Component Analysis (PCA) and Canonical Correspondence Analysis (CCA) were performed on the relative abundances of dinocysts to quantify trends in their distributions (ter Braak and Smilauer, 1998). These calculations were performed with CANOCO for windows version 4.

An initial DCA analysis is performed to test the unimodal or linear character of the dataset. The variation represented by DCA axis is explained as caused by one or more environmental parameters. The perpendicular projection of species and samples point to an axis represents the respective optimum of abundance. This position is given in units of standard deviations (sd). If the length of the first axis is more than 2 sd, we assume the unimodal response of species abundance to environmental parameters. With a PCA, we can relate the variations of environmental parameters and their influence upon dinocyst species. It's a method of ordination which yields projections according to a limited number of orthogonal axes (Principal Components) in order to establish an "ecological grouping" of dinocyst species that may be related to particular environmental conditions.

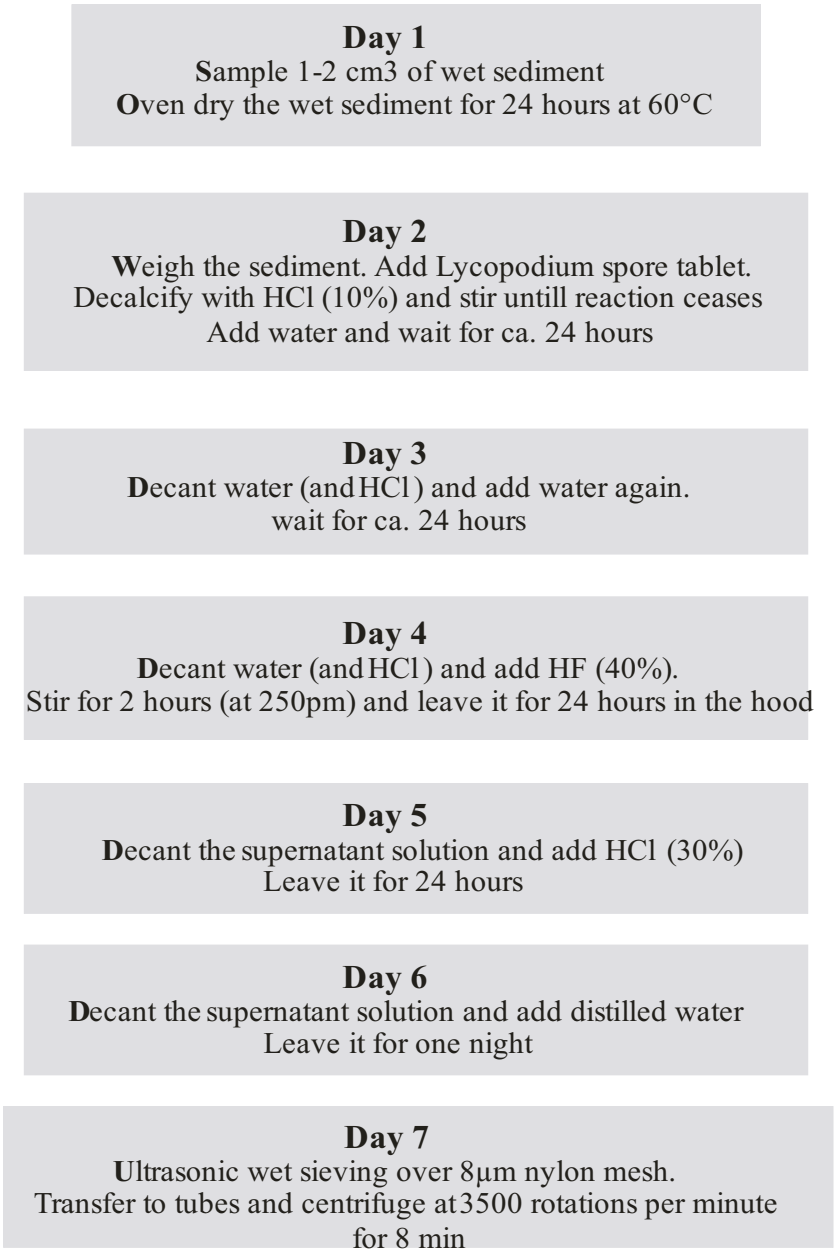

Figure 3.1 Schematic representation of the palynological preparation.

CCA is used to obtain information about the relationship between the variance of selected environmental variables in the water column and relative abundances of dinocyst species. The length of an arrow indicates the length of the gradient. We assume that a species is strongly correlated with an environmental parameter when it is situated near to the tip of this parameter arrow. The optimum of that species is estimated by the perpendicular projection on the variable arrow (ter Braak and Smilauer, 1998).

References

Bard, E., 1988. Correction of accelerator mass spectrometry ^{14}C ages measured in planktonic foraminifera: Paleoceanographic implications. Paleoceanography 6, 635-645.

Bard, E., Rostek, F., Turon, J.L., Gendreau, S., 2000. Hydrological impact of Heinrich events in the subtropical Northeast Atlantic. Science 289, 1321-1324.

Bonnefille, R., Riollet, G. 1980. Pollens des Savanes d´Afrique Orientale. Edition de CNRS, Paris, 140 pp., 113pl.

Damon, P.E., Lerman, J.C., Long, A., 1978. Temporal fluctuations of atmospheric ^{14}C: causal factors and implications. Annual review of Earth and Planetary Science 6, 457-494.

de Vernal, A., Rochon,A., Turon, J-L., Matthiessen, J., 1997., Organic-walled dinoflagellate cysts: palynological tracers of sea-surface conditions in middle to high latitude marine environments. Geobios 30, 905-920.

Faegri, K., Iversen, J., 1989. "Textbook of pollen analysis". IV Edition by Faegri, K., Kaland, P.E., Krzywinski, K.Wiley, New York.

Fensome, R.A., Williams, G.L., 2004. The Lentin and Williams index of fossil dinoflagellate, 2004 Edition. American Association of Stratigraphic Palynologist Foundation contributions series 42. 909 pp.

Franke, J., Paul, A., Schulz, M., 2008. Modelling variations of marine reservoir ages during the last 45 000 years. Climate of the Past 4, 125-136.

Mulitza, S., Bouimetarhan, I., Brüning, M., Freesemann, A., Gussone, N., Filipsson, H., Heil, G., Hessler, S., Jaeschke, A., Johnstone, H., Klann, M., Klein, F., Küster, K., März, C., McGregor, H., Minning, M., Müller, H., Ochsenhirt, W.T., Paul, A., Scewe, F., Schulz, M., Steinlöchner, J., Stuut, J.B., Tjallingii, R., Dobeneck, T., Wiesmaier, S., Zabel, M. and Zonneveld, K., 2006. Report and preliminary results of Meteor cruise M65/1, Dakar – Dakar, 11.06.–01.07.2005. Berichte, Fachbereich Geowissenschaften, Universität Bremen, No. 252, 149 pp.

Pospelova, V., Head, M.J., 2002. Islandinium brevispinosum sp. Nov. (Dinoflagellata), a new species of organic-walled dinoflagellate cyst from modern estuarine sediments of New England (USA). Journal of Phycology 38, 593 – 601.

ter Braak, C.J.F., Smilauer, P., 1998. Canoco 4. Centre for Biometry. Wageningen. Vincens, A., Lezine, A.M., Buchet, G., Lewden, D. and le Thomas, A., 2007.

African pollen data base inventory of tree and shrub pollen types. Review of Palaeobotany and Palynology 145, 135 – 141.

Zonneveld, K.A.F., 1997. New species of organic walled dinoflagellate cysts from modern sediments of the Arabian Sea (Indian Ocean). Review of Palaeobotany and Palynology, 97, 319-337.

Chapter 4

Dinoflagellate cyst distribution in marine surface sediments off West Africa (17 – 6°N) in relation to sea-surface conditions, freshwater input and seasonal coastal upwelling

Ilham Bouimetarhan *[1,3], Fabienne Marret [2], Lydie Dupont [3], Karin Zonneveld [1,3]

[1] Department of Geosciences, University of Bremen, Klagenfurter Strasse, D-28359 Bremen, Germany

[2] Department of Geography, University of Liverpool, L69 7ZT Liverpool, UK

[3] MARUM - Center for Marine Environmental Sciences, University of Bremen, Leobener Strasse, D-28359 Bremen, Germany

Accepted for publication in Marine Micropaleontology

Abstract

An organic-walled dinoflagellate cyst analysis was carried out on 53 surface sediment samples from West Africa (17 – 6°N) to obtain insight in the relationship between their spatial distribution and hydrological conditions in the upper water column as well as marine productivity in the study area.

Multivariate analysis of the dinoflagellate cyst relative abundances and environmental parameters of the water column shows that sea-surface temperature, salinity, marine productivity and bottom water oxygen are the factors that relate significantly to the distribution patterns of individual species in the region.

The composition of cyst assemblages and dinoflagellate cyst concentrations allows the identification of four hydrographic regimes; 1) the northern regime between 17 and 14°N characterized by high productivity associated with seasonal coastal upwelling, 2) the southern regime between 12 and 6°N associated with high-nutrient waters influenced by river discharge 3) the intermediate regime between 14 and 12°N influenced mainly by seasonal coastal upwelling additionally associated with fluvial input of terrestrial nutrients and 4) the low productivity regime characterized by low chlorophyll-*a* concentrations in upper waters and high bottom water oxygen concentrations.

Our data show that cysts of *Polykrikos kofoidii*, *Selenopemphix quanta*, *Dubridinium* spp., *Echinidinium* species and cysts of *Protoperidinium monospinum* are the best proxies to reconstruct the boundary between the NE trade winds and the monsoon winds in the subtropical eastern Atlantic Ocean. The association of *Bitectatodinium spongium*, *Lejeunecysta oliva*, *Quinquecuspis concreta*, *Selenopemphix nephroides*, *and Trinovantedinium applanatum* can be used to reconstruct past river outflow variations within this region.

***Keywords**:* organic-walled dinoflagellate cysts, West Africa, marine surface sediments, sea-surface conditions, upwelling, and river discharge.

4.1 Introduction

The West African region is considered to be one of the most ecologically vulnerable areas on the planet due to the alternation of arid and humid phases associated with weakening and strengthening of the African monsoon circulation that occur on both short - and long - time scales (Gasse, 2000; Nicholson, 2000). The main hypothesis proposed for the cause of this climatic variability invokes a close relationship between changes in African precipitation and changes in ocean surface conditions particularly sea-surface temperature (Folland et al., 1986; Lamb et al., 1995; Schefuß et al., 2005; Weldeab et al., 2005).

The combined study of terrestrial palynomorphs (pollen and spores) and organic-walled dinoflagellate cysts (dinocysts) from the same samples potentially enables the recognition of simultaneous changes in both oceanic and atmospheric mechanisms. Terrestrial palynomorphs (pollen and spores) are used to assess vegetation changes on the adjacent continent and operating transport agents (mainly wind belts and river discharge). Dinocyst associations in marine sediments can be related to environmental conditions in surface waters such as nutrient availability, turbulence, freshwater discharge, sea-surface temperature and salinity (e.g. de Vernal et al., 1994; Dale, 1996). Consequently, they have become a valuable tool for paleoenvironmental and paleoceanographic reconstructions particularly in neritic high productive environments where the microbial degradation of the organic matter causes carbonate dissolution restricting the use of calcareous proxies (Lewis et al., 1990; de Vernal et al., 1994; Harland, 1994; Marret 1994; Dale, 1996; Versteegh, 1997; Zonneveld, 1997; Rochon et al., 1998; Santarelli et al., 1998; de Vernal et al., 2001).

Although studies of dinocyst distributions in marine surface sediments are increasing, the modern dinocyst distribution off West Africa still remains poorly documented (Marret, 1994; Rochon et al., 1999; Marret and de Vernal, 1997; Zonneveld and Brummer, 2000; Zonneveld et al., 2001; Radi et al., 2001; Dale et al., 2002; Marret and Zonneveld, 2003; Radi and de Vernal, 2004; Pospelova et al., 2005, 2006, 2008; Holzwarth et al., 2007). Better and more detailed knowledge about the distribution of dinocysts in marine surface sediments and their relation to environmental parameters have the potential to document changes in ocean

conditions that play an important role in the adjacent continental climate such as atmospheric circulation and river discharge fluctuations.

We present here a detailed study of modern dinocysts in marine surface sediments off West Africa in the subtropical eastern Atlantic Ocean between 17 and 6°N. We relate their spatial distribution to the environmental parameters in the upper water column in order to examine to which extent we can use dinocysts as environmental indicators and to explore which species or combination of species provide the best information about changes in environmental conditions. In this paper, we present the first detailed distribution maps of dinocysts in this region that will serve as a basis for dinocyst based paleoceanographic and paleoenvironmental reconstructions.

4.2 Regional setting

The studied area is located in the subtropical East Atlantic Ocean off West Africa extending from 17 to 6°N (Figure 4.1). Atmospheric circulation in this region is mainly controlled by the West African monsoon characterized by intense precipitation in summer and dry conditions in winter as a result of the seasonal migration of the Intertropical Convergence Zone (ITCZ) (Hsu and Wallace, 1976).

The ITCZ migrates between about 2 and 12°N over the eastern Atlantic Ocean and 8 and 24°N over the continent. Its northern position from July to September is some ten degrees of latitude north of the summer rainfall maximum forming the tropical rainbelt which brings moist monsoon air to West Africa. Its southern position from December to February produces dry conditions associated with hot and dry continental northeastern (NE) trade winds blowing sub-parallel to the West African coast (Nicholson and Grist, 2003). The NE trade winds cause an offshore movement of the surface water masses that result in coastal upwelling.

Another major component of the atmospheric circulation is the Saharan Air Layer (SAL) related to the African Easterly Jet (AEJ), a mid-tropospheric zonal wind system occurring at higher altitudes (1500 – 5500 m). SAL is responsible for transporting dust and terrestrial remains such as pollen grains from the Sahara and Sahel belt to the Atlantic Ocean (Prospero and Nees, 1986; Prospero et al., 2002; Colarco et al., 2003; Stuut et al., 2005) (Figure 4.1).

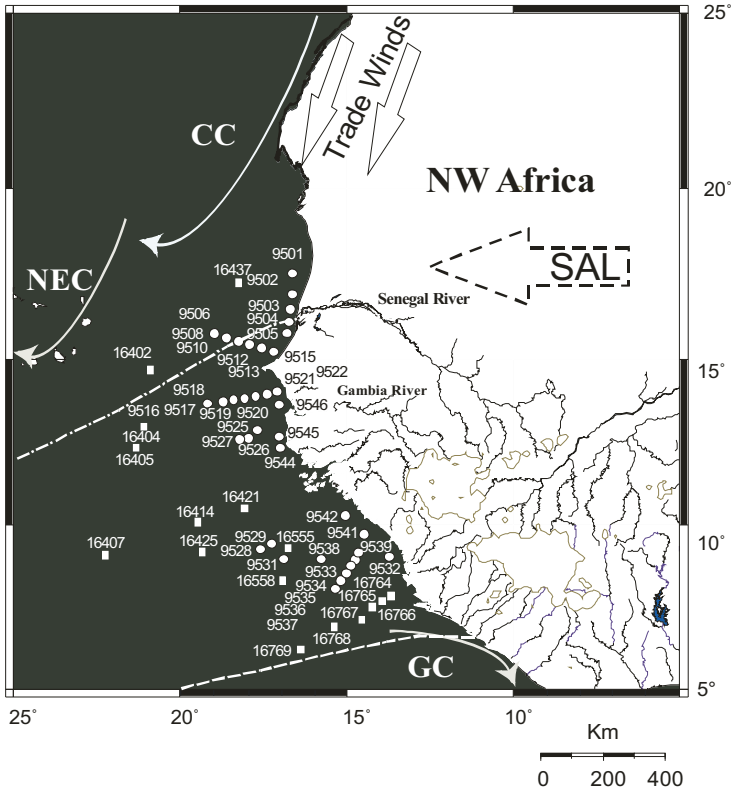

Figure 4.1 Major hydrographic systems with main wind belts (Saharan Air Layer (SAL) and trade winds) and surface oceanic circulation. CC: Canary Currents, NEC: North Equatorial Current, GC: Guinea Current (after Sarnthein et al., 1982 and Mittelstaedt, 1991). White circles denote the location of the 37 GeoB surface sediment samples and white rectangles show the location of the 16 additional GIK samples from Marret and Zonneveld (2003). The dash lines indicate the present day boreal summer (dash-dotted line) and boreal winter (dash line) positions of the Intertropical Convergence Zone (ITCZ).

The hydrology off West Africa is controlled by several oceanic currents (Figure 4.1) that are influenced by the prevailing wind systems. The dominant surface water current is the Canary Current (CC), the easternmost branch of the Azores Current. The CC flows southwestward along the north western African coast as far south as Senegal where it turns westward to join the Atlantic North Equatorial Current (Sarnthein et al., 1982; Mittelstaedt, 1991). The CC is associated with winter upwelling between 20 and 12°N (Nykjaer and Van Camp, 1994; Santos et al., 2005). Primary productivity reaches its maximum during the upwelling season and the phytoplankton community is mainly dominated by diatoms, coccolitophores and dinoflagellates (Nave et al., 2001).

The coastal region of the investigated area has an important network of river drainage basins. The 1790 km-long Senegal River is one of the most active drainage

systems of West Africa (Figure 4.1). The next major river in the northern part of the study area is the 1130 km long Gambia River, followed by the Saloume and Casamance River (World Resources Institute, 2003). Rio Cacheu (Farim), Rio Mansoa, Rio Geba, Rio Corubal, Rio Tombali and Kogon River are the main river systems in the southern part.

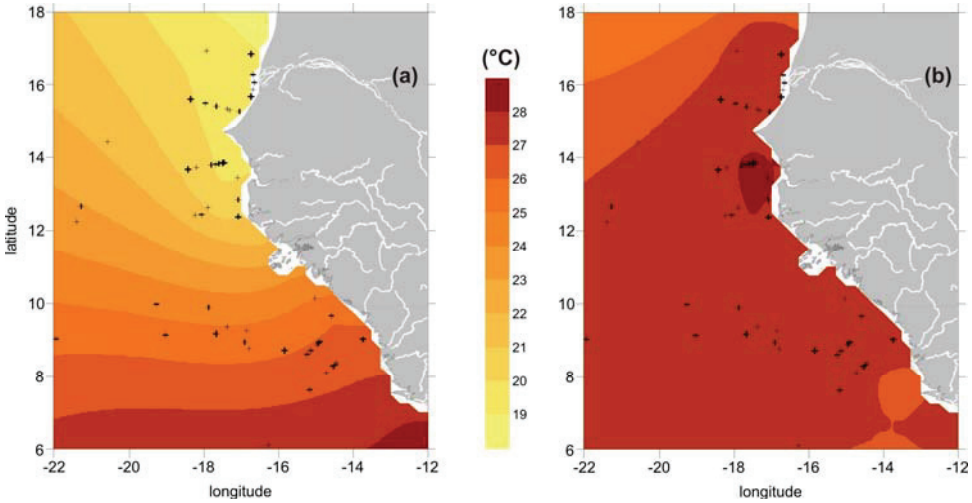

Figure 4.2 Distribution of sea-surface temperature in boreal winter (a) and boreal summer (b). (WOA, 2005)

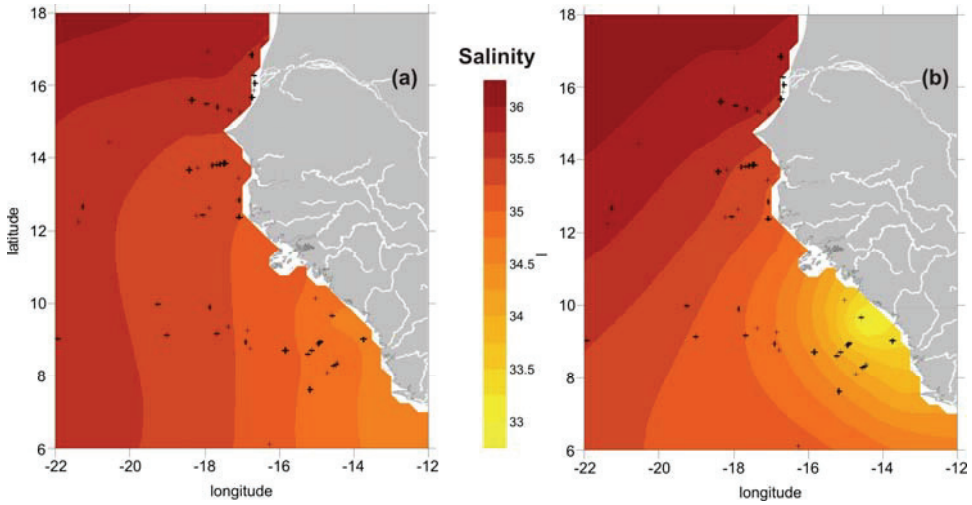

Figure 4.3 Distribution of sea-surface salinity in boreal winter (a) and boreal summer (b). (WOA, 2005)

According to the World Ocean Atlas (WOA), 2005, sea-surface temperature (SST) ranges between 19 and 26 °C in winter and between 26 and 29 °C in summer with an increasing north to south gradient in the investigated area (Figure 4.2). Sea-surface

salinity (SSS) fluctuates between 34 and 36 psu in winter and between 32 and 36 psu during the summer (Figure 4.3).

Satellite images of the chlorophyll-*a* concentrations of the sea surface show a general maximum of about 2.5 to 10 mg/m^3 on the shelf (http://reason.gsfc.nasa.gov) with a decreasing trend from the coast to open ocean (Figure 4.4).

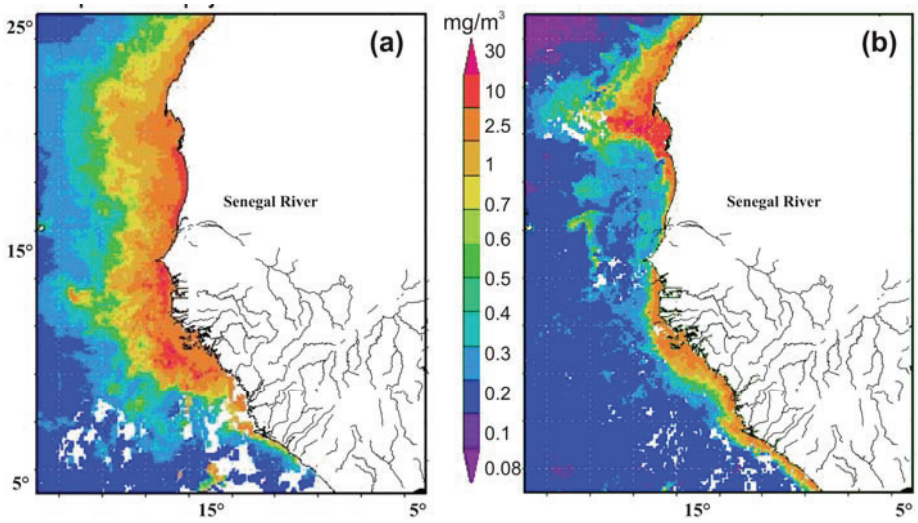

Figure 4.4 Distribution of chlorophyll-*a* concentrations (mg/m^3) at the sea surface in boreal winter (a) and boreal summer (b). (http://seawifs.gsfc.nasa.gov)

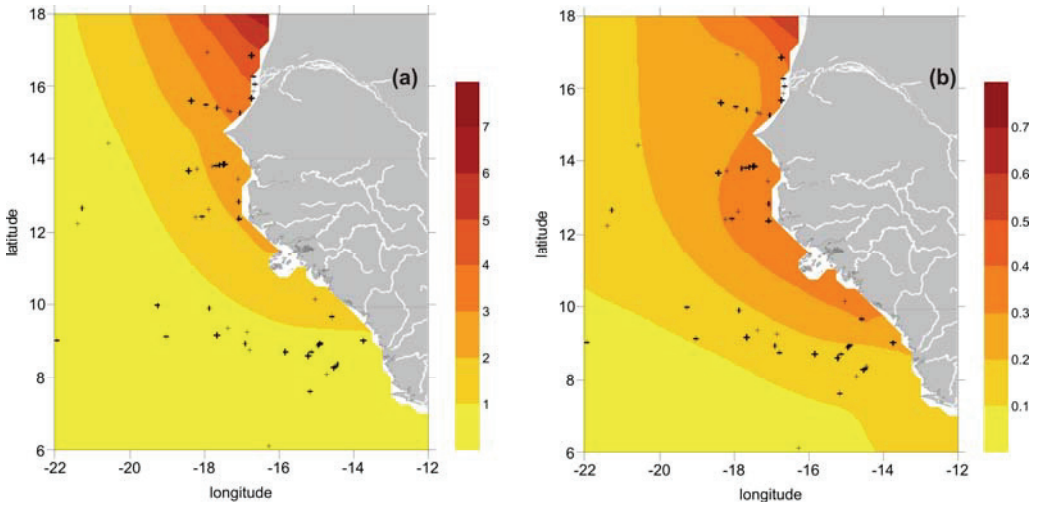

Figure 4.5 Annual values (µmol/l) for nitrate (a) and phosphate (b) at the sea surface. (WOA, 2005)

Bottom water oxygen concentrations measured in the investigated area range between 1.29 and 5.64 ml/l (WOA, 2005) with an average of 4.28 ml/l. Annual

values of nitrate and phosphate at the surface are very low and do not exceed 5 and 0.5 µmol/l respectively (Figure 4.5).

4.3 Material and Methods

The 37 surface samples investigated in the present study were collected from the first upper centimetre of multicores during the R/V *Meteor* cruise M65-1 (Mulitza et al., 2006). The samples were raised from water depths ranging between 10 and 4000 m off West Africa extending from 17 to 8°N and from 20 to 13°W. The results of these sites were combined with 16 additional surface sediment samples derived from the atlas of modern organic-walled dinoflagellate cyst distribution (Marret and Zonneveld, 2003) (Figure 4.1).

Samples (1 cm^3) were oven dried for 24h and subsequently weighed and processed for dinocyst analysis according to standard palynological preparation procedures which include decalcification with 10% hydrochloric acid (HCl) and removal of the siliceous fraction using 40% hydrofluoric acid (HF). One tablet of exotic *Lycopodium* spores (18583 ± 1708 spores/tablet) was added to each sample during the decalcification process in order to calculate palynomorph concentrations based on the dry weight sediments (g). After rinsing, the residue was sieved through a 8 µm mesh size sieve using an ultrasonic bath (5 minutes) to disintegrate lumps of organic matter. An aliquot of 60 µl was mounted in a gelatine-glycerine slide for microscope investigation. Laboratory procedure for the additional 16 samples can be found in Marret and Zonneveld (2003).

Dinocysts were counted up to 300 palynomorphs in each sample where possible. Most types were identified based on published morphological descriptions and the

cyst nomenclature follows de Vernal et al. (1997), Zonneveld (1997), Pospelova and Head (2002) and Fensome and Williams (2004). Besides dinocysts, other palynomorphs such as pollen and fern spores were counted as well (Supplementary Table S4.1).

Dinocyst counts are expressed as percentages of total sum of dinocysts shown in supplementary Table S4.1. Dinocyst and other palynomorph concentrations are

expressed as numbers of individuals per gram of dry sediment (numbers / g) calculated as $C = (N \times L)/(l \times wg)$, where C = palynomorph concentration, N = palynomorph counts, L = *Lycopodium* spores added, l = *Lycopodium* spores counted, and wg = dry weight in gram.

The multivariate analyse techniques Detrended Correspondence Analysis (DCA) and Canonical Correspondence Analysis (CCA) were performed on the relative abundances of dinocysts to quantify trends in their distributions (ter Braak and Smilauer, 1998). These calculations were performed with CANOCO for windows version 4. Prior to statistical analyses, we have grouped dinocyst species together (Supplementary Table S4.2)

An initial DCA analysis was performed to test the unimodal or linear character of the dataset. CCA is used to obtain information about the relationship between the variance of selected environmental variables in the region and relative abundances of dinocyst species. In the present study, the following parameters were used: seasonal values for SST (T), chlorophyll-*a* (Ch) and SSS (S), annual values for upper ocean concentrations of nitrate (Ni) and phosphate (P) and bottom water oxygen content (Ox), as well as water depth (WD). We applied forward selection of variables and a Monte Carlo test based on 199 permutations to determine the significance of each environmental parameter.

Distribution maps of dinocysts have been created by Surfer for windows version 8 using the kriging method.

4.4 Results

Dinocyst counts per sample ranged between 21 and 1405 palynomorphs and two samples turned out to be barren. Dinocyst concentrations fluctuate between ~130 and ~ 65,600 cysts/g with an average of ~ 7250 cysts/g. High cyst concentrations are observed on the continental margin off northern Senegal (Figure 4.6a), whereas the pollen/dinocyst concentration increases towards the south (Figure 4.6b).

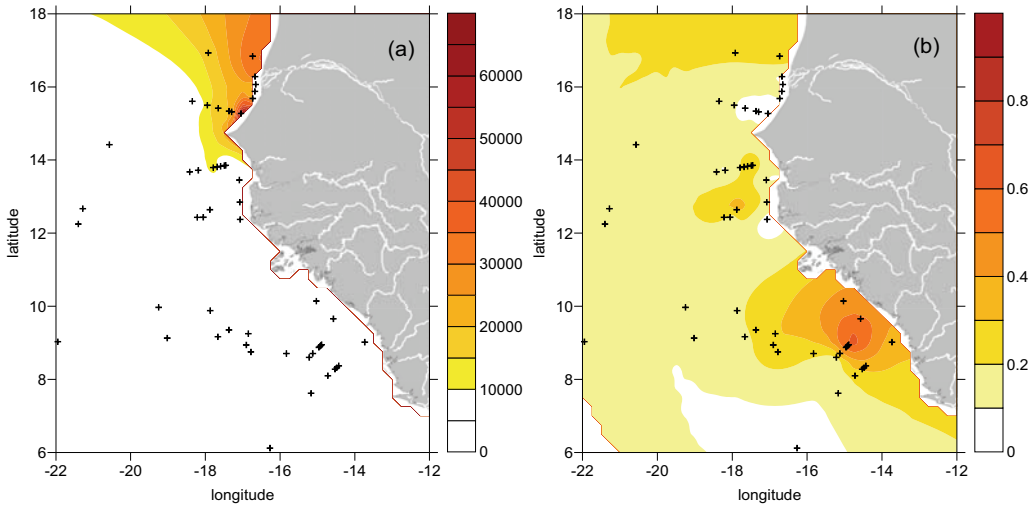

Figure 4.6 Distribution of total concentrations of dinoflagellate cysts (cysts/g) (a) and the ratio pollen to dinoflagellate cysts (b)

4.4.1 Geographic distribution of organic-walled dinocysts

Dinocyst assemblages are dominated by *Lingulodinium machaerophorum* that can form up to 90% of the assemblage. Other species that occur in high amounts are *Brigantedinium* spp. (45%), *Spiniferites* spp. (40%), and *Echinidinium* spp. (25%).

L. machaerophorum is observed mainly at sites off northern Senegal with the highest abundances in the mud-belt of Senegal between 17 and 14°N. High relative abundances of *Brigantedinium* spp. are found at southern sites located between 14 and 7°N. Cysts of *Polykrikos kofoidii* and *Echinidinium* spp. have their highest relative abundances at sites very close to the coast between 14 and 12°N (Figure 4.7).

Based on visual observation and geographic distribution of individual species four groups of species with comparable distribution patterns can be recognized:

Group 1: Is represented by species that show high percentages in the southern part of the research area at sites influenced by river outflow: *Lejeunecysta oliva*, *Quinquecuspis concreta*, *Bitectatodinium spongium, Echinidinium aculeatum,* and *Selenopemphix nephroides* (Figure 4.8 (a)-(e)).

Group 2: Is represented by dinocyst species that have their highest relative abundances in the southern sites of the study area characterized by warm waters. This group includes *Spiniferites* spp.*, Spiniferites ramosus, Spiniferites mirabilis* and

Spiniferites bentorii as well as *Tuberculodinium vancampoae* (Figures 4.8 (f) and 4.9 (a)-(d)).

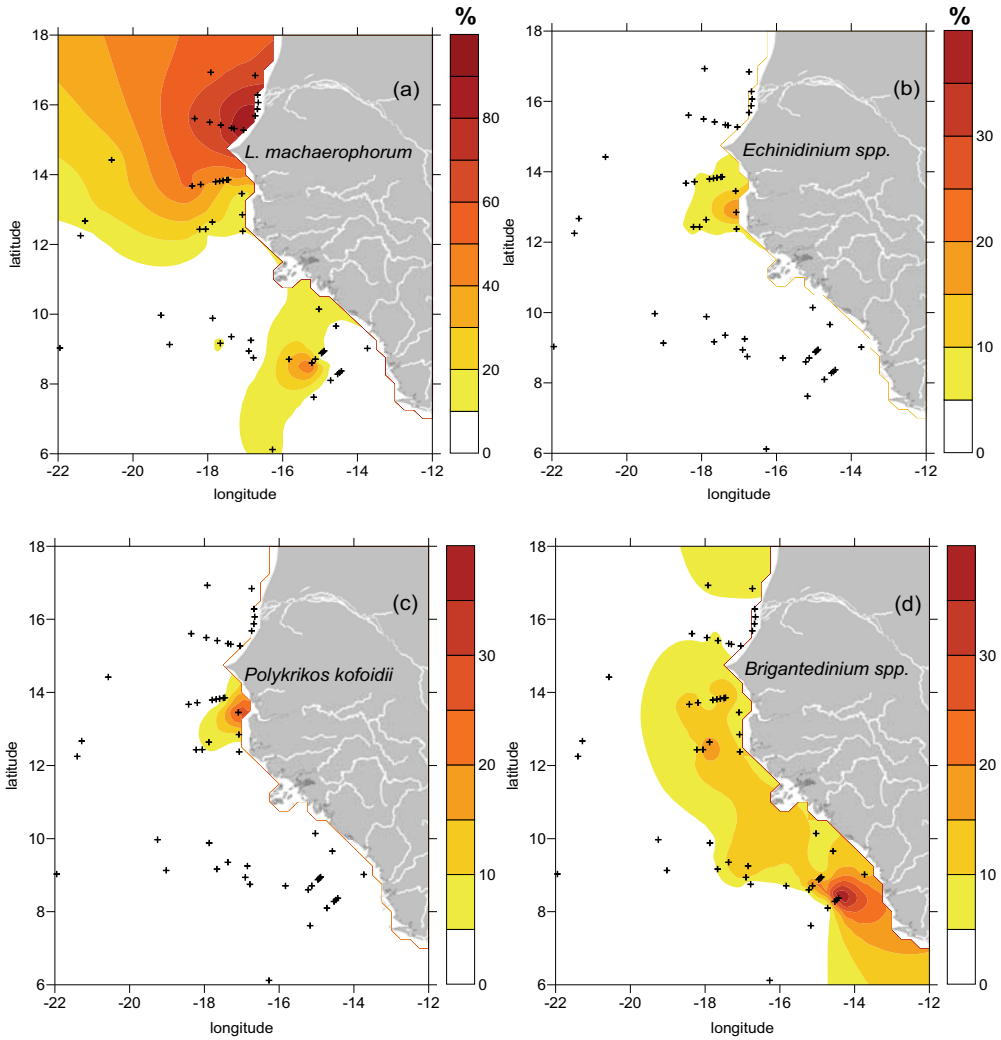

Figure 4.7 Relative abundances of *Lingulodinium machaerophorum* (a), *Echinidinium spp*. (b), cysts of *Polykrikos kofoidii* (c) and *Brigantedinium spp*.(d).

Group 3: Includes dinocyst species that show their highest relative abundances between 14 and 12°N at coastal sites characterized by high chlorophyll-*a* concentrations in surface waters and generally low oxygen concentrations in bottom waters: *Selenopemphix quanta, Dubridinium* spp., *Echinidinium transparantum* and cysts of *Protoperidinium monospinum* and cysts of *Polykrikos kofoidii* (Figures 4.9 (e), (f), 4.10 (a), (b), 4.7 (c)).

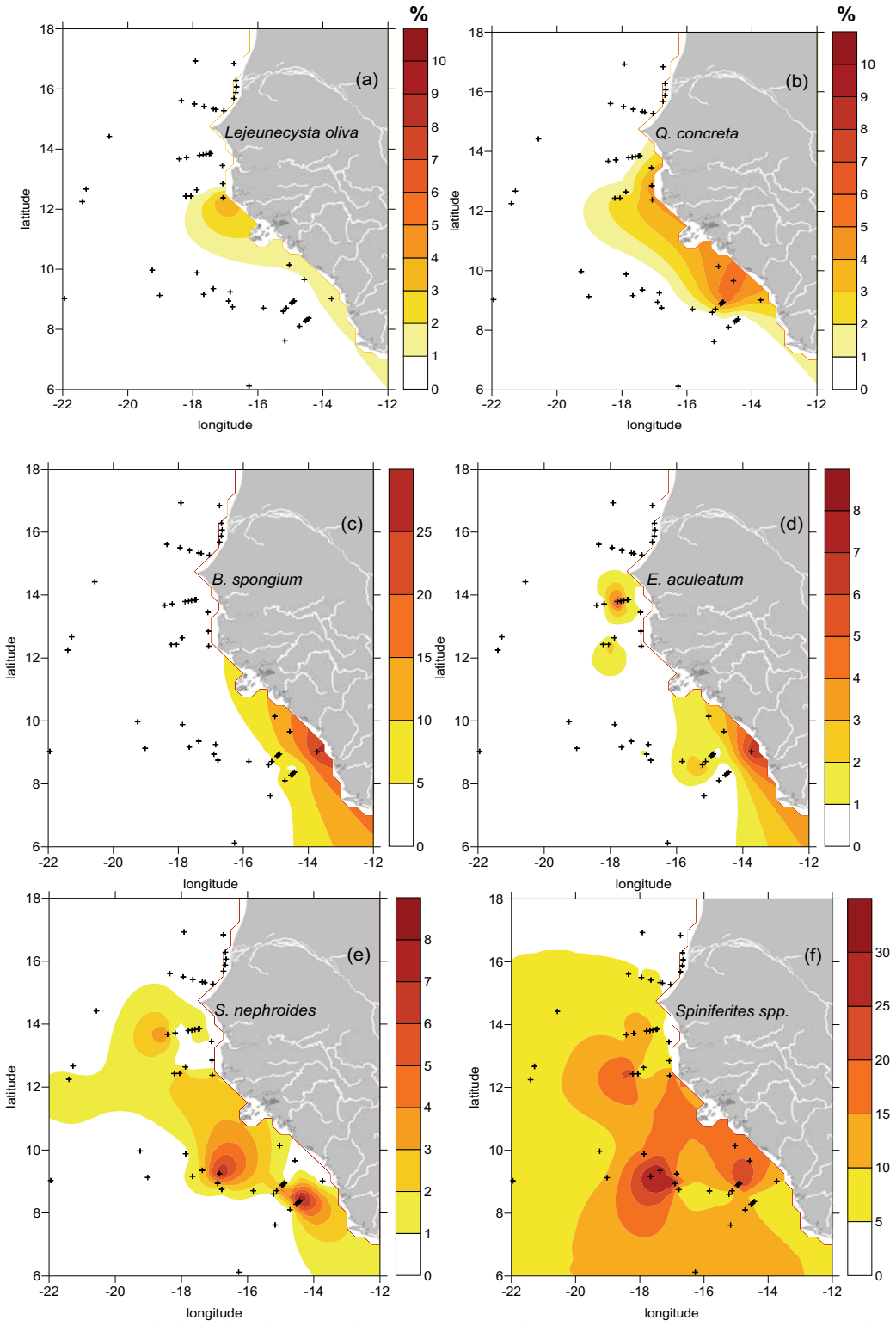

Figure 4.8 Relative abundances of *Lejeunecysta oliva* (a), *Quinquecuspis concreta* (b), *Bitectatodinium spongium* (c), *Echinidinium aculeatum* (d), *Selenopemphix nephroides* (e), *Spiniferites spp*. (f).

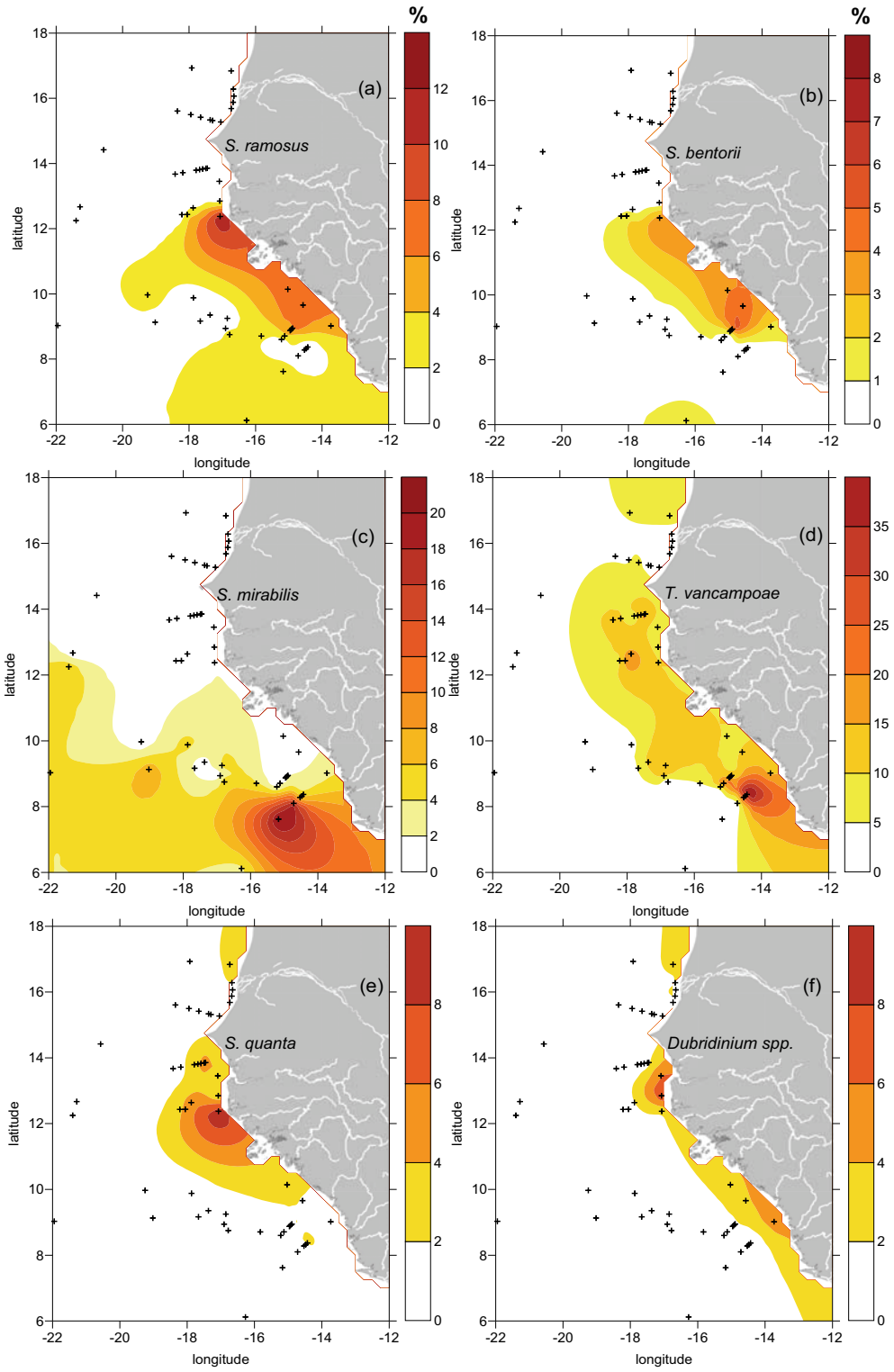

Figure 4.9 Relative abundances of *Spiniferites ramosus* (a), *Spiniferites bentorii* (b), *Spiniferites mirabilis* (c), *Tuberculodinium vancampoae* (d), *Selenopemphix quanta* (e), *Dubridinium spp*. (f).

Group 4: Includes dinocyst species with high relative abundances at sites characterized by relatively low chlorophyll-*a* concentrations and high oxygen concentrations in the bottom waters: *Operculodinium centrocarpum, Nematosphaeropsis labyrinthus, Impagidinium aculeatum*, *Impagidinium spp.*, and *Operculodinium israelianum* (Figure 4.10 (c)-(f) and 4.11 (a)).

Species with random distributions are *Spiniferites pachydermus*, *Polysphaeridium zoharyi* and *Trinovantedinium applanatum*, (Figure 4.11 (b)-(d)).

4.4.2 Detrended Correspondance Analysis (DCA) and Canonical Correspondance Analysis (CCA)

The DCA shows a gradient of 3.275 standard deviation units for our dataset, indicating the unimodal character of the dinocyst distribution that allows the use of the CCA analysis (Figure 4.12).

The CCA indicates that the parameters: nitrate (Ni), SST (autumn, spring and winter), SSS (autumn and summer), water depth (WD), chlorophyll-*a* content (winter and spring) correspond to the highest amount of variance in the dataset of more than 20% (Figure 4.13 and Table 4.1). Although the parameters SSS (winter), chlorophyll-*a* content (autumn and summer), SST (summer) and bottom water oxygen relate to less than 20% of the variance, they are significant at 5% significance level ($p \leq 0.05$) (Table 4.1). Variance in phosphate concentrations does not relate significantly to the dinocyst distribution. The first CCA axis explain 38.8% of the variance and is mostly defined by Ni, chlorophyll-*a* content and SST. The second CCA axis explains additional 25.3% of the variance and is correlated to SSS analysis.

The CCA analysis documents that the highest relative abundances of *L. machaerophorum* can be observed at sites that are characterised by high annual nitrate concentrations, high spring chlorophyll-*a* and relatively low sea-surface temperatures.

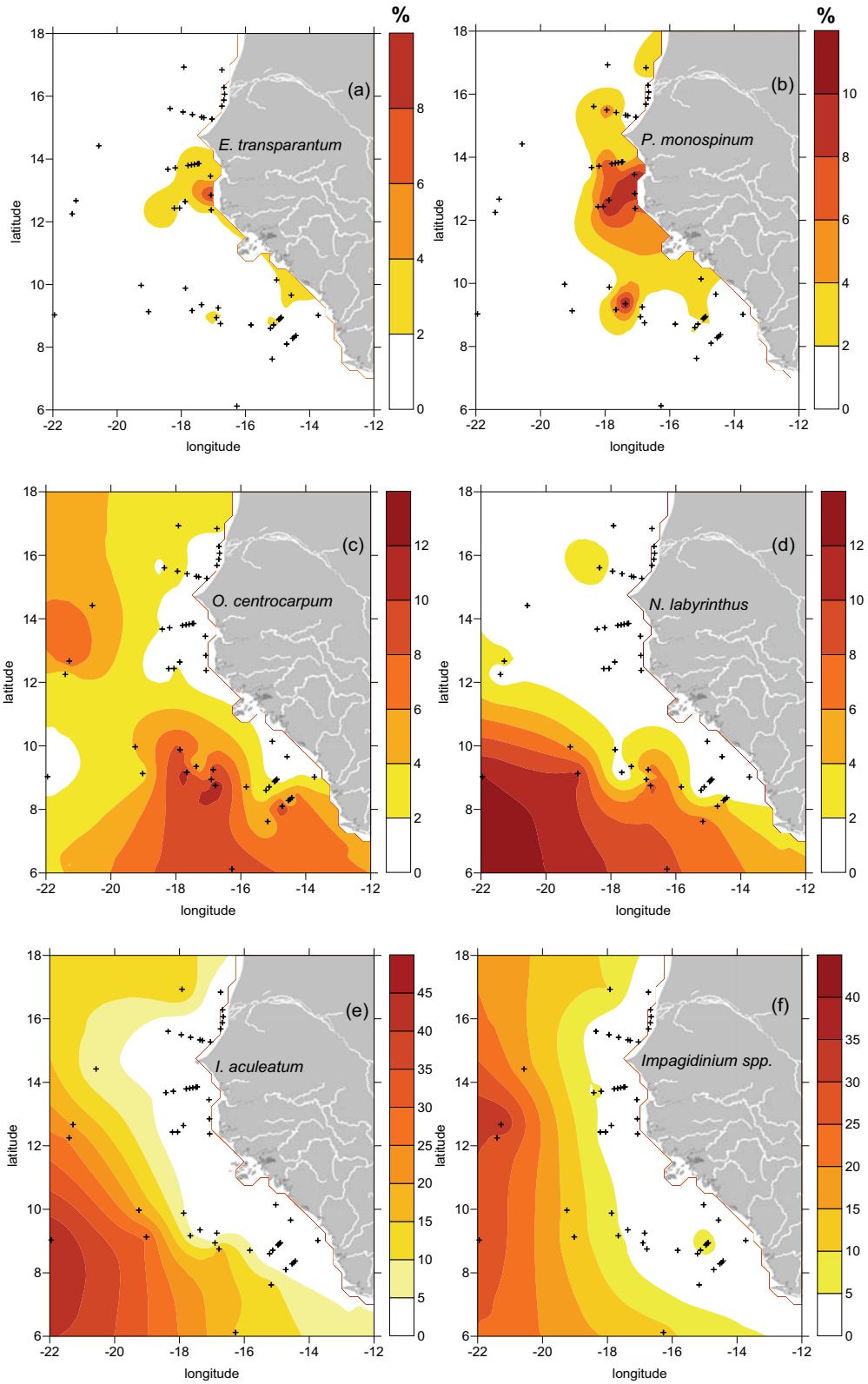

Figure 4.10 Relative abundances of *Echinidinium transparantum* (a), cysts of *Protoperidinium monospinum* (b), *Operculodinium centrocarpum* (c), *Nematosphaeropsis labyrinthus* (d)

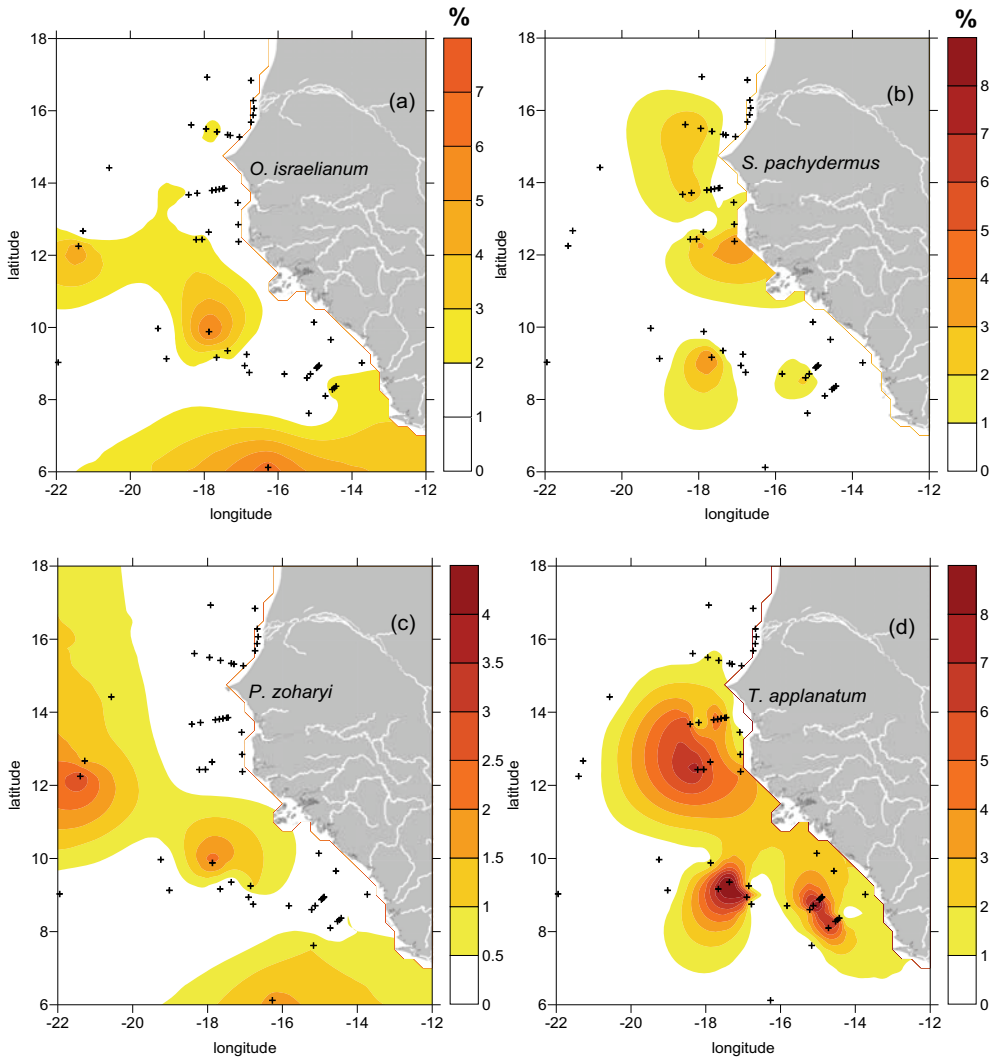

Figure 4.11 Relative abundances of *Operculodinium israelianum* (a), *Spiniferites pachydermus* (b), and *Polysphaeridium zoharyi* (c) and *Trinovantedinium applanatum* (e)

Species that are grouped in group 1 based on the visual examination of the dataset (*L. oliva*, *Q. concreta*, *B. spongium, E. aculeatum,* and *S. nephroides*) are ordinated at the negative side of the SSS gradient but on the positive side of the chlorophyll-*a* gradient in summer and SST in spring and summer.

According to the CCA, highest relative abundances of cysts included in group 2 (*Spiniferites* spp., *S. ramosus, S. mirabilis, S. bentorii* and *T. vancampoae)* correspond to sites with relatively warm SST in winter, spring, and autumn but relatively low nitrate concentrations and spring chlorophyll-*a* concentrations.

Table 4.1 Fraction of variance explained by the environmental variables used in CCA.

(See supplementary Table S4.1 for abbreviations)

Variable	F value for data	*P*-value estimate	explain
Ni	12.928	0.005	0.425
T4	12.327	0.005	0.409
T2	11.393	0.005	0.384
T1	10.528	0.005	0.360
S4	8.254	0.005	0.294
WD	8.110	0.005	0.289
S3	6.580	0.005	0.241
Ch1	6.274	0.005	0.231
Ch2	5.688	0.005	0.212
S1	4.422	0.005	0.169
Ch4	4.120	0.005	0.158
T3	4.016	0.005	0.154
Ox	3.068	0.01	0.120
Ch3	2.993	0.005	0.117

The species *S. quanta, Dubridinium* spp., *E. transparantum* and cysts of *P. monospinum* and cysts of *P. kofoidii* (group 3) are ordinated at the negative side of the bottom water oxygen and water depth gradients but have their highest relative abundances at sites characterised by high chlorophyll-*a* concentrations in winter, autumn and summer.

We observe that species of group 4 (*I. aculeatum*, *I. patulum*, *P. zoharyi* and *N. labyrinthus*) are ordinated at the positive side of water depth and bottom water oxygen gradients and at the most negative side of chlorophyll-*a* gradient in winter, autumn and summer (Figure 4.13).

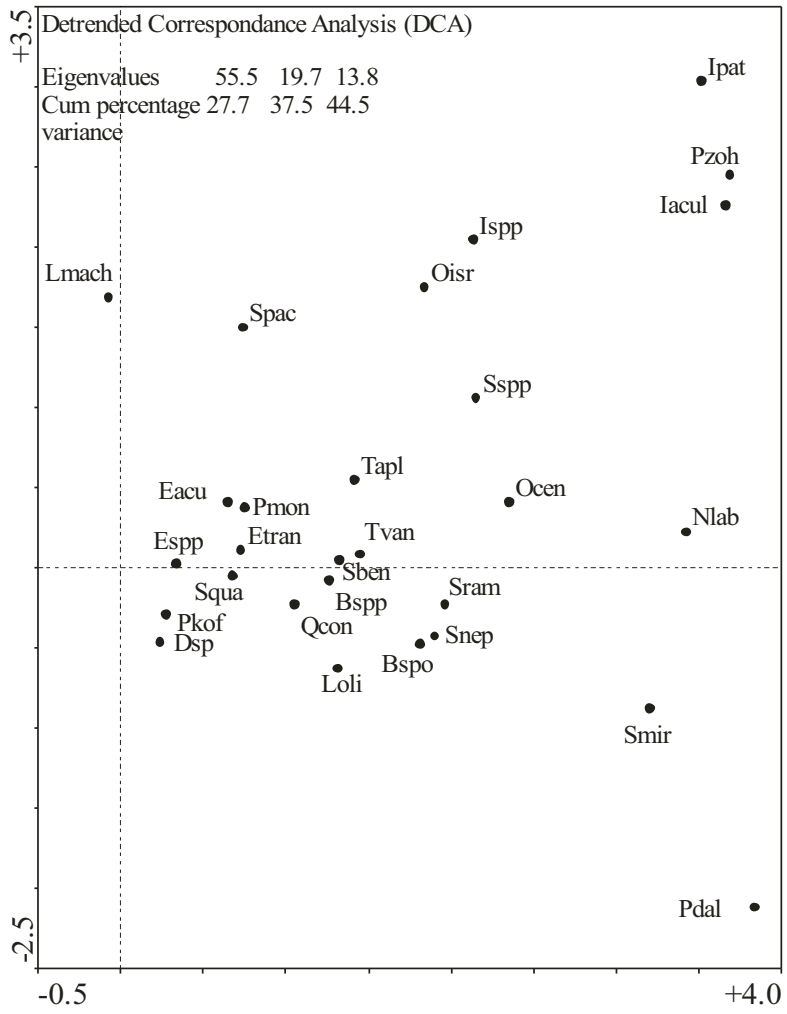

Figure 4.12 Results of the DCA analysis showing the variation within the species distribution. Lmach: *Lingulodinium machaerophorum*, Smir: *Spiniferites mirabilis*, Sspp: *Spiniferites* spp., Sben: *Spiniferites bentorii*, Spac: *Spiniferites pachydermus*, Sram: *Spiniferites ramosus*, Ocen: *Operculodinium centrocarpum*, Pmon: Cysts of *protoperidinium monospinum*, Squa: *Selenopemphix quanta*, Qcon: *Quinquecuspis concreta*, Bspp: *Brigantedinium* spp., Espp: *Echinidinium* spp., Snep: *Selenopemphix nephroides*, Etran: *Echinidinium transparantum*, Pdal: Cysts of *Pentapharsodinium dalei,* Tvan: *Tuberculodinium vancampoae*, Oisr: *Operculodinium israelianum,* Pzoh: *Polysphaeridium zoharyi*, Tapl: *Trinovantedinium applanatum*, Eacu: *Echinidinium aculeatum*, Loli: *Lejeunecysta oliva*, Bspo: *Bitectatodinium spongium,* Pkof: Cysts of *Polykrikos kofoidii*, Dsp: *Dubridinium* spp., Nlab: *Nematosphaeropsis labyrinthus*, Ispp: *Impagidinium* spp., Iacul: *Impagidinium aculeatum*, Ipat: *Impagidinium patulum*.

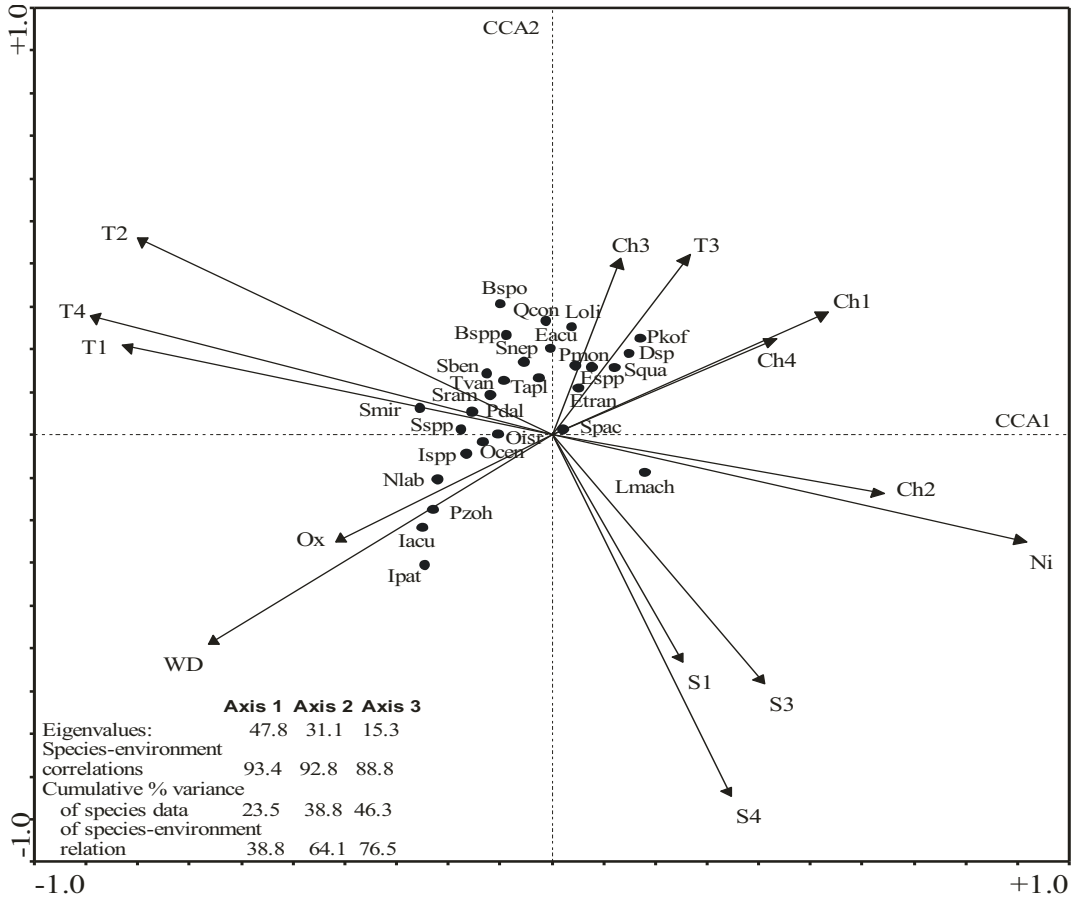

Figure 4.13 Results of the CCA analysis illustrating dinoflagellate species in relation to environmental variables (See Figure 4.12 and Supplementary Table S4.1 for abbreviations)

4.5 Discussion

The present study shows that although the patterns of dinocyst distribution in the subtropical East Atlantic off West Africa are in broad agreement with studies from other regions with relatively similar hydrographic conditions and environmental parameters, this region has its own characteristics. Before discussing the dinocyst species distribution in the sediments in detail, it is important to emphasize the possible effect of non-ecological mechanisms on dinocyst assemblages such as long-range cyst transport and cyst preservation.

Dinocysts can be laterally displaced when they sink to the ocean floor by ocean currents which may cause a wrong interpretation of the data. Hooghiemstra et al. (1986, 2006) who had analysed pollen data from the same study area concluded that pollen distribution over the ocean surface is reflected to a high degree in the ocean

floor sediments without substantial displacement by marine currents. Since pollen and dinocysts are considered to behave as comparable sedimentological particles, we therefore assume that similarly no large scale transport has displaced the dinocysts while sinking into the ocean floor. This assumption is supported by a sediment trap study in Cap Blanc region that documents a relatively fast sinking velocity of dinocysts through the water column with comparable cyst associations in traps at about 1000 and 3000m water depth (Susek, 2005).

In this study, we observe no reworked palynomorphs. As result we have no indication that sediment rearrangement post-depositionally disturbed our cyst distribution patterns.

Recent studies have shown that oxygenated bottom waters can cause species-selective post-depositional degradation, altering dinocyst associations (e.g. Zonneveld et al., 1997, 2001, 2007; Hopkins and McCarthy 2002; Versteegh and Zonneveld, 2002; Reichart and Brinkhuis 2003; Kodrans-Nsiah et al., 2008). We observe in this study, a significant correlation between the relative cyst abundances of individual species and oxygen concentrations in bottom waters which is elucidated by the CCA analysis. Cysts that are traditionally found to be resistant against aerobic degradation have their highest relative abundances in deep ocean sites where bottom waters are characterised by relatively high oxygen concentrations whereas the cysts that are known to be vulnerable to aerobic concentrations are found on the shelf in the oxygen minimum zone. As result we can not exclude oxygen as a factor that could have altered our cyst associations post-depositionally. This hampers the discrimination between the initial ecological signal and the diagenetic effects and prevents the ecological characterisation of individual cyst species based on this dataset.

However, this does not inhibit the determination of cyst associations that are typical for different oceanographic environments when we include bottom water oxygen as an additional factor that characterizes these environments. In this paper we therefore avoid the ecological characterisation of individual cyst species but focus on the characterisation of oceanographic regimes for paleoceanographic purposes.

Based on the variability in dinocyst assemblages and their relationship with oceanographic conditions, we can distinguish typical associations for four major hydrographic regimes off West Africa, 1) the northern regime between 17° and 14°N, 2) the southern regime between 12° and 6°N, 3) the intermediate regime between 14° and 12°N and 4) the low productivity regime (Figure 4.14).

4.5.1 Northern regime

The upper waters of the continental margin off Northern Senegal between 17 and 14°N are characterized by the influence of coastal upwelling that transports nutrient rich subsurface waters into the photic zone and thus stimulating primary productivity (deMenocal, 2000; Adkins et al., 2006). Primary productivity is further enhanced by the additional input of nutrients and trace-elements supplied by the Senegal River and by eolian dust (Sarnthein et al., 1981). The cyst assemblage in this regime is characterized by extremely high dinocyst concentrations with an association that is almost exclusively composed of *L.* machaerophorum (Figure 4.14). Extremely high relative and absolute abundances of *L. machaerophorum* are traditionally found in close vicinity to river mouths where high nutrient concentrations in upper waters prevail (e.g. Lewis 1988; Dale and Fjellså, 1994; Dale et al., 1999; Allen et al. 2002; Dale et al., 2002; Pospelova et al., 2002, 2004, 2005; Marret and Zonneveld, 2003; Sangiorgi and Donders, 2004; Cremer et al., 2007; Siringan et al., 2008). In upwelling regions high abundances of *L. machaerophorum* can typically be related to stratified surface water conditions that are characterised by high nutrient concentrations representative for upwelling relaxation. Within our study we observe that high relative abundances of *L. machaerophorum* are found at sites with high annual nitrate concentrations as well as high spring chlorophyll-*a* concentrations. We do not observe a negative relationship with salinity. We therefore assume that the presence of *L. machaerophorum* is mostly related to “relaxed upwelling” rather than river input in the region. This is consistent with the fact that within this area, maximum upwelling occurs in winter related to the northernmost position of the ITCZ, followed by an upwelling relaxation in spring (Santos et al., 2005). Since the position and seasonality of upwelling in the research area is strongly related to the position of the ITCZ, *L. machaerophorum* might be a valuable key species for reconstructing past variations in the ITCZ position and its associated rainbelt.

Compared to the other regimes, the northern regime is characterised by the highest primary production as reflected by high chlorophyll-*a* concentrations throughout the year and the highest cyst concentrations (Figures 4.4 and 4.6a). Overall, the relationship between primary productivity and dinocyst concentrations has not been clearly established in oceanic or coastal domains (Radi et al., 2007). Zonneveld et al. (2007) suggest that dinocyst concentrations can be considered to reflect marine productivity as long as the aerobic degradation did not affect the dinocyst association. Since the oxygen minimum zone prevails on the shelf and upper slope of this region and oxygen concentrations in bottom waters at these sites are low, we assume that the high total dinocyst concentrations observed here might therefore reflect the high productivity in the surface waters induced mainly by upwelling and/or high Senegal River runoff.

Studies on the modern distribution of dinoflagellate cysts in surface sediments based on relative abundance data often suggest the occurrence of high relative abundances of *Brigantedinium* spp. or cysts of other heterotrophic dinoflagellates in high productivity areas (e.g. Lewis et al., 1990, Dale et al., 2002). Within this study we do not find such a relationship. Our results are consistent with Radi et al. (2007) who observe a relationship between high productivity and high dinocyst concentrations rather than high relative abundances of heterotrophic taxa in coastal inlets of British Columbia.

4.5.2 Southern regime

The coastal sites in the studied area between 12 and 6°N are located in close proximity to the densest fluvial network on the adjacent continent (Figure 4.1). The region is characterized by periods of high rainfall especially in summer. This occurs when the NE trade winds are replaced by the monsoon winds that advect warm and humid air northward along the shore, resulting in high precipitation in this region (Walter and Lieth, 1960). High rainfall results in higher fluvial discharge of relatively warm and fresh waters enhancing input of terrestrial material. This configuration results in relatively low SSS and high SST in the region. We observe here the highest ratio of land-derived pollen to dinocysts reflecting the high continental runoff and strong river discharge (Figure 4.6). Bottom waters of the region are characterised by low oxygen concentrations. We therefore assume that

aerobic degradation did not severely alter the cyst association post-depositionally in this regime. Surface sediments of the most coastal sites of this area are characterised by high relative abundances of *L. oliva*, *Q. concreta*, *B. spongium, E. aculeatum,* and *S. nephroides* (Figures 4.8 and 4.14). These species are clearly correlated with low salinity in the CCA analysis and thus we can associate them to river outflow. However, if this would be the only factor influencing the distribution of these species, we would expect them to occur in the northern part of the study area influenced by the Senegal River as well. Since this is not the case, other factors must have affected their distribution. When looking at the SST distribution, we see that this region is the warmest of the whole study area. SSTs vary seasonally within a very narrow range from 27 to 28°C in contrast to the northern part where SSTs fluctuate between 19 and 26°C. We therefore assume that a combination of low SST seasonality, low SSS, warm waters and high river outflow is favouring the occurrence of these species. We suggest that, within the research area, these species can be used as a proxy for river outflow of warm, fresh and nutrient-rich waters. Our results are in a good agreement with other studies from tropical areas such as the Arabian Sea, the Benguela upwelling system, the China Sea and the western equatorial Atlantic where high relative abundances of these species are observed amongst other species in the vicinity of river mouths (Zonneveld and Jurkschat, 1999; Vink et al., 2000; Wang et al., 2004a, b; Holzwarth et al., 2007). This area is also characterized by high relative abundances of dinocyst species that are traditionally associated to warm or tropical neritic environments such as *T. vancampoae*, *Spiniferites* spp., *S. mirabilis* and *S. ramosus* (Figure 4.14). In our study, these species are ordinated positively at the SST gradient. This observation conforms to the distribution recorded by Marret and Zonneveld (2003), where high abundances of *T. vancampoae* are found in subtropical/tropical regions and *S. mirabilis* are found in temperate to tropical regions with oligotrophic to eutrophic fully marine conditions. High relative abundances of *S. ramosus* related to warm environments have been observed by Pospelova et al. (2008) in the northeastern Pacific.

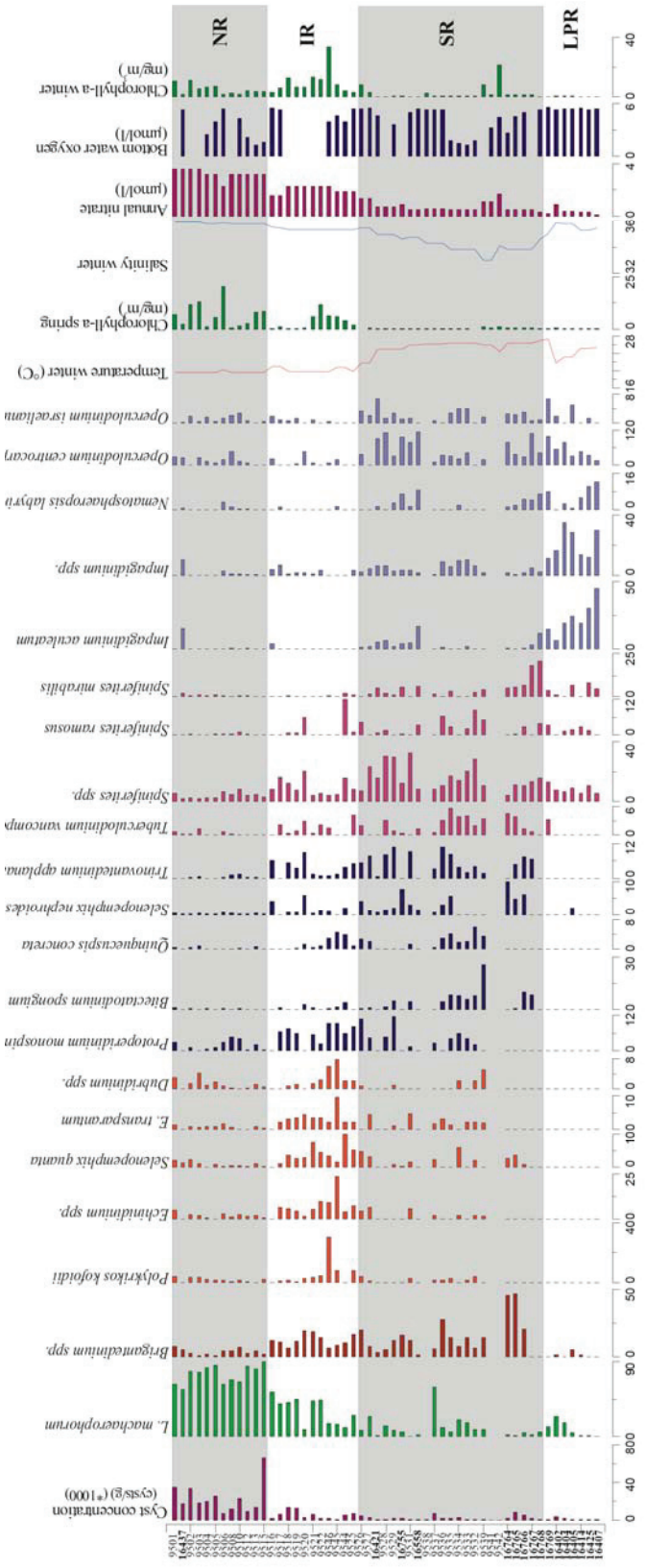

Figure 4.14 Relative abundances of main organic-walled dinoflagellate taxa expressed in percentages of total cysts from marine surface sediments (bold: GIK samples from Marret and Zonneveld (2003), normal: GeoB samples recovered during M65-1 cruise). NR: Northern regime, IR: Intermediate regime, SR: Southern regime, LPR: Low productivity regime. Gray horizontal bands indicate the assemblages of NR and SR.

4.5.3 Intermediate regime

Sites from 14 to 12°N are located in the boundary between NE trade winds and the SE monsoon winds separating arid conditions to the north from humid conditions to the south. This regime is characterized by maximum upwelling during the winter season promoted by the NE trade winds reached far south (Santos et al., 2005) and it is also influenced by river outflow (Figure 4.1). Bottom water oxygen concentrations are relatively low. The dinocyst assemblages of this regime are characterized by an increase in high relative abundances of *S. quanta, Dubridinium* spp., *Echinidinium* species and cysts of *P. kofoidii* related to high winter productivity, relatively low winter SST and high SSS (Figure 4.14). Marret and Zonneveld (2003) suggest a close relationship between high relative abundances of these species and high productivity associated with upwelling. In our investigated area, we can also define such a relationship since these species form a cluster in the DCA as well as in the CCA where they are positively ordinated at the winter chlorophyll-*a* gradient coinciding with maximum upwelling in the region (Figures 4.12 - 4.14). We assume that intense winter upwelling in this region favours the development of cyst assemblages dominated by the mentioned dinocyst species.

Cysts of *P. monospinum* occur in high relative abundances in this area as well. However, unlike the other species it is ordinated positively at the summer chlorophyll-*a* gradient in the CCA analysis corresponding to the high river runoff during summer. Consequently, we can suggest that this species can be associated to high productive regions under the influence of fluvial outflow waters and stratified conditions in this study (Figure 4.10b).

The assemblage composition of this regime suggests the main influence of the seasonal upwelling promoted by NE trade winds in the north and, to a lesser extent, to the river discharge promoted by monsoon precipitation in the south. We therefore assume that cyst of *P. kofoidii*, *S. quanta*, *Dubridinium spp.*, *Echinidinium* species and cyst *of P. monospinum* are ideal to trace the boundary between the NE trade winds and the SE monsoon winds in the subtropical eastern Atlantic Ocean and consequently reconstruct past shifts of the ITCZ position.

The heterotrophic taxon *Brigantedinium spp.* is very often related to high productivity environments. It is one of the most abundant heterotrophic taxon in our investigated samples (Figure 4.14); it is ubiquitously present in nutrient-rich environments both in the vicinity of seasonal upwelling and river mouths confirming its cosmopolitan distribution suggested by Marret (1994) and Marret and Zonneveld (2003).

4.5.4 The low productivity regime

The low productivity regime is represented by samples ranging from the slope to the open ocean off West Africa where cyst assemblages are characterized by the dominance of *Impagidinium* species, *N. labyrinthus* and *O. centrocarpum* (Figure 4.10). Relative abundances of these cysts increase with the distance from the coast towards offshore sites characterized by low productivity and high bottom water oxygen (Figure 4.13). They are particularly resistant to pre- or post-depositional aerobic degradation (Zonneveld et al., 1997; Versteegh and Zonneveld, 2002). The presence of high relative abundances of these species in the offshore sites might therefore be the result of species-selective degradation rather than the ecological affinity of their motiles.

O. centrocarpum is defined as a cosmopolitan species commonly found in coastal environments but also in unstable waters off the outer shelf at the coastal/oceanic boundary (Dale et al., 2002). Figure 4.14 shows that *O. centrocarpum* is present in both coastal sites of the southern regime and offshore sites of the low productivity regime, whereas it is one of the most abundant species in nutrient-rich waters of coastal inlets in British Columbia (Radi et al., 2007) and it is abundant in offshore sites along the California margin (Pospelova et al., 2008).

4.6 Conclusion

The migration of the tropical rainbelt associated with the seasonal migration of the ITCZ has been proposed as the main driving mechanism for hydrologic changes in West Africa (Nicholson, 2001; Wang and Eltahir, 2000; Nicholson and Grist, 2003). The southward migration of the tropical rainbelt causes dry conditions over the northern part of our study area with intensified trade winds along the north western

African coast that would promote seasonal upwelling inducing upwelling-related productivity. Simultaneously, wetter conditions are observed over the southern part leading to enhanced river runoff supplying warm and fresh waters as well as large amounts of terrestrial nutrients.

The cyst distribution reflects four hydrographic regimes that are related to the current position and seasonal variability of the ITCZ and as such the position of its associated tropical rainbelt:

1. The northern regime between 17 and 14°N where surface waters are characterized by high productivity associated with seasonal coastal upwelling. Dinoflagellate cyst association is characterized by high cyst concentrations and dominated by *L. machaerophorum*.

2. The southern regime between 12 and 6°N associated with upper waters that are influenced by river discharge resulting in high nutrient concentrations. The cyst association consisting of *L. oliva*, *Q. concreta*, *B. spongium, E. aculeatum,* and *S. nephroides* can be considered as a good indicator for river discharge.

3. The intermediate regime between 14 and 12°N where surface waters are influenced mostly by seasonal coastal upwelling and in a lesser extent by fluvial discharge of terrestrial nutrients. The cyst association characterized by cysts of *P. kofoidii*, *S. quanta*, *Dubridinium sp.*, *Echinidinium* species and cysts *of P.monospinum* seem ideal to trace the boundary between the NE trade winds and the SE monsoon winds in the subtropical eastern Atlantic Ocean

4. The low productivity regime where surface sediments are characterised by oligotrophic surface waters and oxygen rich bottom waters. The cyst association is characterized by the dominance of *Impagidinium* species, *N. labyrinthus* and *O. centrocarpum.*

The present study shows that at the sites where bottom waters are characterised by relatively low oxygen concentrations, the dinocyst association reflects in detail the upper water conditions and as such the seasonal position of the tropical rainbelt. This

indicates that the fossil dinocyst association in this region forms a very accurate tool for the establishment of detailed reconstructions of past climate change.

Acknowledgements

The authors thank the captain and crew of R/V *Meteor* cruise M65-1 for the logistic and technical assistance to recover the investigated sediment samples. The manuscript benefitted from helpful comments by M. Kölling, J. Groenveld and C. Gonzălez. Thanks to Sven Forke for his assistance with palynological processing. This work is funded through the Deutsche Forschungsgemeinschaft as part of the DFG - Research Centre / Excellence cluster MARUM -The Ocean in the Earth System" of the University of Bremen. This is MARUM publication N° xxx.

Supplementary Table S4.1 Surface sample locations, water depth, total cyst counts and concentrations of dinocysts and pollen together with environmental parameters used in CCA.

Samples	Longitude (°W)	Latitude (°N)	WD (m)	Total cysts	Concent. (cysts/g)	Concent. (pollen/g)	T1	T2	T3	T4	S1	S2	S3	S4	Ch1	Ch2	Ch3	Ch4	Ni	P	Ox
GeoB 9501-4	-16.733	16.84	330	231	35036	14257	19.56	21.53	27.77	25.75	35.70	35.73	35.95	35.67	10.19	6.73	0.28	3.4	3.6	0.3	NA
GeoB 9502-5	-16.67	16.282	65	813	34121	2518	19.56	21.53	27.77	25.75	35.70	35.73	35.95	35.67	10.94	11.70	0.31	1.8	3.6	0.3	NA
GeoB 9503-3	-16.651	16.067	45	477	17614	2511	19.56	21.53	27.77	25.75	35.70	35.73	35.95	35.67	5.52	13.17	0.82	2.49	3.6	0.3	NA
GeoB 9504-4	-16.675	15.877	43	793	19627	2376	19.56	21.53	27.74	25.92	35.70	35.79	35.82	35.44	6.47	1.25	0.95	3.2	3.2	0.3	2.43
GeoB 9505-3	-16.732	15.683	36	916	25486	2921	19.66	21.95	27.74	25.92	35.76	35.79	35.82	35.44	7.16	5.62	0.67	1.82	3.2	0.3	3.95
GeoB 9506-3	-18.35	15.608	2956	260	6638	1174	20.18	22.22	27.39	26.15	35.65	35.82	35.86	35.45	2.03	20.37	2.26	0.48	2.3	0.3	5.43
GeoB 9508-4	-17.947	15.499	2393	437	11124	1476	19.56	21.95	27.74	25.92	35.70	35.79	35.82	35.44	2.65	0.82	0.13	0.36	3.2	0.3	NA
GeoB 9510-3	-17.654	15.417	1565	444	23024	1211	19.56	21.95	27.74	25.92	35.70	35.79	35.82	35.44	1.72	1.41	0.29	0.53	3.2	0.3	4.4
GeoB 9512-4	-17.366	15.337	787	421	9152	1195	19.56	21.95	27.74	25.92	35.70	35.79	35.82	35.44	3.99	2.85	0.31	0.46	3.2	0.3	2.22
GeoB 9513-5	-17.295	15.318	499	251	12973	1539	19.56	21.95	27.74	25.92	35.70	35.79	35.82	35.44	3.79	8.07	0.26	0.42	3.2	0.3	1.26
GeoB 9515-2	-17.045	15.273	102	1405	65602	3922	19.56	21.95	27.74	25.92	35.70	35.79	35.82	35.44	3.34	8.73	0.23	1.75	3.2	0.3	1.56
GeoB 9516-4	-18.419	13.674	3438	48	1858	310	20.93	23.1	27.83	26.95	35.40	35.61	35.56	34.67	3.08	0.27	0.18	5.27	1.6	0.3	5.52
GeoB 9517-5	-18.189	13.718	3107	92	5712	497	20.93	23.45	27.83	26.95	35.40	35.74	35.5	34.67	5.82	1.17	0.21	2.13	1.6	0.3	5.36
GeoB 9518-4	-17.79	13.793	1992	257	13054	3556	19.87	23.10	28.06	26.56	35.27	35.61	35.33	34.09	12.71	0.38	0.17	0.86	2.3	0.4	NA
GeoB 9519-6	-17.683	13.812	1496	374	12733	2996	19.87	23.10	28.06	26.56	35.27	35.61	35.33	34.09	6.42	0.45	0.21	0.62	2.3	0.4	NA
GeoB 9520-4	-17.591	13.829	1099	65	2374	1315	19.87	23.10	28.06	26.56	35.27	35.61	35.33	34.09	6.42	0.60	0.21	0.62	2.3	0.4	NA
GeoB 9521-3	-17.491	13.848	530	210	6514	2016	19.87	23.10	28.06	26.56	35.27	35.61	35.33	34.09	13.21	6	0.25	1.07	2.3	0.4	NA
GeoB 9522-2	-17.454	13.855	151	89	1500	542	19.87	23.10	28.06	26.56	35.27	35.61	35.33	34.09	11.41	11.87	0.27	0.86	2.3	0.4	NA
GeoB 9525-5	-17.879	12.64	2648	93	6928	4407	19.87	24.13	28.02	26.79	35.30	35.70	35.33	33.69	3.19	1.74	0.25	0.53	1.9	0.4	5.43
GeoB 9526-4	-18.056	12.435	3224	145	4057	503	21.72	24.24	27.79	27.15	35.37	35.74	35.47	34.41	7.91	NA	0.25	0.56	1.4	0.3	5.41
GeoB 9527-6	-18.218	12.432	3682	90	2746	808	21.72	24.24	27.79	27.15	35.37	35.74	35.47	34.41	3.24	0.87	0.24	0.29	1.4	0.3	5.5
GeoB 9528-1	-17.664	9.166	3060	63	665	120	24.9	26.76	27.45	28.09	35.28	35.63	34.95	34.23	0.35	0.15	0.22	0.12	0.7	0.2	NA
GeoB 9529-1	-17.369	9.353	1234	99	1342	466	24.9	27.76	27.45	28.09	35.28	35.63	34.95	34.23	0.51	0.14	0.19	0.13	0.7	0.2	3.68
GeoB 9531-2	-16.904	8.941	2288	65	658	288	25.93	27.53	27.30	28.29	35.15	35.50	34.73	33.98	0.29	0.11	0.15	0.12	0.5	0.1	5.07
GeoB 9532-1	-14.889	8.948	315	49	454	945	26.4	28	27.03	28.45	34.90	35.24	33.86	32.80	0.73	NA	0.26	0.19	0.5	0.1	1.76
GeoB 9533-3	-14.911	8.926	394	49	723	1269	26.42	28	27.03	28.45	34.90	35.24	33.86	32.80	0.81	0.11	0.26	0.23	0.5	0.1	1.29
GeoB 9534-4	-14.936	8.901	494	51	2043	2363	26.42	28	27.03	28.45	34.90	35.22	33.86	32.80	0.81	0.11	0.26	0.23	0.5	0.1	1.51
GeoB 9535-5	-14.961	8.876	666	69	1615	1755	26.42	28	27.03	28.45	34.90	35.24	33.86	32.80	0.81	0.12	0.26	0.22	0.5	0.1	1.77
GeoB 9536-4	-15.125	8.709	3076	63	1015	660	26.14	27.74	27.21	28.31	35.01	35.37	34.33	33.38	0.66	0.12	0.25	0.2	0.6	0.1	5.38
GeoB 9537-4	-15.22	8.601	3407	344	6900	923	26.14	27.74	27.21	28.31	35.01	35.37	34.33	33.38	0.40	0.12	0.22	0.18	0.6	0.1	5.33
GeoB 9538-5	-15.829	8.708	4146	21	388	465	26.14	27.74	27.21	28.31	35.01	35.37	34.33	33.38	2.23	0.29	0.13	0.15	0.6	0.1	5.35
GeoB 9539-1	-13.733	9.018	22	58	825	427	25.97	28	27.28	28.20	34.71	35.24	32.96	31.89	8.35	0.98	7.01	1.17	1.1	0.3	NA
GeoB 9541-1	-14.573	9.658	32	0	0	0	25.97	27.57	27.28	28.20	34.71	35.15	32.96	31.89	1.18	0.76	0.71	0.43	1.1	0.3	3.31

Supplementary Table S4.1 *Continued.*

Samples	Longitude (°W)	Latitude (°N)	WD (m)	Total cysts	Concent. (cysts/g)	Concent. (pollen/g)	T1	T2	T3	T4	S1	S2	S3	S4	Ch1	Ch2	Ch3	Ch4	Ni	P	Ox
GeoB 9542-1	-15.03	10.142	33	0	0	0	24.38	27.76	27.52	27.62	35.04	35.53	34.08	32.33	21.52	1.30	1.05	1.29	1.7	0.3	4.41
GeoB 9544-1	-17.068	12.375	21	50	5378	215	20.71	24.13	28.02	26.79	35.30	35.70	35.33	33.69	4.21	4.13	3.04	5.6	1.9	0.4	3.95
GeoB 9545-1	-17.076	12.848	18	62	864	209	20.71	24.13	28.02	26.79	35.30	35.70	35.33	33.69	8.42	5.95	3.29	8.2	1.9	0.4	4.63
GeoB 9546-1	-17.09	13.453	18	200	1367	137	19.87	23.1	28.06	26.56	35.27	35.61	35.33	34.09	33.41	6.30	3.59	5.68	2.3	0.4	3.93
GIK 16769	-16.27	6.12	4933	61	368	-	27.4	28.26	27.14	28.36	35.14	35.39	35.06	34.53	0.14	0.14	0.14	0.13	0.2	0	5.64
GIK 16768	-15.17	7.62	4327	103	758	-	26.86	28.1	27.14	28.37	35	35.31	34.66	33.82	0.19	0.15	0.15	0.14	0.3	0.1	5.38
GIK 16767	-14.72	8.10	3123	120	1369	-	26.42	28	27.03	28.45	34.9	35.24	33.86	32.8	1.07	0.58	0.6	0.62	0.5	0.1	NA
GIK 16766	-14.53	8.28	2383	231	4832	-	26.42	28	27.03	28.45	34.9	35.24	33.86	32.8	1.07	0.58	0.6	0.62	0.5	0.1	5.07
GIK 16765	-14.48	8.32	1500	209	7693	-	26.42	28	27.03	28.45	34.9	35.24	33.86	32.8	1.07	0.58	0.6	0.62	0.5	0.1	4.59
GIK 16764	-14.43	8.37	885	152	1198	-	26.42	28.00	27.03	28.45	34.9	35.24	33.86	32.8	1.07	0.58	0.6	0.62	0.5	0.1	2.63
GIK 16558	-16.78	8.75	3123	148	255	-	25.93	27.53	27.3	28.29	35.15	35.50	34.73	33.98	0.16	0.41	0.14	0.14	0.5	0.1	5.4
GIK 16755	-16.85	9.25	1002	258	1495	-	25	26.99	27.41	28.02	35.15	35.53	34.6	33.58	0.65	0.21	0.19	0.19	0.9	0.2	NA
GIK 16437	-17.92	16.93	2766	341	16762	-	19.66	21.53	27.77	27.75	35.76	35.73	35.95	35.67	1.94	2.55	1.7	1.59	3.6	0.3	5.35
GIK 16425	-19.02	9.13	4802	67	133	-	25.15	26.39	27.43	28.22	35.46	35.75	35.30	35.03	0.20	0.2	0.21	0.2	0.3	0.1	5.36
GIK 16421	-17.87	9.88	1507	169	891	-	24.9	26.7	27.45	28.09	35.28	35.63	34.95	34.23	0.23	0.27	0.26	0.2	0.7	0.2	4.65
GIK 16414	-19.25	9.97	4290	72	303	-	25.15	26.39	27.43	28.22	35.46	35.75	35.30	35.03	0.24	0.26	0.25	0.2	0.3	0.1	5.56
GIK 16407	-21.95	9.03	4586	74	469	-	25.35	26.9	27.31	28.14	35.57	35.84	35.52	35.26	0.16	0.13	0.14	0.14	0.1	0	5.43
GIK 16405	-21.40	12.25	4870	102	879	-	23.23	24.3	27.26	27.28	35.57	35.88	35.84	35.36	0.38	0.21	0.2	0.18	0.4	0.1	5.48
GIK 16404	-21.28	12.67	4787	77	1228	-	23.23	24.3	27.26	27.28	35.57	35.88	35.84	35.36	0.38	0.21	0.2	0.18	0.4	0.1	5.48
GIK 16402	-20.57	14.42	4203	107	3202	-	21.74	23.13	27	26.56	35.61	35.89	35.91	35.43	0.6	0.58	0.34	0.47	0.9	0.2	5.35

T = sea surface temperature (°C), S = sea surface salinity (psu), Ch = chlorophyll_a concentration at the surface (mg/m^3), Ni = nitrate concentration at the surface (µmol/l), P = phosphate concentration at the surface (µmol/l), Ox = bottom water oxygen content (ml/l) and WD = water depth. 1 = winter (January-March), 2 = spring (April-June), 3 = summer (July-September), 4 = autumn (October-December)

.**Supplementary Table S4.2**

List of the identified dinoflagellate cyst species in the investigated surface sediments

(Nomenclature after Marret and Zonneveld. 2003)

Cyst name	Motile affinity	Grouping
Lingulodinium machaerophorum	*Lingulodinium polyedrum*	*L.machaerophorum. L. machaerophorum var. short processes*
Gonyaulacaceae family		
Cysts of *Pentapharsodinium dalei*	*Pentapharsodinium dalei*	
Polysphaeridium zoharyi	*Pyrodinium bahamense*	
Nematosphaeropsis labyrinthus	*Gonyaulax spinifera*	
Operculodinium israelianum	*? Protoceratium sp.*	
Operculodinium centrocarpum	*Protoceratium reticulatum*	*O. centrocarpum* and *O. centrocarpum var. short processes.*
Impagidinium aculeatum	*Gonyaulax sp*	
Imapagidinium patulum	*Gonyaulax sp*	
Imapagidinium spp.		*Impagidinium paradoxum* and *Impagidinium spp.*
Spiniferites mirabilis	*Gonyaulax spinifera*	*S. mirabilis* and *S. hypercanthus*
Spiniferites bentorii	*Gonyaulax digitale*	
Spiniferites pachydermus	*Gonyaulax spinifera*	
Spiniferites ramosus	*Gonyaulax sp*	
Spiniferites spp.	*Gonyaulax sp*	*S. bulloideus. S. membranaceus. Spiniferites delicatus* and *S. spp*
Peridineaceae family		
Brigantedinium spp.		Cyst of *Protoperidinium spp.. Votadinium calvum. Votadinium spinosum. Stelladinium stellatum.* Cysts of *P. americanum* and *Xandarodinium xanthum*
Quinquecuspis concreta	*? Protoperidinium leone*	
Bitectatodinium spongium		
Lejeunecysta oliva	Unknown	
Selenopemphix quanta	*Protoperidinium conicum*	
Selenopemphix nephroides	*Protoperidinium subinerme*	
Trinovantedinium applanatum	*Protoperidinium pentagonum*	
Echinidinium granulatum	Unknown	
Echinidinium spp.	Unknown	*E. delicatum. E. granulatum* and *E.spp*
Echinidinium transparantum	Unknown	
Cysts of *Protoperidinium monospinum*		
Dubridinium sp.		
Polykrikaceae family		
Cyst of *Polykrikos kofoidii*	*Polykrikos kofoidii*	
Pyrophacaceae family		
Tuberculodinium vancampoae	*Pyrophacus steinii*	

References

Adkins, J., deMenocal, P., Eshel, G., 2006. The "African Humid Period" and the record of marine upwelling from excess 230Th in ODP hole 658C. Paleoceangoraphy 21, 4203.

Allen, J. R. M., Watts, W. A., McGee, E., and Huntley, B., 2002. Holocene environmental variability - the record from Lago Grande di Monticchio, Italy. Quaternary International 88, 69-80.

Colarco, P.R., Toon, O.B., Reid, J.S., Livingston, J.M., Russel, P.B., Redmann, J., Schmid, B., Maring, H.B., Savoie, D., Welton, E.J., Campbell, J.R., Holben, B.N., Levy, R., 2003. Saharan dust transport to the Caribbean during PRIDE: 2. Transport, vertical profiles and deposition in simulations of in situ and remote sensing observations. Journal of Geophysical Research 103, 8590.

Cremer, H., Sangiorgi, F., Wagner-Cremer, F., McGee, V., Lotter, A. F., and Visscher, H., 2007. Diatoms (Bacillariophyceae) and dinoflagellate cysts (Dinophyceae) from Rookery Bay, Florida, U.S.A. Carribbean Journal of Science 43(1), 23-58.

Dale, B., Fjellså, A., 1994. Dinoflagellate cysts as paleoproductivity indicators: state of the art, potential and limits. In: Zahn, R., Pedersen, T., Kaminiski, M., Labeyrie, L. (Eds.), Carbon Cycling in the Glacial Ocean: Constrains on the Ocean's Role in Global Change. Springer-Verlag, Berlin, pp. 521 – 537.

Dale, B., 1996. Dinoflagellate cyst ecology: modeling and geological applications. In: Jansonius, J., McGregor, D.C. (Eds.), Palynology: Principles and Applications, vol. 3. American Association of Stratigraphic Palynologists Foundation, Salt Lake City, pp. 1249-1275.

Dale, B., Thorsen, T.A., Fjellså, A., 1999. Dinoflagellate cysts as indicator of cultural eutrophication in the Oslofjord, Norway. Estuarine, Coastal and Shelf Science 48, 371 – 382.

Dale, B., Dale, A.L., Jansen, J.H.F., 2002. Dinoflagellate cysts as environmental indicators in surface sediments from the Congo deep-sea fan and adjacent regions. Palaeogeography, Palaeoclimatology, Palaeoecology 2893, 1 – 30.

de Menocal, P., Oritz, J., Guilderson, T., Sarnthein, M., 2000. Coherent High- and low- latitude climate variability during the Holocene warm period. Science 288, 2198-2202.

de Vernal, A., Turon, J.-L., Guiot,J., 1994. Dinoflagellate cyst distribution in high latitude environments and quantitative reconstruction of sea-surface temperature, salinity and seasonality. Canadian Journal of Earth Sciences 31, 48-62.

de Vernal, A., Rochon,A., Turon, J-L., Matthiessen, J., 1997., Organic-walled dinoflagellate cysts: palynological tracers of sea-surface conditions in middle to high latitude marine environments. Geobios 30, 905-920.

de Vernal, A., Henry, M., Matthiens, J., Mudie, P.J., Rochon, A., Boessenkool, K.P., Eynaud, F., Grøsfjeld, K., Guiot, J., Hamel, D., Harland, R., Head, M.J., Kunz-Pirrung, M., Levac, E., Loucheur, V., Peyron, O., Pospelova, V., Radi, T., Turon, J.-L., Voronina, E., 2001. Dinoflagellate cyst assemblages as tracers of sea-surface conditions in the Northern Atlantic, Arctic and sub-Arctic seas: the new "n=677" data base and its application for quantative paleoceanographic reconstruction. Journal of Quaternary Science 16(7), 681-698.

Fensome, R.A., Williams, G.L., 2004. The Lentin and Williams index of fossil dinoflagellate, 2004 Edition. American Association of Stratigraphic Palynologist Foundation contributions series 42. 909 pp.

Folland, C.K., Palmer, T.N. and Parker, D.E., 1986. Sahel Rainfall and Worldwide Sea Temperatures, 1901-85. Nature 320 (6063), 602-607.

Gasse, F., 2000. Hydrological changes in the African tropics since the Last Glacial Maximum. Quaternary Science Reviews 19, 189-211.

Harland, R., 1994. Dinoflagellate cysts from the glacial/post-glacial transition in the northeast Atlantic Ocean. Palaeontology 37, 263 – 283.

Holzwarth, U., Esper, O. and Zonneveld, K. 2007. Distribution of organic-walled dinoflagellate cysts in shelf surface sediments of the Benguela upwelling system in relationship to environmental conditions. Marine Micropaleontology 64, 91-119.

Hooghiemstra, H., Agwu C.O.C., 1986. Distribution of palynomorphs in marine sediment: a record for seasonal wind patterns over NW Africa and adjacent Atlantic. Geologische Rundschau 75, 81 - 95.

Hooghiemstra, H., Lézine, A.M., A.G. Leroy, S., Dupont, L.M., Marret, F., 2006. Late Quaternary palynology in marine sediments: A synthesis of the understanding of pollen distribution patterns in the NW African setting. Quaternary International 148, 29-44.

Hopkins, J. A. and McCarthy, F. M. G., 2002. Post-depositional palynomorph degradation in Quaternary shelf sediments: a laboratory experiment studying the effects of progressive oxidation. Palynology 26, 167-184.

Hsu, C.P.F., Wallace, J.M., 1976. The global distribution in annual and semiannual cycles in precipitation. Monthly Weather Review 104(9), 1093-1101.

Kodrans-Nsiah, M., 2008. A natural exposure experiment on short-term species-selective aerobic degradation of dinoflagellate. Review of Paleobotany and Palynology (In press)

Lamb, H.F., Gasse, F., Benkaddour, A., El Hamouti, N., van der Kaars, S., Perkins, W.T., Pearce, N.J., Roberts, C.N., 1995. Relation between century-scale Holocene arid intervals in tropical and temperate zones. Nature 373, 134-136.

Lewis, J., 1988. Cysts and sediments: *Gonyaulax polyedra* (*Lingulodinium machaerophorum*) in Loch Ceran. Journal of the Marine Biology Association of the United Kingdom 68, 701-714.

Lewis, J., Dodge, J.D., Powell, A.J., 1990. Quaternary dinoflagellate cysts from the upwelling system offshore Peru, Hole 696B, ODP Leg 112. In: Suess, E., von Huene, R., et al. (Eds.), Proceeding of the Ocean Drilling Program. Scientific results, vol. 112, pp. 323-327.

Lewis, J. and Hallett, R., 1997. *Lingulodinium polyedrum* (*Gonyaulax polyedra*) a blooming dinoflagellate. Oceanography and Marine Biology: an Annual Review 35, 97-161.

Marret, F., 1994. Distribution of dinoflagellate cysts in recent marine sediments from the east Equatorial Atlantic (Gulf of Guinea). Review of Paleobotany and Palynology 84, 1-22.

Marret, F., de Vernal, A., 1997. Dinoflagellate cyst distribution in surface sediments of the Southern Indian Ocean. Marine Micropaleontology 29, 367-392.

Marret, F., Zonneveld, K., 2003. Atlas of modern organic-walled dinoflagellate cyst distribution. *Review of Palaeobotany and Palynology* 125, 1-200.

Mittelstaedt, E., 1991. The ocean boundary along the northwest African coast: Circulation and oceanographic properties at the sea surface. Progress in Oceanography 26, 307-355.

Mulitza, S., Bouimetarhan, I., Brüning, M., Freesemann, A., Gussone, N., Filipsson, H., Heil, G., Hessler, S., Jaeschke, A., Johnstone, H., Klann, M., Klein, F., Küster, K., März, C., McGregor, H., Minning, M., Müller, H., Ochsenhirt, W.T., Paul, A., Scewe, F., Schulz, M., Steinlöchner, J., Stuut, J.B., Tjallingii, R., Dobeneck, T., Wiesmaier, S., Zabel, M. and Zonneveld, K., 2006. Report and preliminary results of Meteor cruise M65/1, Dakar – Dakar, 11.06.–01.07.2005. Berichte, Fachbereich Geowissenschaften, Universität Bremen, No. 252, 149 pp.

Nave, S., Freitas, P., Abrantes, F., 2001. Coastal upwelling in the Canary Island region: spatial variability reflected by the surface sediment diatom record. Marine Micropaleontology 42, 1-23.

Nicholson, S.E., 2000. The nature of rainfall variability over Africa on time scales of decades to millenia. Global and planetary change 26, 137-158.

Nicholson, S.E., 2001. Climatic and environmental change in Africa during the last two centuries. Climate Research 17, 123 – 144.

Nicholson, S.E., Grist, J.P., 2003. The seasonal evolution of the atmospheric circulation over West Africa and Equatorial Africa. Journal of Climate 16 (7), 1013-1030.

Nykjaer, L., Van Camp, L., 1994. Seasonal and interannual variability of coastal upwelling along Northwest Africa and Portugal from 1981 to 1991. Journal of Geophysical Research 99, 14197-14207.

Pospelova, V., Head, M.J., 2002. Islandinium brevispinosum sp. Nov. (Dinoflagellata), a new species of organic-walled dinoflagellate cyst from modern estuarine sediments of New England (USA). Journal of Phycology 38, 593 – 601.

Pospelova, V., Chmura, G.L., Boothman, W.S., Latimer, J.S., 2005. Spatial distribution of modern dinoflagellate cysts in polluted estuarine sediments from Buzzards Bay (Massachusetts, USA) embayments. Marine Ecology Progress Series 292, 23 – 40.

Pospelova, V., Pedersen, T.F., 2006. Dinoflagellate cyst evidence for Late Quaternary climate and marine productivty changes along the californian Margin. In: Poulsen, N.E. (Ed.), The International Workshop on Dinoflagellate and their Cysts: their ecology and Databese for Paleoenvironmental Reconstrutions. Geological Survey of Denmark and Greenland (GEUS), Copenhagen, Denmark, pp. 26 – 27.

Pospelova, V., de Vernal, A., Pedersen, T.F., 2008. distribution of dinoflagellate cysts in surface sediments from the northeastern Pacific Ocean (43 – 25°N) in realtion to sea-surface temperature, salinity, productivity and coastal upwelling.

Prospero, J.M., Nees, R.T., 1986. Impact of the North African drought and El Nino on mineral dust in the Barbados trade winds. Nature 320, 735-738.

Prospero, J.M., Ginoux, P., Torres, O., Nicholson, S.E., Gill, T.E., 2002. Environmental characterization of global sources of atmospheric soil dust identified with the nimbus 7 total zone mapping spectrometer (TOMS) absorbing aerosol product. Review of Geophysics 40, 2-1/ 2-31.

Radi, T., de Vernal, A., Peyron, O., 2001. Relationships between dinocyst assemblages in surface sediments and hydrographic conditions in the Bering and Chukchi seas. Journal of Quaternary Science 16, 667-680.

Radi, T., de Vernal, A., 2004. dinocyst distribution in surface sediments from the northeastern Pacific margin (40 - 60°N) in relation to hydrographic conditions, productivity and upwelling. Review of Paleobotany and Palynology 128, 169-193.

Radi, T., Pospelova, V., de Vernal, A., Barrie, V.J., 2007. Dinoflagellate cysts as indicators of water quality and productivity in British Columbia estuarine environments. Marine Micropaleontology 62, 269 – 297.

Reichart, G. J. and Brinkhuis, H., 2003. Late Quaternary *Protoperidinium* cysts as indicators of paleoproductivity in the northern Arabian Sea. Marine Micropaleontology 937, 1-13.

Rochon, A., de Vernal, A., Sejrup, H.-P., Haflidson, H., 1998. Palynological evidence of climatic and oceanographic changes in the North Sea during the last deglaciation. Quaternary Research 49, 197-207.

Rochon, A., de Vernal, A., Turon, J.L., Matthiessen, J., Head, M.J., 1999. Distribution of recent dinoflagellate cysts in surface sediments from the North Atlantic Ocean and adjacent seas in relation to sea-surface parameters. American Association of Stratigraphic Palynologists Foundation, 23, 1- 150.

Sangiorgi, F., Donders, T.H., 2004. Reconstructing 150 years of eutrophication in the north-western Adriatic Sea (Italy) using dinoflagellate cysts, pollen and spores. Estuarine, Coastal and Shelf Science 60, 69-79.

Santarelli, A., Brinkhuis, H., Hilgen, F., Lourens, L., Versteegh, G.J.M., Visscher, H., 1998. Orbital signatures in a late Miocene dinoflagellate record from Crete (Greece). Marine Micropaleontology 33, 273-297.

Santos, M.A., Kazmin, A.S., Peliz, A., 2005. Decadal changes in the canary upwelling systema s revealed by satellite observations: Their impact on productivity. Journal of Marine Research 63, 359 – 379.

Sarnthein, M., G. Tetzlaff, B. Koopmann, K. Wolter, U. Pflaumann, 1981. Glacial and interglacial wind regimes over the eastern subtropical Atlantic and North-West Africa, *Nature, 293*, 193-196.

Sarnthein, M., Thiede, J., Pflaumann, U., Erlenkeuser, H., Fütterer, D., Koopmann, B., Lange, H.E.S., 1982. Atmospheric and oceanic circulation patterns off Northwest Africa during the past 25 million years. *In* Von Rad, U., Hinz, K., Sarnthein, M., Seibold, E. (Eds), Geology of the Northwest African continental margin. Springer, Berlin, pp. 584-604.

Schefuß, E., Schouten, S. Schneider, R.R., 2005. Climatic controls on central African hydrology during the past 20,000 years. Nature 437, 1003-1006.

Siringan, F. P., Azanza, R. V., Macalalad, N. H., Zamora, P. B., and Maria, M. Y. Y. S., 2008. Temporal changes in cyst densities of *Pyrodiniumbahamense* var. *compressum* and other dinoflagellates in the Manila Bay, Philippines. Harmful Algae , 1-31.

Stuut, J-B., Zabel, M., Ratmeyer, V., Helmke, P., Schefuß, E., 2005. Provenance of present-day eolian dust collected off NW Africa. Journal of Geophysical Research 110, 4202 – 5161.

Susek, E., 2005. Environmental factors influencing cyst formation and preservation of organic-walled dinoflagellate : an environmental and laboratory study. PhD. Thesis. Department of Geosciences at the University of Bremen. 123pp.

ter Braak, C.J.F., Smilauer, P., 1998. Canoco 4. Centre for Biometry. Wageningen. Versteegh, G.J.M., 1997. The onset of northern hemisphere glaciations and its impact on dinoflagellate cysts and acritarchs from the Singa section (south Italy and ODP core 607 (North Atlantic). Marine Micropaleontology 30, 319-343.

Versteegh, G.J.M., Zonneveld, K.A.F., 2002. Use of selective degradation to separate preservation from productivity. Geology 30, 615 – 618.

Vink, A., Zonneveld, K.A.F., Willems, H., 2000. Organic-walled dinoflagellate cysts in western equatorial Atlantic surface sediments: distributions and their relation to environment. Review of Palaeobotany and Palynology 112. 247 – 286.

Walter,H., Lieth,H., 1960. Klimadiagramm - Weltatlas, Fischer Verlag, Jena. Wang, G., Eltahir, E.A.B., 2000. Biosphere –atmosphere interactions over West Africa 2. Multiple equilibria. Quarterly Journal of the Royal Meteorological Society 126, 1261–1280.

Wang, Y. H., Qu, Y. Z., Lu, S. H., Wang, Y., and Matsuoka, K., 2004a. Seasonal distribution of dinoflagellate resting cysts in surface sediments from Changjiang River Estuary. Phycological Research 52(4), 387-395.

Wang, Z. H., Matsuoka, K., Qi, Y. Z., Chen, J. F., and Lu, S. H., 2004b. Dinoflagellate cyst records in recent sediments from Daya Bay, South China Sea Phycological Research 52(4), 396-407.

Weldeab, S., Schneider, R.R., Kölling. M, Wefer, G., 2005. Holocene African droughts relate to eastern equatorial Atlantic cooling. Geology 12, 981-984.

World Ocean Atlas, 2005:http://www.nodc.noaa.gov/OC5/WOA05/pr_woa01.html

World Resources Institute, 2003. http://www.wri.org/

Zonneveld, K.A.F., 1997. Dinoflagellate cysts distribution in surface sediments of the Arabian sea (Northwestern Indian Ocean) in relation to temperature and salinity gradients in the upper water column. Deep-Sea Research II 44, 1411-1443.

Zonneveld, K.A.F., 1997. New species of organic walled dinoflagellate cysts from modern sediments of the Arabian Sea (Indian Ocean). Review of Palaeobotany and Palynology, 97, 319-337.

Zonneveld, K.A.F., Jurkschat, T., 1999. *Bitectatodinium spongium* (Zonneveld, 1997)

Zonneveld et Jurkschat *comb.nov.* from modern sediment and sediment trap samples of the Arabian Sea (northwestern Indian Ocean): taxonomy and ecological affinity. Review of Palaeobotany and Palynology 106, 153-169.

Zonneveld, K.A.F., Brummer, G.A., 2000. Ecological significance, transport and preservation of organic-walled dinoflagellate cysts in the Somali Basin, NW Arabian sea. Deep-sea research. Part 2,9, 2229-2256.

Zonneveld, K.A.F., Hoek, R., Brinkhuis, H. and Willems, H., 2001. Geographical distributions of organic-walled dinoflagellate cysts in surface sediments of the Benguela upwelling Region and their relationship to upper ocean conditions. Progress in Oceanography 48, 25-72.

Zonneveld, K.A.F., Mackensen, A., Baumann, K-H., 2007. Stable oxygen isotopes of *Thoracosphaera heimii* (Dinophyceae) in relationship to temperature; a culture experiment. Marine Micropaleontology 64, 80-90.

Chapter 5

Palynological evidence for climatic and oceanic variability off NW Africa during the late Holocene

Ilham Bouimetarhan[1,*], Lydie Dupont[2], Enno Schefuß[2], Gesine Mollenhauer[1,3], Stefan Mulitza[2], Karin Zonneveld[1]

[1] Department of Geosciences/MARUM, University of Bremen, Klagenfurter Strasse, D-28359 Bremen, Germany

[2] MARUM- Center of Marine Environmental Sciences, University of Bremen, Leobener Strasse, D-28359 Bremen, Germany

[3] Alfred-Wegener Institute for Polar and Marine Research, Am Handelshafen 12, 27570, Bremerhaven, Germany

Quaternary Research (Returned to Journal after moderate revisions)

Abstract

Pollen and organic-walled dinoflagellate cyst assemblages from core GeoB 9503-5 retrieved from the mud-belt (~50m water depth) off the Senegal River mouth have been analyzed to reconstruct short-term palaeoceanographic and palaeoenvironmental changes in subtropical NW Africa during the time interval from ca. 4200 to 1200 cal yr BP. Our study emphasizes significant coeval changes in continental and oceanic environments in and off Senegal and it shows that initial dry conditions were followed by a strong and rapid humidity increase between ca. 2900 and 2500 cal yr BP. After ca. 2500 cal yr BP, the environment slowly became drier again as indicated by slight increases in Sahelian savanna and desert elements in the pollen record. Around ca. 2200 cal yr BP, this relatively dry period ended with periodic pulses of high terrigenous contributions and strong fluctuations in fern spore and river plume dinoflagellate cyst percentages, in the total accumulation rates of pollen, dinoflagellate cysts, fresh-water algae and plant cuticles, suggesting "episodic flash flood" events of the Senegal River. The driest phase developed after about 2100 cal yr BP.

Keywords: Palaeoceanography, palaeoenvironment, pollen, organic-walled dinoflagellate cyst, Senegal River, mud-belt, little humid phase.

5.1 Introduction

Climatic variability has severe consequences for the human populations of West Africa. Most recently, the Sahel drought from the late sixties to early eighties of the last century caused famine and socio-economic decline (e.g. Nicholson, 2000). Recent studies from tropical and subtropical West Africa suggest that increasing humidity during the early to mid-Holocene was followed by an abrupt onset of aridity around 5500 cal yr BP (de Menocal et al., 2000) and by several dry climatic events between ca. 4500 and 2000 cal yr BP characterized by lowered water tables and precipitation estimates (Lézine and Chateauneuf, 1991; Maley and Brenac, 1998; Salzmann and Waller, 1998; Salzmann et al., 2002; Marchant and Hooghiemstra, 2004). These climatic fluctuations detected in several palaeoecological sites have been related to global climatic changes (Maley and Brenac, 1998; Gasse, 2000; Salzmann et al., 2002). A number of studies suggest a close relationship between

changes in ocean circulation and changes in African precipitation. (Lamb et al., 1995; Schefuß et al., 2005; Weldeab et al., 2005; Mulitza et al., 2008). To obtain insight into this relationship, a combined study of terrestrial palynomorphs (pollen and spores) and organic-walled dinoflagellate cysts (dinocysts) enables the recognition of simultaneous changes in both oceanic and atmospheric conditions and offers the opportunity to establish direct land-sea correlations of terrestrial and marine paleoenvironmental changes (Hooghiemstra, 1988b; Hooghiemstra et al., 2006). In this paper, we present an integrated description and interpretation of late Holocene high-resolution pollen and dinocyst records derived from a marine core from the mud-belt deposited on the inner shelf off Senegal close to the mouth of the Senegal River.

5.2 Environmental setting

5.2.1 Regional climate

The study site is located at a mud-belt deposited off the Senegal River mouth in North West (NW) Africa. The climate of NW Africa is mainly controlled by the West African monsoon circulation characterized by intense precipitation in summer and dry conditions in winter (Hsu and Wallace, 1976) caused by the seasonal movement of the Intertropical Convergence Zone (ITCZ). The ITCZ migrates between about 2°N and 12°N over the eastern Atlantic Ocean and 8°N and 24°N over the continent (Nicholson and Grist, 2003). Its northern position from July to September is some ten degrees of latitude north of the summer rainfall maximum forming the tropical rain belt which brings moist monsoon air to NW Africa producing most of the rainfall (Nicholson and Grist, 2003). Its southern position from December to February produces dry conditions in the study area associated with hot and dry continental trade winds blowing almost parallel to the NW African coast. Another main wind system is the Saharan Air Layer (SAL) related to the African Easterly Jet (AEJ), a mid-tropospheric zonal wind system occurring at higher altitudes (1500 – 5500 m) (Prospero, 1990). It is responsible for transporting dust and pollen offshore from the Sahara and Sahel belt to the Atlantic Ocean (Prospero and Nees, 1986; Prospero et al., 2002; Colarco et al., 2003) (Figure 5.1).

5.2.2 Oceanic circulation

The tropical East Atlantic off NW Africa is influenced by several oceanic currents (Figure 5.1) that are controlled by the prevailing wind systems. The dominant surface water current is the Canary Current (CC), the easternmost branch of the Azores Current. The CC flows southwestward along the NW African coast as far south as Senegal where it turns westward to join the Atlantic North Equatorial Current (Mittelstaedt, 1991).

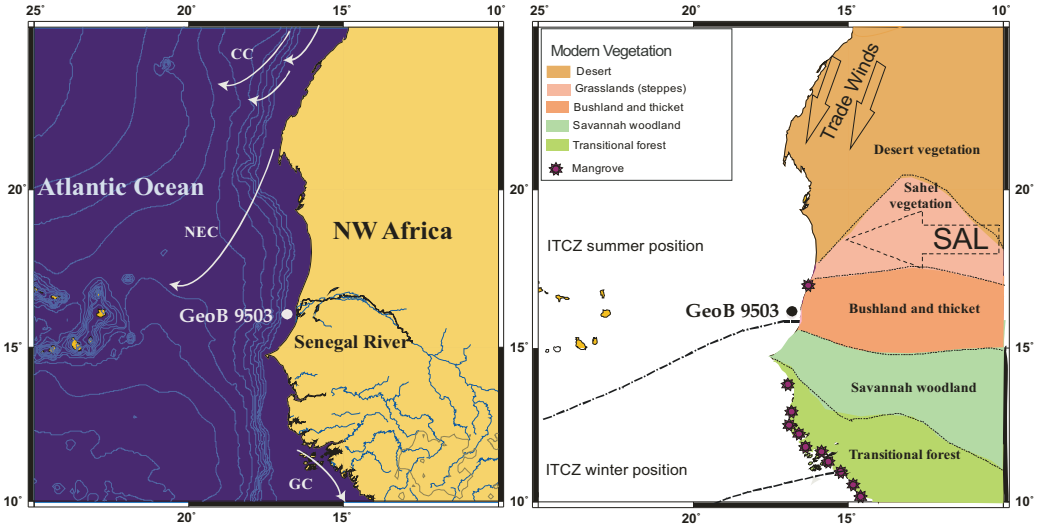

Figure 5.1 (A) Location map of marine core GeoB 9503-5 with major hydrographic systems and surface oceanic currents: CC: Canary Currents, NEC: North Equatorial Current, GC: Guinea Current (after Sarnthein et al., 1982 and Mittelstaedt, 1991). **(B)** Simplified phytogeography and biomes (after White 1983) with main wind belts (Saharan Air Layer (SAL) and trade winds). The dashed lines indicate the present day boreal summer (dash-dotted line) and boreal winter (dashed line) positions of the Intertropical Convergence Zone (ITCZ)

The alongshore flow is associated with upwelling when the position of the subtropical high pressure system strengthens the North East (NE) Trade Winds (Nykjaer and Van Camp, 1994). Filaments and eddies (Johnson and Stevens, 2000) entrain cool, upwelled water rich in nutrients from the coast and transport it up to several hundred km offshore (Mittelstaedt, 1991). The enhanced biological activity in these nutrient-rich waters is documented by diatoms, coccolitophores (Nave et al., 2001), dinocysts (Margalef, 1973) and planktonic foraminifera (Meggers et al., 2002). At the core site, sea surface temperatures (SST) range from 23 to 29°C (WOA, 2001). The sea surface salinities range from 34.8 to 35.6 psu. Salinities are

lower near the coast than offshore due to the freshwater input from the Senegal River.

5.2.3 Senegal River

The 1790 km-long Senegal River located between 10°20' - 17°00' N and 8°00 - 16°30'W, is one of the most active drainage systems of NW Africa. The total area of the Senegal River basin is about 419,650 km^2 (World Resources Institute, 2003). The river's flow regime is characterized by a high-water season from July to October with a peak flow generally occurring in late September and early October (Gac and Kane, 1986), while from November to June, the discharge of the Senegal River drops allowing seawater to penetrate the reduced river channel over a distance of approximately 250 km inland (Gac et al., 1985). The average water discharge at the last downstream point immediately landward of the estuary is 641m^3 / s, and the annual sediment load delivered to the Atlantic Ocean is ~2x10^9kg (Gac and Kane, 1986). Satellite images of the chlorophyll-*a* concentrations of the sea surface during boreal summer indicate that the plume of the Senegal River extends approximately 10 km offshore (http://reason.gsfc.nasa.gov).

5.2.4 Vegetation and pollen transport

The main vegetation belts in NW Africa reflect the North-South precipitation gradient (Figure 5.1). They range from Mediterranean vegetation containing trees and shrubs to the tropical rainforest along the Gulf of Guinea. In between, we find, from North to South, the steppes of the semi-desert area of the western Atlas region, desert vegetation of the Sahara, semi-desert grassland and shrubland of Sahelian (dry savannah) vegetation, and the Sudanian savannah zone (White, 1983). Coastal vegetation is represented by mangrove, occurring in estuaries and near the river mouths (White, 1983). The distribution of mangrove depends on water salinity, river runoff and humidity (Blasco, 1984). Today, mangroves are well developed off the Casamance and Gambia River mouths and the Saloum delta (Spalding et al., 1997). Their abundances decrease near the mouth of the Senegal River (Hooghiemstra et al., 1986).

In the NW African region, aeolian transport of pollen is mainly dependent on the two dominating wind systems, the NE trade winds and the SAL (Hooghiemstra and Agwu, 1986; Hooghiemstra et al., 1986). The Senegal River, on the other hand, is the most important fluvial source of pollen and other terrestrial particles in the study area. The vertical transport mechanisms of palynomorphs through the water column including marine snow formation, mid-water flows and particle repackaging in faecal pellets need to be considered as well (Fowler and Knauer, 1986; Jones et al., 1998). Hooghiemstra et al. (2006) stated that offshore NW Africa, the distribution of pollen over the ocean surface is reflected in the marine sediments without substantial displacement by marine currents.

5.3 Material and methods

We studied the marine sediment core GeoB 9503-5, recovered from the Senegal mud-belt off the mouth of Senegal River at approximately 50 meters water depth (16°03.99'N, 16°39.15'W and 791 cm length) during R/V *Meteor* cruise M65-1 (Mulitza et al., 2006). The entire sediment core consists of homogenous dark olive green mud with shell fragments.

5.3.1 Radiocarbon dating

Ten AMS radiocarbon dates were obtained at the Leibniz-Laboratory for Radiometric Dating and Stable Isotope Research in Kiel University from bivalve shells. Radiocarbon dates were converted to 1 σ calendar age ranges with the CALIB 5.0.2 software (Stuiver and Reimer, 2005) using the Intcal04 calibration curve, (Reimer et al. 2004) with a constant reservoir correction of 400 years (Bard, 1988; Bard et al., 2000) (Table 5.1). Sediment ages between dated core depths were calculated by linear interpolation.

5.3.2 Palynological processing

Fifty-six samples were taken at 10 to 20 cm intervals along the core and they were processed according to standard palynological preparation procedures (Faegri and Iversen, 1989). A volume of 1 cm^3 of wet sediment was oven-dried for 24h and subsequently weighed and decalcified using 10% hydrochloric acid (HCl). In order

to calculate palynomorph concentrations and accumulation rates one tablet of exotic *Lycopodium* spores (10679±426 spores/tablet) was added to the samples. The siliceous fraction was dissolved using 40% hydrofluoric acid (HF). Samples were agitated for 2 hours and left in the HF solution for one day without agitation. The resulting fraction was treated with 30% HCl again for ca. 24h to remove fluorosilicates. Subsequently the solution was decanted and demineralised water was added to the samples. We did not neutralize the samples, though after each of the above steps the supernatant solution was decanted and neutralized by 10% KOH prior to disposal. Finally, demineralised water was added to the samples. After 24 h the residual was washed and sieved through a 8 µm mesh size sieve using an ultrasonic bath (5 minutes) to disintegrate lumps of organic matter.

The residue was concentrated by centrifuging for 8 minutes at 3500 rotations per minute and resuspended in 1 ml of water. A 40µl to 60 µl aliquot was mounted on a slide using glycerine jelly and sealed with nail polish. One to four slides per sample were counted under a light microscope at 400 x and 1000 x magnification to a minimum of 100 pollen grains including herbs, shrubs, trees and aquatics and 200 dinocysts where possible.

The nomenclature of the identified dinocysts was based on published morphological descriptions and the cyst nomenclature follows de Vernal et al. (1997), Zonneveld (1997), Marret and Zonneveld (2003) and Fensome and Williams (2004). Pollen grains were identified using the African Pollen Database (Vincens et al., 2007) and Pollens des savanes d'Afrique orientale (Bonnefille and Riollet, 1980). Besides dinocysts and pollen, other palynomorphs, such as fern spores, plant cuticles and fresh water algae (*Botryococcus*, *Cosmarium*, *Pediastrum*, *Scenedesmus* and *Staurastrum*) were also counted.

Pollen counts are expressed as percentages of total pollen (including pollen of trees shrubs, herbs, and aquatics), spores are expressed as percentages of total pollen and spores. Dinocyst counts are expressed as percentages of total cysts. Additionally, pollen and dinocyst concentrations and accumulation rates were calculated. Calibrated age ranges were estimated using CALIB 5.0.2 and are based on the Intcal04 calibration curve (Reimer et al. 2004; Stuiver et al. 2005).

Table 5.1 Radiocarbon age data used to construct the age model for marine core GeoB9503 -5

Core depth (cm)	Lab Code	^{14}C age yr. B.P	1 σ calendar age ranges	Calibrated age (cal. yr BP)
20	KIA 28454	1675 ± 30	1225 - 1383 BP	1240
70	KIA 29768	1870 ± 30	1327 - 1383 BP	1355
140	KIA 29767	2310 ± 30	1824 - 1883 BP	1855
213	KIA 28452	2555 ± 30	2113 - 2158 BP	2140
320	KIA 29766	2665 ± 30	2205 - 2232 BP	2210
410	KIA 29765	2740 ± 30	2335 - 2358 BP	2350
529	KIA 28451	2925 ± 30	2540 - 2592 BP	2550
600	KIA 29764	2965 ± 30	2710 - 2748 BP	2730
700	KIA 29763	3600 ± 30	3391 - 3445 BP	3420
780	KIA 28450	4140 ± 35	4079 - 4150 BP	4110

5.3.3 Statistical methods

In order to establish a grouping of dinocyst species based on their ecological preferences and to define the diagram zones with more consistency, we performed the multivariate ordination technique Principal Component Analysis (PCA) on the relative abundances (ter Braak and Smilauer, 1998) of dinocyst species as well as on the 56 samples. A Detrended Correspondence Analysis (DCA) conducted prior to PCA indicated that species distributions within the dataset show a linear relationship to underlying gradients validating the application of linear ordination. Prior to statistical analyses, some dinocyst species have been grouped together as indicated in supplementary table S5.1.

5.4 Results

5.4.1 Age model

Radiocarbon dates from 10 samples ranging between 20 and 780 cm core depth are presented in table 1. The time period represented by core GeoB 9503-5 ranges from approximately 1200 cal yr BP to 4200 cal yr BP (Figure 5.2). Maximum sedimentation rates of 1.53 cm / yr occurred at the time period between ca. 2200 and 2100 cal yr BP and a minimum of 0.16 cm / yr is observed between ca. 4200 and 3400 cal yr BP.

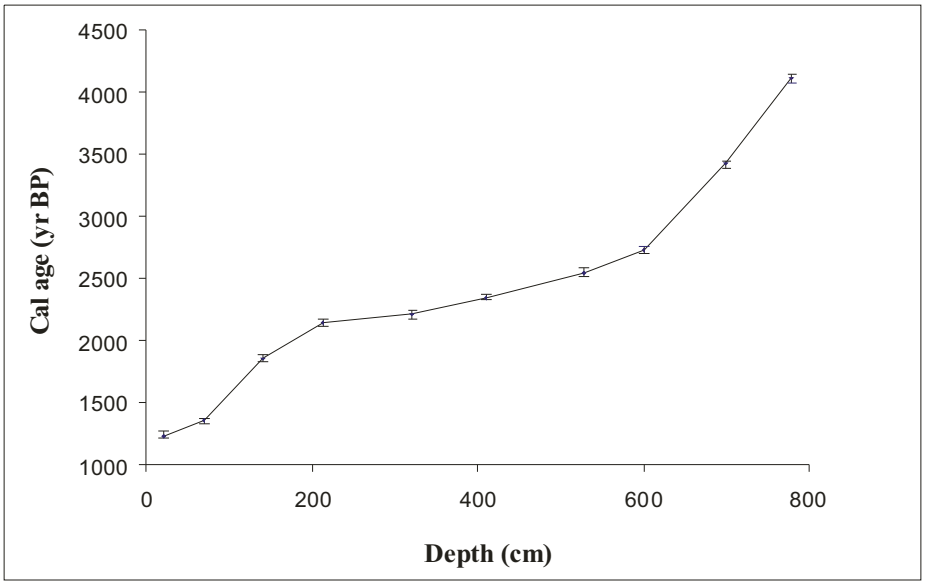

Figure 5.2 Age-depth graph for core GeoB 9503-5.

5.4.2 Principal component analysis (PCA)

Based on the regional distribution of dinocyst assemblages in surface sediments off West Africa (Bouimetarhan et al., in review) and the PCA results, four ecological groups of dinocysts can be distinguished (Figure 5.3A)

Group 1: Shelf association

Spiniferites mirabilis, *Spiniferites ramosus*, *Spiniferites spp*, *Spiniferites pachydermus*, *Spiniferites bentorii* and *Operculodinium centrocarpum.* These species are produced by phototrophic dinoflagellates. In modern sediments they have their highest relative abundances in shelf regions (Marret and Zonneveld, 2003). This association is used as an indicator for high nutrient concentrations in shelf areas (Bouimetarhan et al., accepted).

Group 2: Upwelling association

Brigantedinium spp., *Echinidinium transparantum*, *Echinidinium* spp.,cysts of *Protoperidinium monospinum*, *Protoperidinium* spp., cysts of *Polykrikos kofoidii*, *Quinquecuspis concreta*, *Selenopemphix nephroide*s, *Selenopemphix quanta* and *Xandarodinium xanthum*. These species have their highest relative abundances in areas that are characterized by high productivity in the upper waters such as

upwelling regions (Marret and Zonneveld, 2003; Holzwarth et al., 2007). This group is used as an indicator for nutrient-rich waters, linked to upwelling in the study region (Bouimetarhan et al., accepted).

Group 3: Lagoon assemblage

Lingulodinium machaerophorum, cyst of *Pentaspharsodinium dalei, Polysphaeridium zoharyi, Operculodinium centrocarpum* with short processes, *Operculodinium israelianum* and *Tuberculodinium vancampoae*. This group includes species that are known from regions with extreme changes in sea-surface salinities (SSS) and/or are characteristic for lagoon areas (Marret and Zonneveld, 2003).

Group 4: River plume assemblage

Echinidinium granulatum, *Trinovantedinium appelanatum*, *Lejeunecysta oliva* and *Bitectatodinium spongium*. These species occur at high relative abundances in regions that are influenced by river discharge waters (Zonneveld and Jurkschat, 1999; Marret and Zonneveld, 2003; Holzwarth et al., 2007). This group is used as an indicator for river runoff (Bouimetarhan et al., accepted).

Figure 5.3 (A) PCA ordination plot of individual dinoflagellate species (>1%). **Group1**: Smir: *Spiniferites mirabilis*, Sspp: *Spiniferites* spp., Sbent: *Spiniferites bentorii*, Spach: *Spiniferites pachydermus*, Sram: *Spiniferites ramosus*, O.centro: *Operculodinium centrocarpum*. **Group2**: Pmon: cysts of *Protoperidinium monospinum*, Squa: *Selenopemphix quanta*, Qcon: *Quinquecuspis concreta*, Pspp. cysts of *Protoperidinium* spp., Xanxan: *Xandarodinium xanthum*, Pkof: cysts of *Polykrikos kofoidii*, Espp: *Echinidinium* spp., Sneph: *Selenopemphix nephroides*, Etrans: *Echinidinium transparantum*, Bspp: *Brigantedinium* spp. **Group3:** Pdal: cysts of *Pentapharsodinium dalei,* Tvan: *Tuberculodinium vancampoae*, Oisr: *Operculodinium israelianum,* Lmach: *Lingulodinium machaerophorum*, O.centro shor: *Operculodinium centrocarpum* short, Pzoh: *Polysphaeridium zoharyi*. **Group 4:** Tapp: *Trinovantedinium applanatum*, Egra: *Echinidinium granulatum*, Loli: *Lejeunecysta oliva*, Bitesp: *Bitectatodinium spongium.* **(B)** PCA ordination plot of the 56 samples (ages in 1000 cal yr BP) from core GeoB 9503-5. Light grey triangles stand for the zone B samples, dark triangles for the zone D samples, and grey rectangles denote the zones A, C, and E.

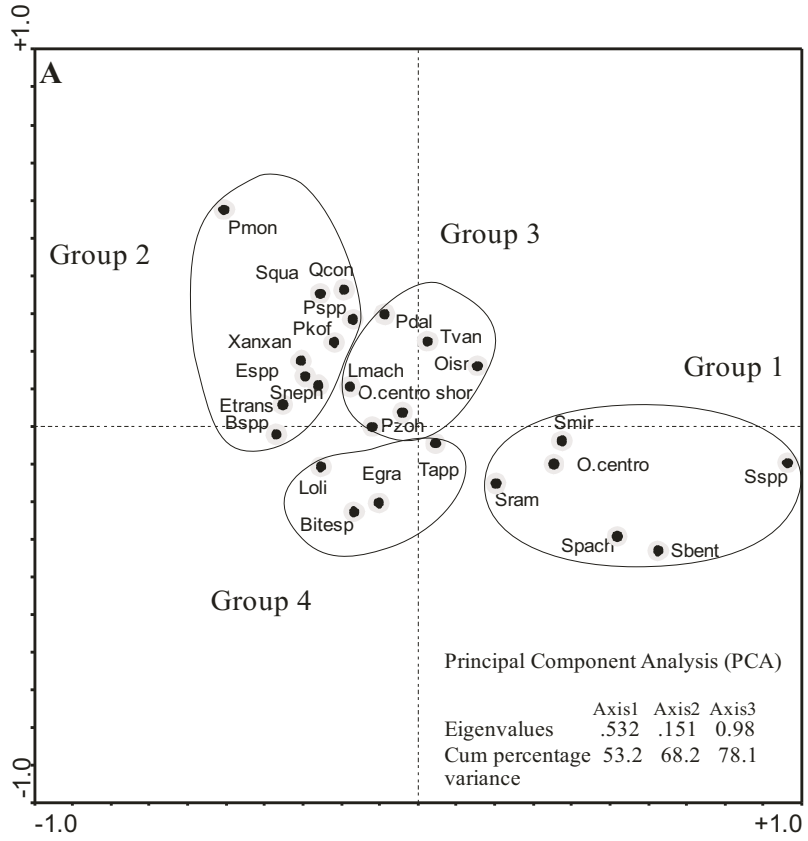
A
+1.0
-1.0
-1.0
+1.0
Group 1
Group 2
Group 3
Group 4
Pmon
Squa
Qcon
Pspp
Pkof
Xanxan
Espp
Sneph
Etrans
Bspp
Pdal
Tvan
Oisr
Lmach
O.centro shor
Pzoh
Tapp
Egra
Loli
Bitesp
Smir
O.centro
Sspp
Sram
Spach
Sbent
Principal Component Analysis (PCA)
Axis1 Axis2 Axis3
Eigenvalues .532 .151 0.98
Cum percentage variance 53.2 68.2 78.1

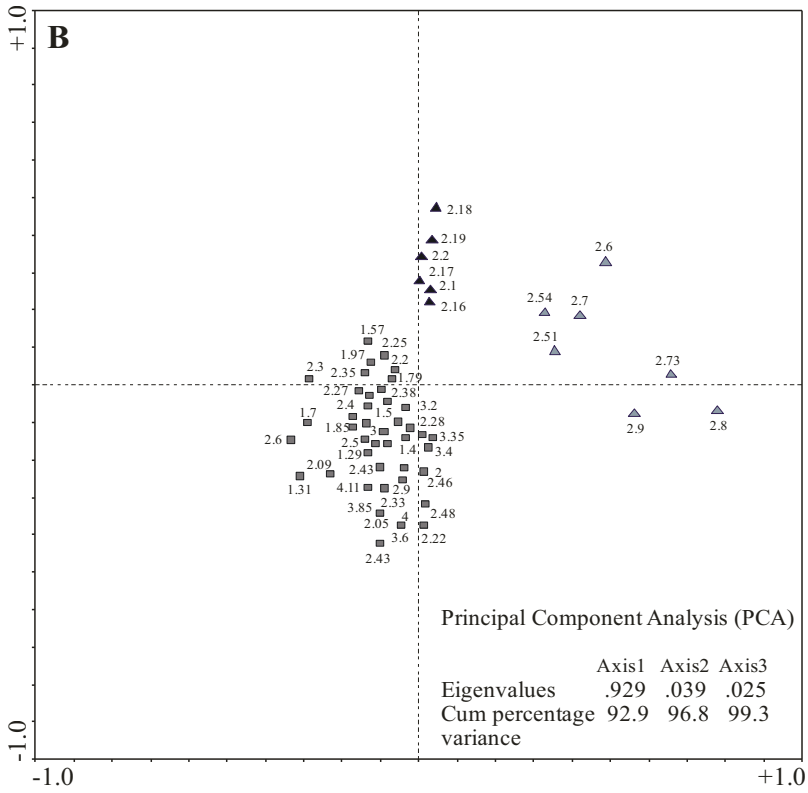
B
+1.0
-1.0
-1.0
+1.0
Principal Component Analysis (PCA)
Axis1 Axis2 Axis3
Eigenvalues .929 .039 .025
Cum percentage variance 92.9 96.8 99.3

The PCA ordination of the samples reveals three distinct clusters. The first cluster comprises samples from 2900 to 2500 cal yr BP that are ordinated at the most positive side of the first axis, samples from 2200 to 2100 cal yr BP are grouped in a second cluster at the positive sides of the first and the second axes, and all the other samples are ordinated at the negative sides of the first and the second PCA axes (Figure 5.3B).

5.4.3 Dinocysts and pollen records

Based on contemporaneous changes in the dinocyst and pollen assemblages as well as on the PCA of the 56 samples, five different zones can be recognised (Figure 5.4). Pollen and dinocysts taxa that never exceed 1% of the total population were excluded from interpretation.

A total of 40 dinocyst taxa were identified (Supplementary Table S5.1). Dinocyst concentrations from core GeoB 9503-5 range between 584 and 45785 cysts / cm^3, reaching maximum values at ca. 2800 cal yr BP (611 cm). The accumulation rates of dinocysts range from 257 to 8231 cysts / cm^2 / yr, reaching maximum values at ca. 2580 cal yr BP (541 cm) (Figure 5.4). A total of 32 pollen taxa were identified and they were grouped according to studies of modern pollen distribution off NW Africa, and their relationship with source areas and transport systems (Hooghiemstra et al., 1986; Dupont and Agwu, 1991; Lézine et al., 1995; Lézine, 1996). The different groups are listed in supplementary table S5.2. Pollen concentrations range between 654 and 7752 pollen grains / cm^3, reaching maximum values at ca. 4030 cal yr BP (771 cm). The accumulation rates of pollen range from 168 to 3780 grains /cm^2 / yr, reaching maximum values at ca. 2160 cal yr BP (251 cm) (Figure 5.4).

Zone A: From ca. 4200 to 2900 cal yr BP. (790 - 630 cm, 11 samples)

The dinocyst concentrations are relatively low in this interval reaching a maximum of 12935 cysts / cm^3 at ca. 3220 cal yr BP (671 cm). Dinoflagellate associations are characterised by high amounts of upwelling species, accounting for up to 59% of the assemblage at ca. 4030 cal yr BP (771 cm), such as cysts of *P. monospinum, S. quanta, S. nephroides* and *Brigantedinium* spp. (Figure 5.4)

Pollen concentrations reach the highest values in the core with a maximum of 7752 pollen grains / cm^3 at ca. 4030 cal yr BP (771 cm). The pollen assemblages are dominated by the Sahelian Savannah elements where Poaceae (grasses) pollen is dominant and percentages reach 82% at ca. 3860 cal yr BP (751 cm). Conversely, percentages of Cyperaceae pollen and Amaranthaceae/Chenopodiaceae (Cheno-Am; representatives of salt-marshes) are low. *Rhizophora* (mangrove tree) pollen values fluctuate between 2 and 17% reaching their highest percentage in this record at ca. 4030 cal yr BP (781 cm) and Asteroideae (Compositae Tubuliflorae) pollen are less than 4%. This interval shows a low occurrence of Sahelian elements such as *Acacia (*2%) and *Mitracarpus* (5%). Percentages of fern spores range from 1 to 11%. Fresh water algae and plant cuticle fluxes have low values (Figure 5.5).

Zone B: From ca. 2900 to 2500 cal yr BP. (630 - 500 cm, 9 samples)

This zone is characterized by an increase in sedimentation rates (Figure 5.4). The time interval is also marked by a strong increase in total dinocyst concentrations and accumulation rates, reaching a maximum of 45758 cysts / cm^3 at ca. 2800 cal yr BP (611 cm) and 8231 cysts /cm^2 / yr at ca. 2580 cal yr BP (541 cm), respectively. It is also characterized by a marked shift from heterotrophic / upwelling association to phototrophic/shelf association dominance. The shelf association accounts for 83% of the assemblage at ca. 2870 cal yr BP (621 cm). Percentages of *S. mirabilis* (12%) and *S. ramosus* (7%) reach their highest values along the core. In addition, this zone is characterised by high amounts of the river plume species with *T. appelanatum* contribution of 8% to the total. Species of the lagoon assemblage are also relatively well represented in this interval, such as cyst of *P. dalei* (5%) and *T. vancampoae* (3%). *P. zoharyi* and *O. centrocarpum* with reduced process length occur in low percentages.

Pollen concentrations decrease markedly during the time interval from 2900 to 2500 cal yr BP. The pollen assemblage shows a slight increase of Cyperaceae pollen (19%) and a considerable occurrence of fern spores (18%) accompanied by an increase of *Acacia* (5%) and Cheno-Am (9%). In this zone, *Rhizophora* pollen values decreases to 1.8 % at ca. 2500 cal yr BP (501 cm) and Asteroideae pollen decreases to 1% at ca. 2630 cal yr BP (561 cm). *Typha* pollen percentages increase and vary from 3 % at ca. 2500 cal yr BP (501 cm) to 7% at ca. 2555 cal yr BP (531 cm). This

interval shows rather high percentages of *Acacia* (5%) and *Mitracarpus* (6%) and low representation of *Mimosa* (1%) (Figure 5.5). The total fresh-water algae fluxes and concentrations increase to a maximum value of 112 / cm^2 / yr and 780 / cm^3 respectively at ca. 2870 cal yr BP (621 cm). Plant cuticles are well represented, their fluxes increase to 2738 / cm^2 / yr at ca. 2700 cal yr BP (591 cm) and concentrations reach a maximum value of 9540 / cm^3 at ca. 2730 cal yr BP (601 cm).

Zone C: From ca. 2500 to 2230 cal yr BP. (500 - 330 cm, 12 samples).

Both the total accumulation rates and concentrations of dinocysts decrease substantially relative to the previous interval (Figure 5.4). This zone is characterized by dominance of the upwelling association (61%), in particular cysts of *P. monospinum* (20%), *S. quanta* (19%), and *Brigantedinium* spp. (17%). Percentages of elements of the phototrophic/shelf association, lagoon and river plume assemblages decrease.

The total pollen flux and concentrations increase gradually to 2070 grains/cm^2/yr and 3220 grains / cm^3, respectively at ca. 2250 cal yr BP (351 cm). Although the Poaceae are still the dominant group, their percentages do not exceed 70% and decreases to 36 % at ca. 2380 cal yr BP (431 cm). The percentages of Cyperaceae pollen vary from 4 to 19%. During this time interval, *Typha* pollen values decrease to 3% at ca. 2470 cal yr BP (481 cm) with an increase in the middle part reaching 7% at ca. 2390 cal yr BP (431 cm). Abundances of semi-desert elements such as Asteroideae pollen increase to 3% at ca. 2270 cal yr BP (361 cm) but Cheno-Am percentages decrease in this interval to 1% at ca. 2470 cal yr BP (481 cm) except for a small increase to 8% at ca. 2380 cal yr BP (431 cm). *Rhizophora* pollen abundance decreases. Percentages of *Acacia* are low while *Mitracarpus* pollen percentages reach a maximum of 11% at ca. 2380 cal yr BP (431 cm). *Olea* pollen is present in this interval but does not exceed 1%. *Pinus* pollen percentages reach 3% at ca. 2470 cal yr BP (481 cm) (Figure 5.5). Spore percentages decrease markedly after the high values of the previous zone. The total fresh-water algae and plant cuticle fluxes are at minimum values in this zone.

***Zone D*:** From ca. 2230 to 2130 cal yr BP. (330 – 210 cm, 10 samples).

This interval is characterized by a rapid increase of sedimentation rates and strong fluctuations in the total accumulation rates of pollen, dinoflagellate cysts, fresh-water algae, and plant cuticles as well as percentages of pollen, spores and dinocysts (Figure 5.4). Dinoflagellate cyst accumulation rates abruptly increase to 7614 cysts /cm^2 / yr at ca. 2170 cal yr BP (261 cm). The upwelling association still dominates the dinocyst assemblages in this part of the diagram. Lagoon and river plume assemblages increase while the phototrophic/shelf association is at minimum values.

Pollen accumulation rates reach their highest values in this interval (3780 grains /cm^2 / yr at ca. 2160 cal yr BP, 251 cm) whereas pollen concentrations decrease (906 grains / cm^3 at ca. 2200 cal yr BP, 311 cm). An exception to this trend occurs in the uppermost part of the interval when pollen concentrations reach 5315 grains / cm^3 at ca. 2130 cal yr BP (211 cm). Percentages of Poaceae are under 72%. The pollen assemblages show a slight increase in Cyperaceae (21%). While *Typha* pollen (10%) reaches the highest percentage along the core, Cheno-Am pollen percentages decrease. The representation of Sahelian elements, including *Mitracarpus* and *Acacia* which were common in the previous zone, decreases abruptly (Figure 5.5). Fern spores increase to 13% at ca. 2170 cal yr BP (271 cm). Fluxes of plant cuticles as well as total fresh-water algae increase markedly in this zone.

Zone E: From ca. 2130 to 1240 cal yr BP. (210 - 20 cm, 14 samples).

Sedimentation rates decrease abruptly (Figure 5.4). Dinocyst accumulation rates and their concentrations are low except for a small increase at ca. 1430 cal yr BP (81 cm). The upwelling association is well represented in the lower part of the interval by cysts of taxa such as *P. monospinum* (26%), *S. quanta* (27%), *and Brigantedinium* spp. (9%). The younger part of this zone is characterized by an increase of the lagoon

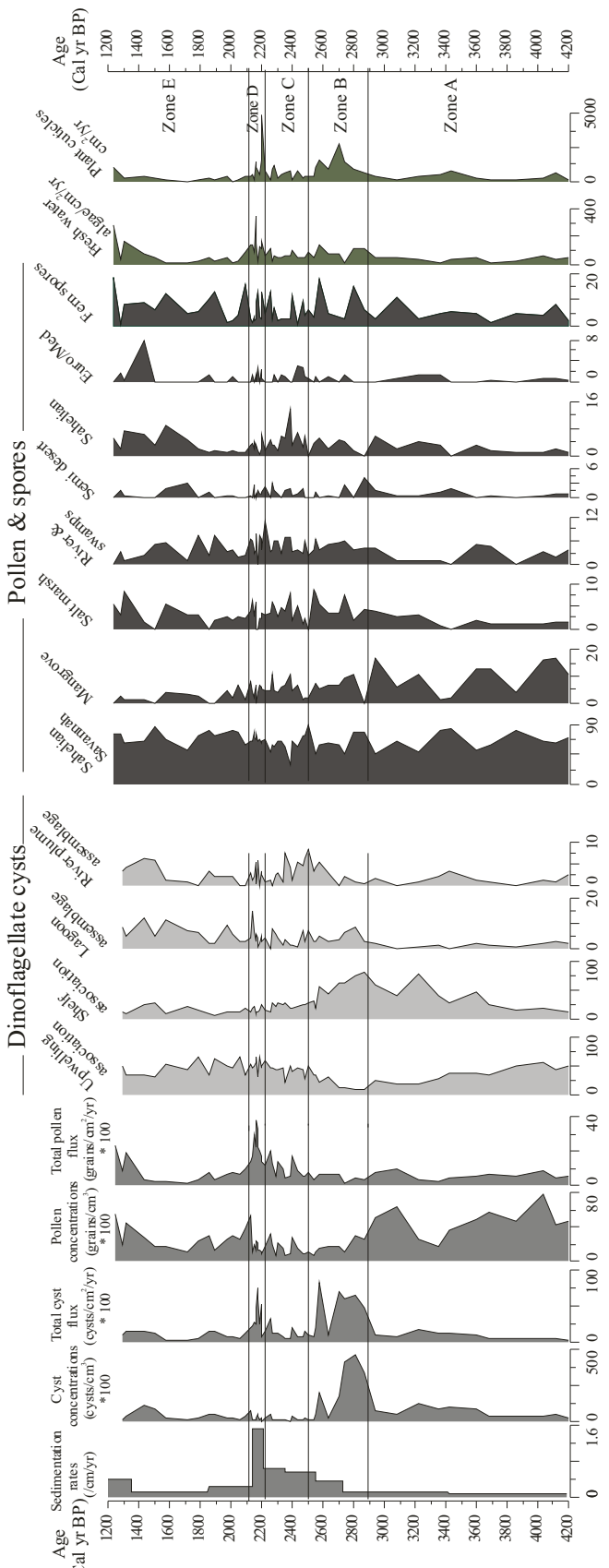

Figure 5.4 Integrated palynological data from marine sediment core GeoB 9503-5 showing concentrations of dinocysts and pollen and their accumulation rates, relative abundances of dinocysts and pollen groups as well as percentages of spores and fluxes of fresh water algae and plant cuticles. Palynological data are subdivided into five zones indicated by the dashed lines. Dinocyst groups are shown as percentages of their own total counted sums. Pollen abundances are calculated as percentages of the sum of total pollen including trees, shrubs and aquatic pollen. Spore percentages are calculated relative to the sum of pollen and spores. Fresh water algae and plant cuticle fluxes are expressed as number of specimens per area and time (##/cm^2/yr)

assemblage with cysts of *P. dalei* (7%) and *T. vancampoae* (8%) as well as the river plume assemblage represented by taxa such as *T. appelanatum* (5%).

Total pollen concentrations and accumulation rates decrease abruptly after the previous zone except for a small increase at 1240 cal yr BP (21 cm). Poaceae pollen values slightly increase to 73% and those of Cyperaceae remain stable compared to the previous zone. *Rhizophora* pollen exhibits its lowest percentages along the core (1%). Percentages of *Mitracarpus* are generally low and do not exceed 2%. *Pinus* pollen is present in three samples of this phase, at ca. 2000 cal yr BP (181 cm), 1430 cal yr BP (81 cm) and ca. 1280 cal yr BP (41 cm) and show high percentages (8%) in the younger part of this zone. The upper part of the interval is also characterized by a marked increase in percentages of Cheno-Am (9%), *Acacia* (6%), *Mimosa* (4%) and Asteroideae (3%). Spore percentages reach 13% and 18% at ca. 1897 cal yr BP (151 cm) and 1240 cal yr BP (21 cm), respectively (Figure 5.5). Plant cuticle fluxes decrease markedly compared to the previous zone. Fresh water algae fluxes follow the same trend with a small increase (285 /cm^2 / yr) at ca. 1240 cal yr BP (21 cm).

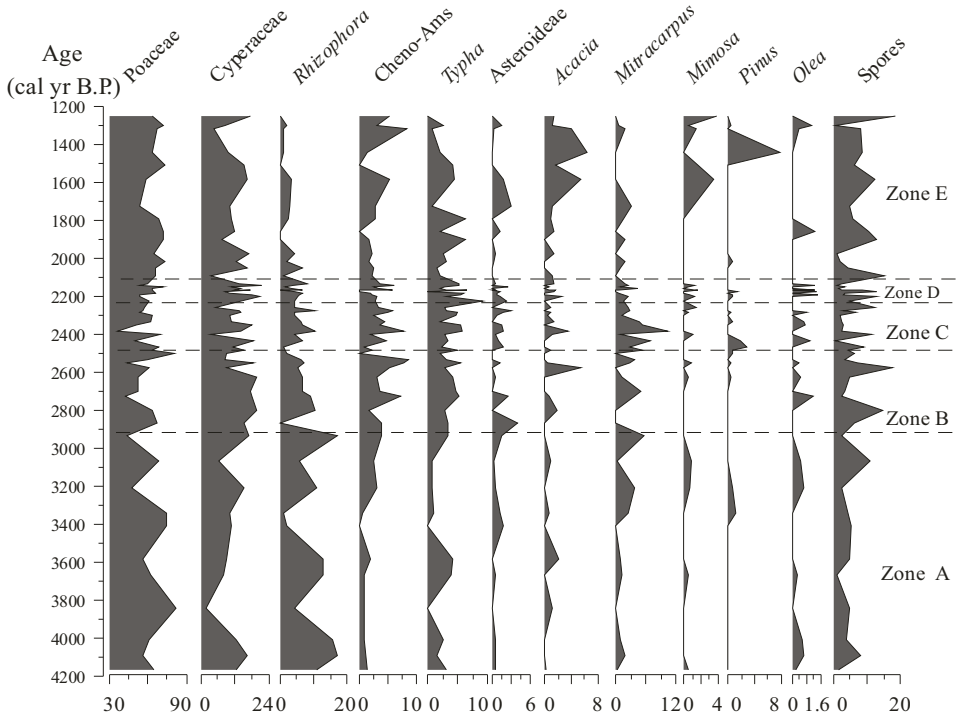

Figure 5.5 Percentage pollen diagram of selected pollen taxa from core GeoB 9503-5.

5.5 Discussion

Organic-walled dinocyst associations in sediments can be related to environmental conditions in surface waters such as nutrient availability, turbulence, sea surface temperature, and sea surface salinity. Consequently, they form a valuable tool for palaeoclimatic and palaeoceanographic reconstructions. (Marret and de Vernal, 1997; Rochon at al., 1999; Marret and Zonneveld, 2003). However, this only holds when species-selective degradation processes under aerobic conditions have not altered the association post-depositionally (e.g. Zonneveld et al., 1997, 2001, 2007; Hopkins and McCarthy 2002; Versteegh and Zonneveld, 2002). At our study site, sedimentation rates and primary production in the surface waters are high. This results in low oxygen concentrations in pore waters and a quick burial of organic matter. We therefore expect that the cyst association at this site has not been altered significantly by degradation processes. Dinocysts are used as proxy to reconstruct sea surface conditions. Pollen and pteridophyte spores are used as indicators of terrestrial conditions indicating source areas of pollen and spores and different transport mechanisms. Plant cuticles and fresh water algae are used to identify changes in the rate of fluvial discharge.

Relatively dry conditions between ca. 4200 and 2900 cal yr BP are indicated by the considerable representation of Sahelian savannah (Poaceae and Cyperaceae) as well as the presence of semi-desert elements, such as Asteroideae. Additional evidence for dry conditions is provided by the low amount of fern spores as well as the low flux values for fresh water algae and plant cuticles, indicative for low river input. Confirmation for low river discharge is provided by the low dinocyst concentrations. The high *Rhizophora* pollen values in this time period therefore reflect the expansion of mangrove vegetation along the Senegal River caused by the reduced freshwater flow and subsequently increased marine influence that would have allowed the mangrove to extend considerably into the estuary despite the relatively dry conditions in the continent (Lézine and Casanova, 1989). There is no evidence for locally wetter conditions and continuous input of fresh water causing the observed high *Rhizophora* values by efficient river transport (Dupont and Agwu, 1991; Lézine et al., 1995; Lézine, 1996).

Supporting evidence for dry conditions at this time has been reported from subtropical NW Africa in the Cap Blanc region (Mauritania). The general trend towards increased aridity, culminated in an abrupt change towards drier conditions indicating the end of the "African humid period" at around ca. 5500 cal yr BP. (e.g. de Menocal et al., 2000). Other evidence for dry conditions between ca. 4500 and 2000 cal yr BP comes from hydrographical and sedimentological records in the late Holocene (e.g. Servant and Servant-Vildary, 1980; Lézine, 1989; Lézine and Casanova, 1989; Maley and Brenac, 1998; Salzmann and Waller, 1998, Salzmann et al., 2002). In addition, in the Sahel of Nigeria (Salzmann and Waller, 1998) and Burkina Faso (Ballouche and Neumann, 1995) the establishment of modern vegetation characterized by Sahelian vegetation and degraded shrubland (Salzmann et al., 2002) ocurred between ca. 3500 and 3000 cal yr BP along with a distinct decrease of lake levels.

Between ca. 2900 and 2500 cal yr BP, the sudden increase of total accumulation rates and concentrations of dinocysts as well as the marked increase of cysts from the river plume assemblage and shelf association species including *Spiniferites* cysts preferring warm and nutrient-rich conditions of neritic environments (Rochon et al., 1999) might therefore reflect an enhanced Senegal River runoff supplying large amounts of terrigenous material and nutrients to the surface waters. In addition, high flux values of plant cuticles and fresh-water algae as well as fern spore and *Typha* swamp elements indicate moister conditions and higher fluvial input. We interpret these features as an indication of more humid conditions that we refer to as a "little humid phase" (LHP). This interval is characterized by increased runoff from the Senegal River possibly related to higher monsoonal precipitation between ca. 2900 and 2500 cal yr BP. Such an increase of precipitation rates could have been caused by the migration of the tropical rain belt towards the north suggesting significant climate variability in the Senegal area between ca. 2900 and 2500 cal yr BP, a period which is generally considered as relatively stable. The dry phase reported in previous studies obviously ended with a "little humid phase" (LHP) in the Senegal area. The LHP was not recorded yet in any other palaeohydrological or palaeoenvironmental data from tropical and subtropical West Africa. The lack of evidence for the LHP in other records might partly be related to lower sampling resolution or different regional climatic responses.

From ca. 2500 to 2200 cal yr BP, the total accumulation rates and concentrations of dinocysts decrease substantially. Dinocyst records reveal a marked shift from the river plume and phototrophic / shelf associations to the upwelling association. These changes were most likely related to changes in atmospheric and/or oceanic conditions adjacent to the Senegal River mouth.

In parallel, the pollen data indicate a dramatic decrease of fern spores and plant cuticles as well as low values of fresh water algae between ca. 2500 and 2200 cal yr BP. This suggests a reduced discharge of fresh water and inefficient transport by the Senegal River. Additionally, *Mitracarpus* pollen originating in the southern Sahelian and Sudanian zone is well represented in the pollen record during this period indicating strong aeolian transport by the NE trades (Hooghiemstra et al., 1986). We therefore interpret this interval as being characterized by lower sediment discharge from the Senegal River and an increase in trade wind strength. The increase in abundance of dinocysts of upwelling association might reflect a response to increasing nutrient availability in the surface waters caused by regional wind-induced upwelling.

These findings are in agreement with the results from a study in the rain forest of western Cameroon, where an abrupt opening of the vegetation took place at 2500 cal yr BP indicating a climatic change toward dry conditions which was followed by a return to wetter climates after ca. 2200 cal yr BP (Maley and Brenac, 1998). Additionally relevant, archeological data indicate the appearance of large settlements in the Senegal delta after ca. 2500 cal yr BP. It is argued that people moved further to the south during times when the Sahelian climate became drier (McIntosh and McIntosh, 1983; McIntosh, 2006). This migration can likely be related to the fact that the drying Senegal delta allowed agricultural activity in previously flooded plains (McIntosh, 1999).

Between ca. 2200 and 2100 cal yr BP, a rapid increase of sedimentation rates and strong fluctuations in percentages of fern spores and dinocysts from the river plume assemblage and in the total accumulation rates of pollen, dinocysts, fresh-water algae, and plant cuticles, indicate large environmental changes in the Senegal area. Wind-induced upwelling might have been associated with strong river discharges. This suggests that the previous dry phase ended with periodic pulses of high

terrigenous contributions. These pulses of terrigenous material could be caused by episodic flash flood events of the Senegal River. These events might have been climatically induced through strengthening of the monsoon system in relation to the northward migration of the tropical rain belt, causing torrential rain and flooding in the catchment area of the Senegal River and supplying large amounts of terrigenous material. Another possible cause for increased terrigenous sediment load in the river would be the intensification of agriculture by the human population established in the Senegal delta after ca. 2500 cal yr BP which could have aggravated the erosion in the area (McIntosh, 1999).

After ca. 2100 cal yr BP, the sudden decrease of sedimentation rates, total accumulation rates of dinocysts, pollen, fresh-water algae and plant cuticles, and an increase of Sahelian savannah elements suggest lower discharge of the Senegal River under more arid conditions. At around 1800 cal yr BP pollen assemblages show a strong occurrence of pollen of Saharan (Asteroideae) and Sahelian elements (*Acacia, Mimosa*). In addition, pollen from *Pinus* and *Olea* which likely originated in North Africa and South-West Europe increased at ca. 1500 cal yr BP indicating a strong increase in trade-wind strength. Simultaneous decline of mangrove pollen at ca. 1800 cal yr BP can be interpreted mainly by lower discharge of the Senegal River. Alternatively, this signal might be related to an increase in human activities in the Senegal delta after 2500 cal yr BP (McIntosh, 1999). Our results corroborate the findings of Alexandre et al. (1997) who report phytolith evidence from Lake Guiers sediments in the Sahelian region which record the occurrence of the driest phase at ca. 2100 cal yr BP. In western Senegal, Lézine (1988, 1989) shows that a second major change affected the Sahel after ca. 2000 cal yr BP and led to the rapid degradation of the vegetation and the establishment of the modern semi-arid environment in the present Sahelian zone. These findings are clearly recorded in our core but not before ca. 1800 cal yr BP.

5.6 Conclusion

Changes in the assemblages, concentrations and fluxes of pollen and dinocysts in marine sediment core GeoB 9503-5 were observed for the time period from ca. 4200 to 1200 cal yr BP providing valuable insights into past climatic, hydrologic and oceanic conditions. Our study emphasizes significant coeval changes in continental

moisture conditions and oceanic environmental changes in and off Senegal. Initial dry conditions between ca. 4200 and 2900 cal yr BP were followed by somewhat moister conditions we refer to as "Little Humid Phase". This phase was characterized by stronger fluvial transport; and, by inference, greater monsoonal humidity between ca. 2900 and 2500 cal yr BP which was likely caused by latitudinal migration of the tropical rain belt towards the north supplying more precipitation. Our data show decreasing Senegal River runoff and increasing Sahelian winds between ca. 2500 and 2200 cal yr BP reflecting a trend towards drier conditions. Around ca. 2200 cal yr BP, this relatively dry period ended with periodic pulses of high terrigenous contributions and strong fluctuations in fern spore and river plume dinocyst percentages and in the total accumulation rates of pollen, dinocysts, fresh-water algae, and plant cuticles. We suggest that these fluctuations were caused by episodic flash flood events of the Senegal River between ca. 2200 and 2100 cal yr BP. Our results show that the LHP and interval of episodic flash floods on the Senegal River interrupt the general climatic trend of increasing aridity in NW Africa that began in the mid-Holocene (deMenocal et al, 2000).

Acknowledgements

This work was funded through the Deutsche Forschungsgemeinschaft as part of the DFG-Research Center/ Excellence cluster "The Ocean in the Earth System" (MARUM) at the University of Bremen. Thanks to the captain and Crew of the R/V *Meteor* for the logistic and technical assistance. Thanks to M. Segl for her help with isotope analyses and to S. Forke for his assistance with palynological processing. The manuscript benefitted from helpful comments by M. Kölling and J. Groenveld. Thanks to Jean-Pierre Cazet for helping with the fresh water algae determination and Anne-Marie Lézine for valuable discussion. We express our gratitude to Wyatt Oswald, Fabienne Marret and Sander van der Kaars for constructive comments and for detailed reviews of an earlier version of this manuscript. This is MARUM publication N° xxx.

Supplementary Table S5.1 List of the identified Dinoflagelate cyst species in marine core GeoB 9503-5. (Nomenclature after Marret and Zonneveld, 2003)

Cyst name	Motile affinity	Grouping
Lingulodinium machaerophorum	*Lingulodinium polyedrum*	*L.machaerophorum, L. machaerophorum var. short processes*
Gonyaulacaceae family		
Cyst of Pentapharsodinium dalei	*Pentapharsodinium dalei*	
Polysphaeridium zoharyi	*Pyrodinium bahamense*	
Operculodinium israelianum	*? Protoceratium sp.*	
Operculodinium centrocarpum	*Protoceratium reticulatum*	*O. centrocarpum* and *O. centrocarpum var. short processes.*
Spiniferites mirabilis	*Gonyaulax spinifera*	*S. mirabilis* and *S. hypercanthus*
Spiniferites bentorii	*Gonyaulax digitale*	
Spiniferites pachydermus	*Gonyaulax spinifera*	
Spiniferites ramosus	*Gonyaulax sp*	
Spiniferites spp.	*Gonyaulax sp*	*S. bulloideus, S. membranaceus* and *S.* spp
Peridineaceae family		
Brigantedinium spp.		Cysts of *Protoperidinium* spp., cyst of *Diplopelta symetrica, Votadinium calvum, votadinium spinosum, Stelladinium stellatum, Dubridinium spp.*, cysts of *Protoperidinium americanum*, *Bitectatodinium spp.*and *Zygabikodinium lenticulatum*
Xandarodinium xanthum	*Protoperidinium divaricatum*	
Quinquecuspis concreta	*? Protoperidinium leone*	
Bitectatodinium spongium.		
Lejeunecysta oliva	Unknown	
Selenopemphix quanta	*Protoperidinium conicum*	
Selenopemphix nephroides	*Protoperidinium subinerme*	
Trinovantedinium applanatum	*Protoperidinium pentagonum*	
Echinidinium granulatum	Unknown	
Echinidinium spp.	Unknown	*E. delicatum, E. aculeatum* and *E.*spp
Echinidinium transparantum	Unknown	*E. zonneveldii* and *E. transparantum*
Cysts of *Protoperidinium monospinum*		
Polykrikaceae family		
Cysts of *Polykrikos kofoidii*	*Polykrikos kofoidii*	*Cyst of P. kofoidii* and *Cyst of P. schwarzii*
Pyrophacaceae family		
Tuberculodinium vancampoae	*Pyrophacus steinii*	

Supplementary Table S5.2 List of the identified pollen taxa in marine core GeoB 9503-5.

Mangrove	**Sudanian elements**
Rhizophora	*Butyrospemum* (Sapotaceae)
	Piliostigma (Caesalpiniaceae)
Rivers and swamps	*Pterocarpus* (Fabaceae)
Typha	*Vernonia*-type (Asteraceae)
	Indigofera-type
Sahelian Savannah	*Tamarindus*
Cyperaceae	*Cuviera*
Poaceae	
	Guinean forest
Salt march	Annonaceae
Amaranthaceae/Chenopodiaceae	*Stereospermum*-type (Bignoniaceae)
	Phoenix-type (Palmae)
Semi-desert	*Uapaca*
Asteroideae	*Psydrax* type *subcordatum* (Rubiaceae)
Artemisia	
	Other elements
Trees and shrubs	*Euphorbia*
European/Mediterranean	Rubiaceae spp.
Olea	*Galium*
Pinus	
Clematis-type	
Fraxinus	
Sahelian elements	
Mitracarpus	
Acacia	
Ziziphus-type	
Boscia	
Borreria	

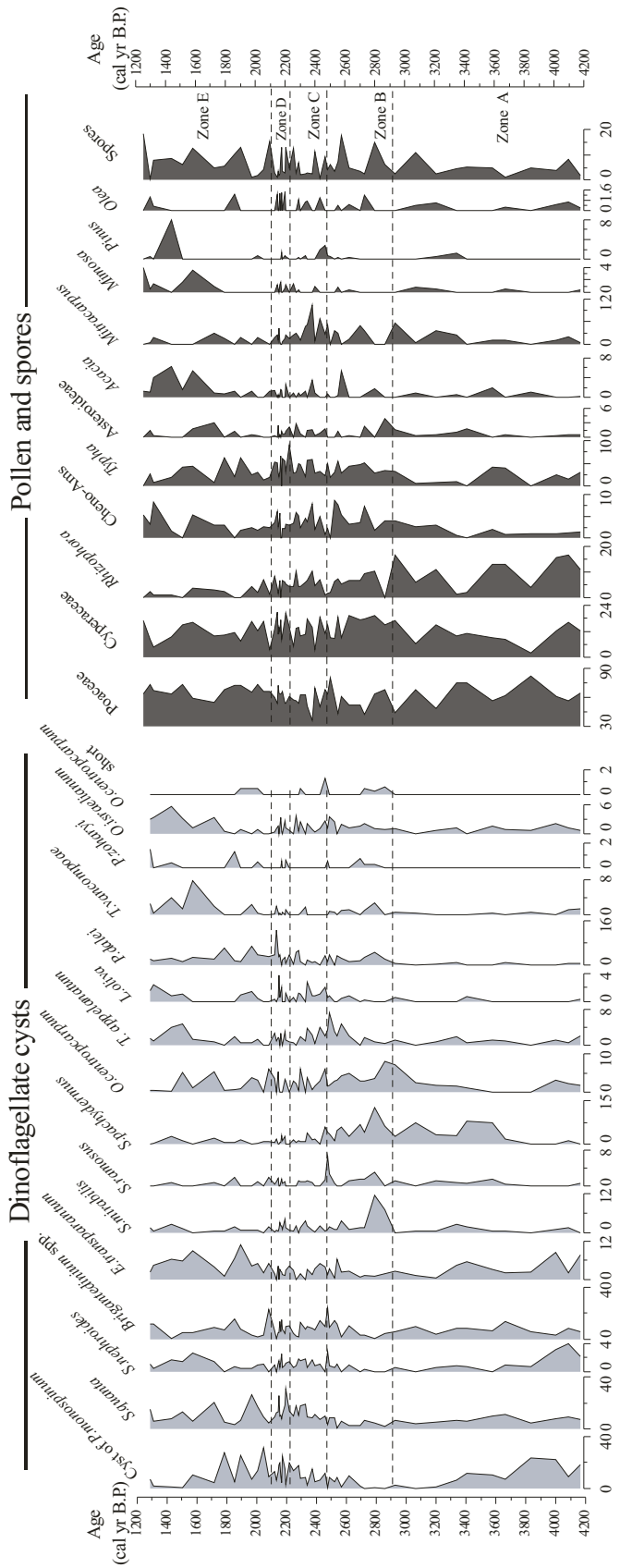

Supplementary figure S5.1 Integrated palynological data from marine sediment core GeoB 9503-5 showing relative abundances of selected organic-walled dinoflagellate and pollen taxa as well as percentages of total spores

References

Alexandre, A., Meunier, J-D., Lézine, A.M., Vincens, A., Schwartz, D., 1997. Phytoliths: indicators of grassland dynamics during the late Holocene in intertropical Africa. Palaeogeography, Palaeoclimatology, Palaeoecology 136, 213-229.

Ballouche, A., Neumann, K., 1995. La végétation du Sahel Burkinabé à l'Holocéne: la mare d'Ousri. *In*: 2nd symposium on African palynology, Tervuren (Belgium), 1995. Publications Occasionnelles CIFEG, 1995/31, Orléans, CIFEG, p. 19-25.

Bard, E., 1988. Correction of accelerator mass spectrometry ^{14}C ages measured in planktonic foraminifera: Paleoceanographic implications. Paleoceanography 6, 635-645.

Bard, E., Rostek, F., Turon, J.L., Gendreau, S., 2000. Hydrological impact of Heinrich events in the subtropical Northeast Atlantic. Science 289, 1321-1324.

Blasco, F., 1984. Climatic factors and the biology of mangrove plants. In: S.C. Sneadaker and J.G. Sneadaker Eds., The Mangrove ecosystem: research methods. –UNESCO, Paris, 18-35.

Bouimetarhan, I., Marret, F., Dupont, L., Zonneveld. K.A.F. (In review). Dinoflagellate cyst distribution in marine surface sediments off West Africa (17-6°N) in relation to sea-surface conditions, freshwater input and seasonal coastal upwelling. Marine Micropaleontology

Bonnefille, R., Riollet, G. 1980. Pollens des Savanes d´Afrique Orientale. Edition de CNRS, Paris, 140 pp., 113pl.

Colarco, P.R., Toon, O.B., Reid, J.S., Livingston, J.M., Russel, P.B., Redmann, J., Schmid, B., Maring, H.B., Savoie, D., Welton, E.J., Campbell, J.R., Holben, B.N., Levy, R., 2003. Saharan dust transport to the Caribbean during PRIDE: 2. Transport, vertical profiles and deposition in simulations of in situ and remote sensing observations. Journal of Geophysical Research 103, 8590.

deMenocal, P., Oritz, J., Guilderson, T., Jess Adkins, Sarnthein, M., Baker, L., Yarusinsky, M., 2000. Abrupt onset and termination of the African humid period: rapid climate response to gradual insolation forcing. Quaternary Science Reviews 19, 347-361.

de Vernal, A., Rochon,A., Turon, J-L., Matthiessen, J., 1997., Organic-walled dinoflagellate cysts: palynological tracers of sea-surface conditions in middle to high latitude marine environments. Geobios 30, 905-920.

Dupont, L.M., Agwu, C.O.C., 1991. Environmental control of pollen grain distribution patterns in the Gulf of Guinea and offshore NW-Africa. Geologische Rundschau 80, 567-589.

Faegri, K., Iversen, J., 1989. "Textbook of pollen analysis". IV Edition by Faegri, K., Kaland, P.E., Krzywinski, K.Wiley, New York.

Fensome, R.A., Williams, G.L., 2004. The Lentin and Williams index of fossil dinoflagellate, 2004 Edition. American Association of Stratigraphic Palynologist Foundation contributions series 42. 909 pp.

Fowler, S.W., Knauer, G.A., 1986. Role of large particles in the transport of elements and organic compounds through the oceanic water column. Progress in Oceanography, 16, 147-194.

Gac, J.Y., Kane, A., Saos, J.L., Carn, M., Villeneuve, J.F., 1985. L'invasion marine dans la basse vallée du fleuve Sénégal. –Dakar-Hann : ORSTOM, 64 p.

Gac, J.Y., Kane, A., 1986. Le fleuve Sénégal : Bilan hydrologique et flux continentaux de matières particulaires à l'embouchure. Sciences géologique bulletin 39, 1, p. 99-130. Strasbourg.

Gasse, F., 2000. Hydrological changes in the African tropics since the Last Glacial Maximum. Quaternary Science Reviews 19, 189-211.

Holzwarth, U., Esper, O. and Zonneveld, K. 2007. Distribution of organic-walled dinoflagellate cysts in shelf surface sediments of the Benguela upwelling system in relationship to environmental conditions. Marine Micropaleontology 64, 91-119.

Hooghiemstra, H., 1988a. Changes of major wind belts and vegetation zones in NW Africa 20.000 – 5000 yr B.P., as deduced from a marine pollen record near Cap Blanc.Review of Palaeobotany and Palynology 55, 101-140.

Hooghiemstra, H., 1988b. Palynological records from northwest African marine sediments: a general outline of the interpretation of the pollen signal. Philosophical Transactions of the Royal Society of London B 318, 431-449.

Hooghiemstra, H., Agwu C.O.C., 1986. Distribution of palynomorphs in marine sediment: a record for seasonal wind patterns over NW Africa and adjacent Atlantic. Geologische Rundschau 75, 81 - 95.

Hooghiemstra, H., Lézine, A.M., A.G. Leroy, S., Dupont, L.M., Marret, F., 2006. Late Quaternary palynology in marine sediments: A synthesis of the understanding of pollen distribution patterns in the NW African setting. Quaternary International 148, 29-44.

Hopkins, J. A. and McCarthy, F. M. G., 2002. Post-depositional palynomorph degradation in Quaternary shelf sediments: a laboratory experiment studying the effects of progressive oxidation. Palynology 26, 167-184.

Hsu, C.P.F., Wallace, J.M., 1976. The global distribution in annual and semiannual cycles in precipitation. Monthly Weather Review 104(9), 1093-1101.

Johnson, J., Stevens, I., 2000. A fine resolution model of the eastern North Atlantic between the Azores, the Canary Islands and the Gibraltar straight. Deep-sea Research I 47, 875-899.

Jones, S.E., Jago, C.F., Bale, A.J., Chapman, D., Howland, R., Jackson, J., 1998.

Aggregation and suspended particulate matter at seasonally stratified site in the southern North Sea: physical and biological controls. Continental Shelf Research 18, 1283-1310.

Lamb, H.F., Gasse, F., Benkaddour, A., El Hamouti, N., van der Kaars, S., Perkins, W.T., Pearce, N.J., Roberts, C.N., 1995. Relation between century-scale Holocene arid intervals in tropical and temperate zones. Nature 373, 134-136.

Lézine, A.M., 1988. Les variations de la couverture forestière mésophile d'Afrique occidentale au cours de l'Holocène. C. R. Académie des Sciences Paris t.307 Série II, 439-445.

Lézine, A.M., 1989. Late Quaternary Vegetation and Climate of the Sahel. Quaternary Research 2, 317-334.

Lézine, A.M., 1996. La mangrove ouest africaine, signal des variations du niveau marin et des conditions régionales du climat au cours de la dernière déglaciation. Bulletin de société géologique, (167) n°6, pp. 743-752.

Lézine, A.M., Casanova, J., 1989. Pollen and hydrological evidence for the interpretation of past climates in tropical West Africa during the Holocene. Quaternary Science Reviews 8, 45 – 55.

Lézine, A.M., Chateauneuf. J.-J., 1991. Peat in the "Niayes" of Senegal: depositional environment and Holocene evolution. Journal of African Earth Sciences 12, 171-179.

Lézine, A.M., Turon, J.L., Buchet, G., 1995. Pollen analyses off Senegal: evolution of the coastal palaeoenvironment during the last deglaciation. Journal of Quaternary science 10, 95-105.

Maley, J., Brenac, P., 1998. Vegetation dynamics, palaeoenvironments and climatic change in the forests of western Cameroon during the last 28000 years B.P. Review of Palaeobotany and Palynology 99, 157-187.

Marchant, R., Hooghiemstra, H., 2004. Rapid environmental change in African and South American tropics around 4000 years before present: a review. Earth Science Reviews 66, 217-260.

Margalef, R., 1973. Assessment of the effects on plankton, p.301-306. In E.A. Pearson and E. De Farja Fragipane (eds.), marine pollution and marine waste disposal proceedings of the 2nd International Congress, san Remo, 17-21 December 1973.

Marret, F., de Vernal, A., 1997. Dinoflagellate cyst distribution in surface sediments of the Southern Indian Ocean. Marine Micropaleontology 29, 367-392.

Marret, F., Zonneveld, K., 2003. Atlas of modern organic-walled dinoflagellate cyst distribution. *Review of Palaeobotany and Palynology* 125, 1-200.

McIntosh, S.K., 1999. A tale of two floodplains: comparative perspectives on the emergence of complex societies and urbanism in the Middle Niger and Senegal Valleys. *In* Proceedings of the Second World Archaeological Congress Intercongress, Mombasa, P. Sinclair, ed. Published on the Uppsala University website: http://www.arkeologi.uu.se/afr/projects/BOOK/Mcintosh/mcintosh.htm

McIntosh, S.K., 2006. The Holocene Prehistory of West Africa (10.000 – 1000 BP). Akeyeampong, E.K. (ed.) Themes in West Africa's History. Ohio University press, Athens.

McIntosh, S.K., McIntosh, R., 1983. Current directions in West African prehistory.Annual Reviews of Anthropology 12, 215-258.

Meggers, H., Freudenthal, T., Nave, S., Targarona, J., Abrantes, F., Helmke, P., 2002. Assessment of geochemical and micropaleontological sedimentary parameters as proxies of surface water properties in the Canary Islands region. Deep Sea Research II 49, 3631-3654.

Mittelstaedt, E., 1991. The ocean boundary along the northwest African coast: Circulation and oceanographic properties at the sea surface. Progress in Oceanography 26, 307-355.

Mulitza, S., Bouimetarhan, I., Brüning, M., Freesemann, A., Gussone, N., Filipsson, H., Heil, G., Hessler, S., Jaeschke, A., Johnstone, H., Klann, M., Klein, F., Küster, K., März, C., McGregor, H., Minning, M., Müller, H., Ochsenhirt, W.T., Paul, A., Scewe, F., Schulz, M., Steinlöchner, J., Stuut, J.B., Tjallingii, R., Dobeneck, T., Wiesmaier, S., Zabel, M. and Zonneveld, K., 2006. Report and preliminary results of Meteor cruise M65/1, Dakar – Dakar, 11.06.–01.07.2005. Berichte, Fachbereich Geowissenschaften, Universität Bremen, No. 252, 149 pp.

Mulitza, S., Prange, M., Stuut, J.B., Zabel, M., von Dobeneck, T., Itambi, C.A., Nizou, J., Schulz, M., Wefer, G., 2008. Sahel Megadrought triggered by glacial slowdowns of Atlantic meridional overturning. Paleoceanography 23, PA4206.

Nave, S., Freitas, P., Abrantes, F., 2001. Coastal upwelling in the Canary Island region: spatial variability reflected by the surface sediment diatom record. Marine Micropaleontology 42, 1-23.

Nicholson, S.E., 2000. The nature of rainfall variability over Africa on time scales of decades to millenia. Global and planetary change 26, 137-158.

Nicholson, S.E., Grist, J.P., 2003. The seasonal evolution of the atmospheric circulation over West Africa and Equatorial Africa. Journal of Climate 16 (7), 1013-1030.

Nykjaer, L., Van Camp, L., 1994. Seasonal and interannual variability of coastal upwelling along Northwest Africa and Portugal from 1981 to 1991. Journal of Geophysical Research 99, 14197-14207.

Prospero, J.M., Nees, R.T., 1986. Impact of the North African drought and El Nino on mineral dust in the Barbados trade winds. Nature 320, 735-738.

Prospero, J.M., 1990. Mineral-aerosol transport to the North Atlantic and North Pacific: the impact of African and Asian sources. *In*: A.H. Knap (Editor), the long-range atmospheric transport of natural and contaminant substances. Mathematical and Physical Sciences. Kluwer Acadameic publishers, Dodrecht, pp. 59-86.

Prospero, J.M., Ginoux, P., Torres, O., Nicholson, S.E., Gill, T.E., 2002. Environmental characterization of global sources of atmospheric soil dust identified with the nimbus 7 total zone mapping spectrometer (TOMS) absorbing aerosol product. Review of Geophysics 40, 2-1/ 2-31.

Reimer, P.J., Baillie, M.G.L., Bard, E., Bayliss, A., Beck, J.W., Bertrand, C., Blackwell, P.G., Buck, C.E., Burr, G., Cutler, K.B., Damon, P.E., Edwards, R.L., Fairbanks, R.G., Friedrich, M., Guilderson, T.P., Hughen, K.A., Kromer, B., McCormac, F.G., Manning, S., Bronk Ramsey, C., Reimer, R.W., Remmele, S., Southon, J.R., Stuiver, M ., Talamo, S., Taylor, F.W., van der Plicht, J. and Weyhenmeyer, C.E., 2004. IntCal04 Terrestrial radiocarbon age calibration, 26-0 ka BP. Radiocarbon 46, 1059-1086.

Rochon, A., de Vernal, A., Turon, J.L., Matthiessen, J., Head, M.J., 1999. Distribution of recent dinoflagellate cysts in surface sediments from the North Atlantic Ocean and adjacent seas in relation to sea-surface parameters. American Association of Stratigraphic Palynologists Foundation, 23, 1- 150.

Salzmann, U., Waller, M., 1998. The Holocene vegetation history of the Nigerian Sahel based on multiple pollen profiles. Review of Palaeobotany and Palynology, 100, 39-72.

Salzmann, U., Hoelzmann, P., Morczinek, I., 2002. Late Quaternary climate and vegetation of the Sudanian zone of Northeast Nigeria. Quaternary Research 58, 73-83.

Sarnthein, M., Thiede, J., Pflaumann, U., Erlenkeuser, H., Fütterer, D., Koopmann, B., Lange, H.E.S., 1982. Atmospheric and oceanic circulation patterns off Northwest Africa during the past 25 million years. *In* Von Rad, U., Hinz, K., Sarnthein, M., Seibold, E. (Eds), Geology of the Northwest African continental margin. Springer, Berlin, pp. 584-604.

Schefuß, E., Schouten, S. Schneider, R.R., 2005. Climatic controls on central African hydrology during the past 20,000 years. Nature 437, 1003-1006.

Servant, M., and Servant-Vildary, S., 1980. L'Environnement quaternaire du basin du Tchad. *In* "The Sahara and the Nile" (M.A.J. Williams and H. Faure, Eds.) pp. 133-162. Balkema, Rotterdam.

Spalding, M., Blasco, F., Field, C., 1997. World mangrove Atlas. The International Society for mangrove Ecosystems (ISME), Smith Settle, Otley, UK: 178p.

Stuiver, M., Reimer, P. J., Reimer, R. W., 2005. CALIB 5.0. (www program and documentation).

ter Braak, C.J.F., Smilauer, P., 1998. Canoco 4. Centre for Biometry. Wageningen. Versteegh, G.J.M., Zonneveld, K.A.F., 2002. Use of selective degradation to separate preservation from productivity. Geology 30, 615 – 618.

Vincens, A., Lezine, A.M., Buchet, G., Lewden, D. and le Thomas, A., 2007. African pollen data base inventory of tree and shrub pollen types. Review of Palaeobotany and Palynology 145, 135 – 141.

Weldeab, S., Schneider, R.R., Kölling. M, Wefer, G., 2005. Holocene African droughts relate to eastern equatorial Atlantic cooling. Geology 12, 981-984.

White, F., 1983. The vegetation of Africa. UNESCO, Paris, 384 pp.

World Ocean Atlas, 2001. http://www.nodc.noaa.gov/OC5/WOA01/pr_woa01.html

World Resources Institute, 2003. http://www.wri.org/

Zonneveld, K.A.F., 1997. New species of organic walled dinoflagellate cysts from modern sediments of the Arabian Sea (Indian Ocean). Review of Palaeobotany and Palynology, 97, 319-337.

Zonneveld, K.A.F., Jurkschat, T., 1999. *Bitectatodinium spongium* (Zonneveld, 1997) Zonneveld et Jurkschat *comb.nov.* from modern sediment and sediment trap samples of the Arabian Sea (northwestern Indian Ocean): taxonomy and ecological affinity. Review of Palaeobotany and Palynology 106, 153-169.

Zonneveld, K.A.F., Hoek, R., Brinkhuis, H. and Willems, H., 2001. Geographical distributions of organic-walled dinoflagellate cysts in surface sediments of the Benguela upwelling Region and their relationship to upper ocean conditions. Progress in Oceanography 48, 25-72.

Zonneveld, K.A.F., Mackensen, A., Baumann, K-H., 2007. Stable oxygen isotopes of *Thoracosphaera heimii* (Dinophyceae) in relationship to temperature; a culture experiment. Marine Micropaleontology 64, 80-90.

Chapter 6

Two aridity maxima in the western Sahel during Heinrich event 1

Ilham Bouimetarhan*, Enno Schefuß, Cletus A. Itambi, Lydie Dupont, Stefan Mulitza, Karin Zonneveld

MARUM - Center for Marine Environmental Sciences and Department of Geosciences, University of Bremen, PO Box 330 440, D-28334, Bremen, Germany

To be submitted to Quaternary Science Reviews

Abstract

High resolution last deglaciation palynological and geochemical records emphasize significant coeval climatic and oceanic changes over western Sahel and in the eastern tropical north Atlantic. During Heinrich Event 1, we identify two aridity maxima occurring between ca. 18,800 and 17,400 cal yr BP and between ca. 16,400 and 15,400 cal yr BP. In both phases, the vegetation in western Sahel is characterized by a maximum representation of Saharan plant community (Chenopodiaceae-Amaranthaceae) simultaneously with an increase of Ti/Ca ratio indicating extremely dry conditions accompanied by strong NE trade winds. Interestingly, dinoflagellate cyst assemblages were dominated, during both intervals, by the upwelling association suggesting nutrient-rich surface waters characteristic for high marine upwelling-related productivity as a response of the NE trade wind intensification. After ca.15,400 yr BP, a small increase of concentration and accumulation rate values of pollen, fern spores and fresh water algae as well as an increase in the representation of mangroves and hygrophile plants and a simultaneous increment of the runoff dinocyst association, point to a shift towards more humid and relatively warm conditions. This new palynological evidence shows the important role played by the latitudinal migration of the inter tropical convergence zone and its associated tropical rainbelt during periods of the AMOC weakening (Strengthening) together with changes in the Indian monsoon and provides a further proof of the close relationship existing between AMOC, North Atlantic SST and western Sahel precipitation.

6.1 Introduction

Life of millions of people in the semi-arid Sahel region relies primarily on the availability of water to drive biological and human activities. Since the Pliocene, this region has been frequently affected by changes towards more arid climate (Leroy and Dupont, 1994; deMenocal, 1995), which resulted in extreme hydrological and environmental variations from extensive grassland with numerous lakes during the early Holocene African Humid Period (AHP) to the present day arid conditions (Claussen et al., 1999; Gasse, 2000; deMenocal et al., 2000).

Historical records suggest millennial scale Sahel droughts to be synchronous with cold north Atlantic sea surface temperature (SST) anomalies (Street-Perrot and Perrot, 1990; Gasse, 2000; Zhao et al., 1995, 2006; Jullien et al., 2007; Itambi et al., 2008; Mulitza et al., 2008; Tjalingii et al., 2008). These abrupt events have been related to changes in the Atlantic meridional overturning circulation (AMOC) (Newell and Hsiung, 1987) and thus to changes in sea-surface temperature patterns (e.g., Lamb, 1978; Folland et al., 1986; Lamb et al., 1995; Schefuß et al., 2005; Weldeab et al., 2005; Mulitza et al, 2008; Tjalingii et al., 2008).

After the last glacial maximum (LGM), a first short-lived meltwater pulse around 19,000 cal yr BP delivered to the Nordic seas (Clark et al., 1996) and subsequent melting of icebergs from the Laurentide ice sheet (Heinrich event 1; H1) (Bond et al., 1992) generated a dramatic quasi-cessation of the AMOC (McManus et al., 2004). The slowdown of the AMOC, due to the reduced northward heat transport lasting until ~ 14,700 cal yr BP could be the driving mechanism of the southward migration of the intertropical convergence zone (ITCZ) and its associated rainbelt (Zhang and Delworth, 2005) thus, resulting in extreme aridity over western Sahel (Mulitza et al., 2008; Itambi et al, 2008).

Recent studies indicate that the glacial climate was far more variable than previously thought. Bard et al. (2000) showed that H1 is a complex period characterized by two depositional phases of the ice-rafted debris (IRD) resulting in Heinrich layers centred at 16,000 (H1a) and 17,500 (H1b) cal yr BP at the Iberian margin. Yet, it is still not clear which mechanism was responsible for the occurrence of these two phases during the H1 stadial.

One possible explanation would be that the cessation of the AMOC started before the ice-berg discharges suggesting a positive feedback leading to ice-berg surges delivering the IRD of Heinrich layers as proposed by Shaffer et al. (2004) and Flückiger et al. (2006). However the scarcity of proxy data with high temporal resolution from sensitive sites such as the tropics, due to their role in altering the global oceanic heat and fresh water balance, has hindered the verification of this hypothesis.

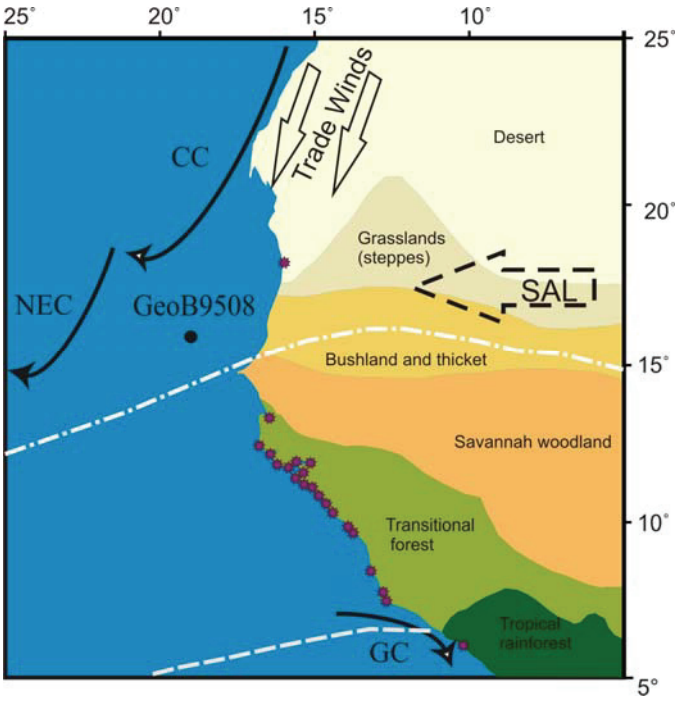

Figure 6.1 Map showing the simplified phytogeography and biomes in the study area (after White 1983), location of marine core GeoB 9508-5, major hydrographic systems and oceanic currents: CC: Canary Currents, NEC: North Equatorial Current, GC: Guinea Current (after Sarnthein et al., 1982 and Mittelstaedt, 1991) and main wind belts (Saharan Air Layer (SAL) and trade winds). The white dashed lines indicate the present day boreal summer (dash-dotted line) and boreal winter (dashed line) positions of the Intertropical Convergence Zone (ITCZ).

Here we address this issue with a high resolution record from the continental slope off northern Senegal GeoB9508-5 for the period 20,000-12,000 cal yr BP, a key location to understand the Sahel climatic variability because of its sensitivity to the African monsoon system (AMS) which controls the amount and distribution of rainfall over West Africa (Figure 6.1). The present study is based on an integrated analysis of terrestrial palynomorphs (pollen and spores) to investigate large-scale shifts in vegetation and hydrological variability related to abrupt climate changes as well as changes in transport pathways (wind and river). In addition, we use organic-walled dinoflagellate cysts (dinocysts) to provide insight into variations of the past sea-surface conditions (e.g., primary productivity, sea-surface temperature and salinity). (e.g., Wall et al., 1977; de Vernal et al., 1994; Marret, 1994; Dale, 1996; Marret and de Vernal, 1997; Marret and Zonneveld, 2003).

6.2 Materials and Methods

We studied a section encompassing the last deglaciation of a high resolution marine core GeoB9508-5 (15°29.90'N, 17°56.88'W, 2384 m water depth) recovered from the continental slope off northern Senegal, west of the Senegal River mouth (Figure 6.1) during R/V *Meteor* cruise M65-1 (Mulitza et al., 2006). The chronology of this core is based on 12 radiocarbon ages (Mulitza et al., 2008). Pollen and dinocyst samples were taken every 5 cm for the time interval 20,000-12,000 cal yr BP resulting in an average temporal resolution of ~ 200 years and were prepared for palynological processing using standard laboratory procedures (Faegri and Iversen, 1989). In brief, 2 cm^3 of sediments was decalcified with diluted HCl (10%) and treated with HF (40%) to remove silicates. *Lycopodium* marker was added to each sample during the decalcification process in order to calculate palynomorph concentrations. The method for obtaining the geochemical data is described in Mulitza et al. (2008). We consider only the concentrations of Ti and Ca in this study. Ti is commonly enriched in loess (Schnetger, 1992) and has widely been used as tracer of Saharan dust (Glaccum, 1978; Schütz and Rahn, 1982; Larrasoaña et al., 2003) and indicates wind strength and continental aridity in NW Africa (Itambi et al., 2008)

6.3 Results

Direct correlation between high resolution pollen and dinocyst records from the core GeoB9508-5 during the last deglaciation between ca. 20,000 and 12,000 cal yr BP documents vegetation shifts that occurred in western Sahel in combination with changes in ocean surface conditions (Figure 6.2).

The pollen associations between ca. 19,800 and 18,800 cal yr BP. show an increase in *Rhizophora* (mangrove) pollen (8.5%) along with the dry savannah elements, mainly grasses (Poaceae) (16%) and total concentrations of fern spores. Conversely, percentages of Cyperaceae pollen and Amaranthaceae/Chenopodiaceae (Cheno-Am; representatives of Saharan elements) as well as concentration and accumulation rates of total pollen are low. Dinocyst concentrations show relatively high values in this interval reaching a maximum of ~ 4300 cysts/cm^3. The dinocyst assemblage is

dominated by *Lingulodinium machaerophorum* accounting for 43% of the dinocyst sum and *Spiniferites* species (13%).

Between ca. 18,800 and 14,800 cal yr BP, contemporaneous changes in dinocyst and pollen assemblages as well as changes in the Ti/Ca ratio representing the variation of terrigenous vs. biogenic input, show four distinct phases (Tables 6.1). First, from ca. 18,800 to 17,400 where Pollen of Saharan vegetation especially Cheno-Am, increased rapidly up to 62% within ca. 500 years reaching their highest values in the pollen record at ca. 18,400 cal yr BP and subsequently decrease at the favour of Cyperaceae pollen (47%). This interval shows low values of fresh water algae. Values for *Rhizophora* decrease abruptly to 1.3% along with the total concentrations of fern spores. Ti/Ca ratio shows a high input of terrigenous materials from the Saharan and Sahel regions reaching maximum values at ca. 17,600 cal yr BP. The main feature within the ocean surface changes in this phase concerns the abrupt increase of the heterotrophic taxon *Brigantedinium* spp. up to 40% at the expense of *L. machaerophorum* and the *Spiniferites* group.

The second phase between ca. 17,400 and 16,400 cal yr BP is characterized by low percentages of Saharan element pollen, low Ti/Ca ratio and an increase of *Boscia* and *Mitracarpus* pollen percentages. The dinocyst assemblage shows a considerable decrease of *Brigantedinium* spp.

Within the third phase between ca. 16,400 and 15,400 cal yr BP, Cheno-Am are again the dominant group and their percentages account for up to 50 % at ca. 15,500 cal yr BP. Cyperaceae pollen show their lowest percentages along the core (20%). Ti/Ca shows a maximum phase during this time interval. The dinocyst assemblage exhibits a strong variability of *Brigantedinium* spp. fluctuating between 18 and 45%.

The fourth phase from 15,400 to 14,800 cal yr BP is marked by a gradual increase in concentrations and accumulation rates values of pollen, fern spore, and fresh water algae as well as an increase of *Rhizophora* and *Typha* (hygrophile plant) pollen percentages. Below 15,000 cal yr BP, Ti/Ca ratio remains low and relatively constant until 12,000 cal yr BP.

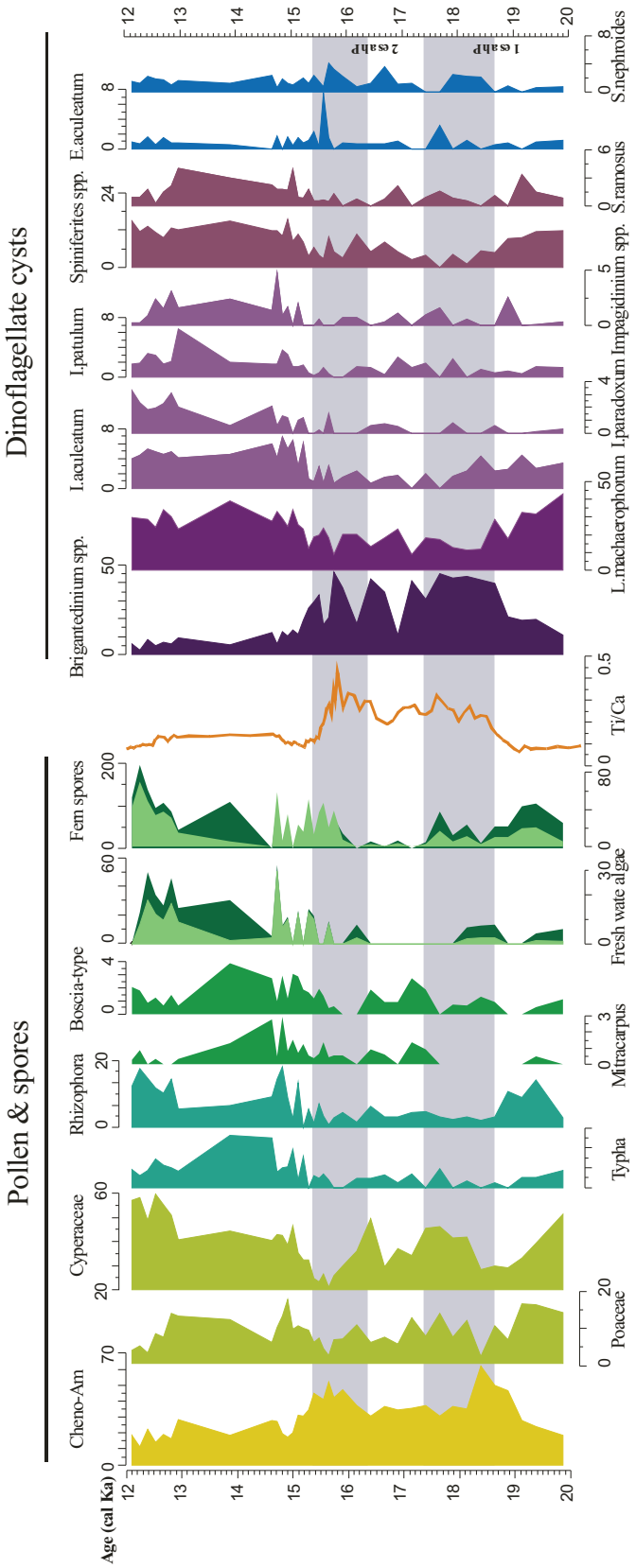

Figure 6.2 Integrated palynological data from marine sediment core GeoB 9508-5 showing percentages of main pollen taxa, concentrations (back diagram, dark green) and fluxes (front diagrams, light green) of fresh water algae and spores, Ti/Ca ratio and percentages of selected dinocyst taxa. Dinocysts species are shown as percentages of their own total counted sums. Pollen abundances are calculated as percentages of the sum of total pollen including trees, shrubs and aquatic pollen. Spore and Fresh water algae concentrations are expressed as number of specimens per gram (# / g) and fluxes as number of specimens per area and time (#/cm^2/yr)*100. Gray horizontal bands indicate the two aridity maxima occurring during Heinrich Event1.

The dinocyst assemblage is characterized by low percentages of *Brigantedinium* spp. decreasing from 40 to 10% at the end of this phase. This interval is also characterized by an abrupt increase of dinocyst accumulation rates whereas dinocyst concentrations increase slightly.

Percentage maxima of Cyperaceae pollen characterize the vegetation development between ca. 14,800 and 12,100 cal yr BP, occurring simultaneously with *Rhizophora* (11%) and *Typha* (6%). Concentrations of pollen, fern spores and total fresh water algae markedly increase whereas Cheno-Am and Poaceae pollen percentages decrease considerably. Dinocyst association is characterized by a strong increase in total dinocyst concentrations and the dominance of *L. machaerophorum* at the expense of *Brigantedinium* spp as well as the significant occurrence of *Spiniferites* and *Impagidinium* species.

Table 6.1 Summary of the main vegetation shifts and oceanic variations described during Heinrich event 1. +++ High increase, ++ increase, ↗ trend towards an increase, ↙ trend towards a decrease.

	Phase 1	**Transition**	**Phase 2**	**Transition**
Pollen concentrations (grains/cm^3)	-	-	+++	++
Amaranthaceae-Chenopodiaceae (Saharan elements/Salt marsh)	+++	↙	+++	-
Cyperaceae	↗	↗	-	+++
Mangrove (Littoral vegetation)	-	↗	-	++
Aquatic elements (River and swamps vegetation)	-	↗	-	++
Dinocyst concentrations (cysts/cm^3)	-	-	++	-
Dinocyst Accumulation rates (cysts/cm^2/ka)	-	-	++	-
Upwelling dinocysts (%)	+++	↙	+++	-
Upwelling dinocysts (Acc. Rate)	++	↙	+++	-
Relaxed upwelling/River runoff association (%) (L. machaerophorum)	-	↗	-	+++
Temperate dinocysts (%) (Spiniferites)	-	↗	-	+++

6.4 Discussion

The high resolution palynological and geochemical data of sediment core GeoB9508-5 reveals the complexity of the last deglaciation, marked by large changes in vegetation cover and oceanic conditions to more complex and extreme conditions during the period between 18,800 and 14,800 cal yr BP and clearly shows four distinct phases within this time interval. The first phase occurs between ca. 18,800 and 17,400, the second phase between 17,400 and 16,400, the third occurs from ca. 16, 400 to 15,400 cal yr BP and the fourth phase from ca.15, 400 to 14,800 cal yr BP (Figure 6.3).

The most striking feature of the first phase is the maximum input of Cheno-Am reaching highest values at ca. 18,400 cal yr BP synchronously with the first elevated phase of Ti/Ca ratio. Cheno-Am are one of the most common representatives of the desert plant community as well as the coastal halophytic vegetation (salt marsh) (Hooghiemstra and Agwu, 1986; Hooghiemstra 1988; Dupont and Agwu, 1991). They indicate dry environments but can also be very sensitive to environmental gradients in the sea-continent interface and thus can provide information on phases of marine lowstand/highstand and transgression /regression (Poumont, 1989; González and Dupont, In press). The ratio Ti/Ca is an indicator for wind strength (Balsam et al., 1995; Larrasoaña et al., 2003). High values point to higher aeolian contribution whereas low values indicate enhanced continental precipitation in NW Africa (Itambi et al., 2008). Interestingly, the abrupt increase of Cheno-Am by 40% within ~500 yrs, in the pollen record, together with the increase of Ti/Ca clearly indicates periods of extremely dry conditions accompanied with strong NE trade winds. Extreme dry conditions are supported by reduced fluvial discharge from the continent as indicated by low Al/Si ratio (Mulitza et al., 2008) and also by changes detected in the dinocyst assemblage. The latest indicates an abrupt increase of the heterotrophic taxon *Brigantedinium* spp. relative abundances, suggesting nutrient-rich environments related to high marine productivity characteristic for active upwelling areas and mixed waters. These observations could be explained by the southward migration of the intertropical convergence zone (ITCZ) and its associated rainbelt (Lohmann, 2003; Zhang and Delworth, 2005; Mulitza et al., 2008) during periods of AMOC weakening due to meltwater pulses in the North Atlantic that

started around 19,000 cal yr BP (Clark et al., 1996). Accordingly, this shift leads to extremely dry conditions over Sahara and Sahel along with strong NE Trade Winds leading to enhanced wind-induced upwelling thus stimulating ocean surface productivity. These conditions define the first aridity maximum phase over western Sahel between ca. 18,800 and 17,400 cal yr BP (Figure 6.3).

Decreasing Ti/Ca ratio and Cheno-Am pollen percentages in the second phase between ca. 17,500 and 16,400 cal yr BP, indicate decreased terrigenous deposition in the marine sediments of GeoB9508-5 and a relative relaxation of the NE trade winds. Indication for relaxed winds is consistent with the considerable decrease of *Brigantedinium* spp. reflecting a weakening of the wind-induced upwelling activity. On the other hand, pollen assemblage shows a modest increase of Sahelian elements (e.g., *Boscia* and *Mitracarpus* pollen) suggesting less arid conditions over western Sahel compared to the previous phase whereas Saharan climate remains dry.

The dominating vegetation type in the third phase, between ca. 16,400 and 15,400 cal yr BP, is the Saharan plant community indicated by the second maximum phase of Cheno-Am occurring syimultaneously with the maximum phase of Ti/Ca suggesting a period of extremely dry conditions over Sahara and Sahel accompanied by an intensification of the NE trade winds. Strong trade winds are supported by an increase of relative abundances of the upwelling taxon *Brigantedinium* spp. indicating similarly to the first phase, considerable southward shift of the ITCZ and its associated tropical rainbelt, during periods of quasi-cessation of the AMOC, leading to enhanced wind-induced upwelling thus stimulating surface productivity and defining the second aridity maximum phase over western Sahel between ca. 16,400 and 15,400 cal yr BP (Figure 6.3).

The salient feature of the fourth phase, between ca. 15,400 yr BP and 14,800 cal yr BP is the increase in concentration and accumulation rate values of pollen, fern spores and fresh water algae as well as the increase of mangrove and hydrophile plants pointing to a shift towards more humid and relatively warm conditions.

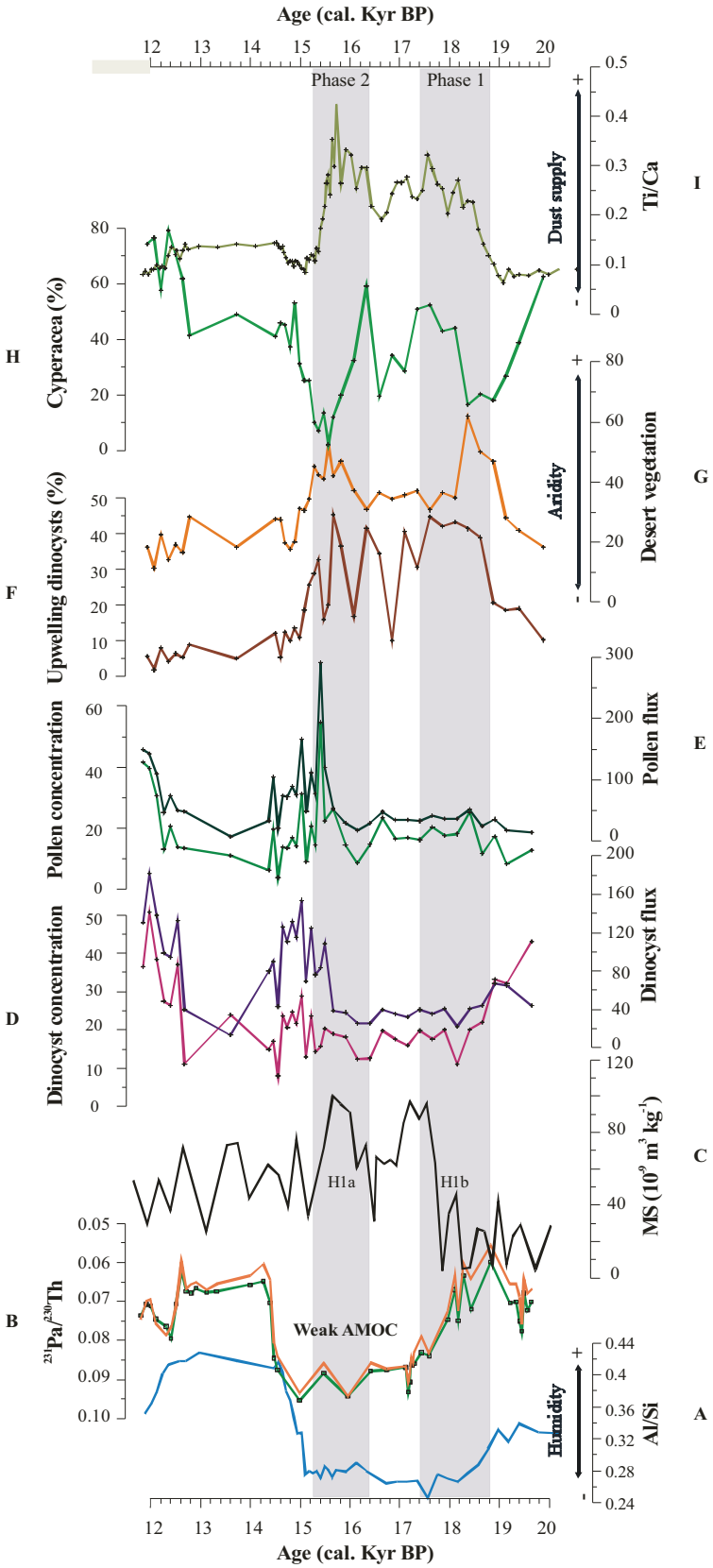
Age (cal. Kyr BP)
12 13 14 15 16 17 18 19 20
Phase 2
Phase 1
H
Cyperacea (%)
0 20 40 60 80
Dust supply
Ti/Ca
0 0.1 0.2 0.3 0.4 0.5
I
F
Upwelling dinocysts (%)
0 10 20 30 40 50
Aridity
Desert vegetation
0 20 40 60 80
G
Pollen concentration
0 20 40 60
Pollen flux
0 100 200 300
E
D
Dinocyst concentration
0 10 20 30 40 50
Dinocyst flux
0 40 80 120 160 200
C
H1a
H1b
MS (10^{-9} m^3 kg^{-1})
0 40 80 120
B
$^{231}Pa/^{230}Th$
0.05 0.06 0.07 0.08 0.09 0.10
Weak AMOC
Humidity
Al/Si
0.24 0.28 0.32 0.36 0.4 0.44
A
Age (cal. Kyr BP)

Figure 6.3 Last deglaciation records of **(A)**: bulk Al/Si ratio from core GeoB9508-5 (Mulitza et al., 2008), **(B)**: Sedimentary $^{231}Pa/^{230}Th$ from core GGC5 (McManus et al., 2004), **(C)**: the MS record from core SU8118 off Southern Portugal (Bard et al., 2000) showing the two depositional phases centred at 16,000 cal yr BP (H1a) and 17,500 (H1b), **(D)**: Dinocyst concentrations (cysts/cm^3)*100 (pink) and accumulation rates (cysts/cm^2/yr)*1000 (purple), **(E)**: Pollen concentrations (grains/cm^3)*100 (light green) and accumulation rates (grains/cm^2/yr)*1000, **(F)**: relative abundances of dinocysts indicative for upwelling, **(G)**: relative abundances of desert vegetation represented by Amarnathaceae-Chenopodiacea (Cheno-Am), **(H)**: relative abundances of Cyperaceae, **(I)**: bulk Ti/ca ratio from core GeoB9508-5. Gray bars indicate the approximate occurrence of the two aridity maxima during Heinrich Event1.

This suggests an enhanced river discharge supplying terrigenous material and nutrients to the marine sediments of GeoB9508-5 leading to the occurrence of runoff dinocyst association indicative of fresh and high-nutrient waters (Bouimetarhan et al., *accepted*) simultaneously with decreased relative abundances of the upwelling taxon *Brigantedinium* spp. suggesting an upwelling weakening. These conditions indicate a major hydrologic change causing simultaneously dry conditions over the Sahara and wetter conditions over Western Sahel supporting the interpretation of high rainfall periods leading to higher runoff and consequently higher inputs of terrestrial nutrients via the Senegal River and more extended periods of weak NE trade winds leading to the cessation of upwelling.

The enhanced humidity that occurred at the fourth phase of H1 stadial is unique and reflects an early reactivation of the western Sahel rainfall suggesting that glacial conditions ended earlier than the high latitudes. This supports the hypothesis of Flückiger et al. (2006) based on modelling simulations, which considers that Heinrich events are a response rather than the cause of AMOC cessation (Hall et al., 2006). Indication for humid conditions in the Sahel region during this time interval has been reported in the Niger basin and Mali, where clear environmental changes from arid to more humid conditions took place at ca. 16,000 cal yr BP with a prominent hydrological change starting at ca. 15,800 cal yr BP, indicating an early re-establishment of rainfall in Sahel (Gasse, 2000) which has been related to the intensification of the Indian monsoon recorded in the Arabian Sea by Sirocko et al. (1996).

Following the H1 stadial between 14,800 and 12,900 yr BP, a drastic decrease of the Saharan vegetation and Ti/Ca ratio simultaneously with an abrupt increase of mangroves and hygrophile plants as well as fern spore and fresh water algae

concentrations and accumulation rates, suggests changes in hydrographic cycle in the Sahel towards more humid and warm environment. These findings are supported by the abrupt increase of Al/Si suggesting a considerable contribution of suspended sediments from the Senegal River (Mulitza et al., 2008) and indicating runoff intensification and continuous freshwater supply. This implies a considerable northward displacement of the ITCZ and its associated tropical rainbelt during the strengthening periods of the AMOC, bringing monsoon winds that advect warm and humid air northward over the Sahel region. These events are thought to match the major Bølling-Allerød warm event identified in high latitudes. According to our age model, the palynological evidences inferred from this study support the results of lake records in the Sahel belt where the African monsoon reactivation at ca. 15,000 cal yr BP had increased rainfall and the runoff in the region (Alayne Street and Grove, 1976; Gasse, 2000). Dinocyst association sees the succession of temperate periods as illustrated by the significant occurrence of the *Spiniferites* group suggesting a considerable warming of the surface waters and *L. machaerophorum* as indicator of nutrient-rich and seasonally stratified waters typical of relaxed upwelling and/or river runoff (Marret and Zonneveld, 2003; Bouimetarhan et al., *accepted*) whereas relative abundances of *Brigantedinium* spp. exhibit a drastic decrease indicating an abrupt weakening of upwelling.

The two aridity maxima observed over the western Sahel reveal the internal complexity of H1 stadial that has earlier been detected further north in mid-latitude core (SU8118) off Portugal where two-depositional IRD phases have been detected at ~ 17,500 cal yr BP (H1b) and 16,000 cal yr BP (H1a) (Bard et al., 2000) and offshore NE Brazil where two forest phases have been recorded during H1, the first phase between ~ 17,900 and 16,600 cal yr BP and the second phase between ~16,600 and 14,900 cal yr BP (Dupont et al., in review). However the processes that provoke the occurrence of these two phases within H1 in western Sahel climate are not yet clear. One explanation would be the peculiar combination of global and regional factors based on the latitudinal position of the studied core: The first factor is associated with the AMOC slowdown due to meltwater pulses in the North Atlantic that causes the southward migration of the intertropical convergence zone (ITCZ) and its associated rainbelt (Lohmann, 2003; Zhang and Delworth, 2005) thus, extreme aridity over West Africa (Mulitza et al., 2008; Itambi et al, 2008) coupled to

strong NE Trade Winds which define the two aridity maxima phases of H1 over western Sahel (Figure 6.3). The second factor is probably related regionally to the Indian monsoon intensification as already suggested by Gasse (2000) resulting in enhanced continental precipitation.

6.5 Conclusions

High-resolution palynological and geochemical records off western Sahel reveal large climatic and hydrologic changes during the last deglaciation. H1 stadial seems to be a complex period characterized by four distinct phases among which two aridity maximum phases were distinguished. The first phase occurs between ca. 18,800 and 17,400 cal yr BP and the second phase between ca.16,400 - 15,400 cal yr BP coinciding with 1) the two-depositional IRD phases detected in the Iberian margin off Portugal at ~ 17,500 cal yr BP (H1b) and ~ 16,000 cal yr BP (H1a) (Bard et al., 2000) and 2) the two forest phases in NE Brazil during H1, between ~ 17,900 and 16,600 cal yr BP and between ~ 16,600 and 14,900 cal yr BP (Dupont et al., in review). Our records are consistent with previous studies and together highlight the close relationship between AMOC, SST changes and Sahel precipitation. The results show that additionally to the latitudinal migration of the ITCZ and its associated tropical rainbelt, Indian mosoon has an impact on the hydrological changes observed in the study area. However, modelling experiments integrating vegetation feedbacks especially the Saharan plant community are needed to better understand the occurrence of these two aridity maxima that punctuated the H1 stadial in western Sahel.

Acknowledgements

This work was funded through the Deutsche Forschungsgemeinschaft as part of the DFG-Research Center/ Excellence cluster “The Ocean in the Earth System” (MARUM) at the University of Bremen. We thank the captain and crew of the R/V *Meteor* for the logistic and technical assistance, André Paul and Xavier Giraud for discussions. Thanks to Mirja Hoins for palynological processing. This is MARUM publication N° xxx.

References

Alayne Street, F., Grove, A.T., 1976. Environmental and climatic implications of Quaternary Lake-level fluctuations in Africa. Nature 261, 385-390.

Balsam, W. L., Otto-Bliesner, B. L., Deaton, B.C., 1995. Modern and last glacial maximum aeolian sedimentation patterns in the Atlantic Ocean interpreted from sediment iron oxide content, Paleoceanography, 10, 493-507.

Bard, E., Rostek, F., Turon, J-L., Gendreau, S., 2000. Hydrological impact of Heinrich events in the subtropical Northeast Atlantic. Nature 289, 1321-1324.

Bond, G., Heinrich, H., Broecker, W., Labeyrie, L., McManus, J., Andrews, J., Huonparallel, S., Jantschik, R., Clasen, S., Simet, C., Tedesco, K., Klas, M., Bonani, G., Ivy, S., 1992. Evidence for massive discharges of icebergs into the North Atlantic sediments and Greenland ice. Nature 365, 143-147.

Bouimetarhan, I., Marret, F., Dupont, L., Zonneveld. K.A.F. (*accepted*). Dinoflagellate cyst distribution in marine surface sediments off West Africa (17-6°N) in relation to sea-surface conditions, freshwater input and seasonal coastal upwelling. Marine Micropaleontology.

Clark, P.U., Alley, R.B., Keigwin, L.D., Licciardi, J.M., Johnsen, S.J., Wang, H., 1996. Origin of the first global meltwater pulse following the last glacial maximum. Paleoceanography 11, 563-578.

Claussen, M., Kubatzki, C., Brovkin, V., Ganopolski, A., 1999. Simulation of an abrupt change in Saharan vegetation in the mid-Holocene. Geophysical research letters 26, 2037-2040.

Dale, B., 1996. Dinoflagellate cyst ecology: modeling and geological applications. In: Jansonius, J., McGregor, D.C. (Eds.), Palynology: Principles and Applications, vol. 3. American Association of Stratigraphic Palynologists Foundation, Salt Lake City, pp. 1249-1275.

deMenocal, P., 1995. Plio-Pleistocene African climate. Science 270, 53-59.

deMenocal, P., Oritz, J., Guilderson, T., Jess Adkins, Sarnthein, M., Baker, L., Yarusinsky, M., 2000. Abrupt onset and termination of the African humid period: rapid climate response to gradual insolation forcing. Quaternary Science Reviews 19, 347-361.

de Vernal, A., Turon, J.-L., Guiot,J., 1994. Dinoflagellate cyst distribution in high latitude environments and quantitative reconstruction of sea-surface temperature, salinity and seasonality. Canadian Journal of Earth Sciences 31, 48-62.

Dupont, L.M., Agwu, C.O.C., 1991. Environmental control of pollen grain distribution patterns in the Gulf of Guinea and offshore NW-Africa. Geologische Rundschau 80, 567-589.

Dupont, L.M., Schütz, F., Teboh, E.C., Jennerjahn, T.C., Behling, H., Paul, A., (In review). Two-step vegetation response to enhanced precipitation in northeastern Brazil during Heinrich event 1.

Faegri, K., Iversen, J., 1989. "Textbook of pollen analysis". IV Edition by Faegri, K., Kaland, P.E., Krzywinski, K.Wiley, New York.

Flückiger, J., Knutti, R., White, J. W. C. 2006. Oceanic process as potential trigger and amplifying mechanisms for Heinrich events. Paleoceanography 21, PA2014, 1-11.

Folland, C.K., Palmer, T.N. and Parker, D.E., 1986. Sahel Rainfall and Worldwide Sea Temperatures, 1901-85. Nature 320 (6063), 602-607.

Gasse, F., 2000. Hydrological changes in the African tropics since the Last Glacial Maximum. Quaternary Science Reviews 19, 189-211.

Glaccum, R. A., 1978. The mineralogical and elemental composition of mineral aerosols over the tropical North Atlantic; the influence of Saharan dust, Master's thesis, University of Miami. Coral Gables, FL, 161 p.

González, C., Dupont, L. (In Press). Tropical salt marsh succession as sea-level indicator during heinrich events. Quaternary Science Reviews.

Hall, I.R., Moran, S.B., zahn, R., Knutz, P.C., Shen, C.-C., Edwards, R.L., 2006. Accelerated drawdown of meridional overturning in the late glacial Atlantic triggerd by transient pre-H event freshwater perturbations. Geophysical Research letters 33, L16616, 1-5.

Hooghiemstra, H., 1988. Changes of major wind belts and vegetation zones in NW Africa 20.000 – 5000 yr B.P., as deduced from a marine pollen record near Cap Blanc.Review of Palaeobotany and Palynology 55, 101-140.

Hooghiemstra, H., Agwu C.O.C., 1986. Distribution of palynomorphs in marine sediment: a record for seasonal wind patterns over NW Africa and adjacent Atlantic. Geologische Rundschau 75, 81 - 95.

Hsu, C.P.F., Wallace, J.M., 1976. The global distribution in annual and semiannual cycles in precipitation. Monthly Weather Review 104(9), 1093-1101.

Itambi A, von Dobeneck T, Mulitza S., Bickert T, Heslop D., 2008. Millennial-scale North West African droughts relates to H Events and D O Cycles: Evidence in marine sediments from off-shore Senegal. Paleoceanography, PA001570.

Jullien, E., Grousset, F., Malaizé, B., Duprat, J., Sanchez-Goni, M.-F., Eynaud, F., Charlier, K., Schneider, R., Bory, A., Bout, V., Flores, J.A., 2007. Low latitude « dusty event » vs high-latitude « ice Heinrich event ». Quaternary Research 68, 379-386.

Lamb, H.F., Gasse, F., Benkaddour, A., El Hamouti, N., van der Kaars, S., Perkins, W.T., Pearce, N.J., Roberts, C.N., 1995. Relation between century-scale Holocene arid intervals in tropical and temperate zones. Nature 373, 134-136.

Lamb, P. J., 1978. Large scale Tropical Atlantic circulation patterns associated with Sub-Saharan weather anomalies. Tellus, 30, 240-251.

Larrasoaña, J. C., Roberts, A. P., Rohling, E. J., Winklhofer, M., Wehausen, R., 2003. Three million years of monsoon variability over the northern Sahara, Clim. Dyn., 21, 689-698.

Leroy, S.A.G., Dupont, A., 1994. Developpmement of vegetation and continental aridity in Northwestern Africa during the late Pliocene: the pollen record of ODP 658. Paleogeography, Paleoclimatology, Paleoecology 109, 295-316.

Marret, F., 1994. Distribution of dinoflagellate cysts in recent marine sediments from the east Equatorial Atlantic (Gulf of Guinea). Review of Paleobotany and Palynology 84, 1-22.

Marret, F., de Vernal, A., 1997. Dinoflagellate cyst distribution in surface sediments of the Southern Indian Ocean. Marine Micropaleontology 29, 367-392.

Marret, F., Zonneveld, K., 2003. Atlas of modern organic-walled dinoflagellate cyst distribution. Review of Palaeobotany and Palynology 125, 1-200.

McManus, J.F., François, r., Gherardi, J.-M., Keigwin, L.D., Brown-Leger, S., 2004. Collapse and rapid resumption of Atlantic meridional circulation linked to deglacial climate changes. Nature 428, 834-837.

Mulitza, S., Bouimetarhan, I., Brüning, M., Freesemann, A., Gussone, N., Filipsson, H., Heil, G., Hessler, S., Jaeschke, A., Johnstone, H., Klann, M., Klein, F., Küster, K., März, C., McGregor, H., Minning, M., Müller, H., Ochsenhirt, W.T., Paul, A., Scewe, F., Schulz, M., Steinlöchner, J., Stuut, J.B., Tjallingii, R., Dobeneck, T., Wiesmaier, S., Zabel, M. and Zonneveld, K., 2006. Report and preliminary results of Meteor cruise M65/1, Dakar – Dakar, 11.06.–01.07.2005. Berichte, Fachbereich Geowissenschaften, Universität Bremen, No. 252, 149 pp.

Mulitza, S., Prange, M., Stuut, J.B., Zabel, M., von Dobeneck, T., Itambi, C.A., Nizou, J., Schulz, M., Wefer, G., 2008. Sahel Megadrought triggered by glacial slowdowns of Atlantic meridional overturning. Paleoceanography 23, PA4206.

Newell, R.E., Hsiung, J., 1987. Factors controlling free air and ocean temperature of the last 30 years and extrapolation to the past, in Aprupt climate change; evidence and implications, edited by Berger, W.H. and Labeyrie, L.D., pp. 67-87.

Poumont, C., 1989. Palynological evidence for eustatic events in the tropical Neogene. Bulletin des centres de recherches Exploration-Production Elf Aquitaine 13, 437-453.

Schefuß, E., Schouten, S. Schneider, R.R., 2005. Climatic controls on central African hydrology during the past 20,000 years. Nature 437, 1003-1006.

Schnetger B., 1992. Chemical composition of loess from a local and worldwide view. N. Jb. Miner. Mh. Jg. 1992 (H. 1), 29-47.

Schütz, L., Rahn, K. A., 1982. Trace element concentrations in erodible soil. Atmospheric Environment, 16, 171-176.

Shaffer G, Olsen SM, Bjerrum CJ., 2004. Ocean subsurface warming as a mechanism for coupling Dansgaard-Oeschger climate cycles and ice-rafting events. Geophysical Research Letters, 31, 1-4.

Street-Perrott, F.A., Perrott, R.A., 1990. Abrupt climate fluctuations in the tropics: the influence of Atlantic Ocean Circulation. Nature 343, 607-611.

Tjallingii, R., Claussen, M., Stuut, J.B., Fohlmeister, J., Jahn, A., Bickert, T., Lamy, F., Röhl, U., 2008. Coherent high- and low-latitude control of the northwest African hydrological balance. Nature Geosciences 1, 670-675.

Wall, D., Dale, B., Lohmann, G. P., Smith, W. K. 1977. The environmental and climatic distribution of dinoflagellate cysts in the North and South Atlantic Oceans and adjacent sea. Marine Micropaleontology 2, 121-200.

Weldeab, S., Schneider, R.R., Kölling. M, Wefer, G., 2005. Holocene African droughts relate to eastern equatorial Atlantic cooling. Geology 12, 981-984.

Zhao, M., Beveridge, N.A.S., Shackelton, N.J., Sarnthein, M., Elington, G., 1995. Molecular stratigraphy of cores off North West Africa: Sea surface temperature history over the last 80 ka. Paleoceanography 10, 661.

Zhang, R., Delworth, T.L., 2005. Simulated tropical response to a substantial weakening of the Atlantic thermohaline circulation. Journal of climate 18, 1853-1860.

Chapter 7

Summary and conclusions

The results compiled in this work investigate the paleoceanographic and paleoclimatic evolution of the eastern tropical North Atlantic and western Sahel during the last deglaciation and the late Holocene with special emphasis on abrupt climate change. This thesis introduces records of pollen and organic-walled dinoflagellate cysts in high temporal resolution from marine gravity cores off western tropical Africa. Palynological results were used with additional informations provided by geochemical data in order to reconstruct past vegetation and hydrological changes as well as changes in past oceanic conditions.

Our investigations on modern sediments off West Africa (17 – 6°N) indicate that both pollen and organic-walled dinoflagellate cysts are sensitive recorders of western Sahel hydrological changes. The composition of dinocyst assemblages and changes in their concentrations as well as those of pollen reflect changes in climatic zones and precipitation regimes in tropical West Africa that are related to the current position and seasonal variability of the ITCZ and the position of its associated tropical rainbelt. The results primarily reflect the southward migration of the tropical rainbelt which causes dry conditions over the northern part of our study area and intensified trade winds along the north western African coast. This promotes seasonal coastal upwelling, which induces upwelling-related productivity. Simultaneously, wetter conditions are observed over the southern part leading to enhanced river runoff supplying warm and fresh waters as well as large amounts of terrestrial nutrients. Four hydrographic regimes have been identified; 1) the northern regime between 17 and 14°N characterized by high productivity associated with seasonal coastal upwelling, 2) the southern regime between 12 and 6°N associated with high-nutrient waters influenced by river discharge, 3) the intermediate regime between 14 and 12°N influenced mainly by seasonal coastal upwelling and additionally associated with fluvial input of terrestrial nutrients, and 4) the low productivity regime characterized by low chlorophyll-*a* concentrations in upper waters and high bottom water oxygen concentrations.

The new palynological evidence from the mud-belt deposited off the Senegal River mouth tracked the decadal-scale history of Sahel drought throughout the period from ca. 4200 to 1200 cal yr BP. The results show significant changes in terrestrial and marine environmental conditions, implying climatic instability during a period that has been generally considered relatively invariable. The record shows changes in the assemblages, concentrations and fluxes of pollen and dinocysts as well as changes in sedimentation rates displaying two main humid periods that have interrupted the general climatic trend of increasing aridity obsereved at the end of the Africa humid period (5500 cal yr BP). The first period occurred between ca. 2900 and 2500 cal yr BP and we refer to it as the "Little Humid Phase". The second occurred between ca. 2200 and 2100 cal yr BP and is thought to be related to episodic flash flood events of the Senegal River. The observed alternating arid and humid phases in western Sahel during the late Holocene most probably reflect the weakening and strengthening of the African monsoon in close association with the latitudinal migration of the ITCZ and its associated tropical rainbelt. These results support the hypothesis of the ITCZ latitudinal migration as the dominant driving mechanism of late Holocene climate variations in this region in contrast to previous beliefs that the tropical African climate is entirely controlled by orbital changes in summer insolation.

On millennial timescales, the history of western Sahel hydrology for the period from 20,000 to 12,000 cal yr BP during the last deglaciation, has been reconstructed through pollen and dinocyst analysis together with geochemical measurments (Ti/Ca ratio) of a marine sediment core GeoB9508-5 located at latitudes nowadays characterized by Sahelian/Saharan conditions. These data indicate that the abrupt onset of arid conditions in the western Sahel were linked to cold North Atlantic sea surface temperatures during times of reduced meridional overturning circulation (AMOC) associated with Heinrich Stadial 1. However, H1 stadial seems to be a more complex and extreme period characterized by four distinct phases among which two aridity maxima were distinguished. The first phase occurred between ca. 18,800 and 17,400 cal yr BP and the second between ca.16,400 and 15,400 cal yr BP. Both phases were characterized by a maximum occurrence of the Saharan plant community coinciding with a maximum of Ti/Ca ratio, indicating extremely dry conditions and strong NE trade winds. Interestingly, dinoflagellate cyst assemblages were dominated, during both intervals, by the upwelling association suggesting nutrient-rich surface

waters characteristic for high marine productivity related to the enhanced Tradewind-induced upwelling in the region. Our results point to a clear impact of the latitudinal migration of the ITCZ and its associated tropical rainbelt during periods of AMOC weakening (Strengthening). It also provides insights into how terrestrial ecosystems (local vegetation, river discharge) responded within a few decades to abrupt climate changes during the last deglaciation and how the upwelling-related productivity changed during this period. These findings show the importance of paleovegetation studies, as an additional source of paleoclimatic information, for comparing and validating the global models that simulate vegetation-climate interactions, vegetation dynamic, and terrestrial ecosystems structure. Our records are consistent with previous studies and together highlight the close relationship between AMOC, SST patterns and Sahel precipitation. The results demonstrate that in addition to the latitudinal migration of the ITCZ and its associated tropical rainbelt, the Indian mosoon has a great impact on the hydrological changes observed in the study area.

Chapter 8

Future perspectives

The present study has shed more light into climate variability over western Sahel and the factors that drive such changes. This work showed that the vegetation of north western Africa is sensitive to rapid climate changes associated with the last deglaciation conditions especially the Heinrich Stadial 1 and the late Holocene. Moreover, the results show the importance of organic-walled dinoflagellate cysts as additional paleoceanographic information concerning paleoproductivity variations in the eastern tropical North Atlantic with respect to abrupt climate changes. However, further research is needed to test and develop the presented ideas and future improvements may be achieved by the following suggestions.

1) The time resolution at site GeoB9503-5 provides a unique opportunity to establish a detailed correlation between terrestrial and marine conditions during the late Holocene. The vegetation signal was reconstructed with decadal-scale resolution together with surface oceanic conditions. In order to establish comparisons with other records, it is necessary to extend the pollen and organic-walled dinoflagellate cyst records to the present. Other studies based on grain size, elemental distribution and mineralogical analyses have been carried out in the nearby cores GeoB9501-5 and GeoB9504-3 covering the last 3000 years. The combined analysis and interpretation of these records would provide a more complete view of the late Holocene climatic and oceanic variations in NW Africa. It would also help to understand how natural and possibly human-induced changes might interact to affect the late Holocene climate. This is especially interesting within the current concern about the apparent rise in global temperature since the second half of the last century. Although it is obvious that human activity influences the natural system, large uncertainties remain about to what extent it is responsible for the current climate change. For this purpose, long, continuous, well dated, high temporal resolution records have to be studied covering both pre-industrial and industrial climate change. Especially interesting, are the intervals corresponding to the “Medieval warm period” and the “Little Ice Age” as well as the 20th century droughts.

2) In the same direction, the pollen record should be extended with particular emphasis on the mangrove record. The variations of mangrove pollen abundances in the core GeoB9503-5 (chapter 5) suggest a decline of the mangrove swamps after ca.1900 cal yr BP that deserves to be further investigated. The variation of mangroves can give information about paleogeographical modifications of the environment such as distance to the coast during periods of sea-level variations and altered marine circulation as well as human impact on the mangrove ecosystem.

3) As shown in chapter 6, the history of western Sahel hydrology during the last deglaciation (20,000 - 12,000 cal yr BP) seems to be more complex than previously thought. The findings in this thesis show that the abrupt onset of arid conditions in the western Sahel were linked to the southward shift of the ITCZ and its associated tropical rainbelt during times of reduced meridional overturning circulation (AMOC) associated with Heinrich Stadial 1. Moreover, the results show the impact of the Indian monsoon on the Sahel rainfall reactivation after ca. 15,400 cal yr BP suggesting that both regional (ITCZ) and probably the Indian monsoon atmospheric patterns interacted to modify the local patterns of western Sahel precipitation. The singularity of this hydrological pattern needs to be further investigated by comparing our palynological record with terrestrial biomarkers (*n*-alkanes and *n*-alkanols from leaf waxes) and SST reconstructions from the same core and/or other cores. The combined interpretation of these records would provide a more complete view of the terrestrial biosphere dynamics and its interaction with oceanic circulation variability.The results shown in chapter 6 highlight the close relationship between AMOC variability, SST changes and Sahel precipitation. However, high temporal resolution palynological analyses will be necessary to address more specific processes.

4) In order to investigate and understand the effect of the Indian monsoon and consequently the effect of the Indian Ocean dipole and the tropical SST variability on the Sahel rainfall, high temporal resolution paleoclimatic and paleoceanographic records bordering the Indian and Atlantic Oceans around Africa would be of a substancial importance. The marine sediment cores retrieved from the tropical western Indian Ocean during RV *Meteor* cruise M75-2 (February 2008) will be used to reconstruct in detail contemporaneous changes in continental vegetation and surface

ocean conditions with respect to climate change. Theses records and their interpretations will be subsequently compared with records of NW Africa to provide more evidence for large-scale linkages that propagate regional climate signals around the globe. Such records will allow the validation of Earth System Models including dynamic vegetation modelling.

Appendix 1

Process length variation in cysts of a dinoflagellate, *Lingulodinium machaerophorum*, in surface sediments investigating its potential use as a salinity proxy

Kenneth N. Mertens [a,*], Sofia Ribeiro [b], Ilham Bouimetarhan [c], Hulya Caner [d], Nathalie Combourieu-Nebout [e], Barrie Dale [f], Anne De Vernal [g], Marianne Ellegaard [b],Mariana Filipova [h], Anna Godhe [i], Evelyne Goubert [j], Kari Grøsfjeld [k], Ulrike Holzwarth [c], Ulrich Kotthoff [l], Suzanne A. G. Leroy [m], Laurent Londeix [n], Fabienne Marret [o], Kazumi Matsuoka [p], Peta J. Mudie [q], Lieven Naudts [r], Jose Luis Peña-Manjarrez [s], Agneta Persson [i], Speranta-Maria Popescu [t], Vera Pospelova [u], Francesca Sangiorgi [v], Marcel T.J Van Der Meer [w], Annemiek Vink [x], Karin Zonneveld [y], Dries Vercauteren [z], Jelle Vlassenbroeck [aa], Stephen Louwye [a]

[a] Research Unit Palaeontology, Ghent University, Krijgslaan 281 s8, 9000 Ghent, Belgium

[b] Department of Biology, Aquatic Biology Section, Faculty of Sciences, University of Copenhagen, Øster Farimagsgade 2D DK-1353 Copenhagen K – Denmark

[c] Centre for Marine Environmental Sciences (Marum), University of Bremen, P.O. Box 330440, D-28334, Germany

[d] Institute of Marine Sciences and Management, Istanbul University, Vefa 34470, Turkey

[e] LSCE/IPSL UMR CEA-CNRS-UVSQ, Domaine du CNRS, Avenue de la Terrasse Bat. 12, F-91198 Gif sur Yvette Cedex, France

[f] Department of Geology, University of Oslo, PB 1047 Blindern, N-0316 Oslo, Norway

[g] GEOTOP, Université du Québec à Montréal, P.O. Box 8888, Montréal, Québec, Canada H3C 3P8

[h] Museum of Natural History, 41 Maria Louisa Blvd., 9000 Varna, Bulgaria

[i] Department of Marine Ecology, Marine Botany, University of Gothenburg, PO Box 461, SE 405 30, Göteborg, Sweden

[j] Université Européenne de Bretagne, Université de Bretagne Sud, Lab-STICC, Campus Tohannic, 56 000 Vannes, France

[k] Geological Survey of Norway, PO Box 3006, Lade, N-7002, Trondheim, Norway

[l] Institute of Geosciences, University of Frankfurt, Altenhöferallee 1, D-60438 Frankfurt/M., Germany

[m] Institute for the Environment, Brunel University (West London), Uxbridge UB8 3PH, UK

[n] Département de Géologie et Océanographie, UMR 5805 CNRS, Université Bordeaux 1, avenue de Facultés, 33405 Talence cedex, France

[o] Department of Geography, University of Liverpool, Liverpool, L69 7ZT, UK

[p] Institute for East China Sea Research (ECSER), 1-14, Bunkyo-machi, Nagasaki, 852-8521, Japan

[q] Geological Survey Canada Atlantic, Dartmouth, Nova Scotia, Canada B2Y 4A2

[r] Renard Centre of Marine Geology (RCMG), Ghent University, Krijgslaan 281 s8, B-9000 Ghent, Belgium

[s] Departamento de Oceanografía Biológica, División de Oceanología, Centro de Investigación Científica y de Educación Superior de Ensenada (CICESE), Km. 107 carretera Tijuana-Ensenada, Ensenada, Baja California, México

[t] Université Claude Bernard Lyon 1, Laboratoire PaléoEnvironnements et PaléobioSphère, UMR 5125 CNRD, 2 Rue Raphaël, Dubois, 69622 Villeurbanne Cedex, France

[u] School of Earth and Ocean Sciences, University of Victoria, Petch 168, P.O. Box 3055 STN CSC, Victoria, B.C. , Canada V8W 3P6

[v] Laboratory of Palaeobotany and Palynology, Budapestlaan 4, 3584 CD Utrecht, The Netherlands

[w] Marine Organic Biogeochemistry, NIOZ Royal Netherlands Institute for Sea Research, P.O. Box 59, 1790 AB Den Burg, Texel, The Netherlands

[x] Federal Institute for Geosciences and Natural Resources, Alfred-Bentz-Haus, Stilleweg 2, 30 655 Hannover, Germany

[y] Fachbreich 5-Geowissenschaften, University of Bremen, P.O. Box 330440, D-28334, Germany

[z] Laboratory of General Biochemistry and Physical Pharmacy, Ghent University, Harelbekestraat 72, 9000 Ghent, Belgium

[aa] UGCT, Ghent University, Proeftuinstraat 86, 9000 Ghent

*Corresponding author: Kenneth.Mertens@ugent.be

Marine Micropaleontology 70 (2009), 54-69

Abstract

A biometrical analysis of the dinoflagellate cyst *Lingulodinium machaerophorum* (Deflandre and Cookson 1955) Wall, 1967 in 144 globally distributed surface sediment samples reveals that the average process length is related to summer salinity and temperature at a water depth of 30 m by the equation salinity/temperature=0.078*average process length + 0.534 with R^2=0.69. This relationship can be used to reconstruct paleosalinities, albeit with caution. This particular ecological window can be associated with known distributions of the corresponding motile stage *Lingulodinium polyedrum* (Stein) Dodge, 1989 that forms the *L. machaerophorum* cysts. Confocal laser microscopy shows that the average process length is positively related to the average distance between process bases (R^2=0.78), and negatively related to the number of processes (R^2=0.65). These results document the existence of two end members in cyst formation: one with many short, densely distributed processes and one with a few, long, widely spaced processes, which can be respectively related to low and high salinity/temperature ratios. Obstruction during formation of the cysts causes anomalous distributions of the processes.

***Keywords*:** *Lingulodinium machaerophorum*, processes, *Lingulodinium polyedrum*, biometry, salinity, temperature, palaeosalinity, dinoflagellate cysts

Introduction

Salinity contributes significantly to the density of seawater, and is an important parameter for tracking changes in ocean circulation and climate variation. Palaeosalinity reconstructions are of critical importance for better understanding of global climate change, since they can be linked to changes of the thermohaline circulation (Schmidt *et al.*, 2004). Quantitative salinity reconstructions have been proposed on the basis of several approaches that use for example foraminiferal oxygen isotopes (e.g. Wang *et al.,* 1995), $\delta^{18}O_{seawater}$ based on foraminiferal Mg/Ca ratios and $\delta^{18}O$ (e.g. Schmidt *et al.*, 2004; Nürnberg & Groeneveld, 2006), alkenones (e.g. Rostek *et al.,* 1993), the modern analogue technique applied to dinoflagellate cyst assemblages (e.g. de Vernal & Hillaire-Marcel, 2000) or δD in alkenones (e.g.

Schouten et al., 2006; van der Meer et al., 2007 en 2008). However, none of these approaches is unequivocal (e.g. alkenones; Bendle *et al.* 2005).

Some planktonic organisms are well-known to show morphological variability depending on salinity, e.g. variable noding in the ostracod *Cyprideis torosa*, van Harten (2000) and morphological variation in the coccoliths of *Emiliania huxleyi* (Bollman & Herrle, 2007). A similar dependence has been reported for *Lingulodinium machaerophorum* (Deflandre & Cookson, 1955) Wall, 1967, the cyst of the autotrophic dinoflagellate *Lingulodinium polyedrum* (Stein) Dodge, 1989 which forms extensive harmful algal blooms reported from coasts of California (Sweeney, 1975), Scotland (Lewis *et al.*, 1985), British Columbia (Mudie *et al.*, 2002), Morocco (Bennouna *et al.*, 2002), West Iberia (Amorim *et al.*, 2001) and other coastal areas. This species can be considered as a model dinoflagellate since it is easily cultured and has been the subject of numerous investigations. An extensive review of these studies is given by Lewis and Hallett (1997). Process length variation of *Lingulodinium machaerophorum* was initially related to salinity variations in the Black Sea by Wall *et al.* (1973), and subsequently investigated by others for other regions (Turon, 1984; Dale, 1996; Matthiessen & Brenner, 1996; Nehring, 1994, 1997; Ellegaard, 2000; Mudie *et al.*, 2001; Brenner, 2005; Sorrel *et al.*, 2006; Marret *et al.*, 2007). Kokinos & Anderson (1995) were the first to demonstrate the occurrence of different biometrical groups in culture experiments. Later culture experiments (Hallett, 1999) discovered a linear relationship between average process length and salinity, but also with temperature.

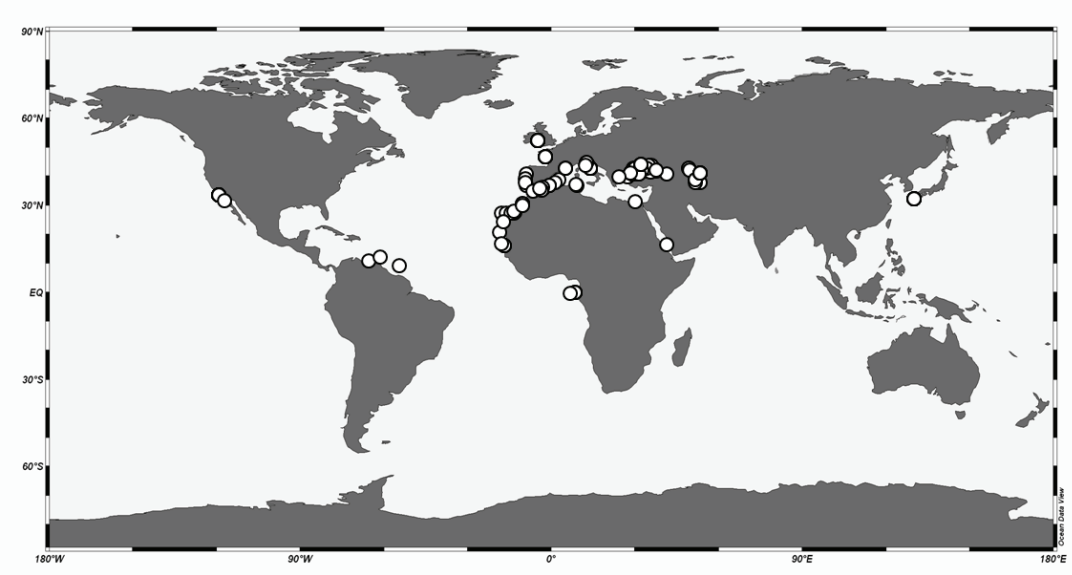

Figure 1 Distribution of the 144 surface samples where *Lingulodinium machaerophorum* process length were studied.

The process length of *L. machaerophorum* as a salinity proxy represents a large potential for palaeoenvironmental studies, since this species currently occurs in a wide range of marine conditions (Marret and Zonneveld, 2003), and can be traced back to the Late Paleocene (Head *et al.*, 1996). The aim of the present study was to evaluate whether the average process length shows a linear relationship to salinity and/or temperature, and to assess its validity for palaeosalinity reconstruction. To achieve this goal, *L. machaerophorum* cysts were studied from surface sediments from numerous coastal areas. Confocal laser microscopy was used for the reconstruction of the complete distribution of the processes on the cyst wall, which has important implications for cyst formation.

Material and Methods

Sample preparation and light microscopy

A total of 144 surface sediment samples were studied for biometric measurements of *L. machaerophorum* cysts from the Kattegat–Skagerrak, Celtic Sea, Brittany, Portuguese coast, Etang de Berre (France), Mediterranean Sea, Marmara Sea, Black Sea, Caspian and Aral Seas, northwest African coast, Canary Islands, coast of Dakar, Gulf of Guinea, Caribbean Sea, Santa Monica Bay (California), Todos Santos Bay (Mexico) and Isahaya Bay (Japan) (Figure 1). Most samples were core top samples

from areas with relatively high sedimentation rates, and ages can be considered recent, i.e. a few centuries (see supplementary data). Five samples have a maximum age of a few thousand years, but since process lengths are as long as processes of recent, nearby samples, these samples can also be considered representative. In general, the cysts studied will give us a global view of the biometric variation of cysts formed during the last few centuries by *L. polyedrum*. It is assumed here that the environmental conditions steering the morphological changes within the cyst are similar to recent environmental conditions.

All the cysts were extracted according to different maceration methods described in the literature (see references in Table 1). Most methods use standard maceration techniques involving hydrochloric acid and hydrofluoric acid, sieving and/or ultrasonication. Regardless of the method used, the cysts all appeared similar in terms of preservation (Plates 1–7).

Almost all measurements were made using a Zeiss Axioskop 2 and Olympus BH-2 light microscope, equipped with a 100x oil immersion objective, and an AxioCam RC5 digital camera (Axiovision v.4.6 software) and Color View II (Cell F Software Imaging System) respectively. The absolute error on a single measurement was 0.5 µm. All measurements were done by Kenneth Neil Mertens, except for the samples from Portugal, which were measured by Sofia Ribeiro. Observer bias did not influence the measurements.

For each sample, the length of the three longest visible processes was measured together with the largest body diameter of 50 cysts for each sample. Measuring 50 cysts gave reproducible results: in sample GeoB7625-2 from the Black Sea, three process lengths. Results are stored by short to long process length per cyst for 50 cysts were measured, and the measurements were then repeated on 50 different cysts, showing no significant differences ($\bar{x}$=13.50 µm ± 2.99 µm and $\bar{x}$=13.21 µm ± 2.62 µm, t-test: p=0.37). The length of each process was measured from the middle of the process base to the process tip. The absolute error in process measurement is 0.4 µm. Within each cyst, three processes could always be found within the focal plane of the light microscope, and for this reason this number seemed a reasonable choice.

.

Table 1. Average of process length from LM measurments, standard deviation, body diameter and standard deviation, average summer temperature and salinity at 30 m water depth, ratio between both and density calculated from both

Region	*# samples*	*Processes measured*	*Average process length (µm)*	*Stdev (µm)*	*Average body diameter (µm)*	*Stdev (µm)*	*Average Summer T_{30m}*	*Average Summer S_{30m}*	*S_{30m}/T_{30m}*	*Denstty (kg/m³)*	*Preservation*	*Reference*
Caspian Sea-Aral Sea	13	1320	5.6	3.4	48.1	6.1	15.72	12.72	0.81	1008.87	Bad to good	Marret *et al.* (2004), Sorrell et al. (2006), Leroy *et al.* (2006) and Leroy (unpublished data), Leroy *et al.* (2007)
Etang de Berre	2	300	7.5	2.5	44.9	4.5	19.91	26.10	1.31	1018.14	Average	Leroy (2001) & Robert *et al.* (2006)
Japan	5	735	8.0	1.9	45.3	5.7	24.54	33.72	1.37	1022.64	Good	Matsuoka (unpublished data)
Caribbean – West Equatorial Atlantic	6	306	13.0	4.4	44.1	6.4	26.19	36.08	1.38	1023.92	Average	Vink *et al.* (2000), Mertens *et al.* (2008) and Vink *et al.* (2001)
Scandinavian Fjords – Kattegat-Skagerrak	26	2271	13.2	4.2	47.9	6.4	16.55*	24.14*	1.46*	1017.43	Bad to good	Grosfjeld & Harland (2001), Gundersen (1988), Ellegaard (2000), Christensen *et al.* (2004) and Persson *et al.* (2000)
East Equatorial Atlantic – Dakar Coast	7	903	13.2	3.4	46.6	6.2	22.88	35.52	1.55	1024.49	Bad to good	Marret *et al.* (1994) and Bouimetarhan *et al.* (unpublished data).
Black Sea and Marmara Sea	35	5196	15.0	4.1	46.3	4.6	12.22	20.08	1.64	1015.14	Good	Verleye *et al.* (2008), Caner & Algan (2002), Caner (unpublished data), Cagatay *et al.* (2000), Naudts (unpublished data), Popescu *et al.* (unpublished), Mudie *et al.* (2007) and van der Meer *et al.* (2008)
Portugal - Brittanny	9	1350	16.8	3.6	45.3	5.5	16.53	35.22	2.13	1025.93	Good	Ribeiro *et al.* (unpublished data), Goubert (unpublished data)
NW Africa	12	1749	18.4	3.8	48.1	6.3	19.47	36.36	1.87	1026.07	Average to good	Holzwarth *et al.* (unpublished data); Kuhlmann et al. (2004), Richter et al.(2007)
Mediterranean – Red Sea	36	3507	19.6	4.4	45.6	6.1	18.39	37.57	2.04	1027.28	Average to good	Sangiorgi *et al.* (2005), Londeix (unpublished data), Combourieu-Nebout *et al.* (1999), Pirlet (unpublished data), Schoel (1974) and Kothoff *et al.* (2008)
Pacific	9	1224	21.2	4.3	47.7	6.1	14.39	33.45	2.32	1025.04	Good	Pospelova *et al.* (2008) and Peña-Manjarrez *et al.* (2005)
Celtic Sea	6	750	21.8	4.1	47.8	5.7	13.50	34.30	2.54	1025.88	Good	Marret & Scource (2002)

*For this region data from 0 m water depth is used

Three reasons can be advanced for choosing the longest processes. Firstly, the longest processes reflect unobstructed growth of the cyst (see below). Secondly, the longest processes enabled us to document the largest variation, and this enhanced the accuracy of the proxy. Thirdly, since only a few processes were parallel to the focal plane of the microscope, it was imperative to make a consistent choice. Sometimes fewer than 50 cysts were measured, if more were not available. Fragments representing less than half of a cyst were not measured, nor were cysts with mostly broken processes.

Salinity and temperature data

The biometric measurements on cysts from the different study areas were compared to both seasonal and annual temperature and salinity at different depths – henceforth noted as T_{0m}, T_{10m},... and S_{0m}, S_{10m}, ..., using the gridded ¼ degree World Ocean Atlas 2001 (Stephens et al. 2002; Boyer et al., 2002) and the Ocean Data View software (Schlitzer, R., http://odv.awi.de, 2008). For the Scandinavian Fjords, in situ data were available from the Water Quality Association of the Bohus Coast (http://www.bvvf.com).

Confocal laser microscopy

Confocal microscopy was performed using a Nikon C1 confocal microscope with a laser wavelength of 488 nm and laser intensity of 10.3%. No colouring was necessary since the cysts were sufficiently autofluorescent. The Z-stack step size was 0.25 µm with a Pixel dwell time of 10.8 µs. The objective used was a 60x/1.40/0.13 Plan-Apochromat lens with oil immersion. After correcting the z-axis for differences in refractive index between the immersion oil and glycerine jelly (here a factor of 78% of correction was used), images were rendered to triangulated surfaces (.stl files) with Volume Graphics VGStudioMax© software. These were imported in Autodesk 3DsMax©, where XYZ coordinates of the base and top of the processes were recorded. From these coordinates Euclidean distances were calculated, enabling the calculation of the process length and the distances between the processes. Distances to the two closest processes of each process were calculated, and by averaging these numbers, the average distance between processes was calculated. A

more detailed description of the methodology is given at http://www.paleo.ugent.be/Confocal.htm.

Results

Preservation issue

To establish the validity of the measurements, preservation needs to be taken into account. Two types of degradation were considered: mechanical and chemical. Three categories were used to describe the mechanical degradation of the cysts: bad (most cysts were fragmented or torn, and processes were broken), average (about half of the cysts were fragmented or torn, and few processes were broken, and good (few cysts were torn or fragmented, and were often still encysted) (see Table 1).

The differences in mechanical breakdown were, from our experience, largely caused by post-processing treatments such as sonication. Prolonged sonication, however, does not significantly change the process length variation. The sample from Gullmar Fjord (average process length 14.6 µm, st. dev. 4.0) was sonicated in an ultrasonic bath for two minutes and the results were not significantly different from samples that were not sonicated (average process length 14.3 µm, st. dev. 4.1) (t-test: p=0.38).

Chemical breakdown could be caused by oxidation or acid treatment. *L. machaerophorum* is moderately sensitive to changes in oxygen availability (Zonneveld *et al.*, 2001). Cysts from samples treated with acetolysis were clearly swollen (Plate 2.8). Most interestingly, both processes and cyst body swell proportionately. These samples were not used for analysis. Similar results were noted after treatment with KOH. These maceration methods should not be used in biometric studies. Cysts extracted using warm HF showed traces of degradation (see Plate 3.23, 3.24), but process length did not change.

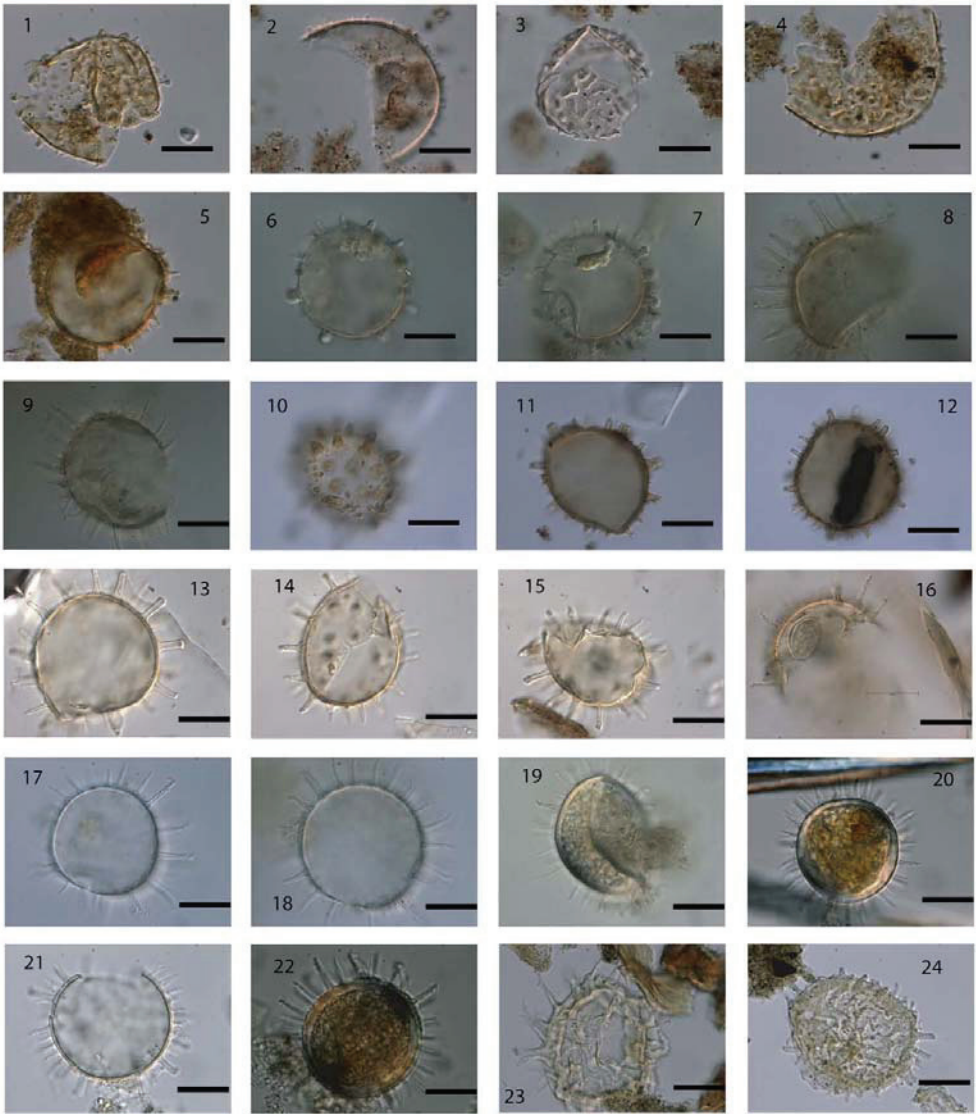

Plate I. *Lingulodinium machaerophorum* cyst from Caspian Sea (1-5), Aral Sea (6-9), Etang de Berre (10-12), Baltic Sea (13-15) and Scandinavian Fjords (16-24). Specific sample names are 1-4. CPO4.5.US02. 6-7.AR23. 8-9. AR17. 10-12. Etang de Berre (19). 13.NG6.14.NG.7.15. NG.9.16. Limfjord. Note inclusion of Nannobarbophora acritarch. 17. Havstenfjorden 18-19. Guumar Fjord 20-21. G2.22.K2. 23-24. Risor Site. All scale bars are 20µm.

Overall cyst biometrics for the multi-regional dataset

The 19,611 process length measurements resulted in a global average of 15.5 µm with a standard deviation of 5.8 µm, and a range from 0 to 41 µm (Figure 2). Most cysts encountered were comparable to the forms described by Kokinos and Anderson (1995), and bald cysts were rare. The range we found is clearly broader than the 2 to 21 µm range postulated by Reid in 1974. The skewness of the distribution was -0.12,

since there is some tailing at the left side of the size frequency curve (Figure 2). The asymmetric distribution was due to a standard deviation that increased synchronously with the average process length. This could be explained partly by the methodological approach – errors on the larger measurements were larger, since larger processes were more often curved or tilted – and by the more common occurrence of cysts with relatively shorter processes in samples that mostly contain cysts with longer processes (also evident in regional size-spectra, Figure 4).

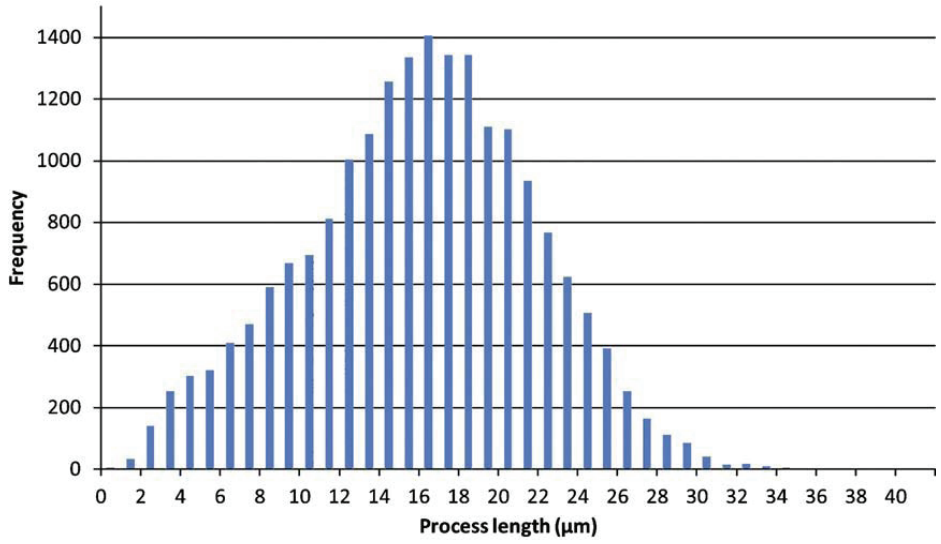

Figure 2 Size-frequency spectrum of 19,611 process measurements.

The 6,537 body diameter measurements resulted in an average body diameter of 46.6 µm with a standard deviation of 5.8 µm. The range was from 26 to 75 µm. This was again a broader range than the 31 to 54 µm given by Deflandre and Cookson (1955) and Wall and Dale (1968). This discrepancy could be explained partly by cysts sometimes being compressed or torn, yielding an anomalously long body diameter. This mechanical deformation of the cyst explains also a positive skewness of the size-frequency spectrum (Figure 3).

The averaged data of *L. machaerophorum* cysts in every region is given in Table 1, sorted from low to high average process length. The individual size-frequency spectra are shown in Figure 4 and the cysts are shown in Plate 1-7. All measurements are available as supplementary data.

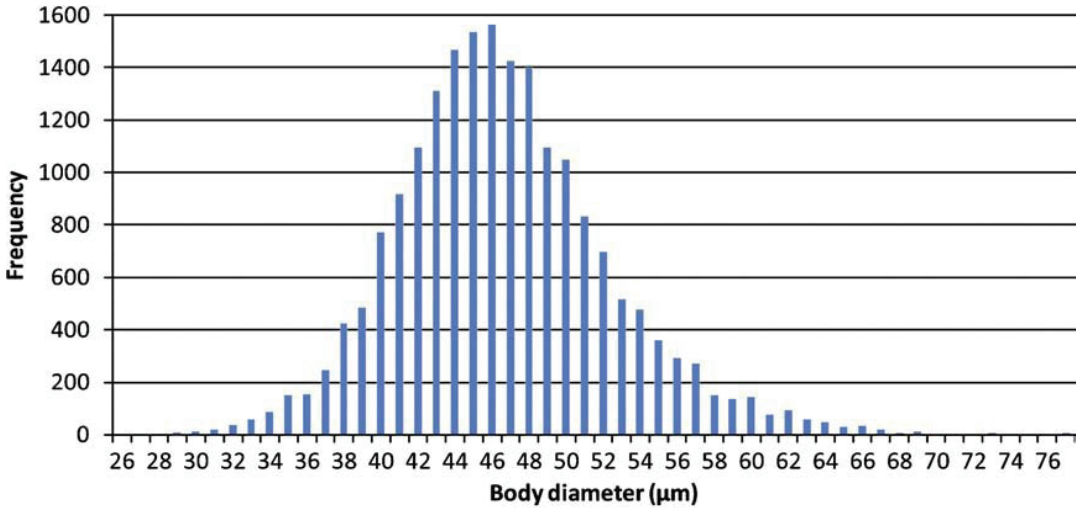

Figure 3 Size-frequency spectrum of 6211 body diameter measurements.

Comparison of process length with salinity & temperature

Firstly, data from the Scandinavian Fjords and the Kattegat–Skagerrak were excluded from all relations since they significantly increased the scatter on all regressions. The reason is given below in the Discussion.

The relation of the average process length of *L. machaerophorum* with only the salinity data, fits best with the winter S_{0m} (R^2=0.54). When compared to temperature data alone, the best relationship is with the winter T_{50m} (R^2=0.06).

A much better relationship can be found with salinity divided by temperature at a water depth of 30 m from July to September (summer). This relationship is expressed as S_{30m}/T_{30m}= 0.078*average process length + 0.534, and has an R^2=0.69 (Figure 5) and a standard error is 0.31 psu/°C. Since seawater density is dependent on salinity and temperature, one could expect that density would have a similar relationship with process length. However, the regression with water density at 30 m water depth shows a stronger relation to process length (R^2=0.50) than with salinity alone (R^2=0.42 with summer S_{30m}), but not better than with S_{30m}/T_{30m}.

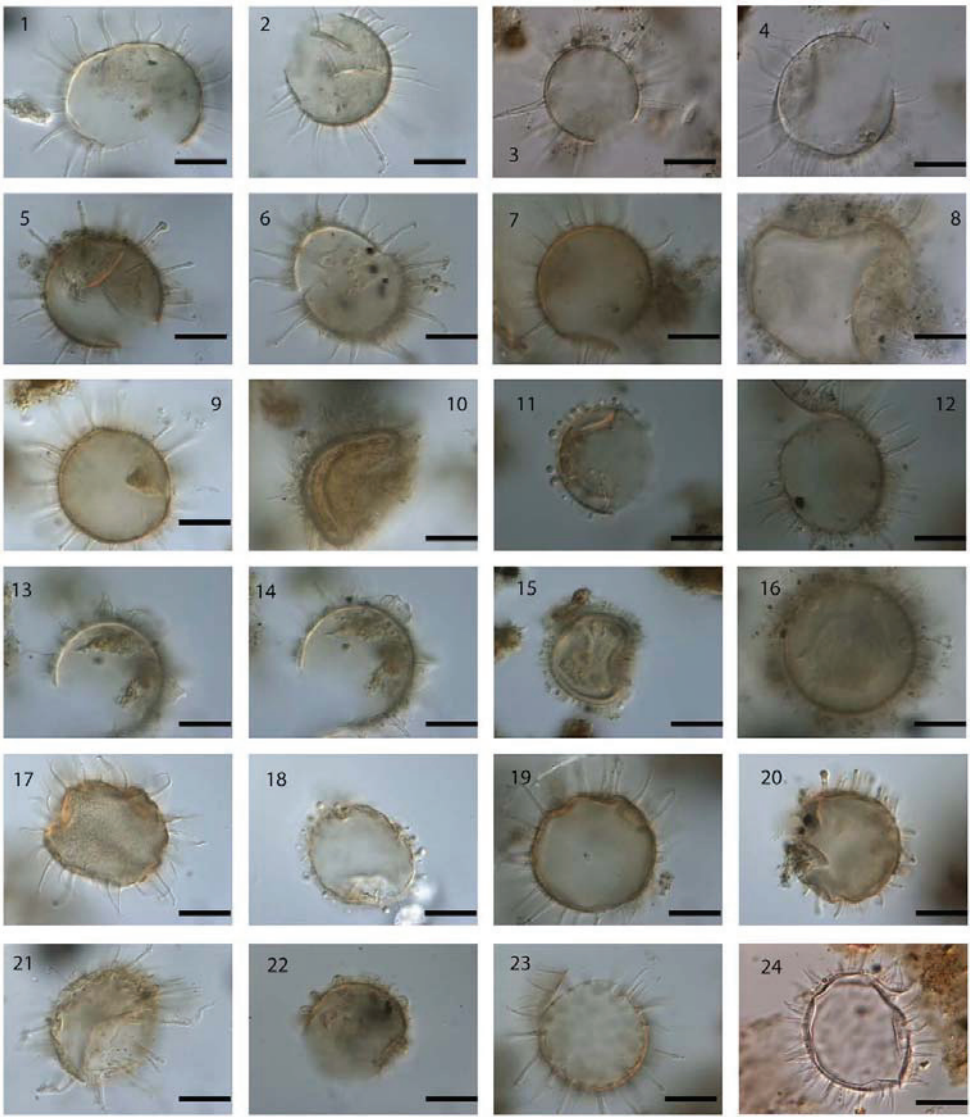

Plate II. *Lingulodinium machaerophorum* cyst from Marmara Sea (1-5) and Black sea (5-24), Note the wide range of morphotypes occurring in these samples. Specific sample names are: 1-2.Dm 13 3-4. Dm5 5-6. Knorr 134.72.7. Knorr 134.51.8. GGC18 Swollen cyst due to use of acetolysis. 9-10. Knorr 134.35.11-12. Knorr134.2. 13-15. B2KS33 0-1. Note merged process in 13 and 14. 16.B2 KS 01 0-1. Note globules at basis of processes. 17-18. All 1443.20-21. All 1438.22. All 434. Note merged processes. 23. All 145.1.24. geoB7625. coloured with safranin-O. All scale bars are 20µm.

An overview of the results in the studied areas is given in Table 1. Next to average process length, salinity, temperature, and S_{30m}/T_{30m}, seawater density data are given, and illustrate that this parameter does not show a better fit than the S_{30m}/T_{30m} ratio. The regression between this averaged data from each region is S_{30m}/T_{30m}=0.085*average process length + 0.468, R^2=0.89 (Figure 6).

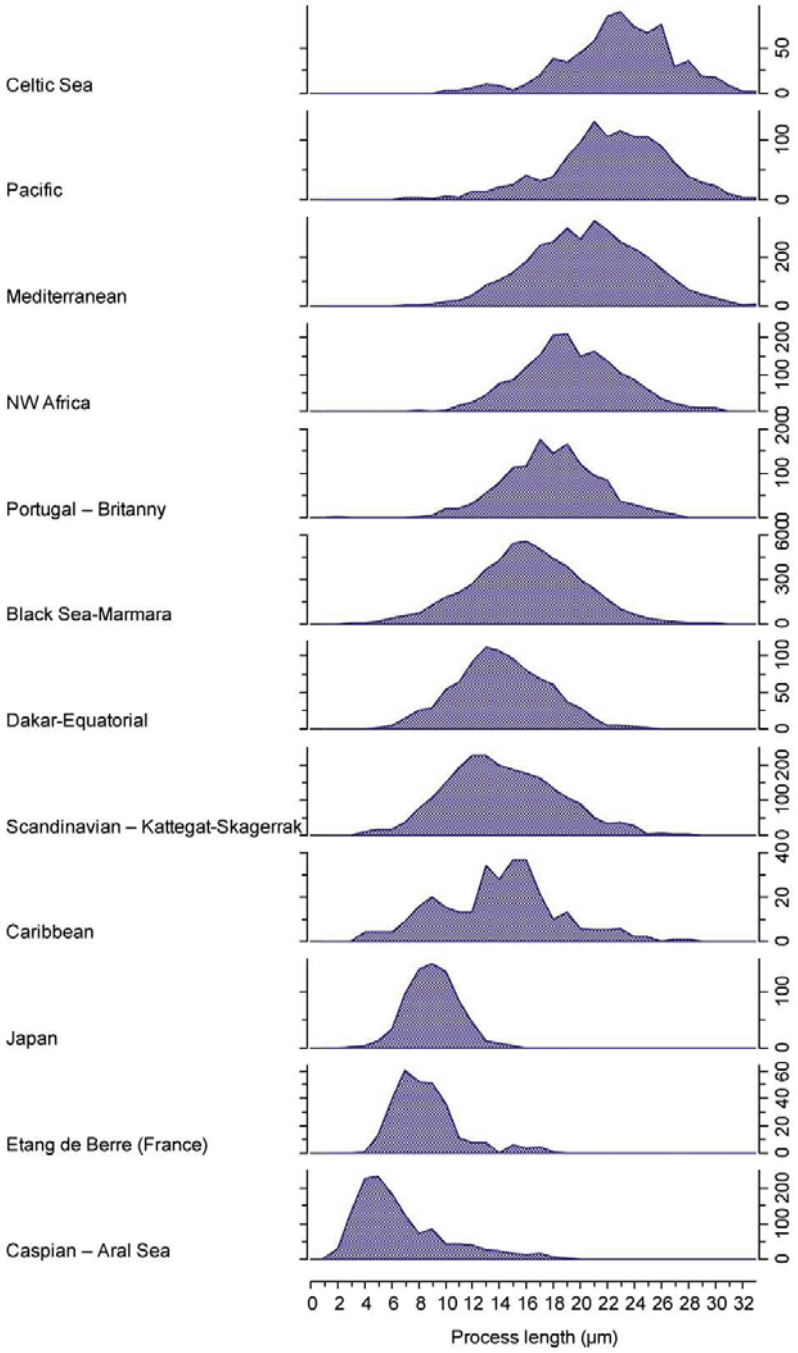

Figure. 4 Sizefrequency spectra of regionam process measurments, sorted from top (long average processes) to bottom (short average processes).

Process length in relation to body diameter

No relation between the process length and cyst body diameter was found (R^2=0.002). This was expected since culture experiments also revealed no relation between the body diameter and the salinity (Hallet, 1999). Furthermore, no

significant relation was found between body diameter with the ratio between salinity and temperature at different depths. Variations in cyst body diameter are probably caused mainly by germination of the cyst or compression

Process length in relation to relative cyst abundance

Mudie et al. (2001) found a correlation of $R^2 = 0.71$ between the relative abundance of *L. machaerophorum* (all forms) and increasing salinity between 16 and 21.5 psu for Holocene assemblages in Marmara Sea core M9. To check this relation in our dataset, the relative abundances of *L. machaerophorum* were determined in 92 surface samples. No significant linear relation between relative abundances in the assemblages and either the process length or the cyst body diameter was found. No significant relationship between relative abundance and temperature or salinity data was found. This is not surprising since the relationship between relative abundances and environmental parameters is not linear, but unimodal (Dale, 1996), and several other factors play a role in determining the relative abundances on such a global scale, mostly relative abundances of other species (closed-sum problems).

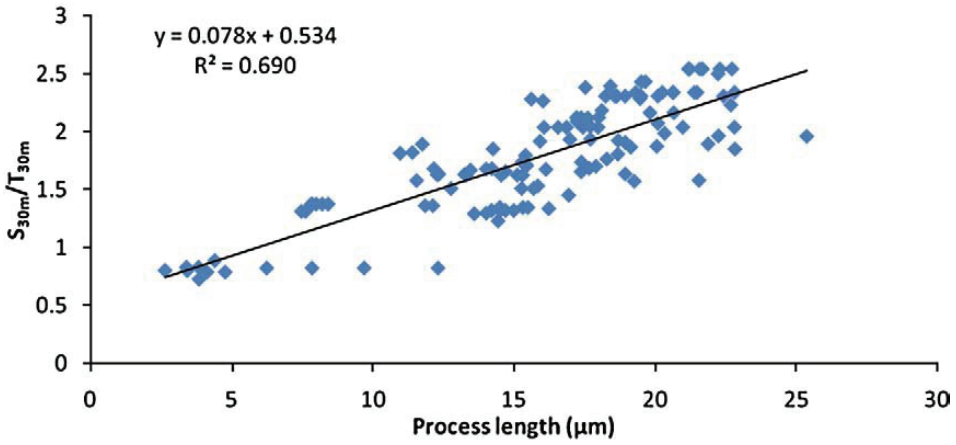

Figure 5 Regression between average process length and summer $S_{30\ m}/T_{30\ m}$ for the 144 surface samples.

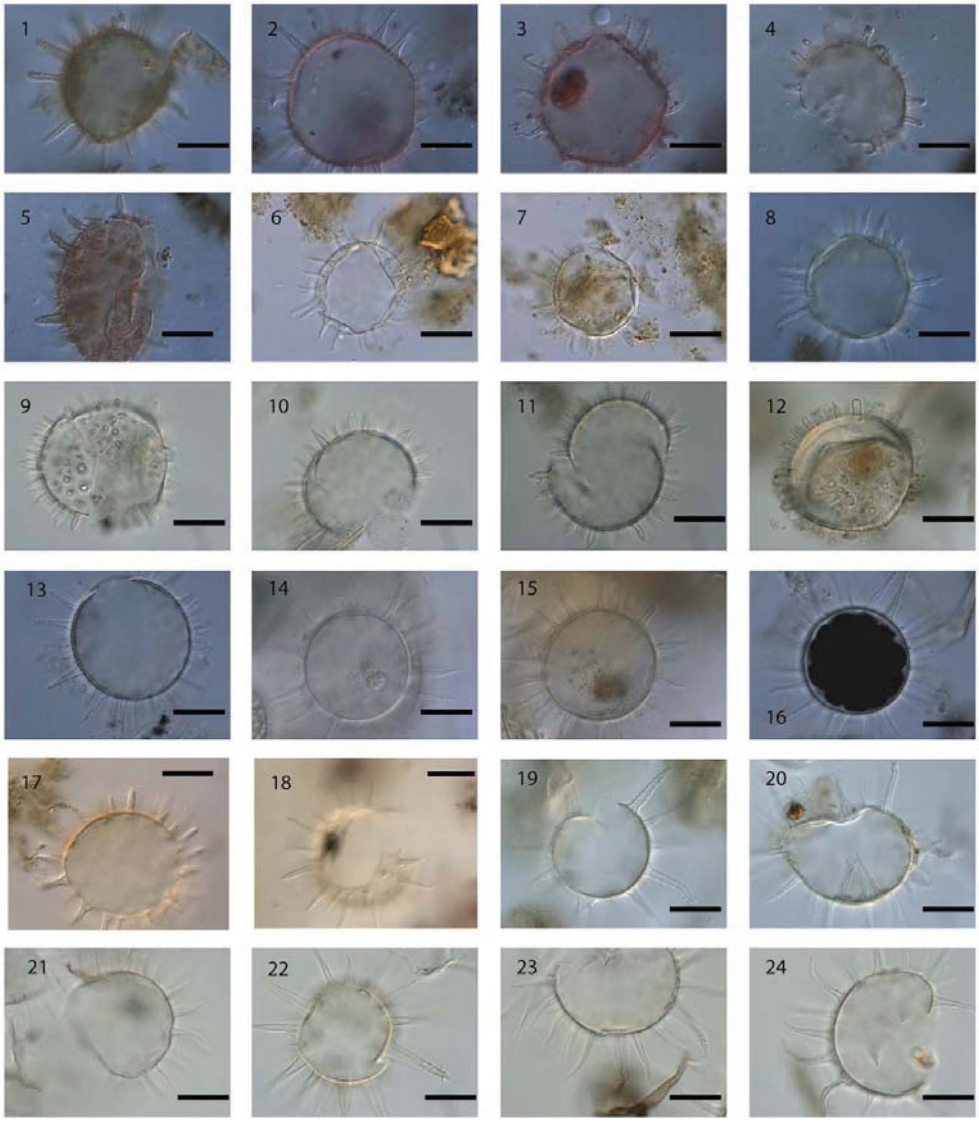

Plate III. *Lingulodinium machaerophorum* cyst from East Equatorial Atlantic (1-7), West Equatorial Atlantic (8), Japan (9-12), Britany (13-16), Portugal (17-18) and NW Africa (19-24). Specific sample names are: 1. 6437-1.2-3.6847-2. 4-5.6875-1.6-7. GeoB9503 Dakar.8.M35003-4. 9-10. AB22. 11. AB40.12.ISA2.13.BV1. 14-15. BV3.16.BV5.17-18. Tejo. 19-20. GeoB4024-121. GeoB5539-2.22-24. GeoB5548. All scale bars are 20µm.

Confocal laser microscopy

All processes on 20 cysts from the North Adriatic Sea (samples AN71 and AN6b) and one from the Gulf of Cadiz (sample GeoB9064) were measured, resulting in 1460 process measurements. The average distances between the processes were also calculated from these measurements. A summary of the results is given in Table 2. Process length ranged from 0 to 31 µm, which differs from the 1,983 process lengths from the North Adriatic Sea samples measured with transmitted light microscopy (6

to 34 µm). The shift in the frequency size spectra was obviously due to the fact that only the longest processes were measured (Figure 7). Most remarkable was the large peak around 3 µm in the confocal measurements. Apparently, a large number of shorter processes were present on most of these cysts.

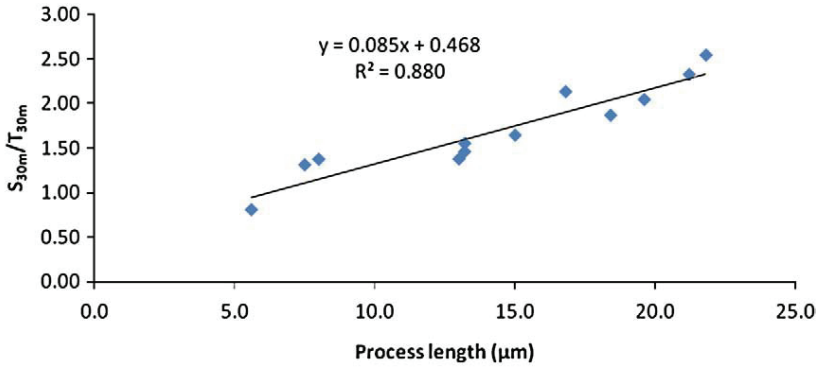

Figure 6 Regression between average process length and summer $S_{30\ m}/T_{30\ m}$ for every region separately.

It is noteworthy that the average process length was significantly related to the average distance between the processes (R^2=0.78) (Figure 9), and that the number of processes is significantly inversely related to the average process length (R^2=0.65) (Figure 8). This lower R^2 can be explained by the incompleteness of the cysts: all cysts were germinated and thus lacking opercular plates, which can number between one and five or indeed more in the case of epicystal archeopyles (Evitt, 1985). This implies that a large number of processes can be missing, and it would be subjective to attempt a correction for the missing processes. It was not possible to use encysted specimens since the strong autofluorescence of the endospore of these specimens obscured many of the least autofluorescent processes. No significant relation was found between the body diameter and the average process length (R^2=0.04), which confirms the observation with transmitted light microscopy.

It is noteworthy that the average process length was significantly related to the average distance between the processes (R^2=0.78) (Figure 9), and that the number of processes is significantly inversely related to the average process length (R^2=0.65) (Figure 8).

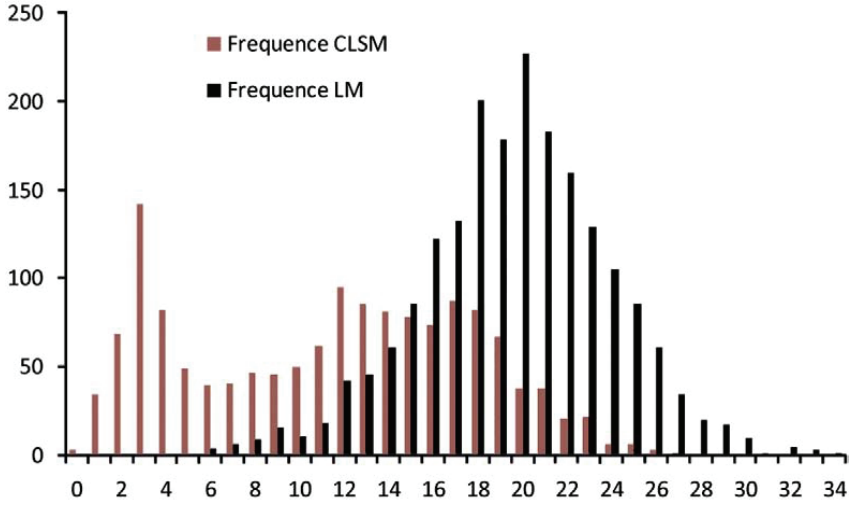

Figure 7 Comparison between the size-frequency spectra from 1460 confocal measurments (CLSM) from the North Atantic Sea (samples AN71 and AN6b) and from the Gulf of Cadiz and 1983 light microscope (LM) measurements from the North Adriatic.

This lower R^2 can be explained by the incompleteness of the cysts: all cysts were germinated and thus lacking opercular plates, which can number between one and five or indeed more in the case of epicystal archeopyles (Evitt, 1985). This implies that a large number of processes can be missing, and it would be subjective to attempt a correction for the missing processes. It was not possible to use encysted specimens since the strong autofluorescence of the endospore of these specimens obscured many of the least autofluorescent processes. No significant relation was found between the body diameter and the average process length (R^2=0.04), which confirms the observation with transmitted light microscopy.

Discussion

Process length correlated to summer S_{30m}/T_{30m}: is it realistic?

The quasi unimodal size frequency spectrum of both process length and cyst body diameter (Figure 2-3), plus the correlation between the average process length and the summer S_{30m}/T_{30m}, strongly confirm that all recorded cysts are ecophenotypes of a single species. It is furthermore not surprising that the most significant relation was found with the summer S_{30m}/T_{30m} depth. These three extra parameters – seasonality, temperature and depth – are discussed below.

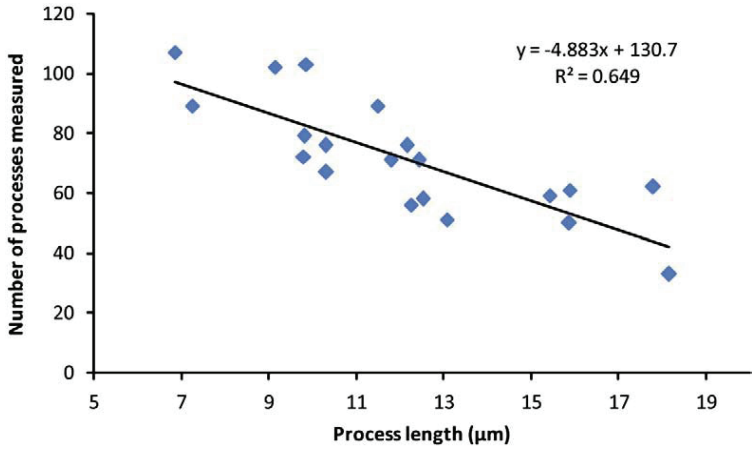

Figure 8 Regression between average process length and the number of processes for the cysts measured with conofocal microscopy.

Late summer–early autumn is generally the time of maximum stratification of the surface waters. Reduced salinity would enhance the water column stability with the generation of a pycnocline, and lowered water column turbulence, conditions that favour growth of *Lingulodinium polyedrum* (Thomas and Gibson, 1990). In most upwelling regions, this would coincide with periods of upwelling relaxation (Blasco, 1977). Late summer-early autumn is the time of the exponential growth phase of *Lingulodinium polyedrum*, which coincides with peak production of *Lingulodinium machaerophorum* cysts, at least in Loch Creran northwest Scotland (Lewis *et al.*, 1985) and Todos Santos Bay, Mexico (Peña-Manjarrez *et al.*, 2005). Culturing suggests that the cyst production is triggered by nutrient depletion, and influenced by temperature (Lewis and Hallett, 1997). A relation between process length and both temperature and salinity is indeed not surprising since the formation of processes can be considered a biochemical process (Hallett, 1999), dependent on both temperature and salinity. The culture experiments by Hallett (1999) confirm a positive relation to salinity and a negative relation to temperature. Moreover, the cysts are probably formed deeper in the water column, which would explain the fit to a 30 meter depth. It is well known that *Lingulodinium polyedrum* migrates deep in the water column (Lewis & Hallett, 1997). A similar vertically migrating dinoflagellate, *Peridiniella catenata,* also forms its cysts deeper in the water column, mostly at 30-40 m depth (Spilling *et al.*, 2006). These cysts are probably formed within a range of water depths, and 30 m depth reflects an average depth.

Table 2. Average process length, stdev, number of processes measured and average distance between processes from CLSM in full measurements.

Cyst number	Sample	Average length (µm)	Stdev length (µm)	# Processes measured	Body diameter (µm)	Average distance (µm)
2	AN71	9.82	5.78	79	44.53	4.35
4	AN71	7.26	5.72	89	39.84	3.76
5	AN71	15.87	5.06	50	56.89	5.79
7	AN71	9.80	6.36	72	45.11	4.68
9	AN71	17.79	6.41	62	43.25	6.78
10	AN71	10.32	6.49	67	39.95	4.55
11	AN71	12.25	1.90	56	43.26	6.21
12	AN71	6.85	4.82	107	39.34	3.98
13	AN71	11.50	7.26	89	43.32	4.76
14	AN71	15.88	7.27	61	51.76	6.90
15	AN71	13.20	6.19	28*	40.54	5.67
16	AN71	15.43	4.19	59	41.93	5.61
17	AN71	12.44	5.43	71	44.69	4.95
2	AN6B	11.79	6.09	71	36.38	4.40
4	AN6B	9.86	5.47	103	45.60	4.88
5	AN6B	9.14	7.13	102	42.87	4.05
6	AN6B	12.17	4.72	76	47.13	4.71
8	AN6B	12.53	4.53	58	57.84	5.66
9	AN6B	13.07	3.50	51	40.77	5.40
10	AN6B	10.30	4.68	76	41.20	4.44
1	GeoB9064	18.16	6.76	33	36.10	6.24
Average		**12.16**	**5.51**	**69.52**	**43.92**	**5.13**
Stdev		**3.11**	**1.33**	**21.06**	**5.68**	**0.91**

* This number was not used in the regression with process length, since less than half of this cyst was preserved.

The ranges of temperature (9–31°C) and salinity (12.4–42.1 psu) at 30 meter depth represent the window in which cyst formation takes place. Cultures show that *Lingulodinium polyedrum* forms cysts at salinities ranging from 10 to 40 psu (Hallett, 1999), and this fits well with the results obtained in this study. The direct link between process length and both salinity and temperature is proven by culture data (Hallett, 1999), and the relation to deeper salinity and temperature data suggests that cyst formation more often than not takes place deeper in the water column, where salinities are higher and temperatures lower, which suggests that caution is needed before linking *Lingulodinium machaerophorum* cyst abundances directly to surface data. This could explain the occurrence of cysts of *Lingulodinium polyedrum* in

regions with surface salinities as low as 5 psu (e.g. McMinn, 1990, 1991; Dale, 1996; Persson *et al.*, 2000).

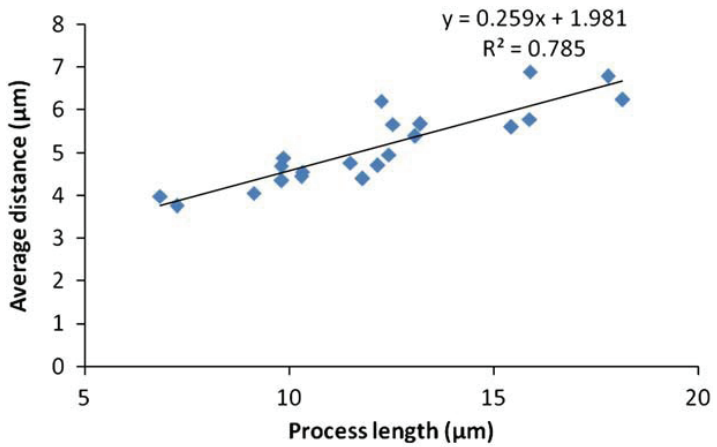

Figure 9 Regression between average process length and the average distance between process bases for the cysts measured with conofocal microscopy.

No better relation was found with density despite its dependence on salinity and temperature. Apparently, density as calculated from salinity and temperature, and pressure (water depth) by Fofonoff & Millard (1983) is much more determined by salinity, and less by temperature, than the measured average process length.

Transport issues

Lingulodinium machaerophorum occurs in estuaries, coastal embayments and the neritic environments of temperate to subtropical regions (Lewis and Hallett, 1997). However, transport of the cysts into other areas by currents must be considered, and the records of *L. machaerophorum* in oceanic environments must be attributed to reworking or long-distance transport (Wall *et al.,* 1977). A classic example is the upwelling area off northwest Africa where the cyst has been recorded over a much wider area than the thecate stage (Dodge and Harland, 1991). In this study, it was assumed that long-distance transport was not an important factor, since the transported cysts would be transported from areas with minor salinity and temperature differences, which would, according to the equation (see above), be reflected in negligible changes in process length.

The Problematic Kattegat–Skagerrak and Scandinavian Fjord samples

It is noteworthy that the inclusion of the Kattegat–Skagerrak and Scandinavian samples increased the scatter of the regression significantly. Two causes can be suggested. Firstly, since most samples plot above the regression line, the average process length could be too short. Most probably this is not linked to a preservation issue, since the average preservation is average to good (except for the Risör site), and broken processes are rare. All recovered cysts are from the uppermost section of box cores, and are thus recently formed. One possible explanation could be that these specimens are genetically different which could result in slightly different morphologies, although there is no *a priori* reason why this should be so, and conflicts with the unimodal size-frequence distribution of process length.

Secondly, summer S_{30m}/T_{30m} could be incorrect, and this can be attributed to several causes. On one hand, the cyst production could have taken place at different water depths. When included in the global dataset of summer S_{30m}/T_{30m}, the relation between average process length is more significant (R^2=0.61) when surface data is used for the Kattegat-Skagerrak and Scandinavian samples. On the other hand, the timing of cyst production might be different. *L. polyedrum* blooms in fjords probably occur very quickly and are short-lived, followed by a long resting period (Godhe and McQuoid, 2003). As for the Kattegat–Skagerrak, the salinity-driven stratification, with higher salinity bottom waters and low salinity surface waters, could result in a very particular environment. In this way, they are formed probably under specific salinity and temperature, and which could explain the scatter increase.

Confocal measurements and implications for cyst formation

First, a short description of cyst formation is given as described by Lewis & Hallett (1997) and Kokinos and Anderson (1995). The motile planozygote ceases swimming, ejects the flagella, and the outer membrane swells. The thecal plates of the planozygote dissociate and are pulled away from the cytoplasm by the ballooning of the outer membrane and underneath this, the formation of the cyst wall occurs. A layer of globules (each ~ 5 µm across) surround the cytoplasm and the spines grow outwards taking the globules with them. These terminal globules collapse to form spine tips and variations in this process confer the variable process morphology

observed in *L. machaerophorum*. Probably, membrane expansion is activated by osmosis (Kokinos, 1994), which causes a pressure gradient. According to Hallett (1999) the outer membrane always reaches full expansion, both for short and long process bearing individuals. The measurements with the confocal laser microscope clearly show that a positive relation exists between the process length and the distance between processes, and a negative relation between the processes length and the number of processes. These findings lead towards three implications. Firstly, the amount of dinosporin necessary for construction the processes would be constant, at least for the studied cysts from the Mediterranean Sea. However, one needs to assume that the amount of dinosporin is proportionate to the number of processes, multiplied by the average process length. This entails that one supposes that the amount of dinosporin needed for formation of the periphragm is constant, which is reasonable since the body diameter is independent of process length. Secondly, the good correlation between the average distance and the process length, together with the observation that globules are all forming simultaneously (Hallett, pers. comm.), suggests that the process length is predetermined. Thirdly, these observations suggest the existence of two end members: one with many closely spaced short processes, and one with a few, more widely spaced, long processes (Figure 10). This gradient in biometrical groups can also be visually observed in transmitted light (Plates 1 to 7).

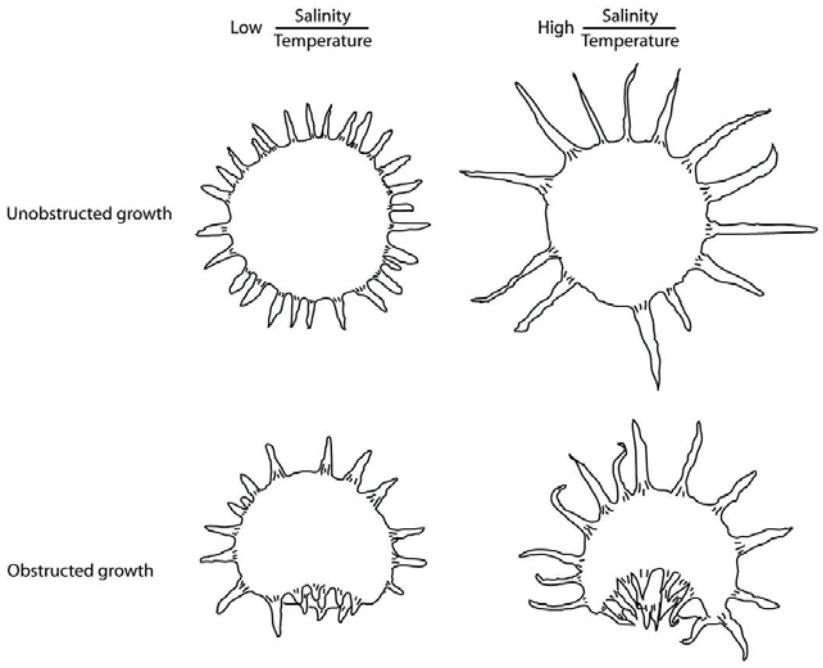

Figure 10. Conceptual model for process formation.

In order to reconcile these observations with observations from cultures, the physico-chemical properties of dinosporin have to be considered. According to Kokinos (1994), dinosporin consists of a complex aromatic biopolymer, possibly made of tocopherols. However, upon re-analysis, De Leeuw *et al.* (2005) showed the tocopherol link to be untrue. It can now be speculated that a certain fixed amount of this precursor monomer (probably a sugar, Versteegh, pers. comm.) for dinosporin is distributed across the sphere, in such a way that a minimum of energy is necessary for this process. This can happen through a process of flocculation (as proposed by Hemsley *et al.* (2004), and is dependent on both temperature and salinity. Fewer but larger colloids of the monomer will be formed when S_{30m}/T_{30m} is higher and these will coalesce on the cytoplasmic membrane. When many small colloids are formed, there is a chance that two or more colloids are merged, and form one larger process (Plate 2, 13-15 & 22). This theory can also explain the rare occurrence of crests on such cyst species as *Operculodinium centrocarpum*, where crests are formed when processes are closely spaced. In the next step, the visco-elastic dinosporin is synthesized on the globules, and stretches out in a radial direction. This stretching is clearly visible in the striations at the base of the processes. Another result of this stretching is the formation of tiny spinules at the distal tip. These are more apparent on the longer processes, and could be the result of a fractal process: what happens at a larger scale, namely the stretching of the processes, is repeated here at a smaller scale, the stretching of the spinules. However, it is unlikely that the stretching is solely caused by membrane expansion. Hallett (1999) indicated that the outer membrane expansion is independent of the definitive process length. Thus the stretching is most probably caused by the combination of outer membrane expansion and a chemical process, similar to the swelling of cysts caused by acetolysis or KOH (see below).

Two types of cysts deserve special attention. Clavate or bulbous process bearing cysts (Plate 1, 13; Plate 2, 11, 20) were frequently encountered in surface sediments from low salinity environments (Black Sea, Caspian Sea, Aral Sea and the Kattegat–Skagerrak). They were frequently encountered in culture by Kokinos and Anderson (1995), but rarely by Hallett (1999). They only seem to differ from normal processes, in that globules were not able to detach from these processes. This is supported by

the fact that the length of normal processes on cysts bearing clavate bearing processes is the same as for clavate processes.

The second type of cyst deserving attention is the bald or spheromorphic cyst. Lewis and Hallett (1997) observed that these cysts are not artifacts of laboratory culturing, since cysts devoid of processes occur in the natural environment of Loch Creran in northwest Scotland. Moreover, as noted by Persson from culturing experiments, these cysts are still viable, and thus cannot be regarded as malformations. Apart from the Aral Sea, very few bald cysts were recorded in surface sediments. It appears that on these cysts, process development did not take place. It can be speculated that this could be caused by a very early rupture of the outer membrane or the inability of the precursor monomer to flocculate at a very low S_{30m}/T_{30m}.

Process distribution

The process distribution on *Lingulodinium machaerophorum* was considered to be intratabular to non-tabular (Wall and Dale, 1968), although some authors noted alignment in the cingular area (Evitt and Davidson, 1964, Wall *et al.*, 1973). Marret *et al.* (2004) showed a remarkable reticulate pattern in the ventral area on cysts with very short processes from the Caspian Sea, suggestive of a tabular distribution. Our findings indicate a regular and equidistant distribution of the processes, with evidence of a tabulation pattern lacking.

The process length distribution is not uniform. In cultures, cysts are formed at the bottom of the observation chambers, and this results in an asymmetrical distribution of the processes on the cysts, where shorter processes are formed at the obstructed side, and longer processes at the unobstructed side (Kokinos & Anderson, 1995; Hallett, 1999). When it is assumed that a constant amount of dinosporin is distributed over the body, aberrantly long processes would form at the unobstructed side, and aberrantly short processes at the obstructed side. Our observations confirm this phenomenon: cysts from shallow areas show a similar asymmetry. The frequent occurrence of short processes on cysts from shallow areas in the Mediterranean Sea can be explained in a similar way (Figure 7). If one measures the longest processes on these cysts, values will be slightly larger than would be expected from our equation.

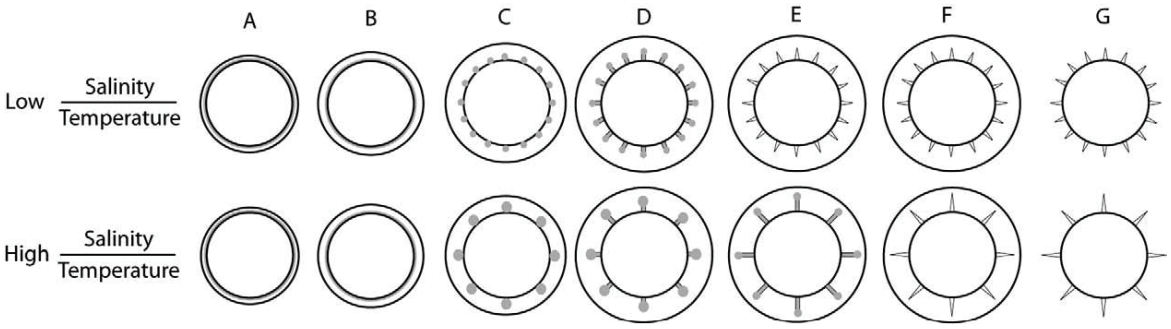

Figure 11 Suggested formation process for the two end members based on observation and documentation by Kokinos and Anderson (1995) and Hallet (1999), and theoretical consideration by Hamsley et al. (2004). Monomer is shown in grey, membranes and polymerised coat in black. (A-B) The outer membrane starts to expand, a fixed amount of monomer is formed and starts to coalesce on the cytoplasmic membrane. (C) depending on environmental parameters (salinity and temperature), a lot of small or few large colloids of the monomer are formed. (D) Visco-elastic dinosporin is synthesized on the globules and stretches in a radial direction. (E) Membrane expansion often comes to a stop before radial stretching ends. (F) Formation of longer process takes longer than shorter process formation. (G) Membrane rupture occurs.

This obstruction factor needs thus to be incorporated into our conceptual model (Figure 10). It is furthermore noticeable that a lot of the non-shallow cysts show this asymmetry to a certain degree (Plate 1-7). So, to a certain extent, this obstruction could be occurring more generally. The frequent occurrence of short processes along the cingulum could also be explained in a similar way, if the cysts were to be formed in a preferred orientation, with the obstructed side along the archeopyle.

Biological function of morphological changes?

The final consideration deals with the biological function of the processes. Possible functions of spines on resting stages are proposed by Belmonte *et al.* (1997), and include flotation, clustering and enhanced sinking, passive defence, sensory activity and/or chemical exchanges and dispersal. Since the link between process length and S_{30m}/T_{30m} exists and density is also dependent on S_{30m}/T_{30m}, it is obvious that either flotation or clustering and enhanced sinking will be the most important biological function of morphological changes of the processes. Longer processes increase the drag coefficient of the cyst and thus increase floating ability according to Stokes' law, but also increase cluster ability. However, the longest processes occur in high density (high S_{30m}/T_{30m}) environments, where floatation would be easier, which is counterintuitive. It seems more logical, then, that longer processes are developed to facilitate sinking (through clustering) in high density environments.

Conclusions

- A total of 19,611 measurements of *Lingulodinium machaerophorum* from 144 surface samples show a relationship between process length and both summer salinity and temperature at 30 m water depth, as given by the following equation: S_{30m}/T_{30m} = 0.078*average process length + 0.534 with R^2=0.69. For salinity the range covered is at least 12.5 to 42 psu, and for temperature 9–31°C. To establish the accuracy of this salinity proxy, future culture studies will hopefully further constrain this relationship.
- Confocal microscopy shows that distances between processes are strongly related to average process length, and that the number of processes is inversely related to average process length. This suggests a two end-member model, one with numerous short, closely spaced processes and one with relatively few, widely spaced, long processes.
- Processes of *Lingulodinium machaerophorum* are hypothesized to biologically function mainly as a clustering device.

Acknowledgements

Warner Brückmann & Silke Schenk (IFM Geomar), Rusty Lotti Bond (Lamont Doherty Earth observatory), Chad Broyles & Walter Hale (IODP), Jim Broda and Liviu Giosan (WHOI), Gilles Lericolais (IFREMER, France), Katrien Heirman and Hans Pirlet (RCMG), Jean-Pierre Arrondeau (IAV) and Rex Harland are kindly acknowledged for providing samples.

Marie-Thérèse Morzadec-Kerfourn is kindly thanked for providing detailed information on sampling locations from Brittany and Philippe Picon (GIPREB) for providing salinity data from Etang de Berre. We are grateful to Zoë Verlaak for helping out with the confocal measurements and Richard Hallett for stimulating discussions on *Lingulodinium machaerophorum* process development.

We express gratitude to Martin Head and one anonymous reviewer for detailed reviews of an earlier version of this manuscript.

References

Amorim, A., Palma, A.S., Sampayo, M.A., Moita, M.T., 2001. On a *Lingulodinium polyedrum* bloom in Setúbal bay, Portugal. In: Hallegraeff, G.M., Blackburn, S.I., Bolch, C.J., Lewis, R.J. (Eds.), Harmful Algal Blooms 2000. Intergovernmental Oceanographic Commission of UNESCO, pp. 133–136.

Bendle J., Rosell-Mele A., Ziveri P., 2005. Variability of unusual distributions of alkenones in the surface waters of the Nordic seas. *Paleoceanography* 20, doi:10.1029/2004PA001025.

Bennouna, A., Berland, B., El Attar, J., Assobhei, O., 2002. *Lingulodinium polyedrum* (Stein) Dodge red tide in shellfish areas along Doukkala coast (Moroccan Atlantic). Oceanologica Acta 25(3), 159-170.

Belmonte, G., Miglietta, A., Rubino, F., Boero, F., 1997. Morphological convergence of resting stages of planktonic organisms: a review. *Hydrobiologia* 355: 159-165.

Blasco, D. 1977. Red tide in the upwelling region of Baja California. *Limnology and Oceanography* 22, 255-263.

Bollmann, J. & Herrle, J.O., 2007. Morphological variation of *Emiliania huxleyi* and sea surface salinity*, Earth and Planetary Science Letters* 255, 273-288.

Boyer, T. P., Stephens, C., J. I. Antonov, M. E. Conkright, R. A. Locarnini, T. D. O'Brien, H. E.Garcia, 2002: *World Ocean Atlas 2001, Volume 2: Salinity.* S. Levitus, Ed., NOAA Atlas NESDIS 50, U.S. Government Printing Office, Wash., D.C., 165 pp., CD-ROMs.

Brenner, W., 2005. Holocene environmental history of the Gotland Basin (Baltic Sea) - a micropalaeontological model, *Palaeogeography, Palaeoclimatology, Palaeoecology* 220, 227-241.

Cagatay, M.N., Görür, N., Algan, O., Eastoe, C., Tchapalyga, A., Ongan, D., Kuhn, T., Kuscu, I., 2000. Late Glacial-Holocene palaeoceanography of the Sea of Marmara: timing of connections with the Mediterranean and the Black Seas. *Marine Geology* 167, 191-206.

Caner, H., Algan, O., 2002. Palynology of sapropelic layers from the Marmara Sea. *Marine Geology* 190, 35-46.

Christensen, J.T., Cedhagen, T. & Hylleberg, J., 2004. Late-Holocene salinity changes in Limfjorden, Denmark. *Sarsia* 89, 379-387.

Combourieu-Nebout, N., Londeix, L., Baudin, F., Turon, J.-L., von Grafenstein, R., Zahn, R. (1999). Quaternary marine and continental paleoenvironments in the western Mediterranean (site 976, Alboran Sea): Palynological evidence. In: *Proceedings of the Ocean Drilling Program, Scientific Results*, vol. 161, p. 457-468.

Dale, B., 1996. Dinoflagellate cyst ecology: modelling and geological applications. In: Jansonius, J., McGregor, D.C. (Eds.), Palynology: Principles and Applications, vol. 3. AASP Foundation, Dallas, TX, pp. 1249-1275.

Deflandre, G., Cookson, I.C., 1955. Fossil microplankton from Australia late Mesozoic and Tertiary sediments. *Australian journal of Marine and Freshwater Research* 6: 242-313.

de Leeuwe, J.W., Versteegh, G.J.M., van Bergen, P.F., 2006. Biomacromolecules of algae and plants and their fossil analogues. *Plant Ecology* 182, 209-233.

de Vernal, A., Hillaire-Marcel, C., 2000. Sea-ice cover, sea-surface salinity and halo/thermocline structure of the northwest North Atlantic: Modern versus full glacial conditions. *Quaternary Science Reviews*, 19 (5): 65-85.

Dodge, J.D., Harland, R., 1991. The distribution of planktonic dinoflagellates and their cysts in the eastern and northeastern Atlantic Ocean. *New Phytologist* 118, 593-603.

Ellegaard, 2000. Variations in dinoflagellate cyst morphology under conditions of changing salinity during the last 2000 years in the Limfjord, Denmark. *Review of Palaeobotany and Palynology* 109: 65-81.

Evitt, W.R., Davidson, S.E., 1964. Dinoflagellate cysts and thecae. Stanford University Publications Geological Sciences 10: 1-12.

Evitt, W.R., 1985. Sporpollenin dinoflagellate cysts. Their morphology and interpretation. Dallas: American Association of Stratigraphic Palynologists Foundation.

Fofonoff, P., Millard, R.C. Jr., 1983. Algorithms for computing of fundamental properties of seawater. *Unesco Technical Papers in Marine Sciences* 44, 1-53.

Godhe, A., McQuoid, 2003. Influence of benthic and pelagic environmental factors on the distribution of dinoflagellate cysts in surface sediments along the Swedish west coast. *Aquatic Microbial Ecology* 32, 185-201.

Grøsfjeld, K., Harland, R., 2001. Distibution of modern dinoflagellate cysts from inshore areas along the coast of southern Norway. *Journal of Quaternary Science* 16(7): 651-659.

Gundersen, N., 1988. En palynologisk undersøkelse av dinoflagellatcyster langs en synkende salinitetsgradient I recente sedimenter fra Østersjø-området. Unpublished candidata scientiarum thesis, University of Oslo, pp. 1-96.

Hallett, R.I. 1999. Consequences of environmental change on the growth and morphology of *Lingulodinium polyedrum* (Dinophyceae) in culture. PhD thesis 1–109. University of Westminster.

Head, M.J., 1996. Late Cenozoic dinoflagellates from the Royal Society borehole at Ludham, Norfolk, Eastern England, *Journal of Paleontology* 70 (4), 543-570.

Hemsley, A.R., Lewis, J., Griffiths, P.C., 2004. Soft and sticky development: some underlying reasons for microarchitectural pattern convergence. *Review of Palaeobotany and Palynology* 130, 105-119.

Kokinos, J.P., 1994. Studies on the cell wall of dinoflagellate resting cysts: morphological development, ultrastructure, and chemical composition. PhD thesis, Massachusetts Institute of Technology/Woods Hole Oceanographic Institution.

Kokinos J.P., Anderson D.M., 1995. Morphological development of resting cysts in cultures of the marine dinoflagellate *Lingulodinium polyedrum* (= *L. machaerophorum*). *Palynology* 19: 143-166.

Kotthoff, U., Pross, J., Müller, U.C., Peyron, O., Schmiedl, G., Schulz, H., Bordon, A., 2008. Climate dynamics in the borderlands of the Aegean Sea during formation of sapropel S1 deduced from a marine pollen record. *Quaternary Science Reviews* 27, 832-845.

Kuhlmann, H., Freudenthal, T., Helmke, P., Meggers, H., 2004. Reconstruction of paleoceanography off NW Africa during the last 40,000 years: influence of local and regional factors on sediment accumulation, *Marine Geology* 209-224.

Leroy, S.A.G., Marret, F., Giralt, S., Bulatov, S.A., 2006. Natural and anthropogenic rapid changes in the Kara-Bogaz Gol over the last two centuries reconstructed from palynological analyses and a comparison to instrumental records. *Quaternary International* 150, 52-70.

Leroy S.A.G., Marret F., Gibert E., Chalie F., Reyss J.L., Arpe K., 2007. River inflow and salinity changes in the Caspian Sea during the last 5500 years, *Quaternary Science Reviews* 26 issue 25-28, 3359-3383.

Leroy, V., 2001. Traceurs palynologiques des flux biogeniques et des conditions hydrographiques en milieu marin cotier: exemple de l'étang de Berre. DEA, Ecole doctorale Sciences de l'environment d'Aix-Marseille, 30 pp.

Lewis, J., Tett, P. & Dodge, J.D., 1985. The cyst-theca cycle of *Gonyaulax polyedra*

(*Lingulodinium machaerophorum*) in Creran, a Scottish west coast Sea-Loch. In: Anderson, D.M., White, A.W., Baden, D.G. (Ed.). Toxic dinoflagellates. Elsevier Science Publishing, 85-90.

Lewis, J. & Hallett, R., 1997. *Lingulodinium polyedrum* (*Gonyaulax polyedra)* a blooming dinoflagellate. In: Ansell, A.D., Gibson, R.N., Barnes, M. (Eds.), Oceanography and Marine Biology: An Annual Review 35, UCL Press, London, 97-161.

Marret, F., 1994. Distribution of dinoflagellate cysts in recent marine sediments from the east Equatorial Atlantic (Gulf of Guinea). Review of Palaeobotany and Palynology 84, 1-22.

Marret, F., Scource, J. 2002. Control of modern dinoflagellate cyst distribution in the Irish and Celtic seas by seasonal stratification dynamics. *Marine Micropaleontology* 47: 101-116.

Marret, F., Leroy, S. A. G., Chalié, F., Gasse, F., 2004. New organic-walled dinoflagellate cysts from recent sediments of Central Asian seas. Review of Palaeobotany and Palynology 129, 1-20.

Marret, F., Zonneveld, K.A.F., 2003. Atlas of modern organic-walled dinoflagellate cyst distribution. *Review of Palaeobotany and Palynology* 125, 1-200.

Marret, F., Mudie, P., Aksu, A., Hiscott, R.N., 2007. A Holocene dinocyst record of a two-step transformation of the Neoeuxinian brackish water lake into the Black Sea. *Quaternary International* doi:10.1016/j.quaint.2007.01.010

Matthiessen, J. & Brenner, W. (1996). Chlorococcalalgen und Dinoflagellaten Zysten in rezenten Sedimenten des Greifswalder Boddens (südliche Ostsee), *Senckenbergiana Maritima* 27 (1/2), 33-48.

Mertens, K., Lynn, M., Aycard, M., Lin, H.-L., Louwye, S. (2008). Coccolithophores as paleoecological indicators for shift of the ITCZ in the Cariaco Basin during the Late Quaternary. *Journal of Quaternary Science* doi:10.1002/jqs.1194.

McMinn, A., 1990. Recent dinoflagellate cyst distribution in eastern Australia. *Review of Palaeobotany and Palynology* 65, 305-310.

McMinn, A., 1991. Recent dinoflagellate cysts from estuarieson the central coast of New South Wales, Australia. *Micropaleontology* 37, 269-287.

Mudie, P.J., Aksu, A.E., Yasar, D., 2001. Late Quaternary dinoflagellate cysts from the Black, Marmara and Aegean seas: variations in assemblages, morphology and paleosalinity. *Marine Micropaleontology* 43: 155-178.

Mudie, P.J., Rochon, A.E., Levac, E. 2002. Palynological records of red tide producing species in Canada: past trends and implications for the future. *Palaeogeography, Palaeoclimatology, Palaeoecology* 180(1): 159-186.

Mudie, P.J., Marret, F., Aksu, A.E., Hiscott, R.N., Gillespie, H., 2007. Palynological evidence for climatic change, anthropogenic activity and outflow of Black Sea water during the Late Pleistocene and Holocene: Centennial- to decadal-scale records from the Black and Marmara Seas. *Quaternary International* 167-168: 73-90.

Nehring, S., 1994. Spatial distribution of dinoflagellate resting cysts in recent sediments of Kiel Bight, Germany (Baltic Sea). *Ophelia* 39 (2), 137-158.

Nehring, S., 1997. Dinoflagellate resting cysts from recent German coastal sediments, *Botanica Marina* 40, 307-324.

Nürnberg, D., J. Groeneveld (2006). Pleistocene variability of the Subtropical Convergence at East Tasman Plateau: Evidence from planktonic foraminiferal Mg/Ca (ODP Site 1172A). Geochemistry, Geophysics, Geosystems, 7-4, Q04P11, doi:10.1029/2005GC000984.

Peña-Manjarrez, J.L., Helenes, J., Gaxiola-Castro, G., Orellano-Cepeda, E. (2005). Dinoflagellate cysts and bloom events at Todos Santos Bay, Baja California, México, 1999-2000. *Continental Shelf Research* 25, 1375-1393.

Persson, A., Godhe, A. & Karlson, B., 2000. Dinoflagellate cysts in recent sediments from the West coast of Sweden. *Botanica Marina* 43, 66-79.

Pospelova, V., de Vernal, A., Pedersen, T.F., 2008. Distribution of dinoflagellate cysts in surface sediments from the northeastern Pacific Ocean (43-25°N) in relation to sea-surface temperature, productivity and coastal upwelling, *Marine Micropaleontology* d10.1016/j.marmicro.2008.01.008.

Reid, P.C., 1974. Gonyaulacean dinoflagellate cysts from the British Isles. *Nova Hedwigia* 25, 579-637.

Richter, D., Vink, A., Zonneveld, K.A.F., Kuhlmann, H. & Willems, H. (2007). Calcareous dinoflagellate cyst distributions in surface sediments from upwelling areas off NW Africa, and their relationships with environmental parameters of the upper water column. *Marine Micropaleontology* 63, 201-228.

Robert, C., Degiovanni, C., Jaubert, R., Leroy, V., Reyss, J.L., Saliège, J.F., Thouveny, N., de Vernal, A., 2006. Variability of sedimentation and environment in the Berre coastal lagoon (SE France) since the first millennium: Natural and anthropogenic forcings. *Journal of Geochemical Exploration* 88, 440-444.

Rostek F., Ruhland G., Bassinot F.C., Muller P.J., Labeyrie L.D., Lancelot Y., Bard E. (1993). Reconstructing sea-surface temperature and salinity using $\delta^{18}O$ and alkenone records. *Nature* 364: 319-321.

Sangiorgi, F., Fabbri, D., Comandini, M., Gabbianelli, G., Tagliavini, E. (2005). The distribution of sterols and organic-walled dinoflagellate cysts in surface sediments of the North-western Adriatic Sea (Italy). *Estuarine, Coastal and Shelf Science* 64, 395-406.

Schmidt, M. W., H. J. Spero, D. W. Lea (2004). Links between salinity variation in the Caribbean and North Atlantic thermohaline circulation. *Nature* 428. 160-163.

Schoell, M. 1974. Valdivia VA 01/03, Hydrographie II und III. Bundesanstalt für Bodenforschung, Hannover, Germany.

Schouten, S., Ossebaar, J., Schreiber, K., Kienhuis, M.V.M., Langer, G., Benthien, A. and Bijma, J., 2006. The effect of temperature, salinity and growth rate on the stable hydrogen isotopic composition of long chain alkenones produced by *Emiliania huxleyi* and *Gephyrocapsa oceanic, Biogeosciences* 3, 113-119.

Sorrell, P., Popescu, S.-M., Head, M..J., Suc, J.-P., Klotz, S., Oberhänsli, H. (2006). Hydrographic development of the Aral Sea during the last 2000 years based on a quantitative analysis of dinoflagellate cysts. *Palaeography, Palaeoclimatology, Palaeoecology* 234: 304-327.

Spilling, K., Kremp, A., Tamelander, T., 2006. Vertical distribution and cyst production of *Peridiniella catenata* (Dinophyceae) during a spring bloom in the Baltic Sea. *Journal of Plankton Research,* doi:10.1093/plankt/fbi149.

Stephens, C., J. I. Antonov, T. P. Boyer, M. E. Conkright, R. A. Locarnini, T. D. O'Brien, H. E. Garcia, 2002: *World Ocean Atlas 2001, Volume 1: Temperature.* S. Levitus, Ed., NOAA Atlas NESDIS 49, U.S. Government Printing Office, Wash., D.C., 167 pp., CD-ROMs.

Sweeney, B.M., 1975. Red tides I have known. In *Toxic dinoflagellate blooms*, V.R. LoCicero (ed). Wakefield, Massachusetts: Massachusetts Science and Technology Foundation, 225-234.

Thomas, W.H., Gibson, C.H. 1990. Quantified small-scale turbulence inhibits a red tide dinoflagellate, *Gonyaulax polyedra* Stein. *Deep-Sea Research*, *37*, 1538-1593.

Turon, J.-L., 1984. Le palynoplankton dans l'environment actuel de l'Atlantic nord oriental. Evolution climatique et hydrologique depuis le dernier maximum glaciaire. *Mémoire de l'institut de Géologie du Bassin d'Aquitaine* 17: 1-313.

van der Meer, M.T.J., Sangiorgi, F., Baas, M., Brinkhuis, H., Sinninghe-Damsté, J.S. & Schouten, S. (2008). Molecular isotopic and dinoflagellate evidence for Late Holocene freshening of the Black Sea. *Earth and Planetary Science Letters* 267, 426-434.

Van der Meer, M.T.J., Baas, M., Rijpstra, W.I.C., Marino, G., Rohling, E.J., Sinninghe Damsté, J.S., Schouten, S., 2007. Hydrogen isotopic compositions of long-chain alkenones record freshwater flooding of the Eastern Mediterranean at the onset of sapropel deposition. *Earth and Planetary Science Letters* 262, 594-600.

van Harten, D., 2000. Variable noding in *Cyprideis torosa* (Ostracoda, Crustacea): an overview, experimental results and a model from Catastrophe Theory. *Hydrobiologia* 419(1): 131-139, doi: 10.1023/A:1003935419364.

Verleye, T., Mertens, K., N., Louwye, S., Arz, H.W., 2008. Holocene Salinity changes in the southwestern Black Sea: a reconstruction based on dinoflagellate cysts. *Palynology* 32.

Vink, A., Rühlemann, C., Zonneveld, K.A.F., Mulitza, S., Hüls, M., Willems, H., 2001.Shifts in the position of the North Equatorial Current and rapid productivity changes in the western Tropical Atlantic during the last glacial. *Paleoceanography* 16 (1):1-12.

Vink, A., Zonneveld, K.A.F., Willems, H., 2000. Organic-walled dinoflagellate cysts. In western equatorial Atlantic surface sediments: distributions and their relation to environment. *Review of Palaeobotany and Palynology* 112, 247-286.

Wall, D., Dale, B., 1968. Modern dinoflagellate cysts and the evolution of the Peridiniales. *Micropaleontology* 14. 265-304.

Wall, D., Dale, B., Harada, K., 1973. Description of new fossil dinoflagellates from the Late Quaternary of the Black Sea. *Micropaleontology* 19: 18-31.

Wall, D., Dale, B., Lohman, G.P., Smith, W.K., 1977. The environmental and climatic distribution of dinoflagellate cysts in modern marine sediments from regions in the North and South Atlantic Ocean and adjacent seas. *Marine Micropaleontology* 2, 121-200.

Wang L., Sarntheim M., Duplessy J.C., Erlenkeuser H., Jung S., Pfaumann U. (1995). Paleo sea surface salinities in the low-latitude Atlantic: the $\delta^{18}O$ record of *Globigerinoides ruber* (White) *Paleoceanography* 10: 749-761.

Zonneveld, K.A.F., Versteegh, G.J.M., de Lange, G.J., 2001. Palaeoproductivity and post-depositional aerobic organic matter decay reflected by dinofagellate cyst assemblages of the Eastern Mediterranean S1 sapropel. *Marine Geology* 181-195.

Appendix 2

Geographic surface sample positions, pollen concentration (grains/g), dinocyst concentration (cysts/g), and count data of the individual dinocyst species

Core No.	Longitude	Latitude	Total pollen	Total dinocyst	Pollen concentration	Dinocyst concentration	*B.spongium*	*Brigantedinium* spp.	*Cyst of P. monospinum*	*Dubridinium* spp.	*E.aculeatum*	*E. delicatum*	*E. granulatum*	*E. transparantum*	*E.* spp.	*I. aculeatum*
GeoB 9501	-16,733	16,840	94	231	14257	35036	2	3	7	7				3	12	
GeoB 9502	-16,670	16,282	60	825	2518	34121	4		10	12				7	21	
GeoB 9503	-16,651	16,067	68	478	2511	17614				20			1	3	10	
GeoB 9504	-16,675	15,877	96	800	2376	19627	3	1	4	7	1			6	5	
GeoB 9505	-16,732	15,683	105	917	2921	25486	2	2	11	17				7	4	
GeoB 9506	-18,350	15,608	46	262	1175	6639	1		8	2				4	8	
GeoB 9508	-17,947	15,499	58	439	1476	11124	1	1	21	1	1			2	5	2
GeoB 9510	-17,654	15,417	69	446	1211	23024	2		18						11	
GeoB 9512	-17,366	15,337	55	421	1196	9152	1		1	1					7	2
GeoB 9513	-17,295	15,318	59	251	1539	12974			5	3				2	5	
GeoB 9515	-17,045	15,273	84	1407	3922	65602	3	8	3	7				3	8	1
GeoB 9516	-18,419	13,674	8	49	310	1858		2								2
GeoB 9517	-18,189	13,718	8	93	497	5712	1	4	6					2	6	
GeoB 9518	-17,790	13,793	70	262	3556	13055		5	20	2	19		2	8	14	
GeoB 9519	-17,683	13,812	88	383	2996	12734		11	22	4	20			13	18	
GeoB 9520	-17,591	13,829	36	68	1315	2375	2	4			1			3	1	
GeoB 9521	-17,491	13,848	65	210	2016	6514	2	9	12	3	3			7	11	
GeoB 9522	-17,454	13,855	54	91	543	1500		2	2	2	1			3	9	
GeoB 9525	-17,879	12,640	51	96	4408	6928		11	8	2				2	7	
GeoB 9526	-18,056	12,435	34	147	504	4058	1	11	16	1	5				7	2
GeoB 9527	-18,218	12,432	36	91	808	2747	1	2	4		1			4	6	2
GeoB 9528	-17,664	9,166	13	63	120	665	1	1	3							4
GeoB 9529	-17,369	9,353	46	102	466	1342	5	1	12	1	1			1		2
GeoB 9531	-16,904	8,941	49	65	288	698	3	2	1		1		1	3	3	3
GeoB 9532	-14,889	8,948	102	49	945	454	4		1	1				1	1	
GeoB 9533	-14,911	8,926	86	49	1269	723	3	2	2					1		1
GeoB 9534	-14,936	8,901	59	51	2363	2043	4	3	3	1	1				1	
GeoB 9535	-14,961	8,876	75	71	1755	1615	6		3		3			1		
GeoB 9536	-15,125	8,709	41	65	661	1015	3	3						2		1
GeoB 9537	-15,220	8,601	46	344	923	6901		4	9		13			5	8	
GeoB 9538	-15,829	8,708	24	21	466	388						1				2
GeoB 9539	-13,733	9,018	30	58	427	825	15	4		3	4			1	1	
GeoB 9541	-14,573	9,658	0	0												
GeoB 9542	-15,030	10,142	0	0												
GeoB 9544	-17,068	12,375	2	50	215	5378	2	4	3	1				1	2	
GeoB 9545	-17,076	12,848	15	63	209	864	1	2	6	5		5		6	10	
GeoB 9546	-17,090	13,453	20	202	137	1367	1	4	19	12	2	7		4	12	

Appendix 2 Continued

Core No.	*I. paradoxum*	*I. patulum*	*I.* spp.	*L. oliva*	*L. machaerophorum*	*L. machaerophorum short*	*N. labyrinthus*	*O. centrocarpum* s.s.	*O. israelianium*	*P. daleii*	*P. kofoidii*	*P. zoharyi*	Cyst of *P. americanum*	*Protoperidinium spp.*	*Q. concreta*	*S. nephroides*	*S. quanta*	*S. bentorii*
GeoB 9501					138	7		6			10			6	1	1	5	
GeoB 9502				1	607	39			16	1	30			1	4	1	19	
GeoB 9503					328	41		10	3	4	17			3	5	2	5	2
GeoB 9504					642	26	2	9	14	3	19	1		3	1	2	1	7
GeoB 9505					760	35	1	3	4	1	17			1	1	1	7	2
GeoB 9506			7		149	15	9	4	4	1	5			8		2	1	1
GeoB 9508		5			279	16	5	19	9	2	4		4	11		2	3	
GeoB 9510			5		270	20	2	5	13		7			25	1	1	3	2
GeoB 9512			2		337	21	2	2	3		2			10		1	2	
GeoB 9513			1		191	14								7	2	1	3	
GeoB 9515				2	1239	26	2		7		33			9		1	7	1
GeoB 9516			2		26			1	1	1				2		2		
GeoB 9517			6		36	1	1		1		1		1	5			1	
GeoB 9518		1	1		101	6			2		4			5		2	10	1
GeoB 9519	2	2	2	1	158	13		1	6		3			18	1	3	10	3
GeoB 9520			1	2	6			3			2			3	1	4	2	1
GeoB 9521			2		82	7		1	2		7			30	1	1	16	
GeoB 9522			3		39	1					4			6	1	1	4	
GeoB 9525			3		24					1	8			2	1		5	
GeoB 9526			3	2	11			5	5	1	6			13	4	6	7	3
GeoB 9527		1	3		20	2			2		1			4	2	1	3	1
GeoB 9528		1	3		8			7	1					2		1		
GeoB 9529			3		8		3	3	3	1				7		2	1	1
GeoB 9531			2				1	5	1		2			6	1	2	1	
GeoB 9532			3		4						2			3	3		1	3
GeoB 9533			5		8			2	2	1	1			4	1			1
GeoB 9534			5		10		1	1	2				2	1	1		3	1
GeoB 9535			4		4			2	2		2			8	3	4		1
GeoB 9536	1		5		7			2			1			1	2	2		
GeoB 9537			2		189	16		3	3		7			15	2	2	8	4
GeoB 9538			2		3				1		1							
GeoB 9539			1	1	5			1	1						2			1
GeoB 9541																		
GeoB 9542																		
GeoB 9544				2	5									1	2	1	5	2
GeoB 9545					9		1	1			5			2	3		1	
GeoB 9546				1	29	3		1	1		62			4	6	2	7	2

Appendix 2 *Continued*

Core No.	*S. bulloides*	*S. hyperacanthus*	*S. mirabilis*	*S. pachydermus*	*S. ramosus*	*S.* spp.	*Stelladinium1 spp.*	*T. applanatum*	*T. vancampoae*	*V. calvum*	*V. spinosum*	*X. xanthum*	Dinocyst indet.
GeoB 9501				1		12	8		2				0
GeoB 9502	2		4	3	2	18	7	2	2				12
GeoB 9503			3	2		9		3	6				1
GeoB 9504			3	8		21	1	1	1			1	7
GeoB 9505			7		3	25	2	1	1		1		1
GeoB 9506			1	7	1	17	2	1	2				2
GeoB 9508				12	1	20	3	5	1	2			2
GeoB 9510			1	7	4	36	4	7					2
GeoB 9512			1	5	1	18	1	1					0
GeoB 9513						12	4	1					0
GeoB 9515	3			3		37	2						2
GeoB 9516				1		4	1	3					1
GeoB 9517				3		15			2				1
GeoB 9518			1	3	2	32	1	14	1				5
GeoB 9519				6	3	29	7	14	4				9
GeoB 9520					4	14	3	6	2				3
GeoB 9521				1		9		3	1				0
GeoB 9522						5	2	1	2			1	2
GeoB 9525			1		1	8		5	4				3
GeoB 9526				6	6	10	1	8	3			2	2
GeoB 9527			1	1	0	21		7					1
GeoB 9528			1	3	1	19		5	2				0
GeoB 9529			1			30	1	11	1				3
GeoB 9531						21		6					0
GeoB 9532			1		4	14		2	1				0
GeoB 9533					1	10	1	1	2				0
GeoB 9534						7		2	2				0
GeoB 9535			2		2	12		6	4				2
GeoB 9536				1	4	7	12	7	2				2
GeoB 9537			4	9		28		11	2				0
GeoB 9538				1		7	1	2					1
GeoB 9539			2		3	6	4	1	2				0
GeoB 9541													
GeoB 9542													0
GeoB 9544			1	2	6	8		2					0
GeoB 9545				1		3		1					1
GeoB 9546			1	3		9	3	2	3				2

Appendix 3

Geographic positions of the investigated surface samples and relative abundances (%) of the individual dinocyst species

Core No.	Longitude	Latitude	*B. spongium*	*Brigantedinium spp.*	*Cyst of P. monospinum*	*Dubridinium spp.*	*E.aculeatum*	*E.delicatum*	*E.granulatum*	*E.transparantum*	*E.spp.*	*I.aculeatum*	*I.paradoxum*	*I.patulum*	*I.spp.*	*L.oliva*
GeoB 9501	-16.733	16.840	0.9	1.3	3.0	3.0				1.3	5.2					
GeoB 9502	-16.670	16.282	0.5		1.2	1.5				0.8	2.5					0.1
GeoB 9503	-16.651	16.067				4.2			0.2	0.6	2.1					
GeoB 9504	-16.675	15.877	0.4	0.1	0.5	0.9	0.1			0.8	0.6					
GeoB 9505	-16.732	15.683	0.2	0.2	1.2	1.9				0.8	0.4					
GeoB 9506	-18.350	15.608	0.4		3.1	0.8				1.5	3.1				2.7	
GeoB 9508	-17.947	15.499	0.2	0.2	4.8	0.2	0.2			0.5	1.1	0.5		1.1		
GeoB 9510	-17.654	15.417	0.4		4.0						2.5				1.1	
GeoB 9512	-17.366	15.337	0.2		0.2	0.2					1.7	0.5			0.5	
GeoB 9513	-17.295	15.318			2.0	1.2				0.8	2.0				0.4	
GeoB 9515	-17.045	15.273	0.2	0.6	0.2	0.5				0.2	0.6	0.1				0.1
GeoB 9516	-18.419	13.674		4.1								4.1			4.1	
GeoB 9517	-18.189	13.718	1.1	4.3	6.5					2.2	6.5				6.5	
GeoB 9518	-17.790	13.793		1.9	7.6	0.8	7.3		0.8	3.1	5.3			0.4	0.4	
GeoB 9519	-17.683	13.812		2.9	5.7	1.0	5.2			3.4	4.7		0.5	0.5	0.5	0.3
GeoB 9520	-17.591	13.829	2.9	5.9			1.5			4.4	1.5				1.5	2.9
GeoB 9521	-17.491	13.848	1.0	4.3	5.7	1.4	1.4			3.3	5.2				1.0	
GeoB 9522	-17.454	13.855		2.2	2.2	2.2	1.1			3.3	9.9				3.3	
GeoB 9525	-17.879	12.640		11.5	8.3	2.1				2.1	7.3				3.1	
GeoB 9526	-18.056	12.435	0.7	7.5	10.9	0.7	3.4				4.8	1.4			2.0	1.4
GeoB 9527	-18.218	12.432	1.1	2.2	4.4		1.1			4.4	6.6	2.2		1.1	3.3	
GeoB 9528	-17.664	9.166	1.6	1.6	4.8							6.3		1.6	4.8	
GeoB 9529	-17.369	9.353	4.9	1.0	11.8	1.0	1.0			1.0		2.0			2.9	
GeoB 9531	-16.904	8.941	4.6	3.1	1.5		1.5		1.5	4.6	4.6	4.6			3.1	
GeoB 9532	-14.889	8.948	8.2		2.0	2.0				2.0	2.0				6.1	
GeoB 9533	-14.911	8.926	6.1	4.1	4.1					2.0		2.0			10.2	
GeoB 9534	-14.936	8.901	7.8	5.9	5.9	2.0	2.0				2.0				9.8	
GeoB 9535	-14.961	8.876	8.5		4.2		4.2			1.4					5.6	
GeoB 9536	-15.125	8.709	4.6	4.6						3.1		1.5	1.5		7.7	
GeoB 9537	-15.220	8.601		1.2	2.6		3.8			1.5	2.3				0.6	
GeoB 9538	-15.829	8.708						4.5				9.1			9.1	
GeoB 9539	-13.733	9.018	25.9	6.9		5.2	6.9			1.7	1.7				1.7	1.7
GeoB 9541	-14.573	9.658														
GeoB 9542	-15.030	10.142														
GeoB 9544	-17.068	12.375	4.0	8.0	6.0	2.0				2.0	4.0					4.0
GeoB 9545	-17.076	12.848	1.6	3.2	9.5	7.9		7.9		9.5	15.9					
GeoB 9546	-17.090	13.453	0.5	2.0	9.4	5.9	1.0	3.5		2.0	5.9					0.5

Appendix 3 *Continued*

Core No.	*L.machaerophorum*	*L.machaerophorum short*	*N. labyrinthus*	*O.centrocarpum* s.s.	*O.israelianium*	*Pentapharsodinium daleii*	*Polykrikos kofoidii*	*Polysphaeridium zoharyi*	*Cyst of P. americanum*	*Protoperidinium spp.*	*Quinquecuspis concreta*	*S.nephroides*	*S.quanta*	*S.bentorii*
GeoB 9501	59.7	3.0		2.6			4.3			2.6	0.4	0.4	2.2	
GeoB 9502	73.6	4.7			1.9	0.1	3.6			0.1	0.5	0.1	2.3	
GeoB 9503	68.6	8.6		2.1	0.6	0.8	3.6			0.6	1.0	0.4	1.0	0.4
GeoB 9504	80.3	3.3	0.3	1.1	1.8	0.4	2.4	0.1		0.4	0.1	0.3	0.1	0.9
GeoB 9505	82.9	3.8	0.1	0.3	0.4	0.1	1.9			0.1	0.1	0.1	0.8	0.2
GeoB 9506	56.9	5.7	3.4	1.5	1.5	0.4	1.9			3.1		0.8	0.4	0.4
GeoB 9508	63.6	3.6	1.1	4.3	2.1	0.5	0.9		0.9	2.5		0.5	0.7	
GeoB 9510	60.5	4.5	0.4	1.1	2.9		1.6			5.6	0.2	0.2	0.7	0.4
GeoB 9512	80.0	5.0	0.5	0.5	0.7		0.5			2.4		0.2	0.5	
GeoB 9513	76.1	5.6								2.8	0.8	0.4	1.2	
GeoB 9515	88.1	1.8	0.1		0.5		2.3			0.6		0.1	0.5	0.1
GeoB 9516	53.1			2.0	2.0	2.0				4.1		4.1		
GeoB 9517	38.7	1.1	1.1		1.1		1.1		1.1	5.4			1.1	
GeoB 9518	38.5	2.3			0.8		1.5			1.9		0.8	3.8	0.4
GeoB 9519	41.3	3.4		0.3	1.6		0.8			4.7	0.3	0.8	2.6	0.8
GeoB 9520	8.8			4.4			2.9			4.4	1.5	5.9	2.9	1.5
GeoB 9521	39.0	3.3		0.5	1.0		3.3			14.3	0.5	0.5	7.6	
GeoB 9522	42.9	1.1					4.4			6.6	1.1	1.1	4.4	
GeoB 9525	25.0					1.0	8.3			2.1	1.0		5.2	
GeoB 9526	7.5			3.4	3.4	0.7	4.1			8.8	2.7	4.1	4.8	2.0
GeoB 9527	22.0	2.2			2.2		1.1			4.4	2.2	1.1	3.3	1.1
GeoB 9528	12.7			11.1	1.6					3.2		1.6		
GeoB 9529	7.8		2.9	2.9	2.9	1.0				6.9		2.0	1.0	1.0
GeoB 9531			1.5	7.7	1.5		3.1			9.2	1.5	3.1	1.5	
GeoB 9532	8.2						4.1			6.1	6.1		2.0	6.1
GeoB 9533	16.3			4.1	4.1	2.0	2.0			8.2	2.0			2.0
GeoB 9534	19.6		2.0	2.0	3.9				3.9	2.0	2.0		5.9	2.0
GeoB 9535	5.6			2.8	2.8		2.8			11.3	4.2	5.6		1.4
GeoB 9536	10.8			3.1			1.5			1.5	3.1	3.1		
GeoB 9537	54.9	4.7		0.9	0.9		2.0			4.4	0.6	0.6	2.3	1.2
GeoB 9538	13.6				4.5		4.5							
GeoB 9539	8.6			1.7	1.7						3.4			1.7
GeoB 9541														
GeoB 9542														
GeoB 9544	10.0									2.0	4.0	2.0	10.0	4.0
GeoB 9545	14.3		1.6	1.6			7.9			3.2	4.8		1.6	
GeoB 9546	14.4	1.5		0.5	0.5		30.7			2.0	3.0	1.0	3.5	1.0

Appendix 3 *Continued*

Core No.	*S.bulloides*	*S.hyperacanthus*	*S.mirabilis*	*S.pachydermus*	*S.ramosus*	*S.spp.*	*Stelladinium1 spp.*	*T. applanatum*	*T. vancampoae*	*V. calvum*	*V. spinosum*	*X. xanthum*	Dinocyst indet.
GeoB 9501				0.4		5.2	3.5		0.9				0.0
GeoB 9502	0.2		0.5	0.4	0.2	2.2	0.8	0.2	0.2				1.5
GeoB 9503			0.6	0.4		1.9		0.6	1.3				0.2
GeoB 9504			0.4	1.0		2.6	0.1	0.1	0.1			0.1	0.9
GeoB 9505			0.8		0.3	2.7	0.2	0.1	0.1		0.1		0.1
GeoB 9506			0.4	2.7	0.4	6.5	0.8	0.4	0.8				0.8
GeoB 9508				2.7	0.2	4.6	0.7	1.1	0.2	0.5			0.5
GeoB 9510			0.2	1.6	0.9	8.1	0.9	1.6					0.4
GeoB 9512			0.2	1.2	0.2	4.3	0.2	0.2					0.0
GeoB 9513						4.8	1.6	0.4					0.0
GeoB 9515	0.2			0.2		2.6	0.1						0.1
GeoB 9516				2.0		8.2	2.0	6.1					2.0
GeoB 9517				3.2		16.1			2.2				1.1
GeoB 9518			0.4	1.1	0.8	12.2	0.4	5.3	0.4				1.9
GeoB 9519				1.6	0.8	7.6	1.8	3.7	1.0				2.3
GeoB 9520					5.9	20.6	4.4	8.8	2.9				4.4
GeoB 9521				0.5		4.3		1.4	0.5				0.0
GeoB 9522						5.5	2.2	1.1	2.2			1.1	2.2
GeoB 9525			1.0		1.0	8.3		5.2	4.2				3.1
GeoB 9526				4.1	4.1	6.8	0.7	5.4	2.0			1.4	1.4
GeoB 9527			1.1	1.1		23.1		7.7					1.1
GeoB 9528			1.6	4.8	1.6	30.2		7.9	3.2				0.0
GeoB 9529			1.0			29.4	1.0	10.8	1.0				2.9
GeoB 9531						32.3		9.2					0.0
GeoB 9532			2.0		8.2	28.6		4.1	2.0				0.0
GeoB 9533					2.0	20.4	2.0	2.0	4.1				0.0
GeoB 9534						13.7		3.9	3.9				0.0
GeoB 9535			2.8		2.8	16.9		8.5	5.6				2.8
GeoB 9536				1.5	6.2	10.8	18.5	10.8	3.1				3.1
GeoB 9537			1.2	2.6		8.1		3.2	0.6				0.0
GeoB 9538				4.5		31.8	4.5	9.1					4.5
GeoB 9539			3.4		5.2	10.3	6.9	1.7	3.4				0.0
GeoB 9541													
GeoB 9542													0.0
GeoB 9544			2.0	4.0	12.0	16.0		4.0					0.0
GeoB 9545				1.6		4.8		1.6					1.6
GeoB 9546			0.5	1.5		4.5	1.5	1.0	1.5				1.0

Appendix 4

Total dinocyst concentration (cysts/cm^3), and accumulation rates (flux) (cysts/cm^2/yr), and count data of the individual dinocyst species from core GeoB9503-5

Depth (cm)	Age (yr)	Total Dinocysts	Dinocyst concentration	Dinocyst flux	*Protoperidinium spp.*	*P.americanum*	*E. delicatum*	*E. granulatum*	*E. aculeatum*	*E.spp.*	*E. zonneveldii*	*E. type 1*	*E.type 2*	*E.transparantum*	*Cyst of P. monospinum*	*Z. leniculatum*	*L. oliva*	*L.sabrina*
21	1240	362	25790	11213	1					4				2	1			
41	1288	197	2138	930	23					12				5	14		3	
51	1311	215	3521	1531	20					25				10	4		5	
81	1434	252	10984	1538				2		31				16	3		2	
91	1505	291	8468	1185	11					6		1	2	17	2		3	
101	1576	78	2532	354	4					7				7	8			
121	1719	148	1838	257	12					6		1		6	7			
131	1791	169	3064	429	12					27		6	4	2	46			
141	1859	152	5839	1496	7		1	1	1	3	1	7	6	9	8	2		1
151	1898	212	5549	1421	10			1		5		4		23	54		2	1
171	1976	208	3340	856	5					9				9	15		3	
181	2015	222	3392	869	3					10		4		11	30		1	
191	2054	96	2101	538	3					11			1	2	30			
201	2093	100	4564	1169	11					2				5	9	1		1
211	2132	334	8070	2067	15					12		3		6	43		1	
221	2145	104	1413	2160	1					9					7			
231	2152	182	1805	2758	9					10			1	8	24		1	
241	2158	136	1685	2575	5					1					25		5	
251	2165	191	3067	4688	22					18				6	37		1	
261	2171	146	4981	7614	1					2				4	14		2	
271	2178	198	3887	5941	6	1		4		4	1	7	3	4	9	1	4	1
281	2184	172	1662	2541	11					11			1	3	43			
301	2198	230	3435	5251	6					4				3	35			
311	2204	174	584	893	7					7				5	5		2	
331	2227	139	2312	1486	13									6	27			
351	2258	339	5247	3373	6					50				10	46		2	1
361	2274	136	2072	1332	3					3			2		21			
371	2289	173	2107	1354	3					9				2	30		2	
381	2305	201	1860	1196	24					1				4	16		2	
401	2336	110	1157	744	9					5					9			
411	2352	185	1096	652	3			1		1		1	3	6	4		5	
431	2385	127	957	569						12				2	19		1	
441	2402	253	3541	2107	11					16				9	13		2	2
461	2436	98	1412	840	5					10				5	6		1	
481	2469	150	1415	842	9					1		1	2	6	17		3	
491	2486	177	2390	1422	5	2		1		16	1	5		2	1	2	1	1
501	2503	259	1916	1140	14	1				3			3	9	21		2	
521	2537	164	1325	788	12					14				1	8			
531	2555	94	5340	2106	2			1					5	6	8			
541	2580	213	20868	8231	3					5				5	2		1	1
561	2631	347	2948	1163	25					17		1		9	33		3	1
591	2707	135	17954	7082	1					4				1	2			
601	2737	397	41109	5958	6					4		1		6			1	
611	2806	369	45758	6632	1					1				4	2			1
621	2875	318	33570	4865	12					2				6				
631	2944	179	7241	1049	4					12				5	5		1	
651	3082	205	5621	815	6					13				3				
671	3220	843	12934	1875	24					23				5	9			
691	3358	259	9158	1327	11					8		4	1	12	17			
701	3429	161	10780	1250	6				1	2		4	1	9	19	2	1	
721	3601	190	9437	1094	11					8				6	20			
731	3687	223	3681	427	18					7		1		5	16	1		
751	3860	157	3718	431	7					10				4	37			1
771	4032	96	3797	440	3					4				8	21			
781	4119	178	4989	578	5					12				4	16			
791	4196	335	3350	388	14					6		1		26	61		1	

Appendix 4 *Continued*

Depth (cm)	Age (yr)	*S. quanta*	*S.nephroides*	*P. dalei*	*Cyst of D. symetrica*	*Brigantidinium spp.*	*P. kofoidii*	*P.schwarzii*	*B. spongium*	*P. zoharyi*	*T. vancompoae*	*Bitectatodinium spp*	*N. labyrithus*	*I. aculatum*	*L. machaerophorum*	*L. machaerophorum short*	*O. israelianum*	*O.centrocarpum*	*O.centrocarpum short*	*S. mirabilis*
21	1240	7	2	1		4	5		2		2				263	30	9	2		
41	1288	30	2	4			30			3	5				3		6	1		3
51	1311	13	1	3		4	12	3	2		1				1		7	1		1
81	1434	21	4	6		1	25	4		1	10	1	1				14	1		7
91	1505	39	4	3		5	46				4				1		9	15		4
101	1576	5	2	2			5				6		1				1	1		
121	1719	30	2	3		2	14				3				1		5	8		1
131	1791	9		10			5						2		2		1	1		1
141	1859	5	1	2		13	2		1	2					4			1		2
151	1898	14	1	2		6	1								8		2	1	1	2
171	1976	55	1	14		2	3				5				1			7	1	2
181	2015	38	2	8		1	2			1	1						2	6	1	2
191	2054	9	1	3			1								1					
201	2093	5		3		11	4								1			6		2
211	2132	31	3	12		6	4				1				1		1	12		1
221	2145	13		13			2				2		1		1		1			1
231	2152	24	2	8		1	2				1						3	10		1
241	2158	35	2	4		2												2		2
251	2165	19	1	7		2	1				1		1	1			3			4
261	2171	16	2	2		8	1										5			3
271	2178	16	5		1	21			1	1							1			4
281	2184	19	1	3		3	2				1									2
301	2198	43	2	6		4	2						1				6	8		8
311	2204	54	2	1		10	1			1	2						2	5		3
331	2227	19	2	5		2	6										1			1
351	2258	34	2	1		10	3						1					10		2
361	2274	24	1	6		1	3								2		5	3		3
371	2289	19	3	9			3								1		1	1		
381	2305	36	3	2		2	3				1						5	11	1	3
401	2336	21	2				3				2									4
411	2352	17	1	3		15	5		1				1		2		4	7		4
431	2385	11	2	1		11	4		1								1	1		1
441	2402	28	2	3		7	5										1	4		1
461	2436	7	1			8	2						1				1	3		2
481	2469	15		5		5	3		1						1		4	7	2	1
491	2486	6	5	2	1	30	7		2	1		1					2	2	1	2
501	2503	22	2	9		9	3				2		1				9	5		3
521	2537	14	1			12	8				1						4	5		2
531	2555	1	1	3		9	1		1									3		1
541	2580	13		5		1	8				2				1		4	9		4
561	2631	11	3	4		12	11				4				3		4	17		4
591	2707	4		2		3	2			1							2	4		2
601	2737	26	1	11		8	28			1	4		1				8	10	2	4
611	2806	17		16		1	7			1	10		5		2		4	12	1	16
621	2875	7		6		2											3	24	2	10
631	2944	12	1	1		6	4				1				2		2	13		
651	3082	8				14	7				1							5		1
671	3220	46	5	2		7	15		1		1		2		1		5	15		4
691	3358	17	2	2		11	7						1		2		3	4		5
701	3429	10	1			6	1		3						1			2		3
721	3601	19				2	10				1						3			
731	3687	26	2	2		12	9								1		2			1
751	3860	8	1			2	7				1						1			
771	4032	8	3				2										2	3		1
781	4119	17	7	1		10	4				2				1		2	4		3
791	4196	24	7	2		5	11				5		1		3		2	6		

Appendix 4 *Continued*

Depth (cm)	Age (yr)	*S.hypercathus*	*S.bulloides*	*S.bentorii*	*S.pachydermus*	*S. ramosus*	*S.membranaceus*	*S.spp.*	*Dubridinium spp.*	*T. appelanatum*	*V. calvum*	*V.spinosum*	*X. xanthum*	*Q. concreta*	*F.cf. Americanum*	*Stelladinium stellatum*	Dinocyst indet.
21	1240			2	1			7	8	1			2				6
41	1288			2				19	5	3			1	11			12
51	1311			2	1			18	61	2	1		4	1			12
81	1434			2	7	2		45	9	10			9				18
91	1505			2	4			55	23	14			8	2			11
101	1576			1				6	8	1			3	5			5
121	1719				3	1		22	12	1			2	2			4
131	1791				1			23	10				2	3			2
141	1859	1		1	1	3		5	48	3	1	1	2		1		5
151	1898				3			9	48	1			4	1			8
171	1976			2				17	42	1				4			10
181	2015			1	1	2		20	58	3			4	5			5
191	2054				1			11	13				2	4			3
201	2093		1		1	2		7	24				2				2
211	2132			3	2	1		29	100	9			24	7			7
221	2145			1	2	1		15	12	1			14	3			4
231	2152			1		3		25	24	3			13				8
241	2158							8	32	2			4	4			3
251	2165	2			1			19	15				11	9		2	8
261	2171			3	1	1		10	55	4			7	1			4
271	2178			3	6	3	1	9	59	2			4				16
281	2184			1	2	1		25	26				5	2			10
301	2198	2		3	6	2		29	28	7			6	7			12
311	2204			4				32	20	2			2	6			1
331	2227			3				20	21	1			6	4			2
351	2258			3	5			26	108	2			8	2			7
361	2274			2	1			32	17				4	1			2
371	2289			2	2	2		31	35	2			2	9			5
381	2305			3	2	2		39	26	4			2	5			4
401	2336				1	1		24	21	1			1	4			2
411	2352			4	7	2	1	26	38	7			4	2			10
431	2385			2	2	1		16	25	3				10			1
441	2402			3	5			40	88	1			4	2			6
461	2436			1				17	14	4			2	7		1	0
481	2469			4	9	2	1	14	21	3	1		4				8
491	2486				8	12		23	17	6	4			1			8
501	2503	2		2	10	7		46	28	19			9	1			17
521	2537			2	2	1		43	23	5				3			3
531	2555			3	5			8	30	2			1	1			3
541	2580	4		10	13			81	16	10			2	1			12
561	2631		1	11	9	4		112	30	7			1	5			5
591	2707			9	9	2		59	18				2				8
601	2737	2		16	17	6		200	6	7				7			14
611	2806	27	1	25	47	11	5	130	7	3			2	1			9
621	2875	13		23	20		1	171	9	1			1				5
631	2944			4	5	2		85	8	2			1	3			0
651	3082			13	15			49	60				2				8
671	3220			22	28	10		574	27	7			3	4			3
691	3358	2		8	8	2	1	78	38	5			4				7
701	3429			7	13	1	1	18	33	1			4				11
721	3601	1		12	14	3		63	8	2			2	1			4
731	3687			9	4	1		45	45	2			1	2			11
751	3860			1				26	37				3	1			10
771	4032							15	8	1			7	1			9
781	4119				2			21	46	1			16	4			0
791	4196			1		2		35	78	7			12	4			21

Appendix 5

Total pollen concentration (grains/cm^3), and accumulation rates (flux) (grains/cm^2/yr), and count data of the individual pollen taxa from core GeoB9503-5

Depth (cm)	Age (yr)	Total pollen	pollen concentration	Pollen flux	Gramineae	Cyperacea	*Rhizophora*	*Typha*	Graminae <25 µm	*Olea*	*Pinus*	*Artemisia*	Asteroideae (Compositae Tubuliflorae)	Amaranthaceae/Chenopodiaceae	*Acacia* (Mimosaceae)	*Boveria spermacore* (Rubeacea)	*Mitracarpus*	*Mimosa type*	*Zizyphus* (Rhamaceae)	*Boscia-type* (Capparidacea)	*Butyrospemum* (Sapotacea)
21	1240	76	5447	2368,3	21	13			27					4	1	1		3	2		
41	1288	190	2062	897	65	16	4	6	73	2	1	1	3	6	2	1	1	1	2		
51	1311	277	4537	1973	94	13	3	3	90	1			1	23	11	1	5	4	3		
81	1434	127	2820	395	23	12	1	3	57		10			2	8						
91	1505	60	1746	244	21	9		3	23						1			1			
101	1576	56	1818	254	19	9	2	3	14				1	3	3			2			
121	1719	100	1242	174	23	10	3	1	31				3	3	1	3	3	1			
131	1791	134	2430	340	45	14	3	10	46					4	1		2				
141	1859	78	2996	767	19	9		2	37	1			1		1	1					
151	1898	54	1413	362	14	4		4	25					1			1				
171	1976	163	2618	670	59	27	7	5	47				1	4	2						
181	2015	273	2966	760	113	33	5	10	86		2		1	5		1	5		1		
191	2054	116	2538	650	29	19	8	2	47					3			1				
201	2093	83	3788	970	32	3	1	2	23			1		2	1						
211	2132	220	5315	1361	77	29	18	14	55				1	8	3		4				
221	2145	81	1101	1682	22	17	3	5	21	1				5			2	1			
231	2152	199	1973	3016	71	21	3	7	73				5	5	1		2	1			
241	2158	116	1437	2197	44	16	4	3	30			1		4			5				
251	2165	154	2473	3780	44	18	10	6	54	2			1	9	1		1	2	2		
261	2171	63	2149	3286	10	11		5	30						1			1			
271	2178	73	1433	2191	14	6	3		33	1	1		1		1				1		1
281	2184	137	1324	2024	37	14	9	10	53				1	3		1	1		1		
301	2198	135	1110	1696	37	24	8	9	35	2	1		1	3			2	1		2	
311	2204	155	905	1384	55	32	8	6	28		1		2	5	4	2	4	2		3	
331	2227	137	1815	1167	40	19	6	15	43				3	4			2				
351	2258	208	3219	2069	60	11	9	7	59					7	2	3	5	3	4		
361	2274	135	2057	1322	38	18	14	5	38				4	8			4			1	
371	2289	236	796	512	71	33	10	14	55	2	1		4	12	2	1	5	1	2	5	
381	2305	242	2239	1440	94	24	10	14	58				2	6	1		3		1	1	
401	2336	151	1589	1021	64	16	9	4	30	1	1			7	2	1	7				
411	2352	134	794	472	30	24	9	9	38	1			2	5			7				
431	2385	115	867	516	20	16	12	8	21				2	9	4		12			8	
441	2402	202	2827	1682	73	7	9	7	67				1	4	2	3	2	2	3		
461	2436	102	1470	875	30	19	7	4	21	1	2		1	5			7			2	
481	2469	109	1028	612	14	12	1	3	60		3		2	1			3		1		
491	2486	134	879	523	42	20	2	8	43		1			3	1		7				
501	2503	164	1215	723	37	15	3	4	95		1					1					
521	2537	81	654	389	23	7	5	3	25					7			3			3	
531	2555	245	1199	473	67	45	18	16	39	1	1		3	19	1	3	7	2	3	3	
541	2580	56	1638	646	9	5	3	2	25					3	3	1					
561	2631	213	1810	714	53	41	14	11	57	1	1		1	7			3	1	1	2	
591	2707	139	1700	671	41	24	9	8	31					5		1	7			2	
601	2737	163	1158	168	37	29	15	10	32	2			4	12	1	2	6		1	2	
611	2806	57	3074	446	11	11	6	2	25					1	1						
621	2875	74	2583	374	24	11		3	26				3	3							
631	2944	125	5056	733	37	21	21	5	18				2	5			7			3	
651	3082	236	6479	939	90	15	14	2	70	1			1	6	2		1	2	2	1	
671	3220	165	2532	367	40	25	18	11	39	1	1		1	5		1	6	1	2	2	
691	3358	170	1860	270	33	17	2	2	94		2		2	1	1	2	4		2	1	
701	3429	55	3694	428	3	6	1		38				1						2		
721	3601	100	4967	576	27	9	13	8	29					2	2	1	1				
731	3687	354	5843	677	156	29	46	17	63	1			2	3		1	4	2		2	
751	3860	196	4641	538	96	4	8		65					2	2				2		
771	4032	196	7752	899	57	24	31	6	62	1			1	2		1	2		1		
781	4119	154	4316	500	53	25	26	3	33	1			1	2			3			1	
791	4196	461	4610	534	168	56	50	17	128	1			3	7	1		2	2			

Appendix 5 *Continued*

Depth (cm)	Age (yr)	*Pliostigma* (Caesalpiniaceae)	*Pterocarpus - type* (Iabaceae)	*Vernonia-type* (Asteraceae)	*Indigofora*	*Tamarindus*	*Stereospermum - type* (Bignoniaceae)	*Phoenix-type* (Palmae)	*Uapaca*	Anonaceae	*Canthium subcordatum* (Rubeaceae)	*Euphorbia-type*	Rubeacea	*Clematis*	*Galium*	*Fraxinus*	*Cuviera*	Pollen indet.	spores	Fungal spores	Total fresh water algae
21	1240											2	1					1	17	1	9
41	1288											5	1						1	7	9
51	1311										1	12	4					8	24	11	24
81	1434				1							1	4					5	12	10	24
91	1505												1					1	4	1	14
101	1576																		8	3	3
121	1719										2	8	2					6	5		6
131	1791										2	4		2				1	8	5	8
141	1859						1					1						5	9	18	5
151	1898											1	2					2	8		3
171	1976										1	5	3					2	2	7	11
181	2015											4	2					5	5	1	4
191	2054					1						3		1	2				5	3	4
201	2093										2	5						11	15	1	8
211	2132											6	2					3	6	3	23
221	2145								2			1	1	1					1	5	7
231	2152										1	4	2					3	7	3	6
241	2158											4	3					2	2	2	5
251	2165											4							4	12	14
261	2171																	5	6	4	3
271	2178	1		1				1	1			1			1			5	11	6	1
281	2184											2	1	1	2			1	5	11	9
301	2198											5	2					3	4	6	9
311	2204											2	1						23	11	18
331	2227											2	2					1	7	5	8
351	2258								7		1	13	5					12	30	4	11
361	2274											3	2						4	11	3
371	2289											8	2	1				7	17	13	27
381	2305											14	6			2		6	5	5	8
401	2336											1	5			1		2	4	12	8
411	2352											4						5	4	12	20
431	2385											3							3	5	13
441	2402	2									1	12	3					4	26	4	12
461	2436											1						2	1	8	6
481	2469		1		1							1	3					3	11	10	9
491	2486											2						5	6	21	7
501	2503	1									1	2		1				3	11	5	19
521	2537								1			3	1						3	12	10
531	2555								2		2	9	3					1	19	7	39
541	2580			1								1						3	12	7	12
561	2631				1				1			8	1					9	11	12	23
591	2707										1	5	2					3	5	3	17
601	2737										1	3	5		1				4	12	16
611	2806																		10	8	14
621	2875									1		2						1	5	1	22
631	2944											4	2						3	8	8
651	3082	1			2				3		2	11	4					6	29	6	13
671	3220											10	2						4	11	16
691	3358					1				1		2	3						8	9	12
701	3429			1								1						2	3	6	5
721	3601											6		1				1	5	8	8
731	3687										1	10	7					10	4	8	7
751	3860										1	8	7					1	10		11
771	4032											2	2	2				2	8	2	15
781	4119										1	4	1						14	7	11
791	4196										3	12	2	1			1	7	8	8	42